**The Dissertation Committee for Malaney Ravae O'Connell Certifies that this is the approved version of the following dissertation:**

# DELINEATING REGULATORY PATHWAYS OF NOVEL CANCER STEM CELL MARKER, DCLK1-S, FOR TARGETING COLON CANCER STEM CELLS

**Committee:**

Pomila Singh, PhD

Thomas Wood, PhD

Heidi Spratt, PhD

Darren Boehning, PhD

Lawrence Sowers, PhD

Anirban Maitra, MD

Dean, Graduate School

# DELINEATING REGULATORY PATHWAYS OF NOVEL CANCER STEM CELL MARKER, DCLK1-S, FOR TARGETING COLON CANCER STEM CELLS

**by**

**Malaney Ravae O'Connell, B.S.**

**Dissertation**

Presented to the Faculty of the Graduate School of

The University of Texas Medical Branch

in Partial Fulfillment

of the Requirements

for the Degree of

**Doctor of Philosophy**

**The University of Texas Medical Branch**

**March, 2016**

# Dedication

To my incredible husband, family, and friends.

## Acknowledgements

I would like to take this opportunity to express my sincere appreciation to my mentor, Dr. Pomila Singh for all of her guidance and support throughout my graduate career. It has been a privilege working with Dr. Singh and I am grateful for the opportunity. I would also like to thank Dr. Shubhashish Sarkar for all of his invaluable support throughout my training both in and out of lab.

I would also like to thank my committee members, Dr. Lawrence Sowers, Dr. Thomas Wood, Dr. Heidi Spratt, Dr. Darren Boehning, and Dr. Anirban Maitra for guidance and commitment to my dissertation project. I truly appreciate all the time and energy you invested in me and my project.

I am also deeply grateful to the administration and staff of the Graduate School of Biomedical Sciences, Cell Biology Graduate program, and the Department of Neuroscience and Cell Biology for all of their support and guidance throughout my graduate career.

I am also sincerely grateful to all of our collaborators for their support of my dissertation project.

Finally I would like to thank my husband, my family, and my friends for their unconditional love, support, and encouragement throughout my graduate career. Thank you for always believing in me.

# DELINEATING REGULATORY PATHWAYS OF NOVEL CANCER STEM CELL MARKER, DCLK1-S, FOR TARGETING COLON CANCER STEM CELLS

Publication No._____

Malaney Ravae O'Connell, PhD

The University of Texas Medical Branch, 2016

Supervisor: Pomila Singh

Colon cancer is third most prevalent cancer in the United States, with significant health consequences for the patient and society. Cancer stem cells are believed to be resistant to conventional treatments resulting in relapse of the disease. Targeting cancer stem cells in addition to conventional therapy may result in better outcomes for patients. Colon cancer stem cells express several stem cell markers, including DCLK1.

Recent reports suggest that the 5' promoter of DCLK1 is increasingly methylated and silenced in colon cancers; however significant levels of DCLK1-protein are expressed by colon cancer cells and human adenocarcinomas, suggesting that DCLK1 measured in colon cancers is likely transcribed from an alternative promoter. As my first goal, this possibility was investigated and led us to discover that colon cancers express a short isoform of DCLK1 from a promoter within intron V, while normal colons mainly express long isoforms of DCLK1 from 5'promoter.

The loss of DCLK1 expression in cancer cells has been reported to result in the loss of proliferative/tumorigenic/metastatic potential of colon cancer cells. RNAi

methods used so far, target both isoforms of DCLK1, therefore my second goal was to use shRNA knockdown methods to specifically target DCLK1-S isoform, in order to delineate the biological role of cancer specific DCLK1-S isoform. The results of our studies suggest that DCLK1-S mediates the activity of transcription factor, NFATC2 (via the NFATC2 $^{53}$SPPS$^{56}$ motif), which in turn results in NFATC2 binding and activation of the COL3A1 promoter which enhances the invasive potential of colon cancer cells.

The 5'(α)-promoter is differentially methylated in normal human colons vs. human colorectal cancers, however the methylation status of the IntronV(β)-promoter does not change. Therefore for my third goal, I investigated if differential expression of DCLK1-S in normal colons vs. human colorectal cancers was perhaps due to differences in transcriptional activity of the promoter in normal vs. cancer cells. Our studies demonstrate for the first time that FOXD3 is a potent transcriptional inhibitor of the IntronV(β)-promoter, resulting in the absence of DCLK1-S expression in normal human colons.

# TABLE OF CONTENTS

# List of Tables

# List of Figures

# List of Abbreviations

| | |
|---|---|
| CRC | Colorectal Cancer |
| US | United States |
| CSC | Cancer Stem Cell |
| NSC | Normal Stem Cell |
| LGR5 | Leucine-Rich Repeat-Containing G-protein Coupled Receptor 5 |
| CD44 | Cluster of Differentiation 44 |
| DCLK1 | DoubleCortin-Like Kinase 1 |
| DCLK1-S | DoubleCortin-Like Kinase 1-Short |
| DCLK1-L | DoubleCortin-Like Kinase 1-Long |
| AdCA | Adenocarcinoma |
| TCF | T-cell Factor |
| LEF | Lymphoid Enhancer-Binding Factor |
| NFκB | Nuclear Factor of Kappa Light Polypeptide Gene |
| RNAi | RNA Interference |
| shRNA | Short Hairpin RNA |
| NFATC2 | Nuclear Factor of Activated T-cells, Cytoplasmic, Calcineurin-Dependent 2 |
| COL3A1 | Collagen, Type III, Alpha 1 |
| ECM | ExtraCellular Matrix |
| SPARC | Secreted Protein, Acidic, Cysteine-Rich |
| vs. | versus |

| | |
|---|---|
| FOXD3 | Forkhead Box D3 |
| FAP | Familial Adenomatous Polyposis |
| APC | Adenomatous Polyposis Coli |
| HNPCC | Hereditary Nonpolyposis Colorectal Cancer |
| MLH1 | MutL Homolog 1 |
| MSH2 | MutS Homolog 2 |
| Fig | Figure |
| IGF | Insulin Like Growth Factor |
| PG | Progastrins |
| KRAS | Kirsten Rat Sarcoma Viral Oncogene Homolog |
| BRAF | B-Raf Proto-Oncogene, Serine/Threonine Kinase |
| TGFβ | Transforming Growth Factor Beta |
| SMAD | Similar to Mothers Against Decapentaplegic |
| P53 | Tumor Protein p53 |
| WNT | Wingless-type MMTV Integration Site Family Member |
| β-catenin | Beta Interacting Protein |
| EMT | Epithelial Mesenchymal Transition |
| CIN | Chromosomal Instability |
| MSI | Microsatellite Instability |
| CIMP | CpG Island Methylator Phenotype |
| FOBT | Fecal Occult Blood Tests |
| FIT | Fecal Immunochemical Tests |
| CDC | Center for Disease Control and Prevention |

| | |
|---|---|
| M cells | Microfold or Membranous cells |
| BMP | Bone Morphogenic Protein |
| BMI | BMI1 Proto-Oncogene, Polycomb Ring Finger |
| DCX | DoubleCortin |
| CAMK | Ca2+/Calmodulin Dependent Kinase |
| VA | Vinca Alkaloids |
| CgA | Glycoprotein Hormones, Alpha Polypeptide |
| BrdU | Bromodeoxyuridine |
| MSI-1 | Musashi RNA-Binding Protein 1 |
| PCNA | Proliferating Cell Nuclear Antigen |
| ChrA | Carcinoembryonic Antigen |
| PTEN | Phosphatase and Tensin Homolog |
| AKT | V-akt Murine Thymoma Oncogene Homolog 1 |
| COX1 | Cytochrome C Oxidase Subunit 1 |
| COX2 | Cytochrome C Oxidase Subunit 2 |
| OCT4 | Octamer-Binding Transcription Factor 4 |
| POU5F1 | POU Class 5 Homeobox 1 |
| SOX2 | SRY (Sex Determining Region Y)-Box 2 |
| NANOG | NANOG Homeobox |
| KLF4 | Kruppel-Like Factor 4 |
| ATM | ATM Serine/Threonine Kinase |
| FABP | Fatty Acid Binding Protein |
| AOM | Azoxymethane |

| | |
|---|---|
| DSS | Dextran Sodium Sulfate |
| HEKC | HEK293 cells Overexpressing Control Vector |
| HEKmGAS | HEK293 cells Overexpressing Full Length Progastrins |
| 2D | Two Dimensional |
| 3D | Three Dimensional |
| Aa | Amino Acids |
| 5-Aza | 5-aza-2'deoxycytidine |
| CD133 | Prominin 1 |
| Bp | Basepairs |
| Abs | Antibodies |
| Mr | Molecular mass |
| RT | Room Temperature |
| Tf | Transcriptional Factor |
| Ad | Adenoma |
| HP | Hyperplastic |
| TA | Tubular Adenoma |
| NORM | Normal |
| MET | Metastatic Lesions |
| TNM | UICC's Criteria for Tumor Node Metastasis |
| CEA | Carcinoembryonic Antigen |
| GAPDH | Glyceraldehyde-3-phophate Dehydrogenase |
| Nt | Nucleotide |
| WB | Western Blot Analysis |

| | |
|---|---|
| NC | Normal Colons |
| CCC | Colon Cancer Cells |
| HCT-C | HCT116 cells overexpressing Control shRNA |
| HCT-D | HCT116 cells overexpressing DCLK1-S shRNA |
| RNAseq | RNA Sequencing Analysis |
| PDGF | Platelet-Derived Growth Factor |
| MMP | Matrix Metalloproteinases |
| DEG | Differentially Expressed Genes |
| PIIP | N-terminal peptide cleaved from the type III collagen precursor molecule |
| P4HA2 | Prolyl 4-Hydroxylase, Alpha Polypeptide II |
| IDC | Invasive Ductal Carcinomas |
| ILC | Invasive Lobular Carcinomas |
| FOXP3 | Forkhead Box P3 |
| GATA4 | GATA Binding Protein 4 |
| AP1 | Activator-Protein 1 |
| C-TERM | C-terminal Domain |
| RHR | Rel-Homology Region |
| TAD | Transactivation Domain |
| NLS | Nuclear Localization Signal |
| NES | Nuclear Export Signal |
| CDS | Calcineurin Docking Site |
| PLCγ | Phospholipase Cγ |

| | |
|---|---|
| IP3 | Inositol Triphosphate |
| DYRK1 | Dual-specificity Tyrosine-phosphorylation Regulated Kinase 1 |
| DYRK2 | Dual-specificity Tyrosine-phosphorylation Regulated Kinase 2 |
| GSK3 | Glycogen-synthase Kinase 3β |
| CK1 | Casein Kinase 1 |
| PKCζ | Protein Kinase C ζ |
| JNK | c-jun N-terminal Kinase |
| VRK2 | Vaccina-related Kinase 2 |
| CN | Calcineurin |
| GFP | Green Fluorescent Protein |
| 205-C | COLO205 cells overexpressing Control GFP plasmid |
| 205-L | COLO205 cells overexpressing GFP-DCLK1-L plasmid |
| 205-S | COLO205 cells overexpressing GFP-DCLK1-S plasmid |
| IF | Immunofluorescence |
| DAPI | 4', 6-diamidino-2-phenylindole |
| IHC | Immunohistochemistry |
| H&E | Hematoxylin and Eosin |
| IP | Immunoprecipitation |
| WT | Wild-type |
| MUT | Mutant |
| FH | Forkhead |
| ERBB3 | Erb-B2 Receptor Tyrosine Kinase 3 |
| Rnd3 | Rho Family GTPase 3 |

| | |
|---|---|
| ERBB3 | Erb-B2 Receptor Tyrosine Kinase 3 |
| TWIST1 | Twist Family BHLH Transcription Factor 1 |
| CXCR4 | Chemokine (C-X-C Motif) Receptor 4 |
| PAX3 | Paired Box 3 |
| CYFIP2 | Cytoplasmic FMR1 Interacting Protein 2 |
| RARB | Retinoic Acid Receptor, Beta |
| HTS | High Throughput Screening |
| FFPE | Formalin-fixed, paraffin-embedded |

# Chapter 1: Introduction

Colorectal cancer (CRC) is the 3rd most common and lethal cancer in the United States (US) (Siegel et al., 2014a; Siegel et al., 2014b). Development of colorectal cancer occurs over many years and is a complex process involving multiple molecular pathways (Grady and Pritchard, 2014; Kuipers et al., 2015; Okugawa et al., 2015). Accumulation of genetic and epigenetic mutations causes mutant epithelial cells to divide uncontrollably leading to a malignant tumor (Grady and Pritchard, 2014; Kuipers et al., 2015; Okugawa et al., 2015). Colorectal cancer represents a significant burden on our public health system and it is estimated that the national expenditure in the year 2015 will be $18.5 billion (Mariotto et al., 2011). Although advances have been made in screening and surveillance, mortality rates remain high among colorectal cancer patients due to the metastasis and spread of the disease and our lack of understanding of these specific mechanisms (Siegel et al., 2012). Cancer stem cells (CSCs) are believed to be resistant to currently available treatments (Cherciu et al., 2014; Kantara et al., 2014; Wang et al., 2015b). Recent literature suggests that targeting cancer stem cells may help to avoid patient relapse and eliminate metastasis (Cherciu et al., 2014; Kantara et al., 2014; Wang et al., 2015b), thus highlighting the importance of identifying and targeting cancer stem cells for treating cancers.

Normal stem cells have been identified at the base of normal colonic crypts in mice and humans, within a stem cell niche (Barker, 2014; Sancho et al., 2015), and are responsible for the constant turnover of proliferating and differentiated cells located along the length of the colonic crypts, due to the short half-life (4-7 days) of differentiated cells (De Mey and Freund, 2013; Humphries and Wright, 2008). Cells in the lower 1/3rd of the crypts (proliferative zone) give rise to differentiated cells in the upper 2/3rds of the crypt, which move upwards and get sloughed off into the lumen due

to apoptotic death (Barker, 2014; Sancho et al., 2015), either in response to injury or as part of normal turnover (Humphries and Wright, 2008).

We previously reported that once normal stem cells (NSCs) are transformed into cancer stem cells, they become morphologically distinct (Sarkar et al., 2012). It is postulated that cancer stem cells unlike normal stem cells, lose the ability to proliferate asymmetrically, and both daughter cells retain proliferative potential, with concomitant loss in their differentiating potential (Ong et al., 2014; Sancho et al., 2015). Additionally, cancer stem cells are believed to be resistant to chemotherapy and radiation therapy, and although though the bulk of the tumor mass is reduced in response to the currently available therapies, the small population of cancer stem cells (< 1-3%) (Kantara et al., 2014; Sarkar et al., 2012) survive treatment and re-grow as primary/metastatic tumors, resulting in relapse of the disease (Cherciu et al., 2014; Kantara et al., 2014; Wang et al., 2015b).

Several putative stem cell markers, including LGR5 (Leucine-rich Repeat-containing G-protein Coupled Receptor 5), CD44 (Cluster of Differentiation 44), and DCLK1 (DoubleCortin-Like Kinase 1), have been reported to identify normal colonic stem cells. However colon cancer stem cells express many of the same markers as intestinal normal stem cells (Barker et al., 2008; Cherciu et al., 2014; Kantara et al., 2014; Nakanishi et al., 2013; Sarkar et al., 2012); therefore targeting cancer stem cells while sparing normal stem cells has remained a challenge.

Recently, DCLK1 was reported to be a specific colon cancer stem cell marker (Nakanishi et al., 2013). High levels of DCLK1 protein have been reported in human colorectal cancers (Gagliardi et al., 2012a; Kantara et al., 2014; Sureban et al., 2009); however in recent years we have learned that the 5' promoter of DCLK1 is epigenetically silenced in human colorectal cancers (Marie Vedeld et al., 2014; Vedeld et al., 2014). Therefore the first aim of my dissertation was to investigate the possibility of an alternate isoform of DCLK1 being expressed from an alternate promoter in human colorectal

cancers. The experiments conducted to address this aim are presented in Chapter 2 of my dissertation. The results of our studies revealed that a short isoform of DCLK1 (DCLK1-S) was the main isoform expressed in human colon cancer cells and in human adenocarcinomas (AdCA), downstream of an IntronV(β)-promoter, while the canonical DCLK1-L (long isoform of DCLK1) was the main isoform expressed in normal human colons, downstream of the 5'(α)promoter (O'Connell et al., 2015). We also demonstrated that TCF/LEF (T-cell Factor/Lymphoid Enhancer-Binding Factor) (5'(α)-promoter) and NF-κB (Nuclear Factor of Kappa Light Polypeptide Gene Enhancer in B-cells) (IntronV(β)-promoter) binding sites were required for transcriptional activation of L/S isoforms in normal vs. cancer cells (O'Connell et al., 2015). The physiological relevance of DCLK1-S expression was examined by plotting survival curves of 92 colorectal cancer patients in relation to high/low expression of DCLK1-S; high-expressers had significantly worse survival, compared to low expressers (O'Connell et al., 2015). Our novel findings regarding alternative usage of promoters by normal vs. cancer stem cells, suggests that specifically targeting DCLK1-S may eliminate cancer stem cells, while sparing DCLK1-L functions in normal colons.

The loss of DCLK1 expression in cancer cells has been reported by us (Kantara et al., 2014) and others (Sureban et al., 2011b; Sureban et al., 2009) to result in the loss of proliferative/tumorigenic/metastatic potential of colon cancer cells. Our laboratory has also reported that down regulation of DCLK1 in other transformed epithelial cells (Sarkar et al., 2012), attenuates the growth of cells and is critically required for maintaining proliferative potential of the colon cancer/transformed cells, *in vitro* and *in vivo*. RNAi (RNA Interference) methods used so far (Kantara et al., 2014; Sureban et al., 2011b; Sureban et al., 2009), target both isoforms of DCLK1. Therefore the second aim of my dissertation was to use shRNA (Short Hairpin RNA) knockdown methods to specifically target the DCLK1-S isoform in representative colon cancer cells, in order to delineate the biological role of cancer specific DCLK1-S isoform. The experiments conducted to

address this aim are presented in Chapter 3 of my dissertation. The results of my Aim 2 studies allowed me to discover some of the pathways which were specifically down-stream of DCLK1-S, but not DCLK1-L (O'Connell et al., 2016c; O'Connell et al., 2016d). A major finding of these studies was that possible direct interaction of DCLK1-S (a kinase), with transcription factor, NFATC2 (Nuclear Factor of Activated T-cells, Cytoplasmic, Calcineurin-Dependent 2), resulted in DCLK1-S mediated phosphorylation (at the $^{53}$SPPS$^{56}$ motif ) and activation of NFATC2 followed by binding of NFATC2 to the promoter of COL3A1 (Collagen, Type III, Alpha 1) resulting in several fold increase in expression levels of COL3A1 (O'Connell et al., 2016c). My *in vitro and in vivo* studies also suggest that DCLK1-S plays a critical role in mediating the invasive potential of colon cancer cells through modulation of the extracellular matrix (ECM) via enhanced expression of associated genes (such as SPARC (Secreted Protein, Acidic, Cysteine-Rich) and COL3A1) (O'Connell et al., 2016c).

As discussed above, the 5'(α)-promoter of DCLK1 is differentially methylated in normal human colons vs. (versus) human colorectal cancers, as confirmed in my studies (O'Connell et al., 2015), however, my findings suggest that the methylation status of the IntronV(β)-promoter does not change in normal vs. colon cancer cells. Therefore the third aim of my dissertation was to determine if differential expression of DCLK1-S in normal colons vs. human colorectal cancers was perhaps due to differences in transcriptional activity of the promoter in normal vs. cancer cells. The results of my third aim are presented in Chapter 4 of my dissertation. As a result of these studies, we identified a role of FOXD3 (Forkhead Box D3) in the regulation of the IntronV(β)-promoter using promoter reporter and ChIP assays (O'Connell et al., 2016a; O'Connell et al., 2016b). Our studies demonstrate for the first time that FOXD3 is a potent transcriptional inhibitor of the IntronV(β)-promoter, resulting in the absence of DCLK1-S expression in normal human colons (O'Connell et al., 2016a; O'Connell et al., 2016b). We also evaluated the pathophysiological relevance of DCLK1-S and FOXD3 expression in the overall survival

of colorectal cancer patients and determined that patients expressing relatively high levels of DCLK1-S and low levels of FOXD3 had significantly worse overall survival as compared to patients expressing relatively low levels of DCLK1-S and high levels of FOXD3, suggesting that measuring DCLK1-S and FOXD3 expression could have diagnostic/prognostic significance (O'Connell et al., 2016a; O'Connell et al., 2016b).

The relevance of my findings towards improvement in the treatment, diagnosis and prognosis of colorectal cancers is discussed in Chapter 5 of my dissertation. The significance of many of the molecules and mechanisms related to my dissertation are described below, as part of chapter 1 itself, and specific aspects of some relevant molecules/pathways are described in the background sections of Chapters 2-4.

## 1.1 COLORECTAL CANCER

### 1.1.1 Colorectal Cancer Demographics

Colorectal cancer is the 3rd most prevalent and deadly cancer for both male and females in the United States with an estimated 137,000 new cases and 50,000 deaths in the year 2014 alone (Siegel et al., 2014a) , as illustrated in **Figure 1.1**.

**Figure 1.1: Colorectal Cancer Demographics**

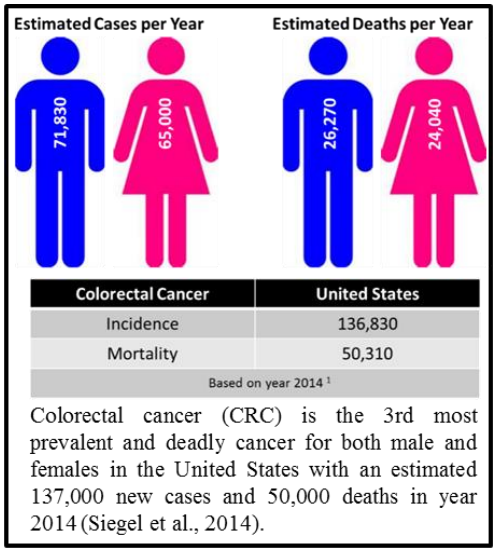

Over the past decade, the overall incidence rates have been steadily decreasing by ~3% per year (Bailey et al., 2015; Siegel et al., 2014a), however in adults 50 years or younger, the incidence rates have increased (Abdelsattar et al., 2016; Bailey et al., 2015; Siegel et al., 2012), suggesting that although the overall incidence of colorectal cancers have declined in 50+ individuals, which can be largely attributed to increased awareness and advances in screening and surveillance, further progress can be accelerated by improving access and use of screening to all populations (Abdelsattar et al., 2016; Bailey et al., 2015; Siegel et al., 2012), which may need to be extended to include individuals 40+ and older, based on recent reports described above. It was estimated in 2015, that the national expenditure for colorectal cancer screening and treatment will be ~$18.5 billion (Mariotto et al., 2011), making it the second most costly cancer in terms of health expenditures (Mariotto et al., 2011). Although great advances have been made to extend the life of colorectal cancer patients, colorectal cancer remains a significant public health burden for our society, due to less than optimal methods of treating and avoiding relapse of this disease, especially in patients with stages II-IV of colorectal cancer.

### 1.1.2 Progression of Colorectal Cancer

Development of colorectal cancer occurs over many years and is a complex process involving multiple molecular pathways (Grady and Pritchard, 2014; Kuipers et al., 2015; Okugawa et al., 2015). Accumulation of genetic and epigenetic mutations causes mutant epithelial cells to divide uncontrollably leading to a malignant tumor (as discussed in recent review articles, (Grady and Pritchard, 2014; Kuipers et al., 2015; Okugawa et al., 2015). Colorectal cancer can be divided into two main subtypes including 1) cancers with a hereditary component, accounting for ~25% of colorectal cancers and 2) sporadic cancers, accounting for ~75% of colorectal cancers (Kuipers et al., 2015).

Cancers with a hereditary component can mostly be attributed to heritable syndromes such as FAP (Familial Adenomatous Polyposis), which is caused by mutation of the *APC* (Adenomatous Polyposis Coli) gene, and HNPCC (Hereditary Nonpolyposis Colorectal Cancer or lynch syndrome), which is caused by mutation of DNA mismatch repair genes such as *MLH1* (MutL Homolog 1) or *MSH2* (MutS Homolog 2) (Kuipers et al., 2015).

Sporadic colorectal cancers are considered genetic/epigenetic diseases, which may be triggered by unhindered hyperproliferation of colonic mucosa in response to sustained and elevated levels of specific growth factors, such as IGFs (Insulin Like Growth Factor 1) and PGs (Progastrins) (Singh et al., 2012; Vigneri et al., 2015), which can potentially result in accumulation of epigenetic changes and/or genetic mutations, of oncogenes and tumor suppressor genes (Grady and Pritchard, 2014; Okugawa et al., 2015). As hyperproliferating colons progress through the adenoma-adenocarcinoma sequence of colon carcinogenesis, several tumor suppressors (coding and noncoding) are silenced while oncogenes are activated due to epigenetic changes or mutations (Kuipers et al., 2015; Okugawa et al., 2015). Typically the *APC* gene is inactivated/mutated which may operate as the initial trigger of colon carcinogenesis (White et al., 2012; Zoratto et al., 2014). Oncogenes such as KRAS (Kirsten Rat Sarcoma Viral Oncogene Homolog), BRAF (B-Raf Proto-Oncogene, Serine/Threonine Kinase), and TGFβ (Transforming Growth Factor Beta)/SMAD (Similar to Mothers Against Decapentaplegic) are then activated (Berg and Soreide, 2012; Sipos and Galamb, 2012; Zoratto et al., 2014), along with significant changes in the expression of several non-coding RNAs (Goel, 2015; Okugawa et al., 2015; Weng et al., 2015), followed by inactivation of gateway tumor suppressors such as p53 (Tumor Protein p53) (Li et al., 2015; Mundade et al., 2014). The APC tumor suppressor protein is a key component of the destruction complex involved in the WNT (Wingless-type MMTV Integration Site Family Member) signaling pathway (White et al., 2012). Loss of APC function results in accumulation of β-catenin (Beta-

Catenin), followed by its activation in response to upregulated oncogenic pathways (such as elevated levels of circulating progastrins, (Singh et al., 2012)), which can transactivate target genes involved in proliferation, differentiation, adhesion, and migration (Vasen et al., 2015; White et al., 2012). Mutations in either oncogenic KRAS or its downstream target, BRAF, results in constitutively activating RAS/RAF/MAPK and PI3K/PTEN/AKT pathways resulting in uninhibited cell growth and proliferation (Berg and Soreide, 2012; Zoratto et al., 2014). Activation of SMAD dimers by TGF-β results in transcriptional activation of key regulators of epithelial to mesenchymal transition (EMT) (Sipos and Galamb, 2012; Zoratto et al., 2014). P53 is a key regulator of apoptosis, in response to DNA damage (Li et al., 2015). P53 mutation results in proliferation of cells harboring damaged/mutated DNA and is involved in advancing the progression of adenomas to adenocarcinomas (Li et al., 2015).

Baseline mutation rates are insufficient to promote carcinogenesis in sporadic cancers. Therefore, progression of sporadic cancers is facilitated by many different molecular pathways of genomic instability, including chromosomal instability (CIN), microsatellite instability (MSI) and CpG island methylator phenotype (CIMP), which increase the number of mutations in transformed cells as illustrated in **Figure1.2** (Kuipers et al., 2015; Mundade et al., 2014). Chromosomal instability is characterized by aneuploidy and frequent loss of heterozygosity and occurs in more than 50% of colorectal cancers (Mundade et al., 2014; Pino and Chung, 2010). Microsatellite instability occurs through inactivation of DNA mismatch repair genes and occurs in ~15% of colorectal cancers (Kim and Kang, 2014; Mundade et al., 2014). Mutation or epigenetic silencing of DNA mismatch repair genes leads to microsatellite instability resulting in accumulation of DNA mutations during replication (Kuipers et al., 2015) (Mundade et al., 2014). CIMP is characterized by widespread hypermethylation of CpG islands within a promoter, resulting in inactivation of tumor suppressor genes in ~20% of colorectal cancers (Mundade et al., 2014; Nazemalhosseini Mojarad et al., 2013). These types of

fundamental changes in stem cells, likely transforms the stem cells into cancer stem cells, which likely sustain the phenotypic changes associated with malignant tumors, arising from benign (adenomatous) growths in the colons (Abetov et al., 2015; Cherciu et al., 2014; Kantara et al., 2014; Kozovska et al., 2014; Sarkar et al., 2012; Singh et al., 2012; Wang et al., 2015b). The challenge therefore is to target the cancer stem cells, which represent the seed of the malignant growth.

**Figure 1.2: Multiple Genetic Pathways in Colorectal Cancer**

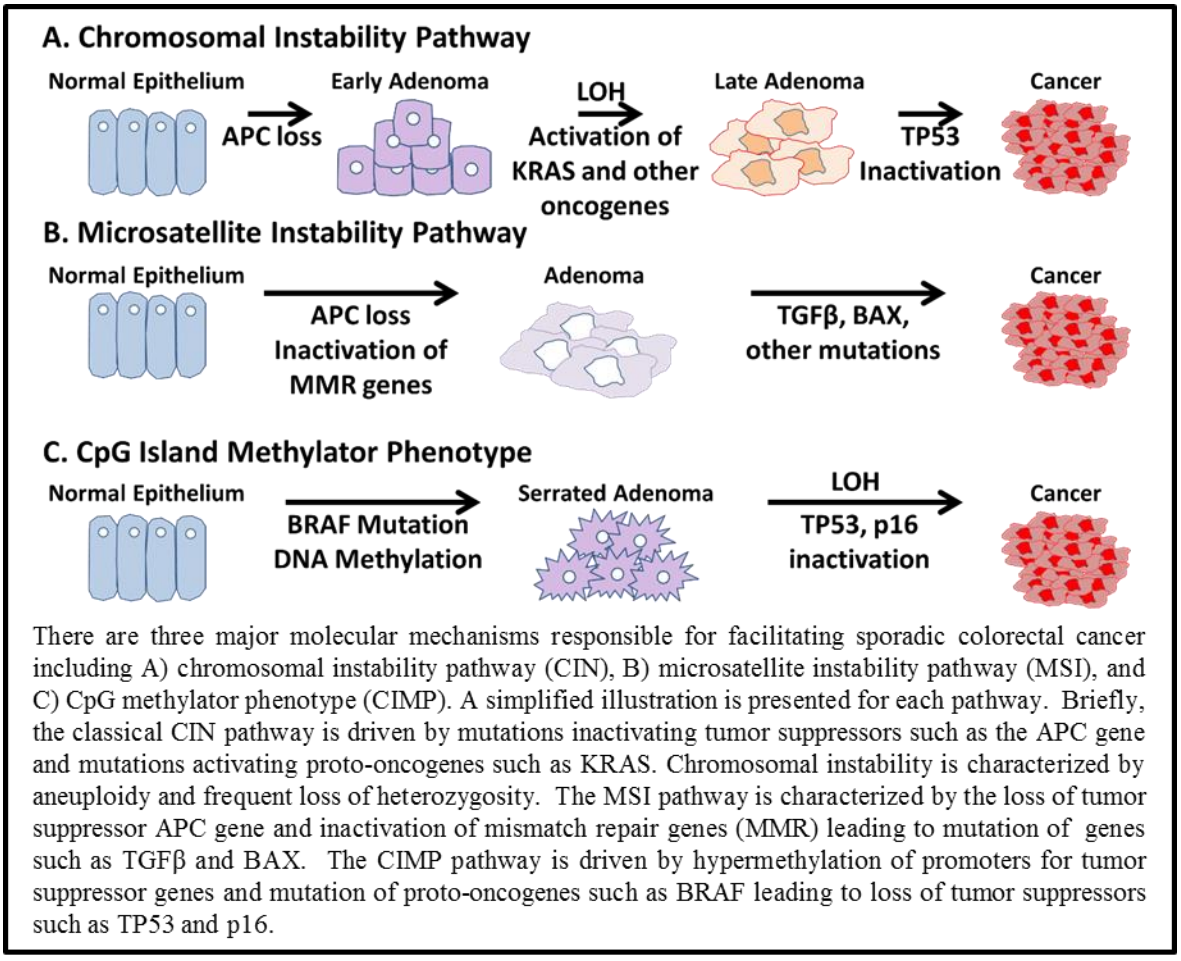


There are three major molecular mechanisms responsible for facilitating sporadic colorectal cancer including A) chromosomal instability pathway (CIN), B) microsatellite instability pathway (MSI), and C) CpG methylator phenotype (CIMP). A simplified illustration is presented for each pathway. Briefly, the classical CIN pathway is driven by mutations inactivating tumor suppressors such as the APC gene and mutations activating proto-oncogenes such as KRAS. Chromosomal instability is characterized by aneuploidy and frequent loss of heterozygosity. The MSI pathway is characterized by the loss of tumor suppressor APC gene and inactivation of mismatch repair genes (MMR) leading to mutation of genes such as TGFβ and BAX. The CIMP pathway is driven by hypermethylation of promoters for tumor suppressor genes and mutation of proto-oncogenes such as BRAF leading to loss of tumor suppressors such as TP53 and p16.

### 1.1.3 Diagnosis and Treatment of Colorectal Cancer

Because adenomas and adenocarcinomas do not present symptoms in the early stages, screening is critical to reduce colorectal cancer mortality rates. Several methods are used to diagnose colorectal cancer including colonoscopy, fecal occult blood tests (FOBT) or fecal immunochemical tests (FIT) and multi-targeted fecal DNA tests (Mundade et al., 2014). To date the golden standard for diagnosis of colorectal cancer is colonoscopy due to its high diagnostic accuracy. During a colonoscopy not only can the location of polyps/tumors be assessed but polyps can also be removed allowing for histological evaluation and molecular profiling of the polyps. (Kuipers et al., 2015). Currently the CDC (Center for Disease Control and Prevention) recommends that regular screening every 10 years should begin at the age of 50 and continue until age 75 (Sabatino et al., 2015). Although there has been significant progress in reducing colorectal cancer incidence due to an increase in screening awareness, colonoscopy remains invasive, expensive, and is not always available to the population at large. Therefore, molecular biomarkers are critically required for accurate identification of patients, who may be at risk of developing colorectal cancer. In my dissertation I describe a novel tool that can be utilized for early detection/diagnosis of transformed colonic epithelium. Utilizing such a tool may help to reduce healthcare costs and improve screening compliance.

Although overall incidence rates have decreased, mortality rates remain high among colorectal cancer patients (~40-50% of patients eventually die from the disease) due to metastatic progression of the disease (Kuipers et al., 2015) (Siegel et al., 2014a). Added to this challenge is the recently observed trend of increasing incidence of late stage colorectal cancers in patients younger than the age of 50 (Abdelsattar et al., 2016; Bailey et al., 2015; Siegel et al., 2014a), due to unknown etiologies. Treatment regimens vary depending on the stage and progression of the cancer. Currently the standard of

treatment includes colectomy, chemotherapy, and radiation therapy (Mundade et al., 2014). Great strides have been made to minimize surgical trauma and preserve function following colectomy and to increase the efficacy of chemotherapeutic agents by targeting colon cancer associated oncogenic pathways, while decreasing their off target effects. However, due to the diverse molecular pathogenesis of colorectal cancer, each patient responds differently to targeted therapy/surgery (van Geel et al., 2015). Each colorectal cancer patient is unique, therefore more precise and individualized treatment strategies must be developed to improve treatment outcomes and prolong the survival of patients (van Geel et al., 2015). Based on previous findings in the cancer stem cell area, and results of my dissertation studies, I strongly believe that diagnosing/targeting cancer stem cells may offer improved methods of prevention and treatment of colorectal cancers, in the future.

## 1.2 STEM CELLS

### 1.2.1 Normal Stem Cells

As part of the final stages of digestion, the colon functions to extract energy and water from solid waste before excretion from the body (Milla, 2009; Peterson and Artis, 2014). The colonic epithelium is a dynamic structure undergoing continuous regeneration (Milla, 2009; Peterson and Artis, 2014). It is composed of epithelial cells arranged in a single layer which fold into finger-like invaginations known as crypts (Milla, 2009; Peterson and Artis, 2014). There are multiple cell types responsible for mediating the function of the colonic epithelium including the well-studied absorptive, enteroendocrine, mucus-secreting (goblet), and Paneth cells (D'Angelo and Wicha, 2010; Ong et al., 2014; Sancho et al., 2015). Absorptive cells in the colonic crypts function to absorb nutrients and water from waste, mucus secreting cells secrete mucus to protect the surface of the crypts/colonic mucosa, enteroendocrine cells control gut physiology, including motility,

by secretion of hormones, and Paneth cells function to control the microbial environment of the mucosa (D'Angelo and Wicha, 2010; Sancho et al., 2015). Recent reports describe three additional cell types that exist in the colonic epithelium including M (microfold or membranous) cells, cup cells, and tuft cells (Gerbe et al., 2012; Ong et al., 2014). M cells function as an interface between the luminal crypt and the underlying immune cells, however the precise functions of cup and tuft cells remains unknown (Gerbe et al., 2012; Ong et al., 2014). Tuft cells are specialized cells, in which the function is not yet known, in the upper 1/3$^{rd}$ of the colonic crypts (Gerbe et al., 2012), and are also labeled as brush cells due to its unique architecture, as described below.

Stem cells are present at the base of the crypts within a stem cell niche and are responsible for the constant cellular turnover and regeneration of the crypt after injury, as described above (Barker, 2014; Sancho et al., 2015). Stem cells are capable of self-renewal by asymmetric proliferation in which one cell reverts back into a quiescent stem cell, and the second daughter cell continues to divide and function as progenitor cells (located in the lower 1/3$^{rd}$ of the crypt), which go on to differentiate into all the functional cell lineages of colonic crypts, as described above (Barker, 2014; Sancho et al., 2015). Differentiated cells are located in the upper 2/3rd region of the crypts (Barker, 2014; Sancho et al., 2015). As cells move upwards through the crypt they lose their proliferating potential and differentiate into mature cells before going through apoptosis and sloughing off into the lumen as demonstrated in **Figure 1.3** (Barker, 2014; Sancho et al., 2015).

**Figure 1.3: Organization of Cells in the Colonic Crypt**

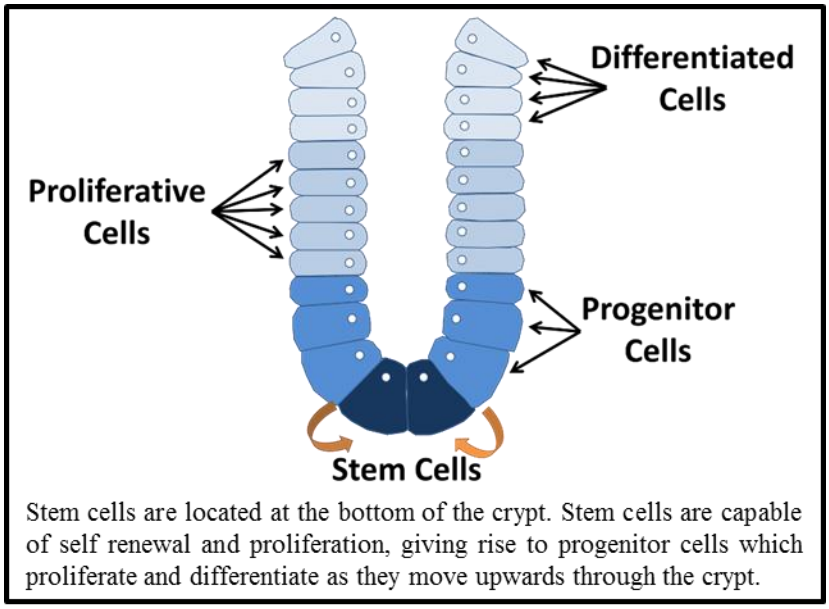


Stem cells are located at the bottom of the crypt. Stem cells are capable of self renewal and proliferation, giving rise to progenitor cells which proliferate and differentiate as they move upwards through the crypt.

Balancing self-renewal, proliferation, and differentiation is required for maintaining epithelial homeostasis. Disruption of this balance in hyperproliferating crypts due to either idiopathic reasons, or in response to elevated levels of specific growth factors (as described above), or inflammatory diseases, can result in uncontrolled growth leading to transformation of stem cells and cancer (Ong et al., 2014; Sancho et al., 2015; Singh et al., 2012). In order for stem cells to maintain normal homeostasis, cells must remain within their protective niche (Sancho et al., 2015). The stem cell niche is a tightly regulated microenvironment in which regulatory and secretory factors allow for crosstalk between epithelial cells and their surrounding mesenchymal cells (Sancho et al., 2015). If signaling pathways crucial for regulating stem cell homeostasis (WNT, Notch, Hedgehog, BMP (Bone Morphogenic Protein), etc.) are disrupted, due to either inflammation/cytokines/altered microbiomes and/or elevated growth factor mediated signaling pathways (such as EGFs, IGFs and progastrins, (Singh et al., 2012; Vigneri et al., 2015)), normal stem cells can become transformed, and lose the ability to asymmetrically divide and produce multi-lineage differentiated cells (Bu and Cao, 2012;

Cherciu et al., 2014; Wang et al., 2015b). Our laboratory has described significant phenotypic differences in isogenic normal and transformed epithelial stem cells (Sarkar et al., 2012), and my studies further suggest expression of cancer specific isoforms of stem cell markers in cancer stem cells (O'Connell et al., 2015), which may allow us, in the future, to diagnose and target colon cancer stem cells.

The vast majority of studies on intestinal stem cells have focused on small intestinal stem cells, especially in rodent models, while human colonic stem cells, remain less well characterized (Zeuner et al., 2014). Within the small intestine two functionally distinct populations of intestinal stem cells have been identified including LGR5+ crypt base columnar stem cells and +4 quiescent stem cells, both of which are reportedly capable of self-renewal and giving rise to differentiated cells (Barker, 2014; Ong et al., 2014). However the contribution of each population towards maintenance of the colonic crypt remains under debate (Ong et al., 2014) (Barker, 2014). The LGR5+ population of stem cells actively proliferates and has been described to be the stem cell population responsible for intestinal homeostasis (Barker, 2014; Ong et al., 2014; Zeuner et al., 2014). The +4, BMI+ (BMI1 Proto-Oncogene, Polycomb Ring Finger), quiescent stem cell population has been described as a reserve stem cell population that is capable of regeneration of the LGR5+ population in case of injury (Barker, 2014; Ong et al., 2014; Zeuner et al., 2014).

To date, the colonic stem cell populations remain largely undefined, and a lack of robust stem cell markers makes studying colonic stem cells, challenging. Therefore, identification of stem cell markers remains crucial to studying stem cell biology. A number of cell surface markers have been proposed to be putative stem cell markers including (but not limited to) LGR5/CD44/DCLK1 (Abetov et al., 2015; Cherciu et al., 2014). As described above, LGR5+ cells have been reported to be actively proliferating stem cells capable of generating all epithelial lineages of the colonic crypt (Barker et al., 2007). CD44+ cells are involved in cell growth, differentiation, and survival and are

capable of both self-renewal and differentiation (Cherciu et al., 2014). DCLK1+ cells are located at the +4 position in normal intestinal crypts and have been described as the quiescent stem cells, capable of giving rise to intestinal lineages (Chandrakesan et al., 2015; May et al., 2008; May et al., 2009). Although several putative stem cell markers have been reported to identify normal colonic stem cells, colon cancer stem cells express many of the same markers as intestinal normal stem cells (Barker, 2014; Cherciu et al., 2014; Hirsch et al., 2014; Nakanishi et al., 2013). Similarly in isogenic clones of normal and transformed embryonic epithelial cells, while we described significant phenotypic differences between normal and transformed stem cells, both expressed a similar array of stem cell markers (Sarkar et al., 2012), therefore targeting cancer stem cells while sparing normal stem cells remains a challenge. However, results of my studies may, for the time, help us identify cancer stem cells, as further discussed in Chapters 2-4.

### 1.2.2 Cancer Stem Cells

Although significant progress has been made to understand the complex molecular pathogenesis of colorectal cancer, the precise origin of colorectal cancer cells remains unclear. Colorectal tumors are a heterogeneous population of cells, composed of different cell types including epithelial, stromal, endothelial and infiltrating white blood cells, all of which enhance tumor growth and progression by influencing physiological, metabolic, and morphological changes (Abetov et al., 2015; Cherciu et al., 2014; Kuipers et al., 2015; Wang et al., 2015b). Currently there are two models describing the process of colorectal tumorigenesis and resulting tumor heterogeneity, these include the stochastic and cancer stem cell models (Abetov et al., 2015; Cherciu et al., 2014; Kozovska et al., 2014; Wang et al., 2015b). The stochastic model suggests that all cells have equal capacity of initiating and promoting tumor growth while the cancer stem cell model suggests that only a small subset of tumor cells have tumorigenic/metastatic

potential, and these transformed cancer stem cells are responsible for maintenance of tumor growth and metastasis (Abetov et al., 2015; Cherciu et al., 2014; Kantara et al., 2014; Kozovska et al., 2014; Singh et al., 2012; Wang et al., 2015b).

Currently several hypotheses have been proposed to describe the origin of cancer stem cells (Bu and Cao, 2012; Cherciu et al., 2014; Sarkar et al., 2012; Wang et al., 2015b). We know that normal colonic stem cells are unspecialized, multipotent cells that have the ability to self-renew through limitless division. Each daughter cell can either revert back to a stem cell or commit to differentiation (Barker, 2014; Ong et al., 2014; Sancho et al., 2015). The first hypothesis suggests that normal stem cells become mutated/deregulated leading to transformation and formation of malignant stem cells that are capable of proliferating continuously, giving rise to a tumor (Bu and Cao, 2012; Cherciu et al., 2014; Wang et al., 2015b). The second hypothesis suggests that a differentiated cell can acquire "stem cell like" capabilities resulting in a cell with a dedifferentiated stem cell phenotype capable of limitless replication (Bu and Cao, 2012; Cherciu et al., 2014; Wang et al., 2015b). Both hypotheses are illustrated in **Figure 1.4**.

**Figure 1.4: Origin of Cancer Stem Cells**

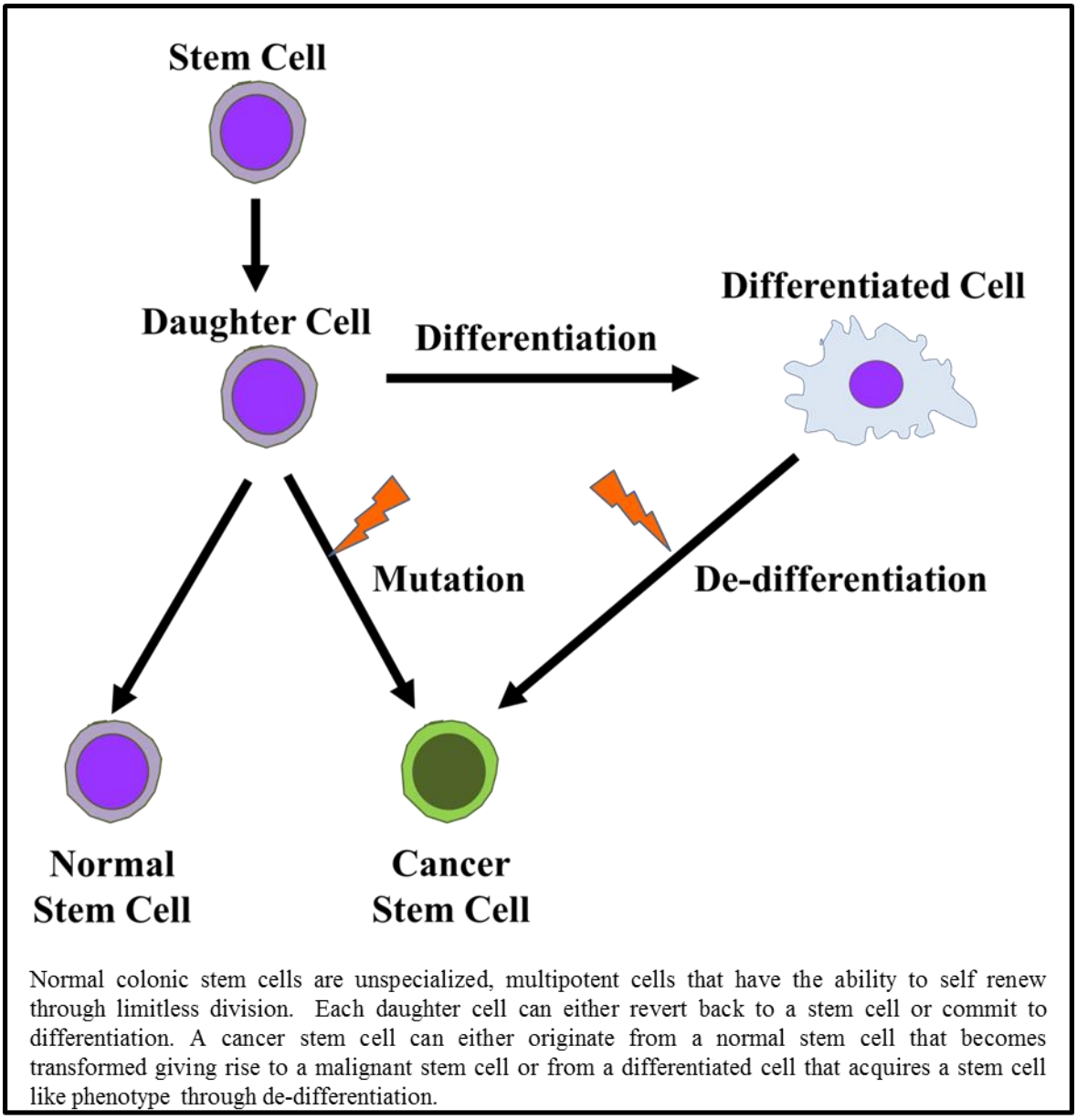


Normal colonic stem cells are unspecialized, multipotent cells that have the ability to self renew through limitless division. Each daughter cell can either revert back to a stem cell or commit to differentiation. A cancer stem cell can either originate from a normal stem cell that becomes transformed giving rise to a malignant stem cell or from a differentiated cell that acquires a stem cell like phenotype through de-differentiation.

Cancer stem cells maintain their capacity to self-renew and differentiate into various cell types; however they are also capable of giving rise to malignant cells and maintaining the whole tumor cell population (Abetov et al., 2015; Kantara et al., 2014; Kozovska et al., 2014; Singh et al., 2012). Due to their limitless replicative capacity, cancer stem cells can divide and feed the growth of tumors (Abetov et al., 2015; Kantara et al., 2014; Kozovska et al., 2014; Singh et al., 2012). However, other cancer cells

within the tumor only have a limited replicative capacity and can only contribute to the bulk of the tumor but not to tumor maintenance (Abetov et al., 2015; Kantara et al., 2014; Kozovska et al., 2014; Singh et al., 2012). Cancer stem cells are potently tumorigenic and have the capability of generating a tumor from a limited number of cells (as few as $10^2$ cancer stem cells have been reported to be capable of generating a tumor) (Abetov et al., 2015; Kantara et al., 2014; Kozovska et al., 2014; Sarkar et al., 2012). Cancer stem cells are also believed to be resistant to chemotherapy and radiation (Cherciu et al., 2014; Kantara et al., 2014; Singh et al., 2012; Wang et al., 2015b). Even though the bulk of the colonic tumor mass is reduced in response to standard current therapies, a small population of cancer stem cells survive treatment and are capable of re-growing as primary/metastatic tumors, resulting in relapse of the disease, as recently reported by our laboratory (Kantara et al., 2014), and confirmed by others (Cherciu et al., 2014; Wang et al., 2015a). This process is demonstrated in **Figure 1.5**.

**Figure 1.5: Targeting of Cancer Stem Cells**

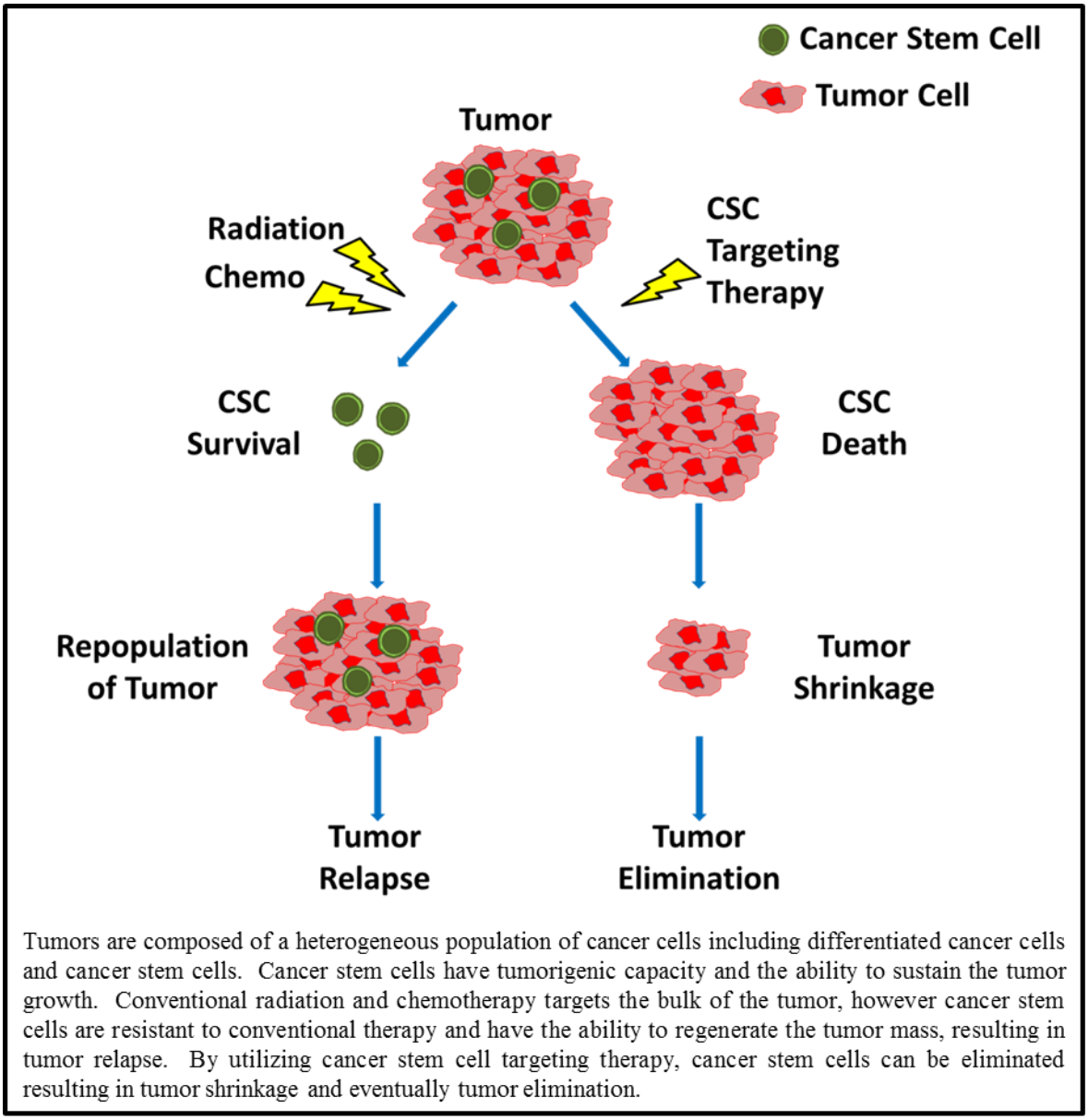


Tumors are composed of a heterogeneous population of cancer cells including differentiated cancer cells and cancer stem cells. Cancer stem cells have tumorigenic capacity and the ability to sustain the tumor growth. Conventional radiation and chemotherapy targets the bulk of the tumor, however cancer stem cells are resistant to conventional therapy and have the ability to regenerate the tumor mass, resulting in tumor relapse. By utilizing cancer stem cell targeting therapy, cancer stem cells can be eliminated resulting in tumor shrinkage and eventually tumor elimination.

It has been proposed that by targeting cancer stem cells, relapse may be eliminated, thus highlighting the importance of identifying and targeting cancer stem cells for treating cancers (Cherciu et al., 2014; Kantara et al., 2014; Singh et al., 2012; Wang et al., 2015b). As described above, several putative stem cell markers, including LGR5, CD44, and DCLK1, have been reported as markers of normal colonic stem cells; however colon cancer stem cells express many of the same markers (Barker, 2014;

Cherciu et al., 2014; Hirsch et al., 2014; Nakanishi et al., 2013; Sarkar et al., 2012), therefore targeting cancer stem cells while sparing normal stem cells remains a challenge. In my dissertation I evaluated stem cell marker DCLK1 and its function as a normal and cancer stem cell marker.

## 1.3 DCLK1 (DOUBLECORTIN-LIKE KINASE 1)

### 1.3.1 DCLK1 in the brain

Human DCLK1 was first described as a putative kinase that was similar to doublecortin in structure but contained an additional calmodulin-dependent kinase-like domain (Omori et al., 1998). The *DCLK1* gene was mapped to chromosome 13q13 and multiple splice variants were described (Omori et al., 1998). Omori et al. demonstrated that variants containing doublecortin (DCX) domains were predominantly expressed in fetal brain tissue while variants that lacked DCX domains were expressed in both fetal and adult brain, therefore it was concluded that the DCX containing variants appeared to be specific to fetal life, playing a role in nervous system development while the variants that lacked the DCX domain appeared to be important in maintaining the mature nervous system (Omori et al., 1998). A subsequent report confirmed the chromosomal location of *DCLK1* and described protein domains of the full length DCLK1 variant (Sossey-Alaoui and Srivastava, 1999). Based on the homology of *DCLK1* to genes expressing only the doublecortin domain, or $Ca^{2+}$/calmodulin dependent kinase (CAMK), a possible role of DCLK1 in cortical development was described (Sossey-Alaoui and Srivastava, 1999).

Importantly, it was reported that the C-terminal kinase domain of DCLK1 lacked calmodulin binding motifs, unlike CAMK, and Silverman et al. concluded that DCLK1 is not calmodulin dependent but instead maybe a cAMP-dependent protein kinase (Silverman et al., 1999). The genomic structure of the full length transcript of *DCLK1* was mapped and individual exon/intron borders were characterized (Matsumoto et al.,

1999). The mouse homolog of DCLK1 was cloned in mouse brains, and expression patterns of variants were evaluated (Burgess et al., 1999). Mouse DCLK1 variants followed a similar pattern of expression to human DCLK1 in fetal and adult brains, and a role in cortical development of mice was suggested (Burgess et al., 1999); however, later studies have questioned the conservation of DCLK1 functions in mouse vs. human brains (Tuy et al., 2008). Expression patterns of DCX and DCLK1 were evaluated in the developing neocortex and it was determined that temporal and spatial patterns of the two proteins were similar, suggesting that both may be involved in a common signaling pathway regulating neuronal migration (Mizuguchi et al., 1999).

Full length DCLK1 was found to co-localize and co-purify with microtubules, while variants lacking the DCX domain remained cytoplasmic and did not appear to co-localize with microtubules, demonstrating that the DCX domains were indeed responsible for microtubule association (Burgess and Reiner, 2000). In primary cultures of embryonic mouse neurons, DCLK1 was shown to co-localize with microtubules in the growth cones of post-mitotic neurons (Burgess and Reiner, 2000). An additional report demonstrated full length DCLK1 was expressed in migrating neuronal populations and was capable of associating with microtubules to stimulate polymerization of tubulin and formation of microtubule structures (Lin et al., 2000). DCLK1 association with microtubules appeared to be a dynamic process and overexpression of full length DCLK1 resulted in microtubule bundling in cell lines and primary neuronal cells (Lin et al., 2000). Lin et al., also demonstrated that the kinase domain of the full length protein remained functional (Lin et al., 2000) in primary neurons. In a later report, Burgess et al., reported that full length DCLK1 was cleaved by calpain resulting in release of the kinase domain from the microtubule binding DCX domain (Burgess and Reiner, 2001). The cleaved kinase domain was structurally similar to the variants lacking DCX domains, previously described (Omori et al., 1998). Omori et al., concluded that localization of the DCLK1 kinase domain in neurons was regulated by calcium responsive cleavage by the

enzyme calpain (Burgess and Reiner, 2001). An extensive study of the differential expression and activity of mouse DCLK1 variants highlighted the complexity of neuronal function and regulation (Burgess and Reiner, 2002). Although the presence of an alternative promoter was eluded to, only splice variants were evaluated with regards to the roles played by the variants in migrating neurons (Burgess and Reiner, 2002).

By identifying the crystal structure of the DCX domains of doublecortin and DCLK1 (Kim et al., 2003b), the Kim et al., demonstrated that the N-terminal end of the DCX domain only binds to assembled microtubules, while the C-terminal DCX domain can bind to both microtubules and un-polymerized tubulin (Kim et al., 2003a). The crystal structure of full length DCLK1 has yet to be resolved, and although two potential regulatory domains of the C-terminal kinase domain have been identified (Shang et al., 2003), substrates and regulators of DCLK1 have remained elusive, and DCLK1 has been termed an **"orphan kinase"**. These gaps in our knowledge remain, and there is thus a need to conduct additional studies to help tease out the specific functions of the two main domains and overall role of DCLK1 variants.

Utilizing a differential protein screen of developmental and mature neuronal tissues, Shu et al., identified DCLK1 as a microtubule-associated protein that was highly expressed in the neocortex and cerebellum during active neurogenesis and it was found to regulate spindle formation during mitotic division (Shu et al., 2006). DCLK1 was also reported to play a key role in axonal projection formation across the midline of migrating cortical neurons (Koizumi et al., 2006) and radial neuronal migration to the cerebral cortex (Friocourt et al., 2007). Knockdown of *DCLK1* gene resulted in disruption of most radial processes in early corticogenesis (Vreugdenhil et al., 2007), once again demonstrating an important role of DCLK1 in neuronal migration and neurogenesis. DCLK1 was shown to be a critical regulator of dendritic development by promoting dendritic growth by enhancing microtubule binding and suppression of synapse maturation (Shin et al., 2013).

Thus, key roles of DCLK1 in neurogenesis, neuronal migration, cortical development, and dendrite growth, have all been well established, but differences in the specific role, if any, of the many variants remains unknown. More recently, a possible role of DCLK1 in human memory and cognitive functions, and in anxiety related behavior of mice was investigated. It was demonstrated that inheritable markers in specific regions of the human *DCLK1* gene influenced cognitive traits such as verbal memory, general cognition, and IQ score (Le Hellard et al., 2009). Overexpression of a DCLK1 variant, lacking the DCX domains in mice, resulted in a more anxious behavioral phenotype as demonstrated in an elevated plus maze assay (Schenk et al., 2010). Thus, the vast amount of work done with DCLK1 in the brain strongly suggests that DCLK1 plays a critical role in neurogenesis, neuronal biology and normal neuronal functions. Recent findings also suggest a possible important role of DCLK1 in tumorous growths as described below.

### 1.3.2 Neuroblastomas and DCLK1

A possible important role of DCLK1 in maintaining tumorous growths was first learned from experiments with neuroblastomas. Co-localization of DCLK1 with mitotic spindles in dividing neuronal precursors was observed (Vreugdenhil et al., 2007), Vreugdenhil et al. evaluated subcellular localization of DCLK1 (and its variants). Several cell lines were evaluated, and surprisingly it was found that only neuroblastoma cell lines endogenously expressed DCLK1, and silencing of DCLK1 resulted in disruption of mitotic spindles and cell cycle arrest at the prometaphase (Vreugdenhil et al., 2007).

As a continuation of these studies, the Verissimo et al. mined data from multiple microarray datasets that contained data from ~20,000 neuroblastoma samples and their normal controls (Verissimo et al., 2010), and discovered that variants of DCLK1 were expressed at significantly higher levels in neuroblastoma tissues, as compared to normal

neuronal tissues (Verissimo et al., 2010), confirming the earlier results with neuroblastoma cell lines In a mouse neuroblastoma cell line, DCLK1 was silenced and changes in gene expression were analyzed (Verissimo et al., 2010). Using pathway analysis, the Verissimo et al. identified significant loss in gene expression related to cell cycle, oxidative stress, and apoptosis pathways, in cells down regulated for DCLK1 expression compared to isogenic control clones (Verissimo et al., 2010). Using a variety of cell growth/death assays, it was confirmed that DCLK1 silencing lead to an inhibition of proliferation and an induction of apoptosis in both human and mouse neuroblastoma cell lines (Verissimo et al., 2010). Because DCLK1 is specifically expressed in proliferative neuroblasts, and silencing resulted in an inhibition of proliferation and an induction of apoptosis of neuroblastoma cell lines, it was suggested that DCLK1 represented a target for the treatment of neuroblastomas (Verissimo et al., 2010). The role of DCLK1 in neuroblastoma was later reviewed (Verissimo et al., 2011) and the Verissimo et al., proposed that DCLK1 represented a potential molecular target that exhibited high specificity and low toxicity for neuroblastoma treatment.

Knockdown of DCLK1 in combination with a current neuroblastoma treatment was evaluated (Verissimo et al., 2012). Treatment with microtubule-destabilizing agent, vinca alkaloids (VAs), resulted in high toxicity and drug resistance (Verissimo et al., 2012). By combining DCLK1 knockdown with lower doses of VAs, cells were sensitized to VA treatment, resulting in inhibition of proliferation and induction of apoptosis, while decreasing toxicity of VA treatment (Verissimo et al., 2012).

In a recent study, it was reported that inhibiting a DCLK1 variant, that contained only the DCX domains but lacked the protein kinase domain, resulted in inhibition of cell proliferation of neuroblastoma cell lines *in vitro* and a delay in neuroblastoma tumor development *in vivo* (Verissimo et al., 2013).

Once an important role of DCLK1 in maintaining growth of neuroblastoma tumors was established, a role of DCLK1 in a number of different cancers, including

colorectal (Chandrakesan et al., 2014; Duckworth et al., 2013; Hammond et al., 2015; Jin et al., 2009; Kantara et al., 2014; Kantara et al., 2015; Kwatra et al., 2013; Li and Bellows, 2013; May et al., 2008; Neradugomma et al., 2014; Ponnurangam et al., 2012; Singh et al., 2012; Vedeld et al., 2014; Westphalen et al., 2014; Weygant et al., 2014), pancreatic (Bailey et al., 2013; Delgiorno et al., 2014; May et al., 2010; Mohammed et al., 2015; Ponnurangam et al., 2015; Qu et al., 2015; Rao et al., 2015; Sureban et al., 2011a; Sureban et al., 2013; Sureban et al., 2014; Weygant et al., 2014), esophageal (Souza et al., 2008; Vega et al., 2012; Whorton et al., 2015), breast (Haakensen et al., 2011; Liu et al., 2015; Oliveras-Ferraros et al., 2014), lung (Powrózek et al., 2015), rectal (Ikezono et al., 2015), renal (Weygant et al., 2015), and hepatocellular (Sureban et al., 2015) cancers has been demonstrated, by either using mouse models of investigation or human tumor samples. For the purposes of my dissertation, I evaluated the role of DCLK1 in colorectal cancer and colorectal cancer stem cells.

### 1.3.3 DCLK1 as a Normal Intestinal Stem Cell Marker

The first evidence of DCLK1 as a gastrointestinal stem cell marker came in 2006 (Giannakis et al., 2006). Using differential gene expression microarray analysis of gut epithelial progenitor cells and whole stomach epithelium, DCLK1 was identified as a potential stem cell marker (Giannakis et al., 2006). DCLK1+ cells did not express neuroendocrine differentiation biomarker, CgA (Glycoprotein Hormones, Alpha Polypeptide), and did not stain for BrdU (Bromodeoxyuridine) (Giannakis et al., 2006). Small intestinal crypts of normal mice contained a single DCLK1+ cell that was positioned directly below the transit amplifying cell population (at the +4 position), therefore DCLK1 was suggested to be a marker of adult gut stem cells (Giannakis et al., 2006).

Later reports confirmed that DCLK1 was expressed at the +4 position in the small intestinal crypts of mice, and that DCLK1 and stem cell marker MSI-1 (Musashi RNA-Binding Protein 1) were co-localized, suggesting that DCLK1+ cells likely represented a subset of MSI-1+ cells (May et al., 2008). In $APC^{min}$ mice, DCLK1+ cells were negative for PCNA (Proliferating Cell Nuclear Antigen) staining suggesting that DCLK1+ cells were not proliferating, therefore DCLK1+ cells were termed quiescent stem cells (May et al., 2008). In normal appearing crypts, DCLK1+ cells exhibited membrane β-catenin staining while in a crypt adenoma, DCLK1+ cells exhibited nuclear β-catenin (May et al., 2008). May et al., suggested that DCLK1 and nuclear β-catenin could distinguish adenoma stem cells from normal intestinal stem cells and DCLK1 and PCNA staining could distinguish an adenoma stem cell from a proliferative adenoma cell (May et al., 2008).

In a later study, May et al., reported that DCLK1+ cells were primarily located at the +4 position of the crypt within the small intestine of mice, and DCLK1+ cells did not co-localize with other putative stem cell markers (such as LGR5) or any other marker of differentiated intestinal cells, such as ChrA (Carcinoembryonic Antigen), pPTEN (Phosphatase and Tensin Homolog), pAKT (V-akt Murine Thymoma Oncogene Homolog 1), somatostatin, secretin, suggesting that DCLK1 marked a unique +4 quiescent stem cell population (May et al., 2009). Using PCNA staining to assess the proliferative status of LGR5+ and DCLK1+ stem cell populations, LGR5+ cells were found to be PCNA+ while DCLK1+ cells were PCNA-, suggesting that LGR5 does indeed represent actively proliferating stem cells while DCLK1 represents the +4 quiescent stem cell population (May et al., 2009). DCLK1 was found to be expressed on the cell surface and when cells were sorted and grown in suspension culture, DCLK1+ cells formed spheroids *in vitro* while DCLK1- cells lacked the ability to form spheroids, providing proof of stemness of DCLK1+ cells (May et al., 2009). When injected into nude mice, DCLK1+ cells grew as organoids and gave rise to intestinal lineages and

produced gland like structures, providing proof of pluripotency of DCLK1+ cells (May et al., 2009). May et al., determined that DCLK1 is not only a marker of +4 quiescent stem cells, but also DCLK1+ cells could be distinguished from actively proliferating LGR5+ cells, providing a reliable marker to distinguish the two stem cell population located within the small intestine (May et al., 2009).

In an author reply, the identification of DCLK1 as a putative stem cell marker was challenged (Gerbe et al., 2009). In the reply, Gerbe et al., stated that DCLK1 expression did not identify stem cells within the intestinal epithelium but instead identified differentiated tuft cells or brush cells. Gerbe et al., questioned the authenticity of a stem cell marker that identified non-proliferating cells; a well-established feature of stem cells (Gerbe et al., 2009). To determine the identity of DCLK1+ tuft cells, Gerbe et al., co-stained the cells with known markers of differentiated cell types (Gerbe et al., 2009). DCLK1 was not found to co-stain with any known markers of the well-studied absorptive, enteroendocrine, goblet, or Paneth cells; however, DCLK1 did co-stain with COX1 (Cytochrome C Oxidase Subunit 1), COX2 (Cytochrome C Oxidase Subunit 2), villin, and α-tubulin, all molecular markers of differentiated tuft cells (Gerbe et al., 2009). Therefore Gerbe et al., concluded that DCLK1 was not a quiescent stem cell marker but was instead a bona fide tuft cell marker (Gerbe et al., 2009). In a subsequent report, Gerbe et al., described DCLK1+ cells as postmitotic, short lived differentiated tuft cells that are derived from LGR5+ active cycling columnar base stem cells (Gerbe et al., 2011). These conflicting reports rendered it difficult to establish the functional significance of DCLK1as a stem cell marker, in normal biology of mouse intestines.

In another attempt to elucidate the potential function of DCLK1, DCLK1+ cells were FACS sorted from intestinal epithelium of Dclk-CreER;Rosa26-YPF mice (Chandrakesan et al., 2015). DCLK1+ cells were found to be positive for BMI1 and negative for LGR5, while DCLK1- cells were positive for LGR5 and negative for BMI1, suggesting that DCLK1+ cells represented the +4, BMI+, quiescent stem cell populations

and DCLK1- cells represented the LGR5+ actively proliferating columnar base stem cell populations (Chandrakesan et al., 2015). The DCLK1+ cell population also demonstrated increased expression of pluripotency genes (OCT4/POU5F1 (Octamer-Binding Transcription Factor 4/ POU Class 5 Homeobox 1), SOX2 (SRY (Sex Determining Region Y)-Box 2), NANOG (NANOG Homeobox), and KLF4 (Kruppel-Like Factor 4)) and pro-survival genes (ATM (ATM Serine/Threonine Kinase), Tp53, and survivin) (Chandrakesan et al., 2015). DCLK1 +/- cell populations were grown as enteroids (colonies grown on soft agar) to determine the self-renewal properties (determined by enteroid formation) of the two populations (Chandrakesan et al., 2015). Both DCLK1 +/- cell populations grew enteroids; however only 1-2% of the DCLK1- population displayed the ability to self-renew, as compared to 18% of the DCLK1+ population (Chandrakesan et al., 2015), which is supported by our findings with embryonic stem cells (Sarkar et al., 2012). Authors (Chandrakesan et al., 2015), concluded that DCLK1+ cells represent the quiescent and pluripotent cells, which maintain survival and have self-renewal capabilities, and are reminiscent of the +4 quiescent intestinal stem cell populations, that these May et al., had initially described in 2008 and 2009 (May et al., 2008; May et al., 2009). We and others had similarly described the presence of DCLK1+ cells at the +4 position in the colonic crypts of mice, which were responsive to the growth effects of progastrins, resulting in hyperproliferation of the colonic crypts of these mice (Jin et al., 2009; Sarkar et al., 2011). Hence it is possible that both the +4 cells in the stem cell niche, and the tuft cells, located towards the upper end of colonic crypts, function as a reserve of stem cell populations, capable of regenerating the active cycling stem cell population in case of injury. However, most of these findings are based on mouse models and remain to be confirmed in humans.

### 1.3.4 DCLK1 as a Cancer Stem Cell Marker

As described above, initial reports demonstrated that there were variable expression patterns of DCLK1 between normal epithelium and the epithelium of $APC^{min}$ mice and DCLK1 expression was found to be increased in adenomas (May et al., 2008). May et al., had suggested that DCLK1/nuclear β-catenin staining could distinguish adenoma stem cells from normal intestinal stem cells and that DCLK1+ cells may be the origin of neoplastic cells (May et al., 2008). As described above, our laboratory and other investigators had also described the expression of DCLK1 in mouse colonic crypts at the +4 position, and reported a significant elevation in the expression of DCLK1 in the +4 cells, in response to progastrins (Jin et al., 2009; Sarkar et al., 2011); progastrins have been described by many investigators as potent mitogens for colonic epithelial cells and colon cancers (discussed in a recent review article (Singh et al., 2012). Increased expression of progastrin in the intestines of Fabp-PG (Fatty Acid Binding Protein) mice was reported by our laboratory to induce hyperproliferation of colonic crypts (Singh et al., 2000b) and increase colon carcinogenesis in mice in response to AOM (Azoxymethane) ± DSS (Dextran Sodium Sulfate) (Cobb et al., 2004; Singh et al., 2000a). Progastrin overexpression (in hGAS/+ mice, expressing high levels of progastrin in the livers of the mice) led to increased expression of DCLK1 in the colonic crypts of the mice; upon treatment with AOM (a colon carcinogen), and colonic tumorigenesis was significantly enhanced in the hGAS/+ mice, in relation to increased expression of DCLK1 in the tumors of the mice (Jin et al., 2009). We further reported that DCLK1 expression was increased in an annexin A2 (non-canonical receptor for progastrins, (Singh et al., 2007)) dependent manner in response to autocrine and endocrine progastrins (Sarkar et al., 2011). Using isogenic clones of human embryonic epithelial cells (HEK293), which either expressed the control vector (HEKC) or the mutant gastrin gene vector, for over-expressing full length progastrin (HEKmGAS clones), we reported that

both the relative levels and the proportion of cells expressing DCLK1 were significantly increased in HEKmGAS cells compared to that in HEKC cells (Sarkar et al., 2011). Treatment of cells with annexin A2 siRNA reversed stimulatory effects of autocrine PG on DCLK1,suggesting that annexin A2 was required for mediating stimulatory effects of progastrins on expression levels of DCLK1 in target cells, which was confirmed *in vivo*, using annexin A2 knock down mice (Sarkar et al., 2011). Taken together, these reports indicated that DCLK1 likely mediated growth factor and co-carcinogenic effects of progastrins on colon carcinogenesis in mice.

An important role of DCLK1 in maintaining growth/proliferative potential of human colon cancer cells became evident in studies with human colon cancer cells. Downregulation of DCLK1 expression in human colon cancer cells (HCT116 cells) using siRNA against all isoforms of DCLK1, resulted in the loss of growth of HCT116 tumor xenografts in athymic nude mice (Kantara et al., 2014; Sureban et al., 2011b), which was reported to be mediated by loss of Let-7a miRNA (Sureban et al., 2009). Utilizing isogenic clones of embryonic epithelial cells, HEKC and HEKmGAS cells (described above), DCLK1+ cell populations were found to be significantly upregulated in progastrin overexpressing HEKmGAS cells, when grown either as mono layer cultures in 2D or as 3D growths *in vitro* (spheroids) or *in vivo* (xenografts), compared to that of HEKC cells (Sarkar et al., 2012). Downregulation of DCLK1 in HEKC and HEKmGAS cells (using DCLK1 siRNA), resulted in significant downregulation of proliferation in both cell types, demonstrating that DCLK1 likely plays a functional role in maintaining proliferation of both normal and cancer stem cells (Sarkar et al., 2012). More recently, we reported that a subset of DCLK1+ cells were resistant to inhibitory effects of chemopreventive/chemotherapeutic agents, including the dietary agent, curcumin (Kantara et al., 2014). Our studies demonstrated that unlike control (non-treated cells), which formed secondary spheroids within 4 days of re-plating, curcumin treated cells formed secondary spheroids much later, by ~ 30-45 days, suggesting that curcumin

treatment delayed re-growth of secondary spheroids, but did not avoid relapse (Kantara et al., 2014). On further investigation, we discovered that a subset of cancer stem cells, expressing DCLK1, underwent autophagic survival and regrew as spheroids, while other stem cells, expressing LGR5, did not, but the sub–set of DCLK1+ that re-grew, gave rise to LGR5+ cells as well (Kantara et al., 2014). Curcumin treatment of primary HCT116 spheroids resulted in complete attenuation of LGR5 expression, however low levels of DCLK1 continued to be expressed, suggesting that a subset of DCLK1+ cells are resistant to curcumin treatment (Kantara et al., 2014). Co-treatment with DCLK1 siRNA and curcumin eliminated relapse/re-growth of spheroids from colon cancer stem cells, while treatment with LGR5/CD44 siRNAs were not as effective (Kantara et al., 2014). These findings strongly support a critical role of DCLK1 in colon cancer stem cell biology (Kantara et al., 2014). Effects of DCLK1 ± curcumin on HCT116 cells grown *in vitro* in 2D or 3D culture or *in vivo* as xenografts were evaluated (Kantara et al., 2014). DCLK1 siRNA was more effective than curcumin against growth of HCT116 cells both *in vitro* and *in vivo* suggesting that DCLK1 plays a functional role in the proliferative/tumorigenic potential of cancer stem cells (Kantara et al., 2014). DCLK1 downregulation combined with curcumin treatment was significantly more effective both *in vitro* and *in vivo*. When treated with a combination of DCLK1 siRNA and curcumin, primary HCT116 spheroids did not form secondary spheroids, suggesting that the combined regimen resulted in augmentation of both apoptotic and autophagic cell death pathways, and complete elimination of cancer stem cells, thus resulting in loss of relapse in the time frame of our studies (Kantara et al., 2014). These findings highlighted a critical role of DCLK1, not only as a marker of cancer stem cells, but also as a functional protein, which may be playing an important role in maintaining the cancer stem cell population in human colonic tumors.

Recent literature also strongly implicates a possible important role of DCLK1 in mouse colon tumorigenesis. The role of DCLK1 as a normal/cancer stem cell marker was evaluated in normal mouse intestines and during intestinal tumorigenesis using DCLK1$^{creERT2/+}$ knock in mice (Nakanishi et al., 2013). Using tamoxifen induced cre-mediated lineage tracing of both the small intestine and the colon (via Dclk1$^{Cre/ERT2/+}$; Rosa26R mice), it was demonstrated that DCLK1+ cells originated in the lower crypt and that these DCLK1+ cells migrated up along the length of the crypt and were eventually shed within a couple of weeks (Nakanishi et al., 2013). BrdU incorporation was not observed in DCLK1+ cells located within the normal intestine; therefore the Nakanishi et al., concluded that DCLK1 did not mark stem cells in the normal intestine but instead marked postmitotic cells (Nakanishi et al., 2013). In Dclk1$^{CreERT2/+}$; Rosa26R; Apc$^{Min/+}$ mice, lineage tracing analysis showed that polyps were positive for LacZ labeled cells (Nakanishi et al., 2013). When tracing LacZ expression within the polyps over time, labeled cells (~3.1% of tumor cells) were initially located at the polyp base and then expanded daily to eventually occupy the whole polyp within 5-7 days (Nakanishi et al., 2013). Based on the data, Nakanishi et al., concluded that DCLK1 only marked cancer stem cells, that formed tumors, and that DCLK1 expression was required for forming intestinal adenomas (Nakanishi et al., 2013). Using Dclk1$^{CreERT2/+}$; Rosa26R; Apc$^{Min/+}$; Rosa26$^{iDTR/+}$ mice, diphtheria toxin mediated ablation of DCLK1+ cells resulted in regression of the tumors without damaging the normal intestine, based on which the Nakanishi et al., concluded that ablation of DCLK1+ cancer stem cells resulted in tumor regression without causing damage to the normal intestine or normal intestinal stem cells. DCLK1+ cells in mutant mice have similarly been described as colon cancer initiating cells, giving rise to colonic tumors, especially in mice with non-functional APC, and in the presence of an inflammatory stimulus (DSS induced colitis) (Westphalen et al., 2014). Westphalen et al., however suggested that DCLK1+ tuft cells were required for initiating colonic tumors in mice, giving credence to possible importance of tuft cells in

colon carcinogenesis in mice. Taken together, these reports demonstrate that DCLK1+ cells function as colon cancer stem cells that are capable of giving rise to intestinal tumors in mice.

Due to the reported specificity of DCLK1 to cancer stem cells, our laboratory evaluated the use of DCLK1 as a novel circulating cancer stem cell marker (Kantara et al., 2015). As described above, cancer stem cells are believed to be resistant to chemotherapy and radiation and a small sub-set of cancer stem cells can survive chemotherapeutic treatment and re-grow as primary/metastatic tumors, resulting in relapse of the disease (Cherciu et al., 2014; Kantara et al., 2014; Wang et al., 2015b). Therefore utilizing circulating cancer stem cells to screen patients for risk of relapse or for presence of metastatic disease, could significantly improve clinical outcomes. Using DCLK1 and several additional cancer stem cell markers/epithelial cell markers, we reported a novel approach for detecting cancer stem cells in circulation (Kantara et al., 2015).

### 1.3.5 Epigenetic Silencing of DCLK1

In recent years, the 5' promoter of the human *DCLK1* gene was reported to be hypermethylated in a number of cancers, including colorectal cancers (Andresen et al., 2012; Marie Vedeld et al., 2014; Powrózek et al., 2015; Vedeld et al., 2014). Hypermethylation of the 5'promoter of the human *DCLK1* gene was first described in cholangiocarcinoma (Andresen et al., 2012). The promoter of the human *DCLK1* gene displayed high methylation frequency in primary cholangiocarcinoma tumors when compared to normal mucosal controls (Andresen et al., 2012). A subsequent report demonstrated that the 5'promoter of the human *DCLK1* gene was hypermethylated in ~82% of colorectal cancer samples with minimal methylation of the promoter in normal mucosal samples (Vedeld et al., 2014). In a panel of 74 cancer cell lines derived from 15

different tissues, Vedeld et al. observed a negative correlation of 5'promoter of *DCLK1* methylation and DCLK1 expression, suggesting that when the promoter of *DCLK1* is hypermethylated, DCLK1 expression is silenced (Vedeld et al., 2014). Treatment of 20 cell lines with epigenetic drug, 5-aza-2'deoxycytidine (5-Aza), resulted in a significant increase in DCLK1 expression, again demonstrating that reduced gene expression of DCLK1 in human cancer cell lines was a result of hypermethylation of the DCLK1 promoter (Vedeld et al., 2014). Vedeld et al. suggested that methylation of the DCLK1 promoter represented a novel epigenetic biomarker for colorectal cancers (Vedeld et al., 2014). It has since been demonstrated that the 5'promoter of the human *DCLK1* gene is hypermethylated in gastric (Marie Vedeld et al., 2014), pancreatic (Marie Vedeld et al., 2014), and lung cancers (Powrózek et al., 2015).

### 1.3.6 DCLK1 Overexpression in Colorectal Cancers

Although the 5'promoter of *DCLK1* gene has been reported to be epigenetically silenced in human colon cancer cell lines and human colorectal cancers, high levels of DCLK1 protein have been reported throughout literature (Gagliardi et al., 2012a; Kantara et al., 2014; Sureban et al., 2009). Using human cancer tissue microarrays, staining of DCLK1 was found to be increased in human colorectal cancer specimens as compared to normal colonic mucosa (Sureban et al., 2009). DCLK1 expression was also observed in a variety of human colon cancer cell lines (Sureban et al., 2009). In a large scale patient study, DCLK1 was found to be frequently expressed in colorectal neoplasia and patients whose tumors had high levels DCLK1 staining had an increased risk for cancer specific mortality, suggesting that DCLK1 expression may be associated with poor prognosis (Gagliardi et al., 2012a). Reports from our laboratory demonstrated that colon cancer cell lines express high levels of DCLK1 in both 2D and 3D cultures (Kantara et al., 2014). These reports demonstrate that although the 5' promoter of the human *DCLK1* gene is

epigenetically silenced, DCLK1 protein levels remain elevated in human colon cancer cell lines and colorectal cancers.

### 1.3.7 Human *DCLK1* gene

The *DCLK1* gene encodes a member of the protein kinase family and doublecortin family. The *DCLK1* gene is located on the long arm of chromosome 13 at position 13 (13q13) (Omori et al., 1998; Sossey-Alaoui and Srivastava, 1999). Previous names of DCLK1 include DCAMKL1 and KIAA0369 (as described in the NCBI database). According to the NCBI database, four transcript variants of human DCLK1 have been described; additional isoforms have been described in the SwissProt database. The full length transcript of isoform 1 (NM_004734.4) is 8463 bps, contains 18 exons, and results in a 729 aa peptide with a molecular mass of 82.224 kDa (NP_004725) (as described in the NCBI database). DCLK1 isoform 2 (NM_001195415.1) is 7592 bps, and lacks several 5' exons as compared to isoform 1. The resulting transcript contains 14 exons and results in a 422 aa peptide (NP_001182344.1) that has a shorter N-terminus as compared to isoform 1. DCLK1 isoform 3 (NM_001195416.1) is 7518 bps and lacks several 5' exons as compared to isoform 1. Isoform 3 also lacks a coding exon in the 3' region that results in a frame-shift, as compared to isoform 1. The resulting transcript contains 13 exons and results in a 433 aa peptide (NP_001182345.1), that has a shorter N-terminus and different C-terminus as compared to isoform 1. DCLK1 isoform 4 (NM_001195430.1) is 5432 bp and shares only one exon with isoform 1. The resulting transcript contains 3 exons and results in a 56 aa peptide (NP_001182359.1) that has a shorter N-terminus and C-terminus as compared to isoform 1. Key differences in the 4 transcripts of human DCLK1 are highlighted in **Figure1.6**.

**Figure 1.6: Nucleotide Sequence Homology between the Transcripts for the 4 Isoforms of Human DCLK1**

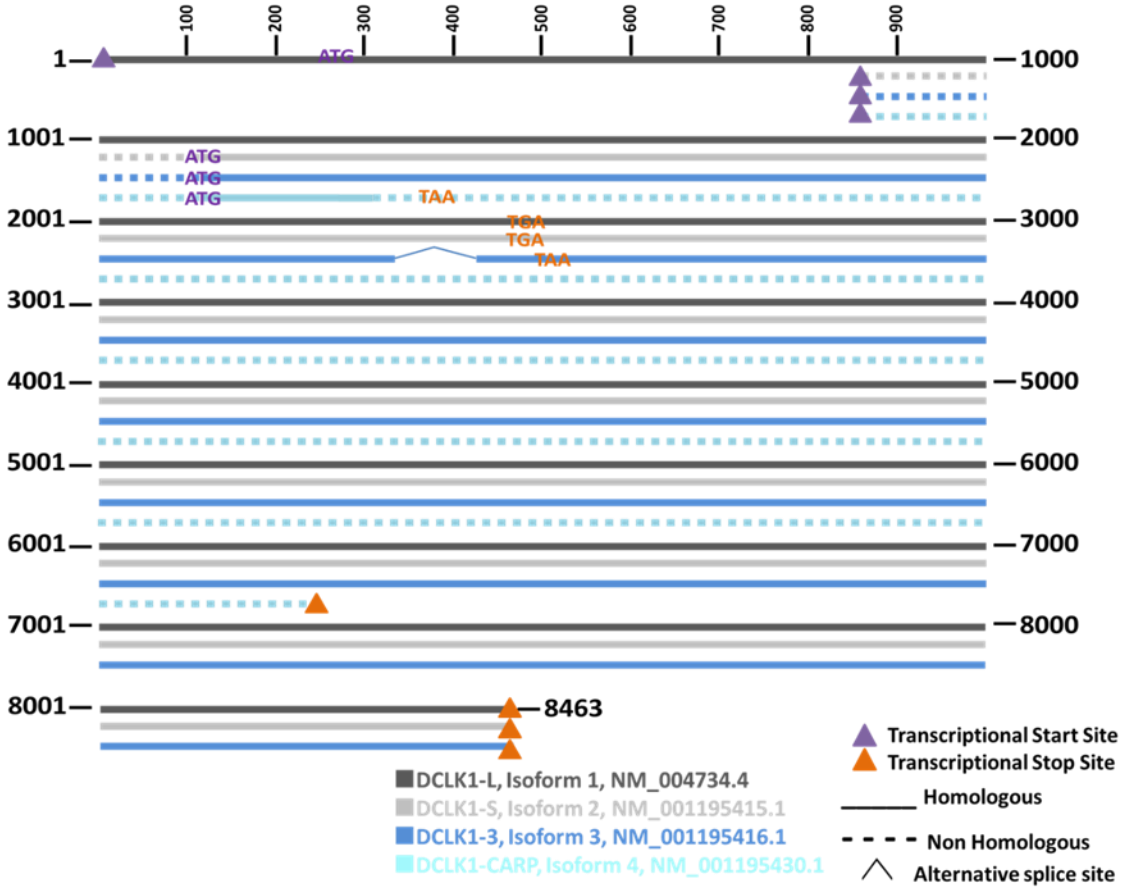


Diagrammatic representation of the nucleotide sequence homology of isoforms of *hDCLK1* as described in the NCBI database. Dark Grey=isoform 1 (NM_004734.4), Light Grey=isoform 2 (NM_001195415.1), Dark Blue=isoform 3 (NM_001195416.1), and Light blue=isoform 4 (NM_001195430.1). Solid lines=homologous regions, dashed lines=non-homologous regions, arrow head=alternative splice site, purple triangles=transcriptional start sites, orange triangles=transcriptional stop sites. Start (purple) and stop (orange) codons are indicated. The coding region of *DCLK1* isoform 1 starts at bp 284 (from exon 2) and ends at bp 2473 (exon 18). The 5' untranslated region includes exon 1 and part of exon 2.The 3' untranslated region includes most of exon 18 (3301 bp). The coding region of *DCLK1* isoform 2 starts at base 334 (of exon 1), and ends at base 1602 (in exon 14). Isoform 2 consists of 14 exons. The 5' untranslated region includes most of exon 1 (352 bp) and 3' untranslated region includes most of exon 14 (3301 bp). The coding region of *DCLK1* isoform 3 (DCLK1-3) starts at base 334 (in exon 1) and ends at base 1635 (exon 14). Isoform 3 is transcribed from 13 exons rather than 14 exons. Isoforms 2 and 3 represent splice variants of transcripts originating in the same exon of the gene that are different by 74 bps, since isoform 2 contains sequences that are transcribed from an additional exon compared to isoform 3.The coding region of *DCLK1* isoform 4 starts at base 334 and ends at base 504, and is transcribed from 3 exons. The 5' untranslated region is homologous between isoforms 2, 3, and 4. The 3' untranslated region of isoform 4 includes most of exon 3.

### 1.3.8 Human DCLK1 Protein

The full length DCLK1 isoform 1 contains: two N-terminal doublecortin domains which bind microtubules, a C-terminal serine/threonine kinase domain with homology to Ca2+/calmodulin dependent protein kinases and a middle serine/proline rich domain, which mediates protein interactions (Sossey-Alaoui and Srivastava, 1999). The serine/proline-rich domain has been shown to mediate multiple protein-protein interactions. Isoforms 2 and 3 retain the protein kinase domain but lack the doublecortin domains, compared to isoform 1. Isoform 4 lacks both the doublecortin domains and the protein kinase domain. A diagrammatic representation of the 4 isoforms of DCLK1 is provided in **Figure 1.7**.

**Figure 1.7: Diagrammatic Representation of Protein Domains of the hDCLK1 Isoforms**

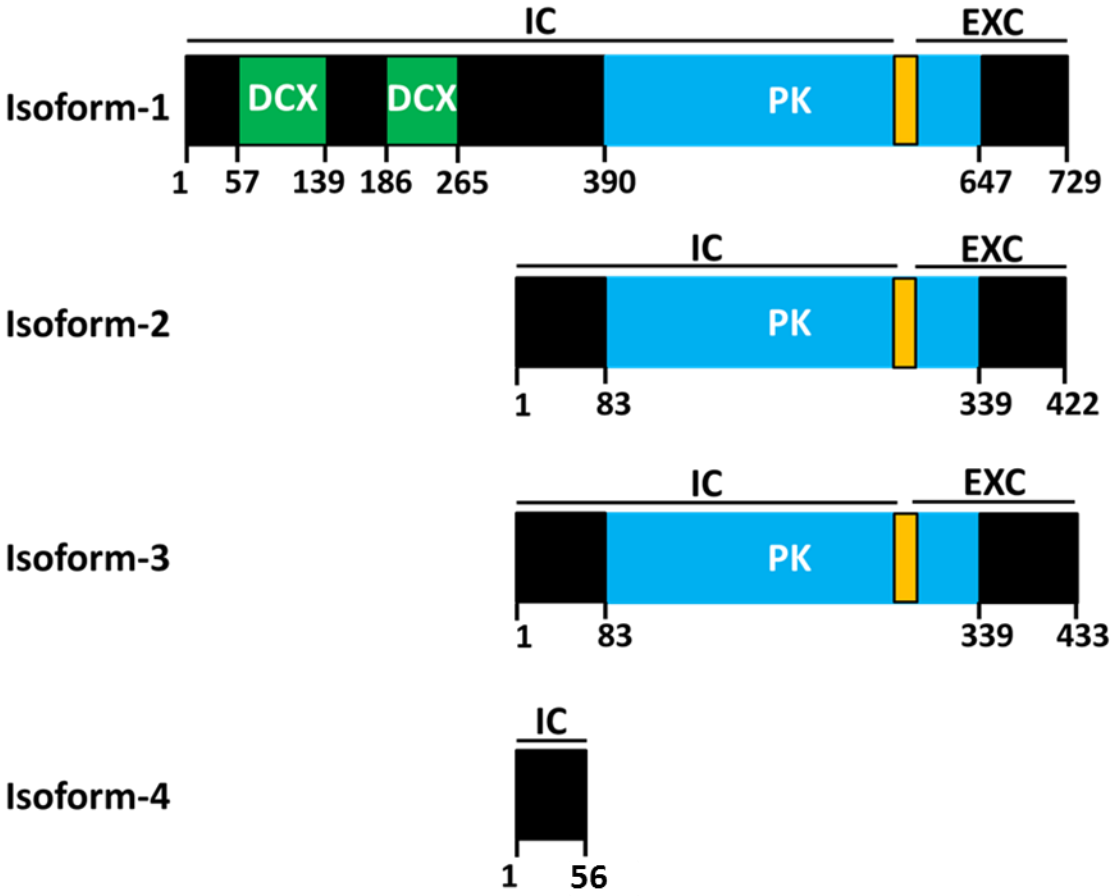


DCX=doublecortin domain; PK=calmodulin-like proten kinase domain; IC=intracellular domains of the indicated isoforms; EC=extracellular domain of the four isoforms; Isoforms are named according to the NCBI database. The total number of amino acids in the four isoforms, as it relates to the various domains is indicated. Briefly, isoform 1 consists of two doublecortin domains, a protein kinase domain, and a serine/proline rich area. The transmembrane domain was present only in isoforms 1, 2 and 3. Protein analysis using PSORT (www.psort.nibb.ac.jp.org), University of Tokyo, Japan) suggested only one transmembrane domain (located between 568-584 AAs of isoform 1). However, protein analysis using BCM Search Launcher (http://searchlauncher.bcm.tmc.edu/multi-align/multi-align.html), Baylor College of Medicine, Houston, TX) identified 2 transmembrane domains (located between AA 534-559 and 568-585). Isoforms 2 and 3 retain the protein kinase domain but lack the doublecortin domains, compared to isoform 1. Isoform 4 lacks both the doublecortin domains and the protein kinase domain. It is important to note that SwissProt describes a 740 AA isoform (015075-1) that is not described in the NCBI database. This 740 AA protein consist of two doublecortin domains, a protein kinase domain, and a serine/proline rich area.

Various names have been used to describe the different human isoforms of DCLK1 throughout literature. Isoform 1 (NP_004725.1) has been previously referred to as DCLK1-long-B (Engels et al., 2004), KIAA0369AS (Omori et al., 1998), DCK-α1 (Pal et al., 2011), and DCLK1-β (Burgess and Reiner, 2002). Isoform 2 (NP_001182344.1) has been previously referred to as DCLK1-short-B (Engels et al., 2004), DCK-β1 (Shang et al., 2003), and KIAA0369-BS (Omori et al., 1998). Isoform 3 (NP_001182345.1) has been previously referred to as DCLK1-short-A (Engels et al., 2004), DCK-β2 (Shang et al., 2003), KIAA0369-BL (Omori et al., 1998), and CPG16 (Burgess and Reiner, 2002; Silverman et al., 1999). Isoform 4 has been previously referred to as ania-4 (Berke et al., 1998) and CARP (Vreugdenhil et al., 1999). The 740 AA protein described in the SwissProt database (015075-1) has been referred to as DCLK1-long-A (Engels et al., 2004), KIAA0369-AL (Omori et al., 1998), DCK-α2 (Shang et al., 2003), and DCLK α (Burgess and Reiner, 2002).

### 1.3.9 Mouse DCLK1

Although the human *DCLK1* gene is conserved in mouse, chimpanzee, dog, chicken, and C. elegans, the associated transcripts described for each species differs significantly, demonstrating the complexity of this gene in different species. There are 7 mouse DCLK1 isoforms described in the NCBI database. A diagrammatic representation of the 7 transcripts described is provided in **Figure 1.8**.

**Figure 1.8: Diagrammatic Representation of the Transcripts for the 7 Mouse Isoforms of *DCLK1***

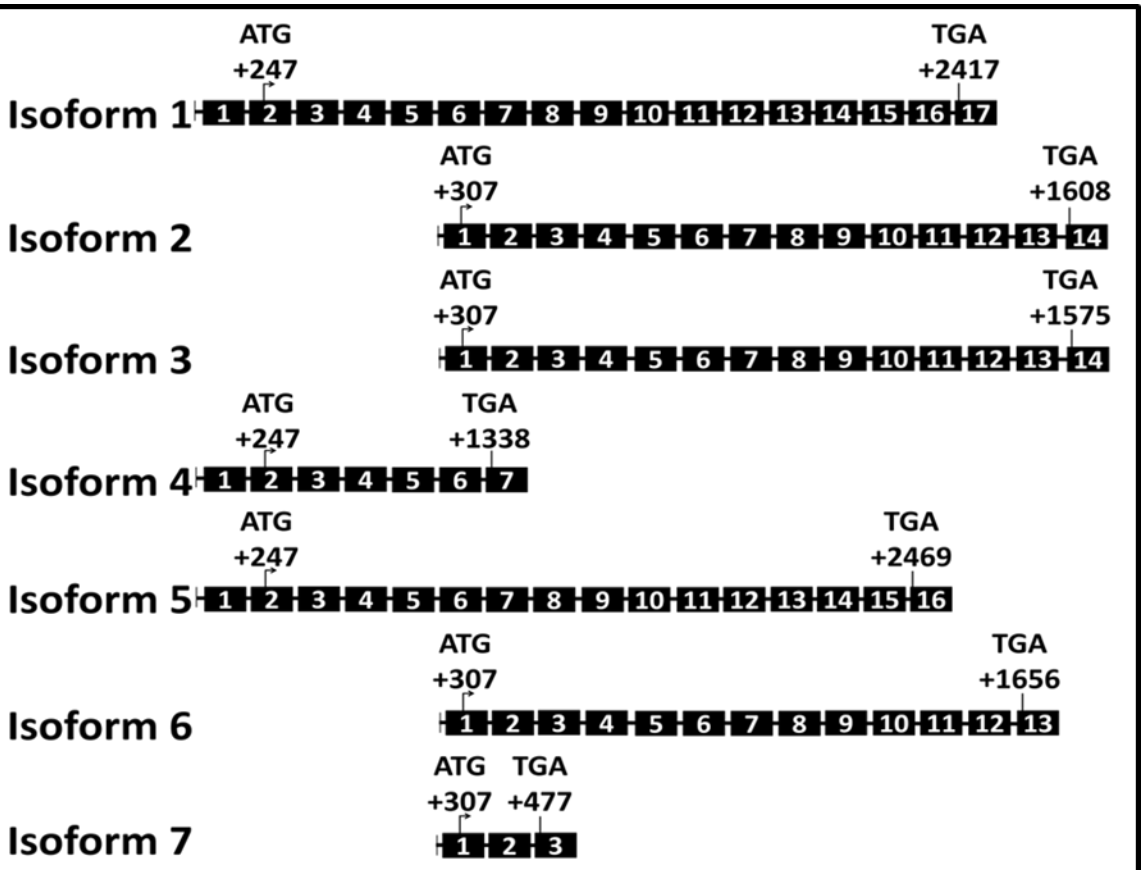


Isoform 1 (NM_019978.3), Isoform 2 (NM_001111051.1), Isoform 3 (NM_001111052.1), Isoform 4 (NM_001111053.1), Isoform 5 (NM_001195538.1), Isoform 6 (NM_001195539.1), and Isoform 7 (NM_001195540.1). Transcriptional start sites (ATG) and end sites (TGA) are shown. Numbered boxes=exons; lines between boxes=introns. Introns and Exons are not drawn to scale.

There are 7 unique resulting polypeptides in mice. In brief, isoform 1 consists of two doublecortin domains and a protein kinase domain. Isoforms 2 and 3 retain the protein kinase domain but lack the doublecortin domains, compared to isoform 1. Isoform 4 retains the doublecortin domains but lacks the protein kinase domain. Isoform 5 consists of two doublecortin domains and a protein kinase domain. Isoform 6 lacks the doublecortin domains and consists of a protein kinase domain. Isoform 7 lacks both the doublecortin and protein kinase domains. A diagrammatic representation of the protein domains present in the 7 mouse isoforms is provided in **Figure 1.9**.

**Figure 1.9: Diagrammatic Representation of the Protein Domains Present in the 7 Isoforms of mouse DCLK1**

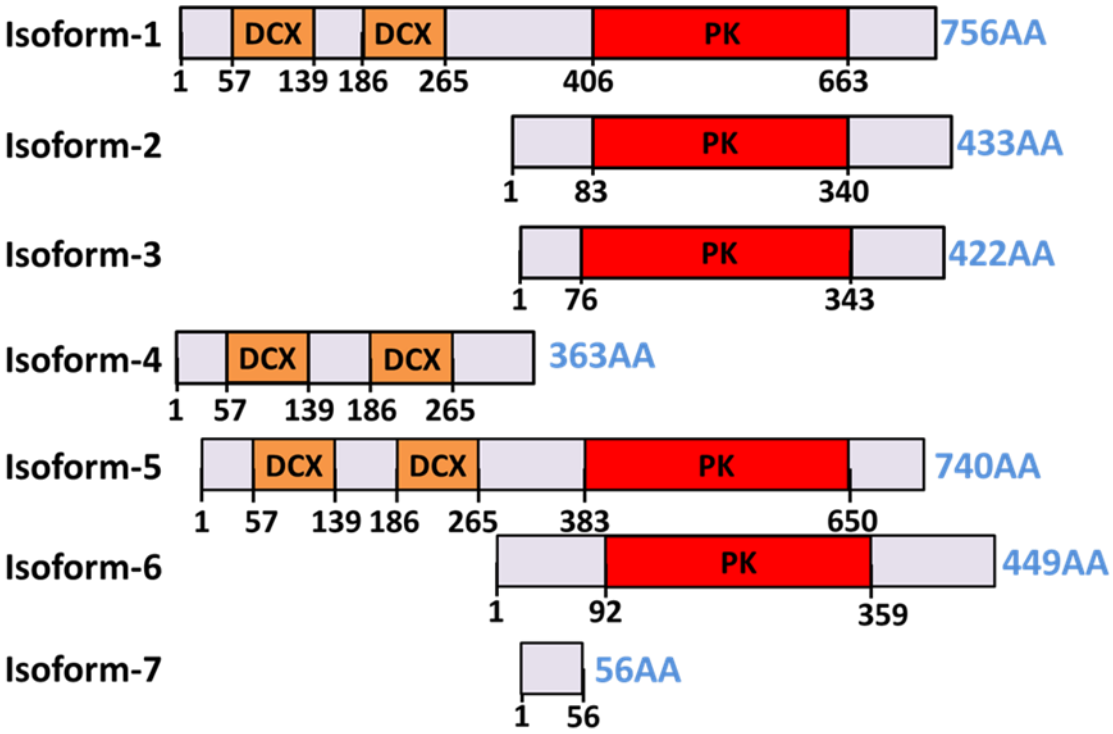


DCX=doublecortin domain; PK=calmodulin-like protein kinase domain. The total number of amino acids in the seven isoforms, as it relates to the various domains is indicated. Briefly, isoform 1 consists of two doublecortin domains and a protein kinase domain. Isoforms 2 and 3 retain the protein kinase domain but lack the doublecortin domains, compared to isoform 1. Isoform 4 retains the doublecortin domains but lacks the protein kinase domain. Isoform 5, like, isoform 1, consists of two doublecortin domains and a protein kinase domain. Isoform 6 lacks the doublecortin domains and consists of a protein kinase domain. Isoform 7 lacks both the doublecortin and protein kinase domains.

# Chapter 2: Epigenetic Changes and Alternate Promoter Usage by Human Colon Cancers for Expressing DCLK1-Isoforms: Clinical Implications

***This chapter is a copy of a manuscript published from our laboratory in 2015 (O'Connell et al., 2015). I retain copyright permission by Nature Publications to reuse the full article for dissertations purposes.**

## 2.1 INTRODUCTION

CRC is the third most prevalent cancer in the U.S. (Siegel et al., 2014a). Several cancer stem cell (CSC) markers have been identified in the literature, including CD44, CD133 (Prominin 1), Lgr5 and DCLK1 (Kemper et al., 2012; May et al., 2008; Nakanishi et al., 2013; Ning et al., 2013; Nomura et al., 2015; Park et al., 2012; Schepers et al., 2012). Besides marking cancer cells, CD44, CD133 and Lgr5 have been reported to play an important functional role in either maintaining the growth of cancer cells and/or in aiding in the metastatic potential of cells (Kemper et al., 2012; Nomura et al., 2015; Park et al., 2012; Schepers et al., 2012). More recently, an equally important role of DCLK1 has been implicated in colon tumorigenesis in mice (Bailey et al., 2014; Nakanishi et al., 2013; Westphalen et al., 2014) and in maintaining the proliferative potential of human colon cancer cells (Kantara et al., 2014; Sarkar et al., 2012; Sureban et al., 2011b). We recently reported that a subset of DCLK1+CSCs were resistant to inhibitory effects of chemopreventive/chemotherapeutic agents, and down-regulation of DCLK1 combined with chemoprevention was required for eliminating CSCs, *in vitro* and *in vivo*, and for avoiding relapse (in terms of re-formation of tumorospheres from treated cells) (Kantara et al., 2014). These findings highlighted a possible critical role of DCLK1 in maintaining the growth of human colon cancer cell lines. Isogenic clones of human

embryonic epithelial cells (HEK293), that were either poorly tumorigenic (HEKC) or highly metastatic (HEKmGAS), expressed identical set of markers, including DCLK1 (Sarkar et al., 2012). Thus, specifically targeting CSCs has remained a challenge.

*DCLK1*-gene encodes a member of the protein kinase family and doublecortin family (Lin et al., 2000), and was initially reported to play a critical role in neurogenesis and neuronal migration (Lin et al., 2000; Shin et al., 2013; Shu et al., 2006). Thereafter, investigators reported an important role of DCLK1 in dictating cognitive behavior of mice and humans (Le Hellard et al., 2009; Shin et al., 2013). A possible important role of DCLK1 in maintaining tumorous growths was first learned from experiments with neuroblastomas (Verissimo et al., 2013; Verissimo et al., 2010). Only in the past 7-8 years, epithelial expression of DCLK1 was described for the first time in mouse gastric epithelial cells (Giannakis et al., 2006), and Giannakis et al. speculated that DCLK1 was being expressed by gastric stem cells. Soon afterwards, laboratories of Drs. Anant and Houchen published several papers describing DCLK1 expression in mouse intestinal crypts (May et al., 2008; May et al., 2009). Expression of DCLK1 in mouse colonic crypts was reported to be significantly elevated in response to progastrins (potent mitogens for colonic epithelial cells and colon cancers) (Jin et al., 2009; Sarkar et al., 2011), which correlated with hyperproliferation of the crypts (Sarkar et al., 2011)). DCLK1 is also expressed by acetylated Tuft cells, located in the upper 1/3 of colon crypts in mice (Gerbe et al., 2009). More recently, a critical role of DCLK1+Tuft cells was reported in developing colon and pancreatic tumors/lesions in mutant mouse models of carcinogenesis (Bailey et al., 2014; Westphalen et al., 2014). DCLK1+Tuft cells were reported to be required for restitution of mouse intestinal crypts in response to inflammation/radiation damage (May et al., 2014). Thus the literature so far strongly implicates a possible important role of DCLK1 in mouse colon tumorigenesis and in maintaining the growth of human colon cancers.

A number of long (~80-82KDa) and short (~45-50KDa) isoforms of DCLK1 have been identified in human brains/neurons (Burgess and Reiner, 2002; Engels et al., 2004; Omori et al., 1998; Shang et al., 2003; Silverman et al., 1999) (as described in 1.3.8). The ~82kDa long isoform of DCLK1 contains: two N-terminal doublecortin domains which bind microtubules, a C-terminal serine/threonine kinase domain with homology to Ca2+/calmodulin dependent protein kinases and a middle serine/proline rich domain, which mediates protein interactions. The nomenclature for the various isoforms has remained a source of confusion, and differs even in the Swiss-Prot and NCBI databases (as described in **Figure 1.3.8**). The specific biological function of the various isoforms has remained undefined. The shorter isoforms lack the two N terminal doublecortin domains. Thus the 3D structure of the long vs. short isoforms can be expected to be quite different, with perhaps some differences in their biological interactions and activities. The longer isoforms and their splice variants are presumed to be transcriptionally regulated by the 5'(α)-promoter. The origin of the shorter isoforms has not been investigated to a significant extent, but a 3' promoter (termed β-promoter (Shang et al., 2003)), downstream of the 5'(α)-promoter has been implicated in transcribing shorter-transcripts of DCLK1 in mouse cerebellum (Pal et al., 2011). In at least one report, a TATA box containing promoter was described in the IntronV of *DCLK1*-gene in neuronal cells (Le Hellard et al., 2009). Unlike in neuronal cells, possible expression of different isoforms of DCLK1 by normal colonic epithelial cells and colon cancer cells/tumors has not been investigated to-date. The presence of DCLK1 protein in epithelial cells has so far been mainly examined by using commercial antibodies, generated against the common C terminal end of long and short isoforms (Femia et al., 2013; Kantara et al., 2014; Kikuchi et al., 2010; May et al., 2008; Sarkar et al., 2012). Thus the specific isoform(s) being expressed by epithelial cells has remained unknown.

In studies with mutant mouse models of colon/pancreatic tumorigenesis, described above, a bac construct, expressing either the reporter gene or diphtheria toxin,

downstream of the 5'promoter of mouse *DCLK1* gene was used, suggesting that 5'promoter remains functional during intestinal/pancreatic tumorigenesis in mice, which likely results in the expression of the long isoform(s). The 5'promoter of h*DCLK1*-gene, however, was recently reported to be hypermethylated in hCRCs, by several investigators (Marie Vedeld et al., 2014; Vedeld et al., 2014), suggesting the possibility that the 5'promoter of h*DCLK1*-gene may be epigenetically silenced in hCRCs. This intriguing possibility was examined in the current studies, and our findings suggest that hypermethylation of 5'promoter is an early event during adenoma-carcinoma sequence of colon carcinogenesis in humans, unlike mice. Our data also suggests an absence of expression of long transcripts/isoforms in all 15 human colon cancer cell lines (hCCCs) screened to-date by us, suggesting epigenetic silencing of the 5'(α)-promoter due to its hypermethylation in hCRCs, as described above.

Even though the 5'(α)-promoter is epigenetically silenced in hCCCs/hCRCs, high levels of DCLK1 protein have been reported in hCCCs/hCRCs (Gagliardi et al., 2012a; Gagliardi et al., 2012b; Kantara et al., 2014; Singh et al., 2012). The discrepancy between the reported presence of DCLK1 protein in hCCCs/hCRCs, and hypermethylation/epigenetic silencing of 5'(α)-promoter, suggests the possibility that hCCCs/hCRCs may be utilizing an alternate promoter for expressing alternate isoforms of DCLK1. This novel possibility was examined as described below.

*In silico* analysis of h*DCLK1* gene, led us to confirm the presence of a canonical TATA box within the β promoter located within IntronV. We report for the first time, that IntronV-(β)-promoter is used as an alternate-promoter by hCCCs/hCRCs for expressing a short transcript. Based on sequence homology, the long (L) and short (S) transcripts of DCLK1, found in normal human colon cell lines/normal human colons (hNCs) vs. hCCCs/hCRCs, respectively, were determined to be identical to isoforms 1 (NM_004734.4) and 2 (NM_001195415.1) in the NCBI data base. For the purpose of our studies we have termed the isoform 1 as DCLK1-L and the isoform 2 as DCLK1-S, to

clearly differentiate between the molecular sizes of the two isoforms. Colon tumors and normal colons from mice, on the other hand, were confirmed to only express the long isoform(s).

Transcriptional regulation of the α/β promoters in the h*DCLK1*-gene in epithelial cells remains largely unknown. Activation of β-catenin and NF-κBp65 was reported to be critically required for upregulating DCLK1 protein in response to autocrine and endocrine progastrins (Sarkar et al., 2011). We therefore conducted *in silico* analysis of the two promoters followed by promoter-reporter/ChIP assays, in the presence or absence of the known activator (progastrin), and report for the first time an important role of β-catenin binding to TCF4/LEF binding-sites for activating 5'(α)-promoter, and an important role of NF-κB binding-site for activating IntronV-(β)promoter.

In order to define pathophysiological relevance of DCLK1-S expression by hCRCs, the overall-survival of a cohort of 92 CRC patients was examined in relation to high/low expression of DCLK1-S. A clinically important finding was that high-expressers of DCLK1-S had significantly worse overall-survival, and disease free interval. DCLK1-S expression represented an independent diagnostic/prognostic marker for CRC patients.

## 2.2 MATERIALS AND METHODS

### 2.2.1 Reagents Used

Antibodies used in these studies included: anti-total-p65NF-κB, anti-β-catenin (total) (Cell Signaling Technology, Danvers, MA); anti-β-actin (total) (Sigma, St. Louis, MO); anti-DCLK1 antibody (Abcam AB31704, Cambridge, MA). Mono-specific rabbit polyclonal anti-progastrin-antibody and eukaryotic plasmid, expressing triple mutant

human gastrin gene, for overexpressing human progastrin (PG) peptide, were generated in our laboratory as previously described (Sarkar et al., 2011). Smart Pool of target-specific small interfering RNA (siRNA) and non-targeting (control) siRNA Pool were purchased from Dharmacon (Lafayette, CO). Sepharose beads and all other chemical reagents were purchased from Sigma. TissueScanTM Disease Tissue qPCR array (Catalogue Number HCRT102) for colon cancer and normal colons was purchased from OriGene (Rockville, MD). cDNA synthesis master mix was purchased from GeneDEPOT (Baker, TX). Syber green qRT-PCR kit was purchased from Bio-Rad (Hercule, CA). Promega GoTaq®green Master Mix (Maddison, WI) was used for PCR amplification, using a Thermal Cycler from Eppendorf (Hauppauge, NY). Cloning vector pGL2 was from Promega, and TOPO-TA cloning vector was purchased from Invitrogen (Grand Island, NY). Restriction enzymes and competent cells were purchased from New England BioLabs (Ipswich, MA). Transfection reagent FuGENE®6 was bought from Roche (Branford, CT), and all primers used were synthesized by Sigma.

### 2.2.2 Cell Culture

HEK293 and HCT116 cell lines were obtained from ATCC, and have been maintained in the laboratory for several years. CCD841 and CT26 cells were generously gifted to our laboratory from Dr. Carla Kantara (Department of BMB, UTMB) and Dr. Iryna Pinchuk (Department of Surgery, UTMB). CCD841 and CT26 were purchased from ATCC within the past two years, and confirmed by ATCC. CT26 cells were previously termed MC-26 mouse colon cancer cells (Siddheshwar et al., 2001). All cell lines were monitored regularly for absence of mycoplasma and HEK293 and HCT116 cell lines were confirmed to represent human epithelial cell lines with the help of Biosynthesis Company (Lewisville, TX). Stable clones of HEK293 cells were generated to overexpress either the control vector (HEKC) or a triple mutant hGAS vector, in order

to overexpress full length progastrin (PG) peptide (HEKmGAS cells), as described previously (Sarkar et al., 2012; Sarkar et al., 2011). The wild type parental cell lines (HEK293, HCT116) were cultured in DMEMF12 medium (Invitrogen, Grand Island, NY), supplemented with 10% FCS containing 1% penicillin/streptomycin in a humid atmosphere at 37°C with 5% CO2. The stable clones of HEKC and HEKmGAS cells were cultured in the same medium supplemented with 100µg/mL Geneticin (Invitrogen) under similar conditions. CCD841 and CT26 were similarly cultured using MEM (CCD841) and RPMI-1640 (CT26), media, along with supplements as described above. In addition, for screening purposes only, several panels of human colon cancer cell lines were purchased in January of 2015 from ATCC, and maintained in culture as suggested by the company.

### 2.2.3 Procurement of Samples from Normal Colonic Mucosa and Colonic Tumors of Patients

Samples of normal colonic mucosa were obtained from consented patients at the time of endoscopy for screening purposes, as per our approved IRB protocol (UTMB IRB#03-237). Normal samples were obtained only if the colons were free of adenomas (Ads) and adenocarcinomas (AdCAs), but positive for small hyperplastic (Hp) growths. Pinch biopsies of tubular adenomas (TAs) (polyps) were also obtained at the time of screening endoscopy, from patients who were positive for polyps but negative for AdCAs, as per our approved IRB Protocols; rest of the snared polyps were sent to pathology department. Samples of primary or metastatic tumors, with or without the adjoining uninvolved colonic tissue (matched paired sample) were obtained as discarded samples (as per our approved UTMB IRB protocol #91-310) from either UTMB Hospital, at time of surgery, or from Tissue Core Facility at Cancer Center, University of Alabama, as part of CHTN Program funded by NIH. All samples were collected and

flash-frozen and stored in liquid nitrogen or -80°C until analyzed. Pathology of all samples, thus obtained, was confirmed. In few experiments we also harvested tissue samples from colons, liver and brain of male FVB/N mice (2-4 month old) (Taconic, Hudson, NY) by our published methods (Cobb et al., 2004), as per our approved IACUC protocols (UTMB IACUC protocol #01-12-055). Ninety-two colorectal carcinoma tissues were used for clinical validation of DCLK1-S expression from an independent cohort, for data presented in **Fig 2.14** and **Tables 2.4 & 2.5**. These specimens were preserved immediately after surgical resection in RNA later (QIAGEN, Chartsworth, CA) and stored at -80°C until RNA extraction. The surgical samples were obtained from the Mie University Hospital, Japan, from patients enrolled during 2005 to 2011. The patients included 57 men and 35 women with a mean age of 68 years (range 37-89 years). None of the patients received chemotherapy and radiotherapy before surgery and no perioperative mortalities were observed. The primary lesion was located in the rectum in 41 patients, sigmoid colon in 19, ascending colon in 16, transverse colon in 9, and descending colon in 7. Eleven patients were diagnosed with synchronous liver metastasis. Clinicopathological findings were based on the UICC's criteria for tumor node metastasis (TNM) classification. There were 19 patients with stage I (T1-2N0M0), 30 with stage II (T3-4N0M0), and 22 with stage III (TXN1-2M0) disease. Twenty-one patients with distant metastasis were classified as having stage IV (TXNXM1) disease. Ten patients had poorly differentiated or mucinous adenocarcinoma, whereas 82 patients had well or moderately differentiated colorectal tumors. Postoperative follow-up data were obtained from all patients, and the median follow-up duration was 21.8 months (range: 1-88). All patients were followed up after the initial hospital discharge, with physical examination and tumor marker assays (CEA (Carcinoembryonic Antigen), CA19-9) performed every 1-3 months and computed tomography performed every 6 months. Endoscopic examinations were performed when necessary. Written informed consent was obtained from each patient (as per approved BCM IRB protocol #005-134). All tissues were

collected in accordance with the approved guidelines set forth by UTMB and BCM for the IRB and IACUC protocols.

### 2.2.4 Analysis of Tissue Samples and Cell Lines by RT-PCR/qRT-PCR

Total RNA was isolated from cell lines in monolayer cultures at 60-70% confluency, or from human and mouse tissues (described above), using Trizol Reagent (Invitrogen), as previously described (Siddheshwar et al., 2001; Singh et al., 2007). For qRT-PCR, the iTaq Universal SYBR Green Supermix (Bio-Rad, CA) was used as per the manufacturer's instructions. Expression levels of DCLK1-S in tissues for data presented in **Fig 2.14** were normalized against GAPDH (Glyceraldehyde-3-phophate Dehydrogenase) using the 2-ΔCt method, as previously described (Hur et al., 2014). The primer sequences used for PCR amplification of cDNA for both RT-PCR/qRT-PCR amplification of the long (L) and short (S) isoforms of DCLK1 from either human (h) or mouse (m) specimens are provided in **Table 2.1**. Electrophoresis gels presented were cropped to present all the bands observed within the range covered by the molecular markers used (between 100 bp and 1000 bp for RT-PCR data), in order to avoid primer-dimers seen towards the end of the run. Processing of the electrophoresis blots was applied equally across the entire image. Touch-up tools were not used to manipulate data. Relative band-density of electrophoresis blots was analyzed using Image J program (rsbweb.nih.gov/ij/download) and expressed as a ratio or % of β-actin in the corresponding samples.

### 2.2.5 3'-5' Primer Extension Assay

Total RNA was extracted from HCT116 and HEK293 cells as described above. Nascent RNA was isolated using a Click-iT Nascent RNA Capture Kit (Life

Technologies) according to the manufacturer's instructions. 5ug of total RNA or nascent RNA was reverse transcribed using a DCLK1-common primer (**primer 2 in Fig 2.74a**), that encompassed the nt sequence from homologous coding sequence of both long and short isoforms of DCLK1. The pool of cDNA was purified using a column (Oligo Clean & Concentrator, Zymogen). The purified cDNA was ligated to a non-mammalian adapter sequence (atgctgaaacgcgagagaaaccgcgtatcaacccc) at the 5'-end by T4 DNA ligase followed by purification of the ligated cDNA product. 2µl of the ligated product was PCR amplified using the forward adapter primer (primer 1) and reverse primer 2. Using these primers, the expected size for the DCLK1-S transcript is 498bps (NM_001195415.1) and for the DCLK1-L transcript is 1300bps (NM_004734.4) as shown in **Fig 2.7a**.

### 2.2.6 Treatment of colon cancer cells with 5-Azacytidine (de-methylating agent)

HCT116 cells were seeded in 100 mm dishes at a density of $5x10^6$ cells/dish, one day prior to drug treatment. The cells were treated with 10 µM 5-aza-2′-deoxycytidine (5-Azacytidine) on days 2 and 5 of culture. The cells were harvested on day 6 of culture and total RNA isolated. RNA was processed for measuring relative levels of DCLK1-L/S by RT-PCR.

### 2.2.7 Generation of DCLK1 5'(α)-promoter-reporter (luciferase) constructs

The long isoform (Isoform 1) of human DCLK1 is transcribed from 5'-promoter (NM_004794.4 in the NCBI data base). Based on the published promoter sequence (AL160392.12), several primer sets were designed to amplify three promoter segments of 0.5 to > 2.0Kb of the 5'-promoter from -100 through -2234 nts using genomic DNA from either normal colonic mucosa or HEK-293 cells, which gave identical results. The

primers were synthesized with the restriction sites Xho1 at 5'-end and HindIII at 3' end, in order to clone into PGL2 basic vector (**as shown in Table 2.1**). The PCR products were purified using QIAquick PCR Purification kit (Qiagen, Valencia, CA), cloned into luciferase expression vector (PGL2 basic vector, Promega, WI) and amplified in DH5α competent cells (New England Biosciences, MD). Positive colonies were processed for purifying the promoter-reporter expression plasmids; control plasmids lacked the DCLK1 5'-promoter sequences. In initial experiments promoter-reporter plasmids were transfected into HEKC/HEKmGAS and HCT116 cells, and the construct which demonstrated the maximum luciferase activity (-2234/-504 promoter-luciferase construct) (termed DCLK1-L-LUC), was used in all the studies presented in **Fig 2.8 & 2.9**. For a control experiment, the two functional TCF/LEF binding sites in the DCLK1-L-Luc construct (-1904 and -1591) were disrupted. The -1904 TCF/LEF binding site was disrupted by insertion of a Not1 restriction site and the -1591 TCF/LEF binding site was disrupted by insertion of a SacII restriction site. Using the PGL2 luciferase expression vector, the DCLK1-L-Luc-F primer (**as shown in Table 2.1**) and Not1-R primer (GCGGCCGCAGTGCTCTCACTAGAAATAGTT) were used to amplify a 5' Xho1 and 3' Not1 fragment. Not1-F primer (GCGGCCGCGATCAATATCTTAGTAATATAAAGGAAG) and SacII-R primer (CCGCGG AGTGCTCTCACTAGAAATAGTT) were used to amplify a 5' Not1 and 3' SacII fragment. SacII-F primer (CCGCGGTTGCTACTGAGAGAGTCAAACAC) and DCLK1-L-Luc-R primer (**as shown in Table 2.1**) were used to amplify a 5' SacII and 3' HindIII fragment. The 3 fragments were then ligated together and cloned into the PGL2 luciferase expression vector as described above. The mutant plasmid was confirmed and reporter-promoter assays were conducted as described above.

### 2.2.8 Generation of promoter-reporter constructs for IntronV-(β)promoter of *DCLK1*-gene

The short isoform of DCLK1 (isoform 2) (NM_001195415.1 in NCBI data base) is transcribed from a promoter within IntronV, as recently reported for neuronal cells (Le Hellard et al., 2009). Unlike the 5'-promoter, the IntronV-promoter has a consensus TATA binding site at -918nt (**Fig 2.12a**), and promoter-reporter constructs surrounding the TATA box have been shown to be active in promoter-reporter assays (Le Hellard et al., 2009). Therefore, promoter fragments within IntronV (-2503/-771 and -1348/-771) were amplified using genomic DNA, described above, and cloned into PGL2 basic vector at XhoI and HindIII sites. The purified IntronV-promoter-reporter constructs, DCLK1-Luc-S1 (-2503/-771) and DCLK1-Luc-S2 (-1348/-771), were confirmed by DNA sequencing in the recombinant Core Facility at UTMB. Primer sequences used for PCR amplification of the promoter segments are listed in **Table 2.1**.

### 2.2.9 Promoter-Reporter assays

Cells were transiently transfected with the indicated promoter-reporter constructs using FuGENE6 for 24-48h, as per manufacturer's instructions; control cells were transfected with empty pGL2 vector, lacking promoter sequences. In some experiments promoter-reporter plasmids were used for measuring activation of β-catenin (TOPFlash wild type and FOPFlash mutant), obtained from Dr. Bert Vogelstein (John Hopkins, Baltimore, MD), as previously described (Sarkar et al., 2011). Transfected cells were lysed in luciferase assay lysis buffer and luciferin was added according to instructions of the manufacturer (E2510, Promega WI). Luciferase activity was measured using a luminometer (Dynex Technologies, VA) after 10sec of addition of substrate, as previously described (Sarkar et al., 2011).

### 2.2.10 Chromatin Immunoprecipitation Assays (ChIP)

For ChIP assays, cells in culture (60-70% confluent), were fixed in 1% formaldehyde for 10 min RT to crosslink DNA to bound proteins, and reaction stopped by adding 0.125M glycine. Cells were washed with cold PBS, pelleted at 4ºC in the presence of protease inhibitor cocktail (Sigma) and re-suspended in 600µl of ChIP sonication buffer (1%Triton X-100, 0.1% deoxycholate, 50mM Tris-pH 8.1, 150mM NaCl, 5mM EDTA and protease inhibitors), followed by sonication and centrifugation of fragments (600-700bp long) at 10,000 RPM. The crosslinked chromatin supernatant was immunopreciptated using target-specific antibody (2-5µg purified IgG) at 4ºC, overnight. Control samples contained no antibody. For obtaining input levels of the corresponding proteins, equivalent numbers of cells were also processed for Western Immunoblot analysis. Protein A/G Sepharose beads, pre-absorbed by Herring sperm DNA (100µg/ml) was added to the chromatin-antibody complex and centrifuged to sediment the beads. The beads were washed with cold buffers, and DNA eluted from the beads with elution buffer (1%SDS, 0.1%NaHCO3, 0.01%mg/ml Herring Sperm DNA). DNA in the supernatant was precipitated using high-salt method as described by Ishizawa et al (Ishizawa et al., 1991). The extracted DNA was purified using a kit from Zymogen (Catalog number D4060), and 2µl of the purified DNA was used for PCR amplification of the immunoprecipitated DNA with specific primers designed around the transcription factor binding site of interest. The primer sequences used for this purpose are listed in **Table 2.1**.

### 2.2.11 DNA Methylation Analysis using the method of bisulfite conversion

Genomic DNA was purified from cell lines and colon tissues using a kit from Qiagen, and 2-5µg of gDNA was used for methylation analysis. Methylation analysis was conducted as described by Clark et al (Clark et al., 1994). Briefly, DNA was treated with

sodium hydroxide (3M) for denaturation followed by bisulfite deamination using hydroquinone/sodium bisulfite treatment (16mM hydroquinone, 4 M sodium bisulfite), overnight at 50ºC. The reaction mixture was desalted using Wizard DNA clean-up kit (Promega) and NaOH (3.0M), followed by incubating at 37ºC for 20min for alkali de-sulphonation reaction. The DNA was precipitated in the presence of 10mg/ml glycogen as a carrier by the method used by Ishizawa et al (Ishizawa et al., 1991). Bisulfite converted DNA (2µl) was amplified by PCR using bisulfite converted primers (**primers used are listed in Table 2.1**). The PCR products were purified by a column (Wizard DNA clean-up kit, Promega) and cloned into a TA cloning vector (Sigma). Clones were confirmed by EcoR1 digestion and positive clones were sequenced using T7 primers in the Recombinant DNA Core Facility at UTMB.

### 2.2.12 Western Immunoblot (WB) analysis

Treated and control cells growing as mono-layer cultures, were harvested and processed for preparing cellular lysates, followed by electrophoresis and transferred to PVDF-membranes as previously described (Kantara et al., 2014; Sarkar et al., 2012; Sarkar et al., 2011). Frozen tissue samples obtained from patients as described above were homogenized and processed for preparation of tissue lysates in RIPA buffer as described previously (Kantara et al., 2014; Sarkar et al., 2012; Sarkar et al., 2011). Samples containing 30-50µg of proteins were subjected to electrophoresis and transferred to PVDF-membranes as previously described (Kantara et al., 2014; Sarkar et al., 2012; Sarkar et al., 2011). Blots were cut into horizontal strips containing target or loading-control proteins (β-actin), and processed for WB, as described previously (Kantara et al., 2014; Sarkar et al., 2012; Sarkar et al., 2011). Antigen-antibody complexes were detected with a chemiluminescence-reagent kit (Thermoscientific, IL or GE Healthcare, UK). Membrane-strips containing either target or loading control proteins were simultaneously

exposed for equal time to autoradiographic films. Western blots presented were cropped to exclude bands beyond the range of the molecular markers, at the running end and at the loading end, as is customary, which helps to develop both weak and strong signals within the relevant range. Processing of films was applied equally across the entire image. Touch-up tools were not used to manipulate data. Relative band-density on scanned autoradiograms was analyzed using Image J program (rsbweb.nih.gov/ij/download) and expressed as a ratio or % of β-actin in the corresponding samples.

### 2.2.13 Transient-transfection of cells with oligonucleotides

Cell lines, seeded in 96-well plates were transfected with 5pmol of either target-specific or control-siRNA, as indicated, using Lipofectamine 2000 (Invitrogen), as described (Kantara et al., 2014; Sarkar et al., 2011). Transfected cells were propagated in normal growth medium containing 10% FCS, and processed for WB analysis after 48h of transfection for confirming down-regulation of the target transcription factor (β-catenin or NF-κBp65). In order to examine the role of the indicated transcription factors in modulating the transcriptional activation of the promoter-reporter constructs, cells in culture were pre-transfected with the indicated promoter-reporter constructs, followed by transient transfection with the indicated siRNA molecules, followed by processing the cells after 48h of treatment for relative levels of luciferase, as described above.

### 2.2.14 Statistical analysis

Data are presented as mean±SEM of values obtained from indicated number of patient samples or experiments. To test for significant differences between means, nonparametric Mann Whitney test was employed using STAT view 4.1 (Abacus

Concepts, Inc, Berkley, CA). Chi-square tests were used to analyze the relationship between DCLK1-S expression and clinicopathological factors. Overall survival curves were analyzed using Kaplan-Meier method, and comparisons were made using the log-rank test. The cut off threshold between high and low expression group for DCLK1-S transcript was defined by the median values of the gene's expression in cancerous tissue. The cox proportional hazards regression model, using Medcalc version 12.3.0 was utilized to estimate univariate and multivariate hazard rations for prognosis. In addition to target mRNA expression, a list of clinical variables was considered for univariate and multivariate analysis to determine its impact on prognosis of patients with colorectal cancer: sex, age at diagnosis (continuous), pathological differentiation (differentiated or undifferentiated), tumor size (>41mm median or <41 mm), lymph node metastasis (present or absent), and distant metastasis (presence or absence). All p values were two-sided and differences were considered to be statistically significant if <0.05.

## 2.3 RESULTS

### 2.3.1 5'(α)promoter is methylated during colon-carcinogenesis in humans

In preliminary studies we discovered that 5'(α)-promoter of *DCLK1*-gene was hypermethylated in hCCCs, as recently reported (Vedeld et al., 2014). We mapped a total of 20 CpG sites within 200bps of the 5'(α)-promoter (**Fig 2.1a**). All the 20 CpG sites were non-methylated in the human normal colon (hNC) cell line (CCD841), but were methylated by >80% in 5 hCCC-lines, examined to-date. Mapping of the methylation status of individual CpG sites obtained from representative cell lines, by bisulfite sequencing is diagrammatically presented in **Figure 2.1b**. Samples obtained from either normal (Norm) colons, adenomas (Ad), adenocarcinomas (AdCA) or metastatic-lesions

(Met), from 5-8 patients, were also analyzed for methylation status of the indicated CpG sites, as described in Methods, and data from representative samples are presented diagrammatically in **Figure 2.2a**. The percentage of 20 CpG sites, that were methylated in all the samples examined, was in the order of: AdCA/Met(85±15)>TA(67±30)>Norm (19±8%) (**Fig 2.1c**).

### 2.3.2 Human normal colons (hNCs)/cells mainly express long-isoform of DCLK1 while hCCCs/hCRCs mainly express short-isoform

Hypermethylation of 5'-promoter of some genes during neoplastic-transformation is associated with expression of shorter transcripts from an alternate promoter (Archey et al., 1999; Hoivik et al., 2013). Since 5'(α)-promoter of the *DCLK1*-gene is hypermethylated in hCRCs, but DCLK1 protein is measured in hCRCs, usage of an alternate-promoter was suggested.

Molecular mass of DCLK1 was determined by Western Blot (WB) analysis using DCLK1-antibodies, which detect isoforms 1&2 in human brain. Almost all normal colonic mucosal samples (hNC) from patients were positive for the ~82kDa DCLK1 protein, corresponding to long isoform (isoform 1 in NCBI data base) of hDCLK1; Less than 10% samples (1/22) were also strongly positive for S-isoform (**Table 2.2**), which may be of prognostic value, since the patient was positive for large adenomas. Representative WB data from hNC (normal colon) patient samples are presented in **Figure 2.3a**. A minor band of S-isoform was also seen in a few hNC samples (**Fig 2.3a,b;Table 2.2**), which may reflect expression of the short isoform by stromal and enteric neuronal cells, present within the colonic mucosa. The AdCA samples from patients with hCRCs were predominantly positive for ~45-48kDa DCLK1 protein, corresponding to short(S) isoform (isoform 2 in NCBI data base) of hDCLK1. Representative WB data from AdCA samples in presented in **Figure 2.3c**. The ratios of

S/L DCLK1 to β-actin in hNCs vs. hCRC samples, demonstrated opposite profiles (**Figs 2.3b,d**). A hNC cell line (CCD841) only expressed DCLK1-L while HCT116 hCCC (colon cancer cells) only expressed DCLK1-S (**Fig 2.3e**). All 15 hCCC cell-lines, examined by RT-PCR, were negative for DCLK1-L; but the majority (13/15) expressed DCLK1-S (**Table 2.3**). Representative RT-PCR data from hCCC cell-lines, wild type or mutant for KRAS/BRAF, are presented in **Figure 2.4**; the expression of DCLK1-S did not appear to be associated with any specific mutant phenotype of hCCC-cell lines. HEK293 cells, transduced to over-express progastrin (HEKmGAS), develop tumorigenic/metastatic potential (Sarkar et al., 2012), and express elevated levels of both S/L DCLK1; control non-tumorigenic, HEKC cells, however, only express DCLK1-L (**Fig 2.3f**). Thus, tumorigenic-transformation alone can apparently up-regulate the expression of the short-isoform, in the absence of epigenetic-silencing of 5'(α)-promoter.

Genomic structure of h*DCLK1*-gene was mapped from contig NC_40000013.1 (**Fig 2.5a**). Primer sets were designed for isoforms listed in NCBI database, to identify the isoforms being expressed by normal/non-transformed (CCD841/HEKC) and transformed (HCT116/HEKmGAS) cells. Long (NM_004734.4) and short (NM_001195415.1) transcripts, transcribed from the indicated exons (**Fig 2.5a**), were detected (**Figs 2.5b,c**). Only the 5'UTR and 17bps, downstream of ATG, are non-homologous in S vs. L transcripts; the rest of the coding sequence for DCLK1-S is homologous with DCLK1-L (**Fig 2.5a;** as described in background). Amino acid sequence of DCLK1-S was also >98% homologous with C-terminus of DCLK1-L (as described in background). We took advantage of slight differences in nucleotide sequences of L/S DCLK1, and developed isoform specific primers for amplifying L/S transcripts from human/mouse samples (**Table 2.1**). HCT116 cells only expressed DCLK1-S, while normal CCD841 cells only expressed L-transcript (**Fig 2.5b**). Non-tumorigenic HEKC cells only expressed L-transcript, while tumorigenic/metastatic HEKmGAS cells expressed both DCLK1-L/S (**Fig 2.5c**), corresponding to protein data (**Fig 2.3f**). Both L/S transcripts were expressed

in mouse brain (**Fig 2.5d**), as reported (Omori et al., 1998), but mouse colonic epithelium only expressed DCLK1-L (**Fig 2.5d**). Unlike hCRCs, 5'-promoter of mouse *DCLK1* gene does not appear to be epigenetically silenced in intestinal/pancreatic tumors (Bailey et al., 2013; Nakanishi et al., 2013; Westphalen et al., 2014), as recently confirmed (Borinstein et al., 2010). Norm/Ad samples from mouse colons (generated as described in methods), were subjected to RT-PCR, using mouse primers (**Table 2.1**), and only L-transcript was amplified in both (**Fig 2.5e**). In a mouse cancer cell line (CT26), only L-transcript was amplified (**Fig 2.5f**). Thus, even though 5'-promoter of many common genes are epigenetically silenced in both mouse/human colon tumors (Grimm et al., 2013), 5'(α)-promoter of h*DCLK1* gene is silenced only in human colon tumors, as recently confirmed (Vedeld et al., 2014). The loss or gain of DCLK1-L/S transcripts during different stages of colon-carcinogenesis was examined in patient samples, and representative RT-PCR data are presented in **Figure 2.6a**. Data from all samples (**Figs 2.5g,h**), show that hNCs from patients mainly express L-transcript, while adenomas/adenocarcinomas mainly express S-transcript, albeit at significantly different levels. The fold-change in DCLK1-S expression by hCRC samples, at stages I-III, was examined by qRT-PCR, compared to that in hNCs, free of colonic growths (**Fig 2.6b**); higher levels were measured at stages I/II than stage III in the four samples analyzed/stage, using a commercial cDNA plate.

### 2.3.3 Identification of transcriptional start site of DCLK1-transcripts in normal vs. cancer cells

A common reverse-primer (primer-2) from coding sequence of L/S transcripts was designed (**Table 2.1**), and either nascent-mRNA or total-RNA was reverse transcribed, as diagrammatically shown (**Fig 2.7a**). A non-mammalian adapter-sequence was ligated to the products and PCR amplified using primers 1/2 (**Fig 2.7a**); results are shown in **Figures 2.7b,c**. HCT116 cells only expressed a 498bp-product, matching the

expected size of short-isoform (NM_001195415.1) (**Fig 2.7b**). HEK293 samples only expressed a 1,300bp-product, matching the expected size of DCLK1-L transcript (NM_004734.4) (**Fig 2.7c**). Sequencing confirmed the expected products. All other bands were fragments thereof or non-specific. The results confirm that hCCCs express DCLK1-S from the β promoter in IntronV of hDCLK1-gene. HCT116 cells, treated with 5-Azacytidine, re-expressed DCLK1-L transcript (**Figs 2.7d,e**), confirming that 5'-promoter of h*DCLK1* gene is epigenetically-silenced in HCT116 cells.

### 2.3.4 Role of TCF4/LEF binding-sites in up-regulating transcriptional activity of 5'(α)-promoter of hDCLK1 gene

We used progastrin (PG) as an activator of DCLK1 expression in target cells, based on previous findings (Jin et al., 2009; Sarkar et al., 2011). PG is a potent co-carcinogen and increases colon-carcinogenesis in mice, in response to AOM±DSS (Cobb et al., 2004; Jin et al., 2009; Singh et al., 2000a). Two potent transcription-factors (TFs) (NF-κBp65/β-catenin) mediate hyperproliferative/co-carcinogenic effects of PG on mouse colonic crypts (Rengifo-Cam et al., 2007; Sarkar et al., 2011; Umar et al., 2009) associated with significant up-regulation of stem-cell-markers, including DCLK1 (Jin et al., 2009; Sarkar et al., 2011). Since colon-carcinogenesis in mice is associated with increased expression of DCLK-L (**Fig 2.5**), and NF-κB/β-catenin mediate up-regulatory effects of PG (Rengifo-Cam et al., 2007; Sarkar et al., 2011; Umar et al., 2008; Umar et al., 2009), we conducted *in silico* analysis of 5'(α)-promoter. Several potential binding-sites for TCF4/LEF, and NF-κB, were found within 5kb of start-site (**Fig 2.8a, Fig 2.9a**). A 5'-promoter-reporter construct, containing TCF4/LEF and NF-κB binding-sites, was generated. Relative transcriptional-activity of promoter-reporter construct was examined in transiently transfected HEKC/HEKmGAS/HCT116 cells (**Fig 2.8b**). CCD841 cells were not used as they were difficult to transfect. Corresponding levels of activated β-

catenin were indirectly examined by measuring relative activation of TOP vs. FOP plasmids, as described in Methods. Non-tumorigenic HEKC cells demonstrated relatively low levels of activated β-catenin (TOP-activity), while HEKmGAS/HCT116 cells were positive for significant levels of activated β-catenin/NF-κB (**Fig 2.8b, Fig 2.9b**), probably in response to autocrine PG (Sarkar et al., 2011). Transcriptional activity of 5'(α)-promoter-reporter construct (DCLK1-L-LUC) was several-fold higher in HEKmGAS/HCT116 cells compared to that in HEKC cells, suggesting that β-catenin binding to 5'(α)-promoter may contribute to increased activation of DCLK1-L-LUC vector (**Fig 2.8b**). HEK293 cells were transiently co-transfected with either control-vector or mGAS-vector to express high levels of PG (Sarkar et al., 2012; Sarkar et al., 2011), along with DCLK1-L-LUC vector. Transcriptional activity of DCLK1-L-LUC in the presence of PG expression was significantly increased in HEK293 cells (**Fig 2.8c**). Transcriptional activity of DCLK1-L-LUC-vector was significantly reduced in HEKmGAS/HCT116 cells to control HEKC levels, on co-transfection with β-catenin siRNA (**Figs 2.8d,e**); efficacy of β-catenin-siRNA was confirmed (**Fig 2.10**). Possible role of NF-κB-binding-sites in regulating 5'(α)-promoter was examined by co-transfecting HEKC/HEKmGAS cells with NF-κBp65-siRNA and DCLK1-L-LUC vector. Relative activity of DCLK1-L-LUC vector was similar in control-siRNA vs. NF-κBp65-siRNA treated cells, corresponding to relative levels of DCLK1-L transcript in control vs. treated cells (**Fig 2.9b**); the latter results strongly suggest that NF-κB-binding-sites do not play a significant role in activating/regulating the 5'(α)-promoter in these cells.

β-catenin binding to the five potential TCF4/LEF binding-sites in 5'(α)-promoter (**Fig 2.11a**), was determined in ChIP assays. TCF4/LEF sites at -1904 and -1591 were the only functional β-catenin binding-sites in the indicated cells (**Fig 2.11a**). Representative ChIP data from all three cell-lines confirmed that non-tumorigenic HEKC cells, lacking activated β-catenin (**Fig 2.8b**), were negative for β-catenin binding to both sites, while tumorigenic cell lines (HEKmGAS, HCT116) were positive (**Figs 2.11b-d**). HEK293

cells were transiently transfected with either control or mGAS (PG expressing) vector, and analyzed by ChIP assays (**Figs 2.11e,f**). Relative binding of β-catenin to the two TCF4 binding-sites, in the presence or absence of mGAS expression, from several experiments, is presented as % of total β-catenin (input) in the cells (**Fig 2.11g**). β-catenin binding to both sites increased significantly in HEK293 cells transfected with mGAS-vector. For reasons unknown, relative binding of β-catenin to -1904 site was significantly higher than that to -1591 site in HEKmGAS/HCT116 cells (**Fig 2.11g**).

To confirm a role of the -1904 and the -1591 TCF4/LEF binding-sites in transcriptional regulation of DCLK1-L-LUC vector, the two sites were mutated as described in Methods, and confirmed. All three cell lines were transfected with either the mutant DCLK1-L-Luc construct (termed DCLK1-L-Mutant) or the wildtype DCLK1-L-Luc construct. The transcriptional activity of DCLK1-L-Mutant construct was significantly down-regulated in HEKmGAS/HCT116 cells, to control levels measured in HEKC cells (**Fig 2.8f**), mimicking the results obtained with the wildtype DCLK1-L-Luc construct in the presence of β-catenin siRNA (**Figs 2.8d,e**). Results in **Figure 2.8f** provide further evidence that the two TCF4/LEF binding sites play a critical role in transcriptional regulation of the 5'promoter.

### 2.3.5 Role of NF-κB binding-site in regulating transcriptional activity of IntronV(β)-promoter of hDCLK1-gene

By *in silico* analysis, a single NF-κB binding site (~439bps, 5' of a consensus TATA box), but no TCF4/LEF sites, were identified within 3 kb of IntronV(β)-promoter (**Fig 2.12a**). Role of NF-κB in regulating transcriptional activity of IntronV(β)-promoter was examined by using two promoter-reporter constructs (**Fig 2.12a**). NF-κB *cis*-element was present in DCLK1-S-LUC-1, but absent in DCLK1-S-LUC-2 (**Fig 2.12a**). Transcriptional activity of both promoter-reporter constructs was negligible in HEKC

cells (**Fig 2.12b**), known to be negative for activated NF-κBp6522. Relative transcriptional activity of LUC-1 was ~2-4 fold higher in HEKmGAS/HCT116 cells, compared to that of LUC-2 construct (**Fig 2.12b**), suggesting an important role of NF-κB binding-site in mediating increased activation of IntronV(β)-promoter. Transcriptional activity of LUC-2 was also elevated in HEKmGAS/HCT116 cells (**Fig 2.12b**), suggesting endogenous factor(s), other than p65, may also activate IntronV(β)-promoter. PG is overexpressed in hCRCs (Singh et al., 1996; Singh et al., 2012), and maybe a prognostic marker for hCRC patients (Do et al., 2012). In the presence of PG (mGAS-vector), transcriptional activity of LUC-1 increased by ~10-15-fold in HEK293 cells (**Fig 2.12c**), confirming an important role of NF-κB binding site in transcriptional activation of IntronV(β)-promoter in response to PG. Surprisingly transcriptional activity of LUC-2 (negative for NF-κB binding-site) was also increased by ~3-5-fold, suggesting that *cis*-elements other than NF-κB, might also respond to PG. Cells transfected with LUC1-vector were also co-transfected with either control- or NF-κBp65-siRNA (**Figs 2.12d,e**). Loss of NF-κBp65 expression in NF-κBp65-siRNA transfected cells (**Fig 2.10b**), resulted in reduction of transcriptional activity of LUC-1 in HEKmGAS/HCT116 cells by >50% (**Figs 2.12d,e**), to levels measured with LUC-2 (**Fig 2.12b**). The results suggest that the single NF-κB *cis*-element plays an important role in transcriptional activation of IntronV(β)-promoter, and hence the expression of S-isoform, in transformed/cancer cells.

Representative ChIP data confirms binding of NF-κBp65 to NF-κB binding-site in IntronV-promoter (**Fig 2.13a**), *in situ* (**Figs 2.13b,c**). Almost 80-90% of total NF-κBp65 was bound to NF-κB binding-site in HEKmGAS/HCT116 cells. Surprisingly, ~30-40% of total NF-κBp65 was also bound in HEKC cells (**Fig 2.13d**), even though transcriptional activity of the promoter-reporter construct was negligible in these cells (**Figs 2.12b,d**), suggesting that either a threshold of NF-κB binding is required, or other factors activate IntronV(β)-promoter, in the presence of NF-κBp65. The % bound NF-κBp65 increased by ~5-fold in HEK293 cells overexpressing PG (mGAS vector) (**Figs**

**2.13e,f**), corroborating our previous findings of significant increase in phosphorylation/activation of NF-κBp65 in response to PG (Rengifo-Cam et al., 2007; Sarkar et al., 2011).

### 2.3.6 High expression of DCLK1-S in AdCA samples from CRC patients is associated with poor patient survival

The expression pattern of DCLK1-S transcript in relation to clinicopathological parameters was analyzed using an independent cohort of patient specimens, as described in Methods. High-expression of DCLK1-S significantly correlated with overall poor patient survival in patients with Stages I-IV disease (**Fig 2.14a**), or patients with only curatively resected Stages I-III disease (**Fig 2.14b**), with significantly worse disease free survival (**Fig 2.14c**), which significantly correlated with pathological T-category and lymphatic vessel involvement (**Table 2.4**). Moreover, by multivariate analysis, overexpression of DCLK1-S emerged as an independent prognostic factor in CRC patients (**Table 2.5**).

**Figure 2.1: Methylation of 5'(α)-promoter of h*DCLK1***

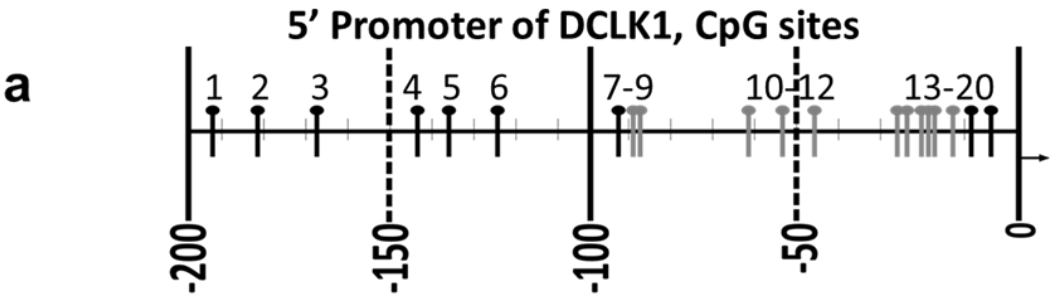


b

| | CpG Sites (● Methylated:○ Unmethylated) | | | | | | | | | | | | | | | | | | | |
|---|---|---|---|---|---|---|---|---|---|---|---|---|---|---|---|---|---|---|---|---|
| Cell line | 1 | 2 | 3 | 4 | 5 | 6 | 7 | 8 | 9 | 10 | 11 | 12 | 13 | 14 | 15 | 16 | 17 | 18 | 19 | 20 |
| CCD841 | ○ | ○ | ○ | ○ | ○ | ○ | ○ | ○ | ○ | ○ | ○ | ○ | ○ | ○ | ○ | ○ | ○ | ○ | ○ | ○ |
| HCT116 | ● | ● | ● | ● | ● | ● | ● | ● | ● | ● | ● | ● | ● | ● | ● | ● | ● | ● | ● | ● |

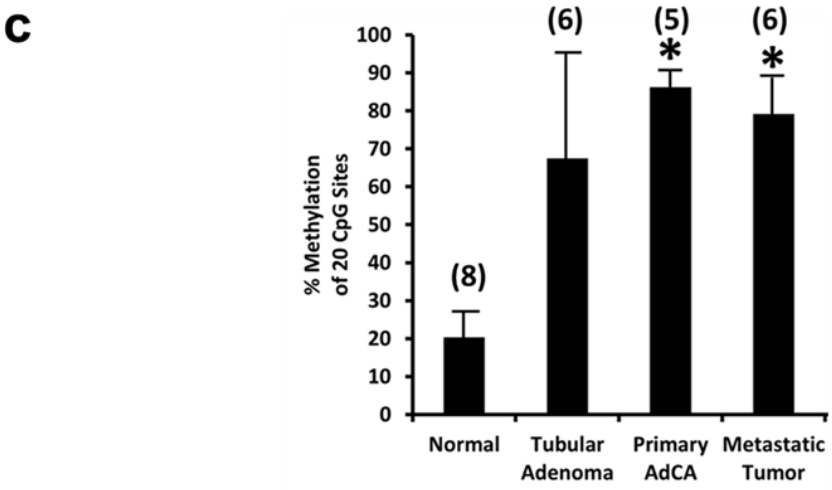


(a) = CpG sites that can be potentially methylated within 200bps of the 5'(α)-promoter of DCLK1-gene are depicted as vertical black/grey lines, and numbered 1-20. Grey vertical lines depict CpG sites used for assessing DNA methylation of 5'(α)-promoter of DCLK1-gene in a recent study (as described in results). (b) = Methylation status of 20 CpG sites was determined using the bisulfite method of sequencing as described in Methods. Methylation status of the 20 sites is shown for representative normal (CCD841) and colon cancer (HCT116) cell lines. Open circles=unmethylated CpG sites; filled circles=methylated CpG sites. (c) = Methylation status is presented as bar graphs, and represents % CpG sites methylated (of the 20 sites analyzed) in samples from normal colons (Normal), colonic tubular-adenomas (TAs), primary adenocarcinomas (AdCAs), and metastatic (MET) tumors. Each bar graph = mean±SEM of data from the indicated number of samples in parentheses, that were analyzed. *=$p<0.05$ vs methylation status of normal-colons that were obtained from patients free of adenomas and adenocarcinomas. The procurement of samples is described in methods.

**Figure 2.2: DNA Methylation Analysis of 5'(α)-promoter of h*DCLK1* in Human Samples**

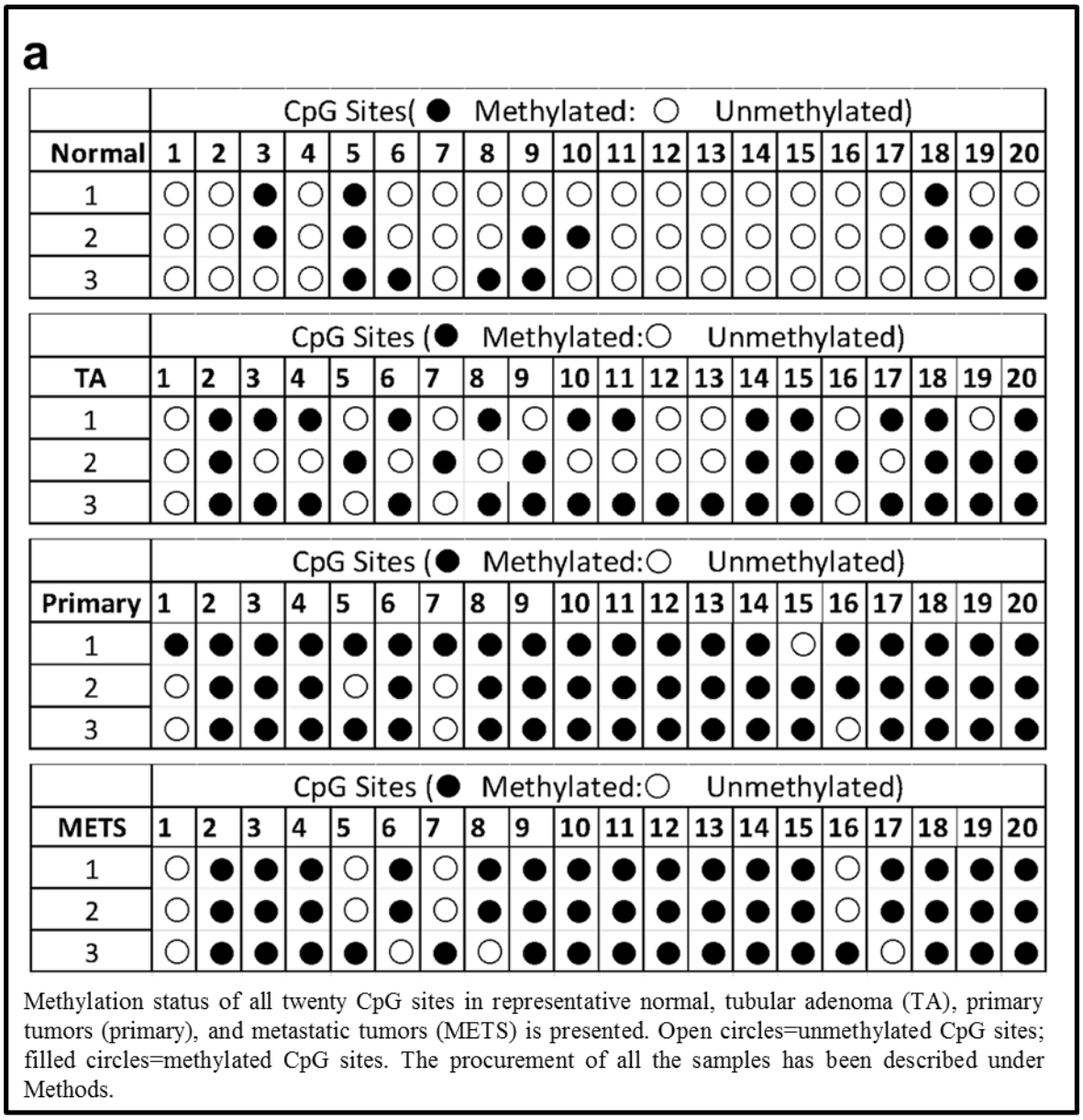


Methylation status of all twenty CpG sites in representative normal, tubular adenoma (TA), primary tumors (primary), and metastatic tumors (METS) is presented. Open circles=unmethylated CpG sites; filled circles=methylated CpG sites. The procurement of all the samples has been described under Methods.

**Figure 2.3: Western Blot (WB) Analysis of DCLK1 Protein in Human Cell Lines and Patient Samples**

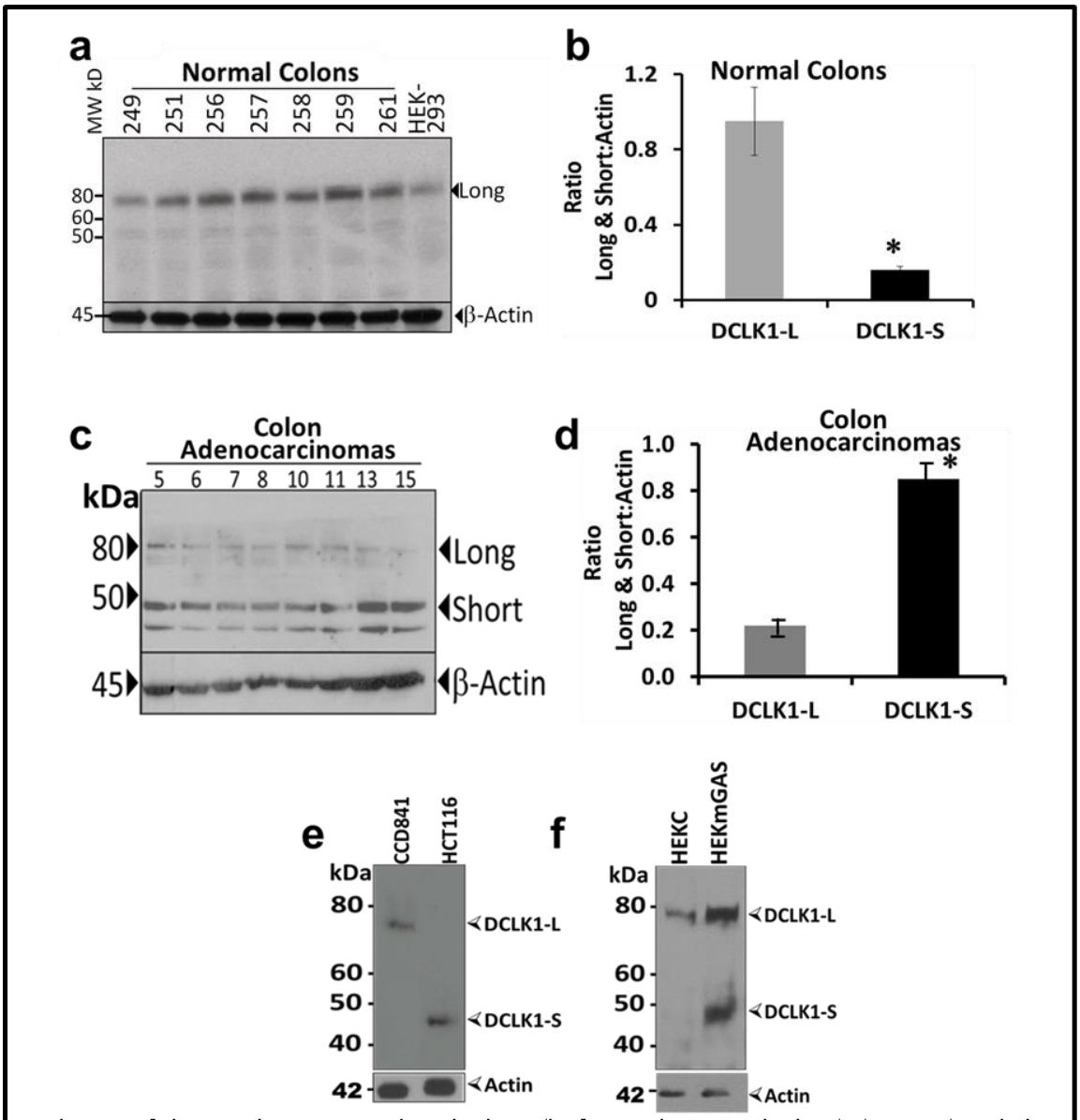


The Mr of the proteins correspond to the long (isoform 1 in NCBI database) (~80KDa) and short (Isoform 2 in NCBI database) (~45KDa) DCLK1 protein in human cells. (a-f) = Tissue samples were obtained from patients with either normal-colons (hNCs), free of Ads/AdCAs, or from patients with adenocarcinomas, as described in methods. Representative WB of samples from hNCs (a) and hCRCs (c) are presented, demonstrating relative expression of L/S DCLK1; laboratory numbers for patient samples are indicated above the Blots in a and c. WBs in each case were densitometrically analyzed and ratio of relative levels of L/S DCLK1 to corresponding β-actin levels are presented as bar-graphs, from all samples analyzed (b, normal-colons; d, adenocarcinomas). Each bar-graph in b and c = mean±SEM of calculated ratios for the two isoforms in patient samples obtained from 8-22 patients, as described in methods. (e) = Representative Western Blots from normal (CCD841) and colon cancer (HCT116) cell lines. (f) = Representative WBs from isogenic HEKC/HEKmGAS cells. Western blots presented in a, c, e, and f were cropped to improve clarity. All bands within the range of the molecular markers were retained and processing of the film was applied equally across the entire image. *=$p<0.05$ vs. DCLK1-L

**Figure 2.4: Representative RT-PCR Analysis of Long and Short Transcripts of DCLK1 in Human Colon Cancer (hCCC) Cell Lines**

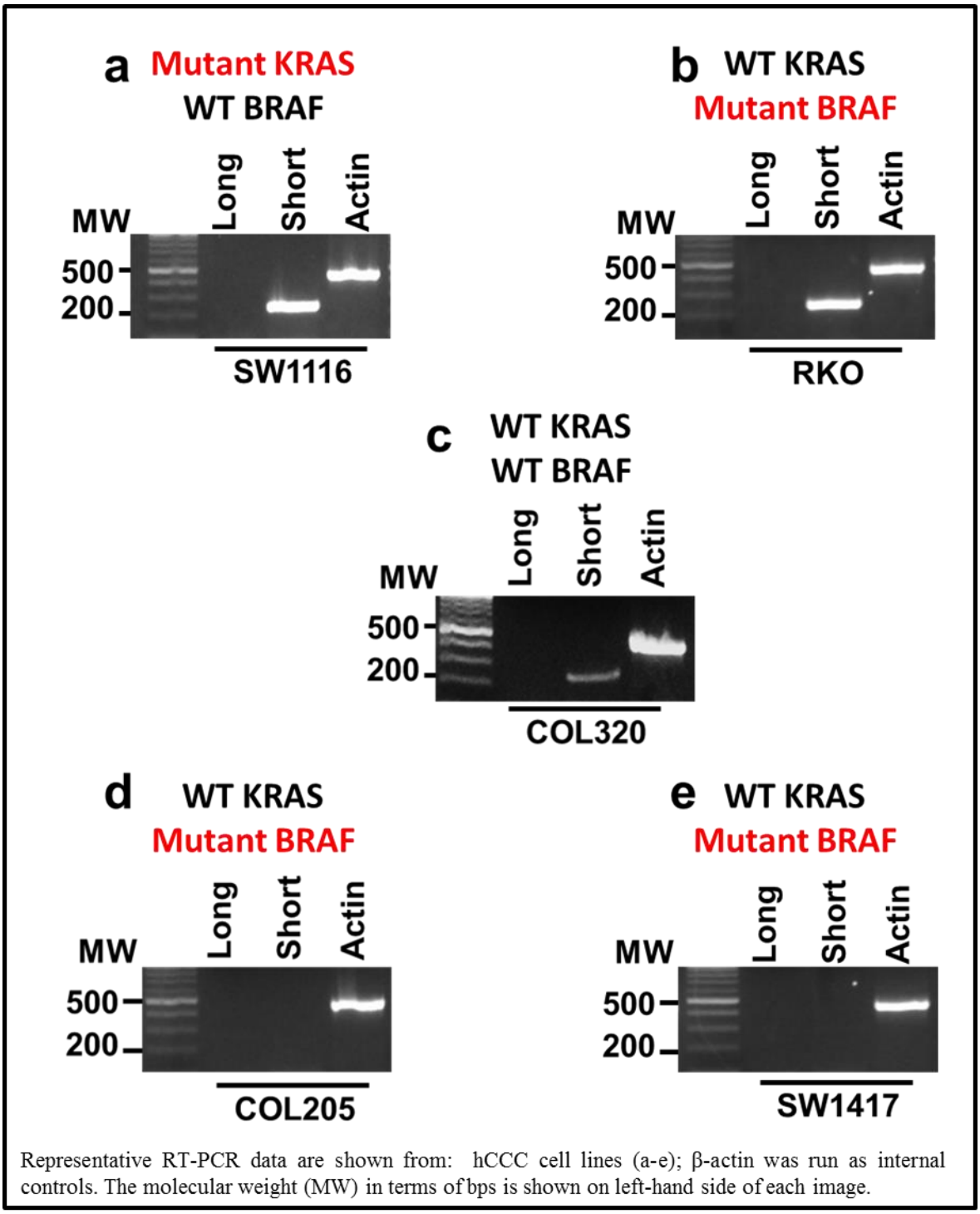


Representative RT-PCR data are shown from: hCCC cell lines (a-e); β-actin was run as internal controls. The molecular weight (MW) in terms of bps is shown on left-hand side of each image.

**Figure 2.5: RT-PCR Analysis of Long and Short Transcripts of *DCLK1* in Human and Mouse Cell Lines and in Patient Samples**

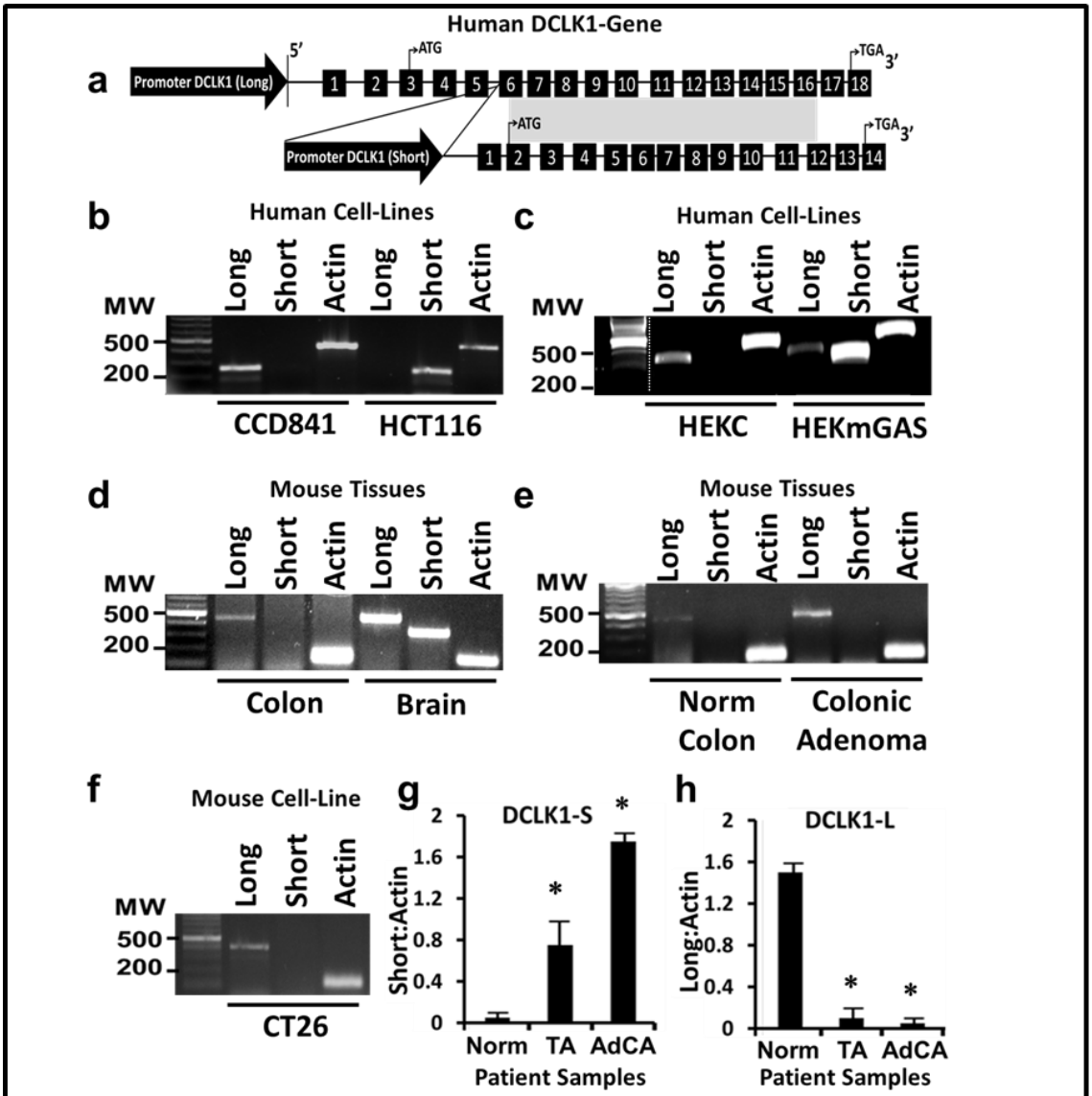


(a)=Diagrammatic representation of h*DCLK1* gene with transcription of DCLK1-L/S transcripts from the indicated exons. The α promoter for DCLK1-L is located at 5'-end and the alternate β promoter for DCLK1-S is located within IntronV of the gene. Transcriptional start sites (ATG) and end sites (TGA) are shown and homologous sequences between the two transcripts are shaded. Numbered boxes=exons; lines between boxes=introns. (b-h)=Samples from mice and humans (patients) were obtained as described in methods and processed for RT-PCR using human/mouse primers for DCLK1-L/S transcripts. Representative RT-PCR data are shown from: human cell lines (b,c); Normal-colonic-mucosa and brain tissues from wild type FVB/N mice (d); uninvolved mouse colon-mucosa (Norm) and mouse colon-tumor samples (Ads) (e); mouse cancer cell line (CT26) (f). Human (b,c) and mouse (d-f) β-actin was run as internal controls. The molecular weight (MW) in terms of bps is shown on left-hand side of each image in b-f. Representative RT-PCR data from patient samples are presented in Figure2.6a. Relative levels of short (g) and long (h) DCLK1 transcripts in human patient samples are presented as a ratio of the corresponding β-actin levels; hNC samples=Norm, tubular-adenomas=TA and colon-adenocarcinomas=AdCAs. Each bar-graph in g and h = mean±SEM of 5-8 separate patient samples, analyzed in duplicate. *=$p<0.05$ vs expression in normal patient samples.

**Figure 2.6: Relative Expression Levels of Long and Short Transcripts of DCLK1-isoforms in Patient Samples**

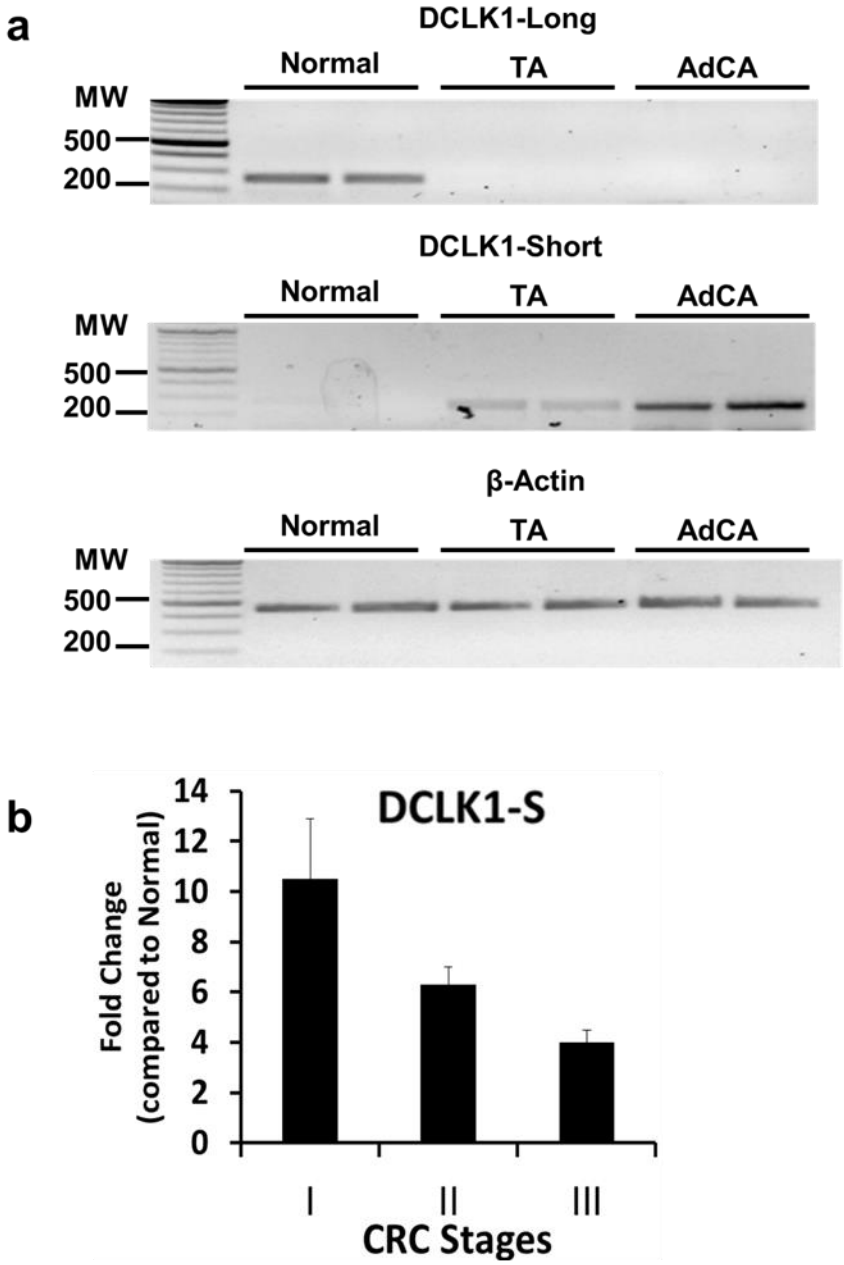


Total RNA from indicated tissue samples were amplified by RT-PCR by using sense and anti-sense primers for amplifying either DCLK1-L transcripts or DCLK1-S transcripts, as described in Methods. Representative data are presented from normal colons, tubular adenomas (TA) and advanced adenocarcinomas (AdCAs), obtained from two patients each; the samples were co-amplified and co-run at the same time for L/S transcripts and corresponding β-actin levels. Densitometric data from all samples that were similarly analyzed are presented as a ratio of β-actin levels in the corresponding samples, and are presented as bar-graphs in Figure2.5g,h.

**Figure 2.7: Primer Extension Analysis for Confirming Transcription of DCLK1-L/S Transcripts & Confirmation of Epigenetic Silencing of 5'(α)-promoter of *DCLK1*-gene in HCT116 cells**

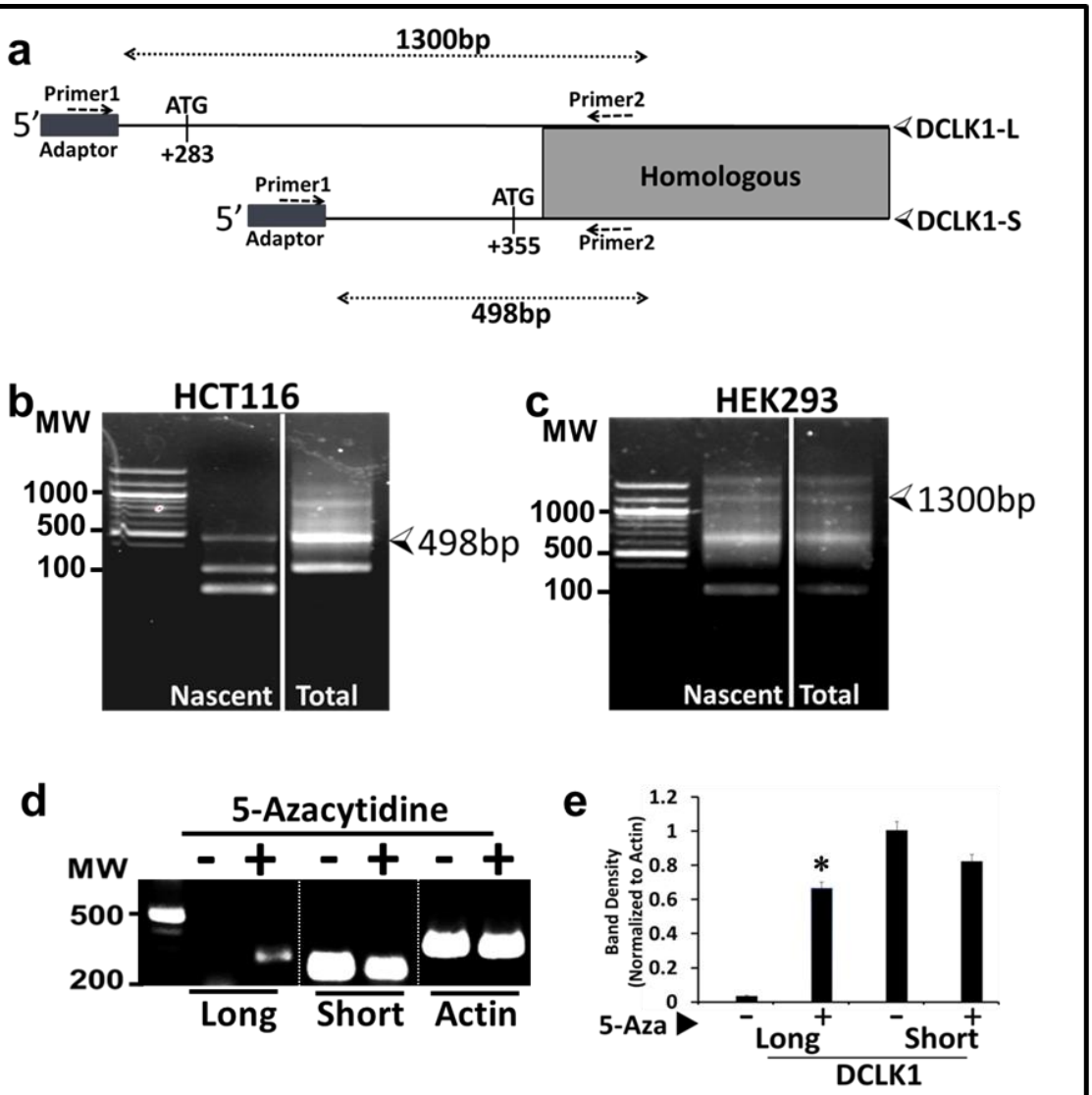


Schematic representation of 3'-5' primer-extension analysis. The shaded portion shows 100% homology in the sequences between the two isoforms. A common primer-2 from the two transcripts was used for 3'-5' extension, followed by ligating with non-mammalian adapter sequence (black box), as described in methods. Primers 1 and 2 were used for PCR amplification of the products. (b-c) = Both nascent mRNA and total RNA were used for primer extension analysis, followed by PCR amplification, as described above. Resulting PCR products are presented in b (HCT116 cells) and c (HEK-293 cells). HCT116 cells were positive for only the short transcript (498bps) and HEK-293 cells were positive for only the long transcript (1,300bps). All other bands were either non-specific or fragments thereof, as confirmed by sequencing. Electrophoresis gels shown in b and c, were not cropped. A white line is provided to clearly separate the nascent RNA from the total RNA.

Relative expression (RT-PCR) of L/S DCLK1 in HCT116 cells, in presence or absence of treatment with 5-aza-2′-deoxycytidine (5-azacytidine) is shown. d = Representative RT-PCR data. e = densitometric data presented as % of β-actin in corresponding samples. Each bar-graph in e = mean±SEM of three experiments. *=$p<0.05$ vs. DMSO treated cells.

**Figure 2.8: Role of TCF4/LEF Binding-sites in Activation of 5'(α)-promoter**

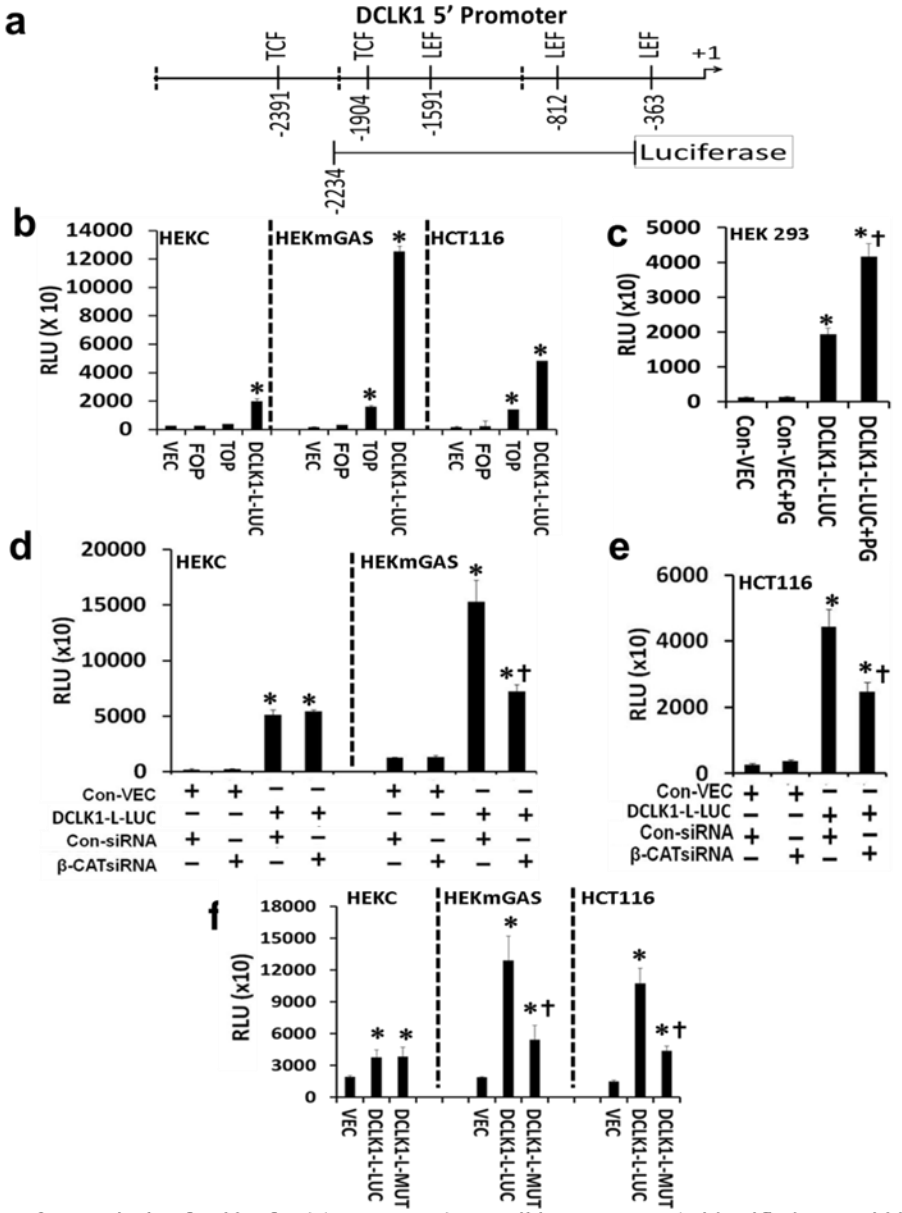


(a) = *In silico* analysis of ~3kb of 5'(α)-promoter (transcribing DCLK1-L), identified several binding sites for TCF-4/LEF and NF-κB, with >90% conserved sequences. The construct (DCLK1-L-LUC) used for the promoter-reporter assays is diagrammatically shown below the mapped promoter. (b-f) = Relative transcriptional/luciferase activity (RLU) in the indicated cells, transiently-transfected with the plasmids for 48h, in the presence or absence of transfection with either PG expressing plasmid (p-mGAS) (c), or the indicated siRNA (d,e), or a mutant plasmid (DCLK1-L-Mutant), containing insertions in the -1904/-1591 TCF/LEF binding sites (f), as shown. Methods used to generate the mutant plasmid are described under methods section. Cells were co-transfected with promoter-reporter construct±p-mGAS/siRNA for data presented in c-e. VEC=control LUC vector; TOP=TOPFlash plasmid with wild type TCF4/LEF binding sites for β-catenin binding; FOP=mutant FOPFlash plasmid. Each bar-graph in b-f represents mean±SEM of three separate experiments conducted in duplicate or triplicate/experiment. *=$p<0.05$ vs corresponding values with control vector. † in b=$p<0.05$ vs corresponding values in HEKC cells; † in c=$p<0.05$ vs corresponding values with DCLK1-L-LUC vector alone. † in d and e =$p<0.05$ vs control siRNA values; † in f=$p<0,05$ vs wild type DCLK1-L-LUC values.

**Figure 2.9: Role of NFκB Binding Site in Activation of the 5'(α)-promoter of DCLK1**

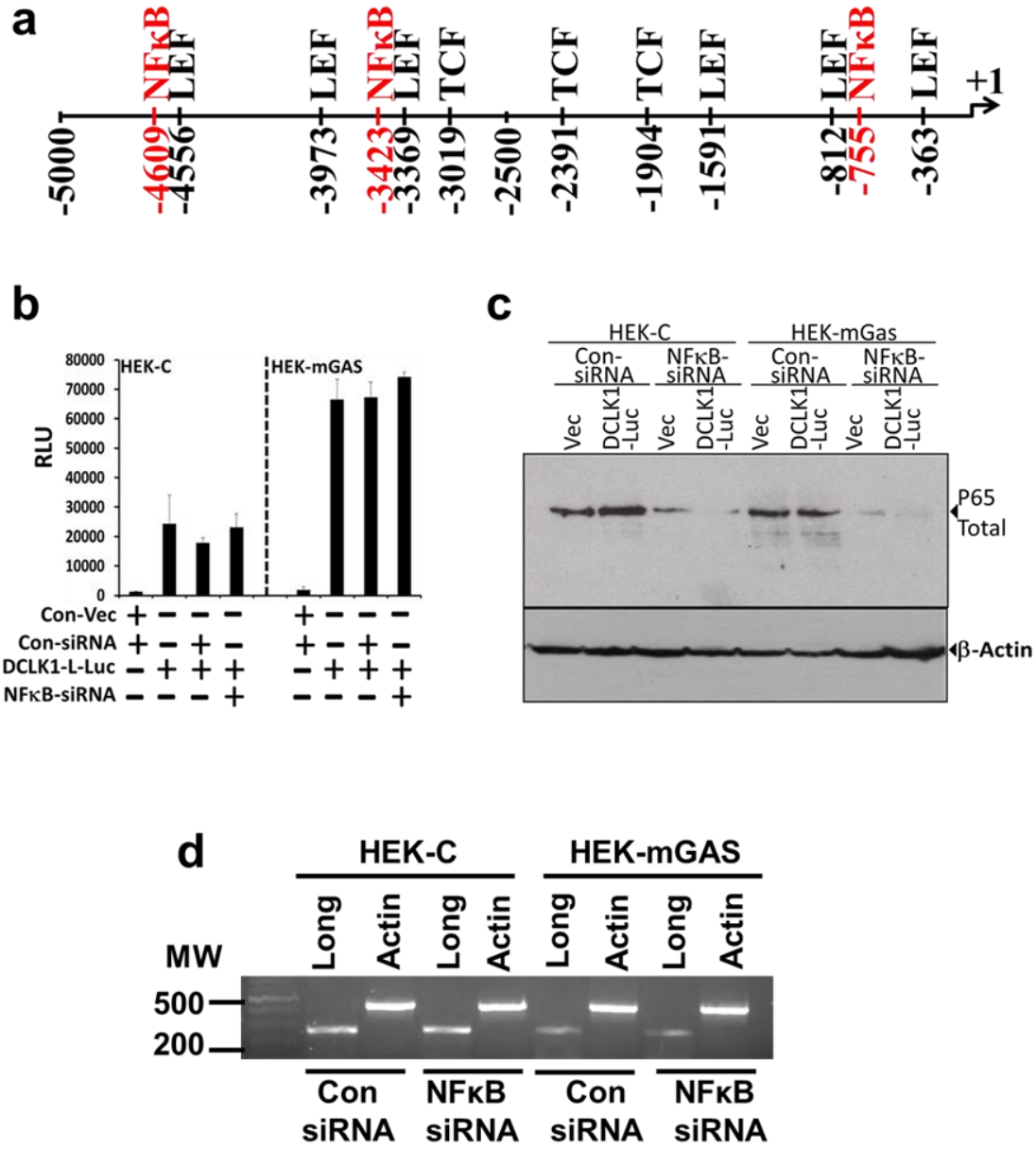


(a) *In silico* analysis of ~5kb of 5'-promoter of human *DCLK1*-gene (transcribing DCLK1-L), identified several binding sites for TCF-4/LEF and three NFκB binding sites, with >90% conserved sequences. (b) = Relative transcriptional/luciferase activity (RLU) in the indicated cells, transiently-transfected with the plasmids for 48h, in the presence or absence of transfection with either control or NFκBp65-siRNA. Cells were co-transfected with promoter-reporter construct±siRNA. VEC=control LUC vector. Each bar represents mean±SEM of four experiments. (c) = Western-Blot analysis, demonstrating efficacy of NF-κBp65-siRNA for down-regulating the expression of NF-κBp65 protein in the cell lines. (d) = Representative RT-PCR data for DCLK1-L isoform from indicated cells, in the presence of absence of either control-siRNA or NFκBp65-siRNA. The indicated cell lines were transfected with either (scrambled) siRNA (con-siRNA) or target-specific NF-κBp65-siRNA for 48h, before processing the cells by RT-PCR.

**Figure 2.10: Western-Blot Analysis, Demonstrating Efficacy of β-catenin-siRNA and NF-κBp65-siRNA for Downregulating the Expression of the Corresponding Protein in the Cell Lines**

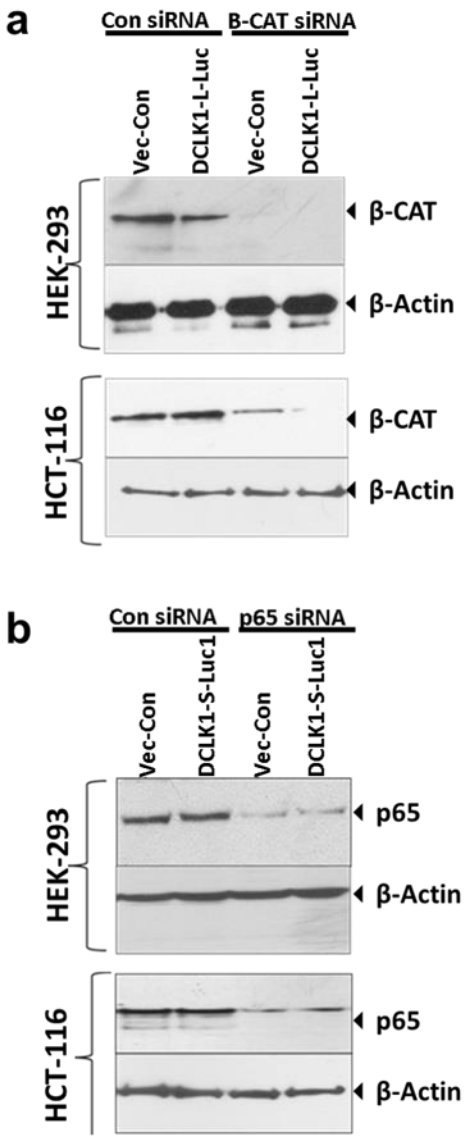


The indicated cell lines were transfected with either empty vectors (Vec-con) or vectors expressing promoter-reporter constructs (DCLK1-L-LUC) (a), or DCLK1-S-LUC-1) (b), and co-transfected with either control (scrambled) siRNA (con siRNA) or target-specific siRNA: β-catenin-siRNA (a) or NF-κBp65-siRNA (b), for 48h, as described in Methods. In each case the target specific siRNA was effective in significantly down-regulating the expression of the target proteins by >80-90%. The data presented are representative of three separate experiments conducted similarly in duplicate. β-cat=β-catenin; p65=NF-κBp65; Vec-con=empty vector; Con=control. The corresponding β-actin levels in each sample are shown.

**Figure 2.11: In situ Binding of Endogenous β-catenin to the Two Functional TCF4/LEF Binding Sites in the 5'(α)-promoter of *DCLK1*-gene**

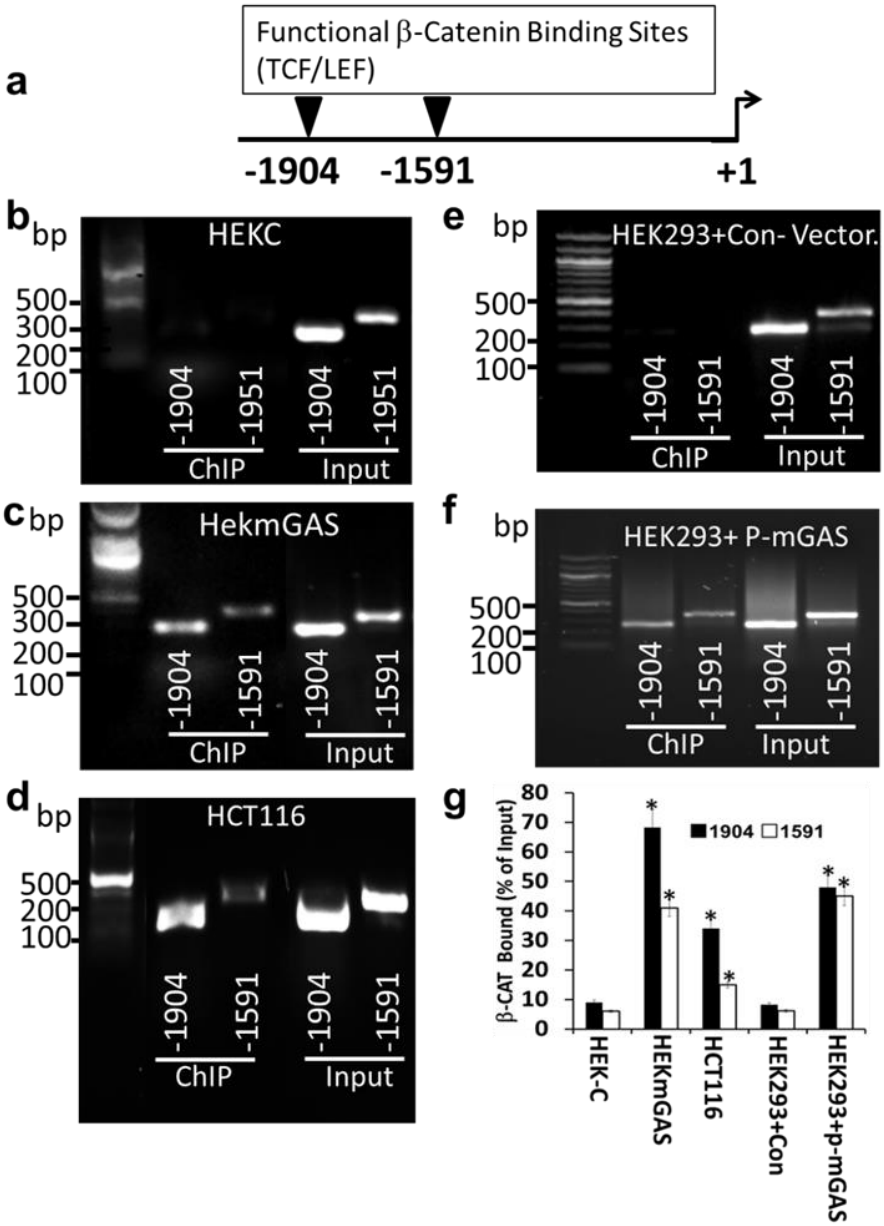


(a) = Map of functional TCF4/LEF binding sites in 5'(α)-promoter of *DCLK1*-gene, as determined by ChIP analysis for β-catenin binding. (b-d) = Relative binding of β-catenin to the indicated TCF4/LEF binding sites in the indicated cell lines, by ChIP analysis. Total level of β-catenin in the samples is presented as input. Electrophoresis gels were not cropped. (e-f) = Relative binding of β-catenin to functional TCF4/LEF binding sites in HEK-293 cells, transfected with either control vector (e) or PG expressing (p-mGAS) vectors (f), 48h before ChIP. Data presented in b-f is representative of six observations from three experiments. (g) = Relative binding of β-catenin, in situ, to functional binding sites in 5'(α)-promoter of *DCLK1*-gene, in different cell-lines, in presence or absence of mPG expression (described above), presented as % of input. Each bar-graph=mean±SEM of duplicates from three experiments. % binding of β-catenin was determined by densitometric analysis of indicated bands. *=$p<0.05$ vs. HEKC or HEK293+Con

**Figure 2.12: Role of NF-κB Binding Site in Activation of IntronV(β)-promoter of *DCLK1* gene**

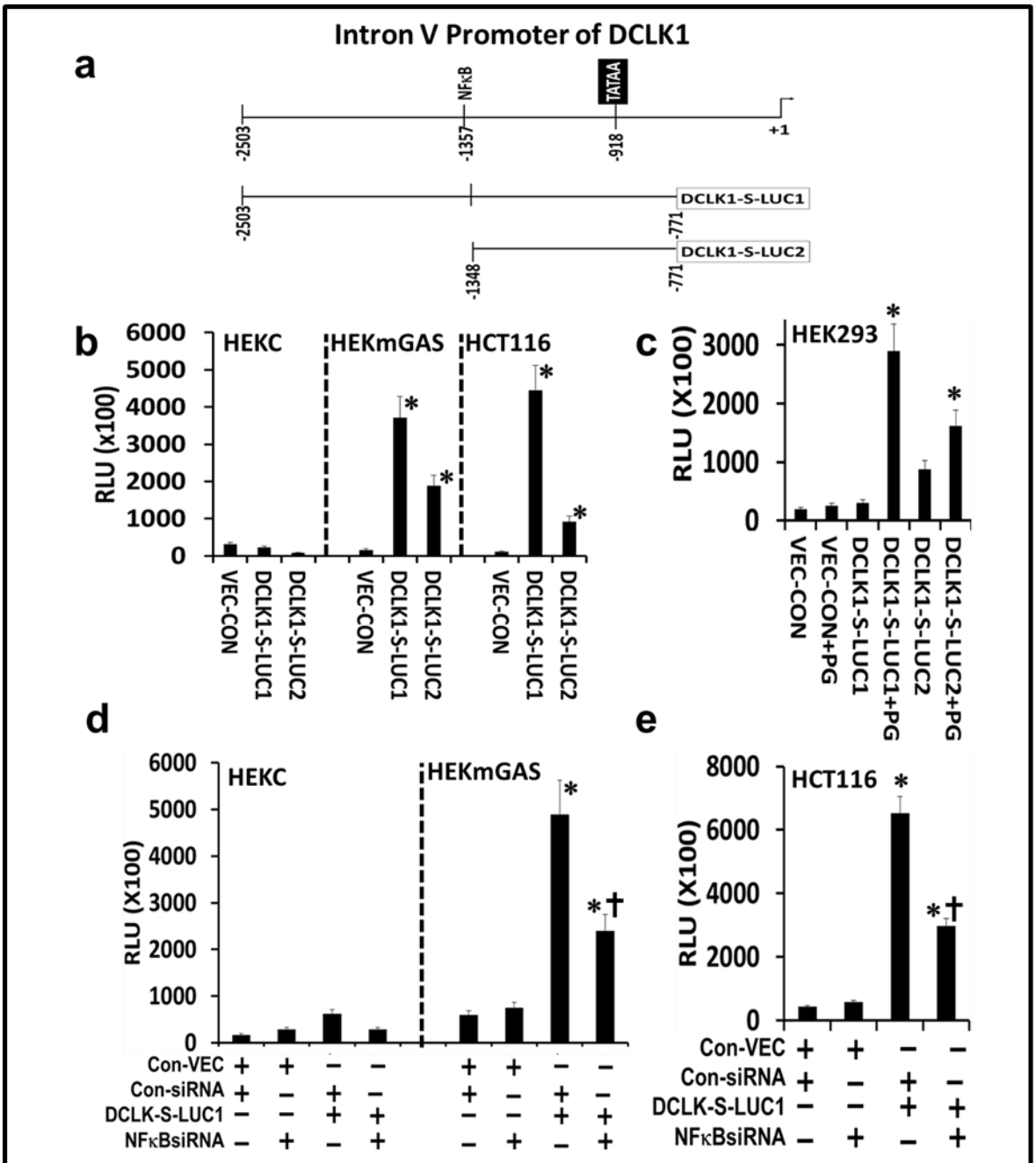


(a) = *In silico* analysis of IntronV(β)-promoter demonstrated presence of a consensus TATA box and a consensus NF-κB binding site, as shown. IntronV(β)-promoter-luciferase constructs, used in the current studies, are diagrammatically shown as DCLK1-S-LUC-1 and DCLK1-S-LUC-2. (b-e) = Transcriptional activity of promoter-reporter constructs in the indicated cell lines (b), in the presence or absence of PG expression (c) or treatment with either control or NF-κBp65-siRNA (d-e), as described in the legend of Figure 2.8. Transcriptional activation in terms of luminescence (RLU) is presented in b-e. Each bar-graph=mean±SEM of data from three experiments, conducted in triplicate. *=$p<0.05$ vs control vector in (b-e). † in (c)=$p<0.05$ vs LUC-1 or LUC-2 vector alone, in the absence of PG expression. † in (d,e)=$p<0.05$ vs corresponding data with control siRNA treated samples.

**Figure 2.13: Binding of Endogenous Activated NF-κBp65 to the Single NF-κB Binding Site in the IntronV(β)-promoter, *in situ*, in Human Cell Lines**

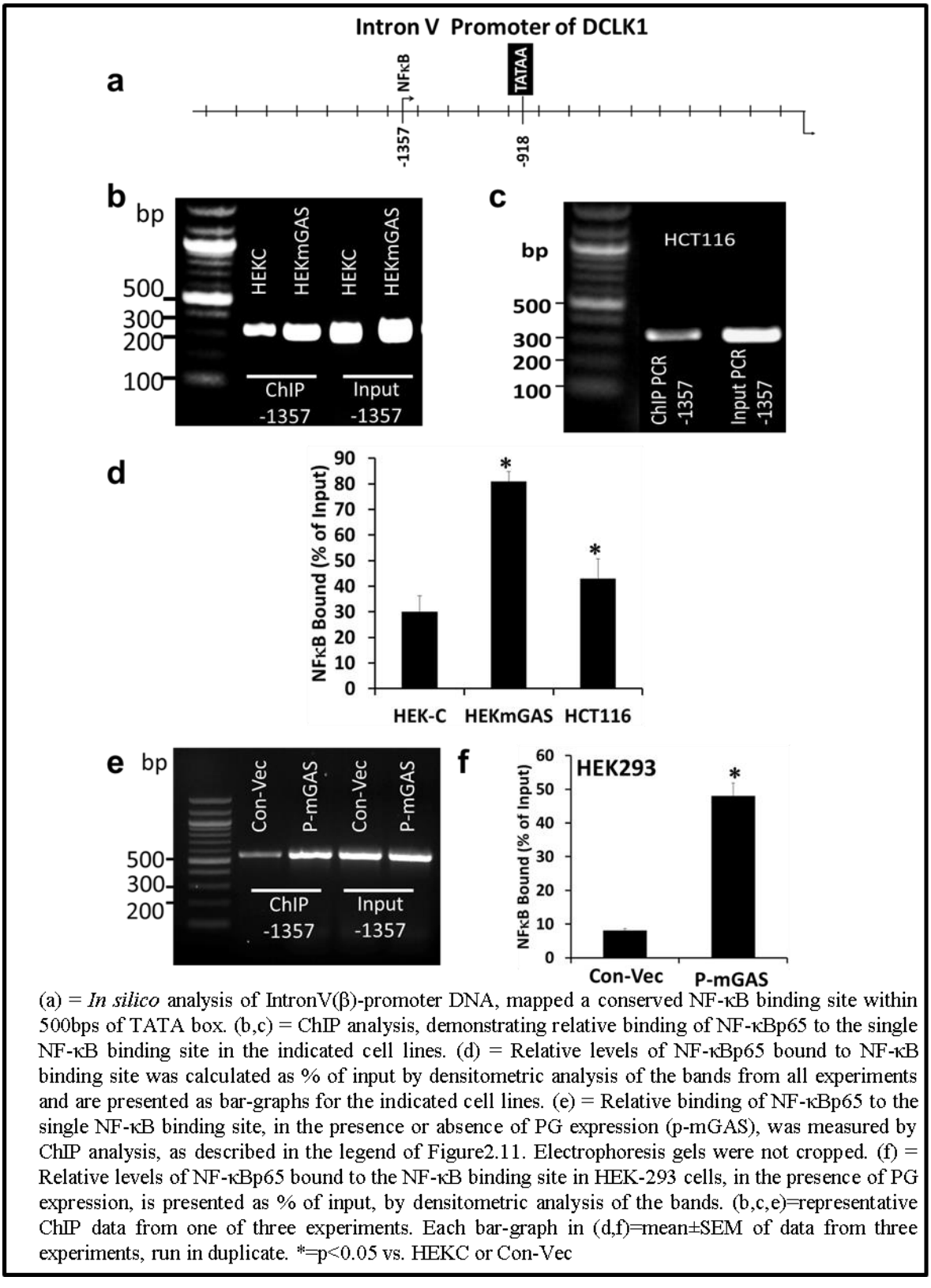


(a) = *In silico* analysis of IntronV(β)-promoter DNA, mapped a conserved NF-κB binding site within 500bps of TATA box. (b,c) = ChIP analysis, demonstrating relative binding of NF-κBp65 to the single NF-κB binding site in the indicated cell lines. (d) = Relative levels of NF-κBp65 bound to NF-κB binding site was calculated as % of input by densitometric analysis of the bands from all experiments and are presented as bar-graphs for the indicated cell lines. (e) = Relative binding of NF-κBp65 to the single NF-κB binding site, in the presence or absence of PG expression (p-mGAS), was measured by ChIP analysis, as described in the legend of Figure2.11. Electrophoresis gels were not cropped. (f) = Relative levels of NF-κBp65 bound to the NF-κB binding site in HEK-293 cells, in the presence of PG expression, is presented as % of input, by densitometric analysis of the bands. (b,c,e)=representative ChIP data from one of three experiments. Each bar-graph in (d,f)=mean±SEM of data from three experiments, run in duplicate. *=$p<0.05$ vs. HEKC or Con-Vec

**Figure 2.14: Overall Survival and Disease Free Survival of Patients with CRC, in Relation to Low or High Expression of DCLK1-S**

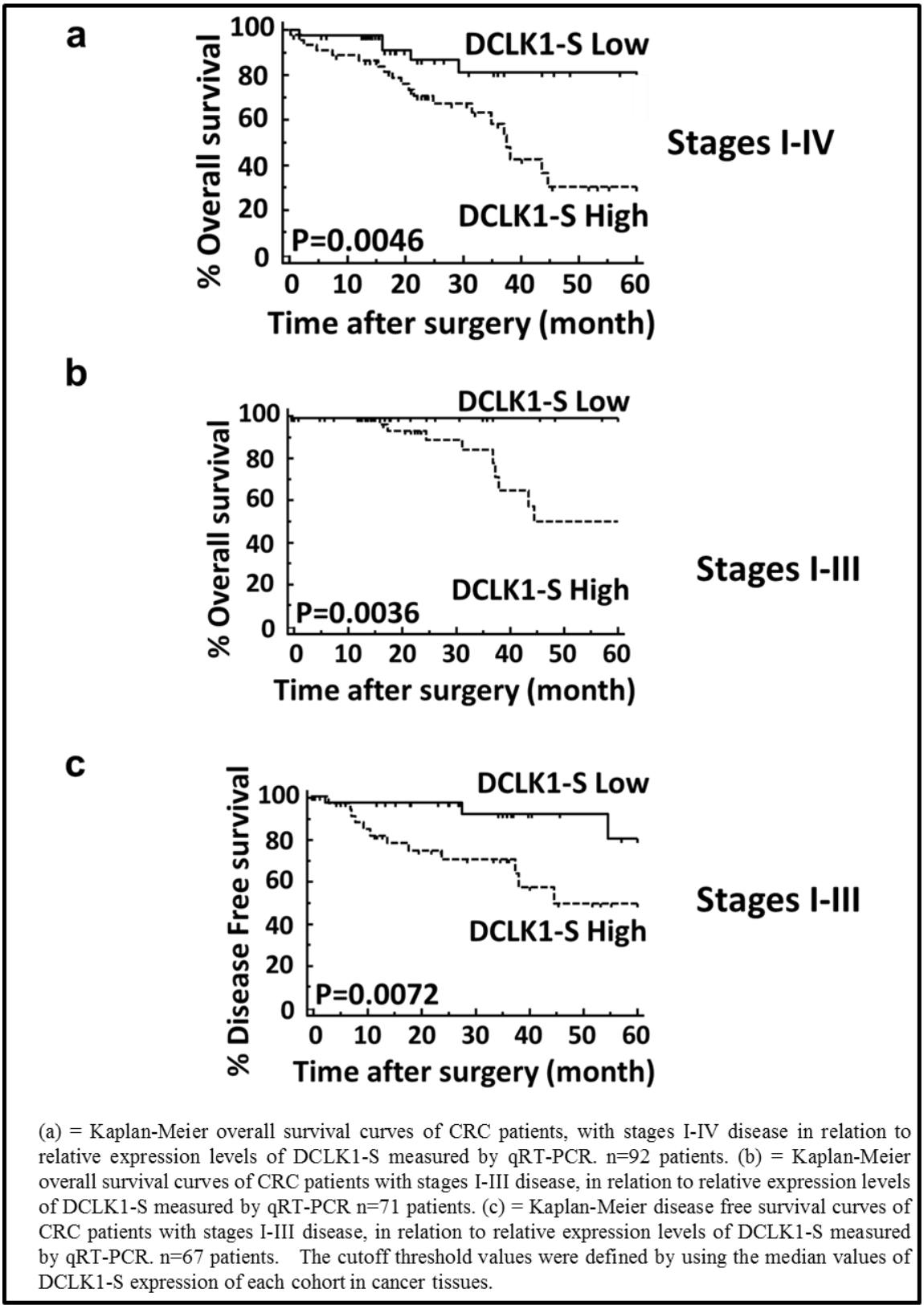


(a) = Kaplan-Meier overall survival curves of CRC patients, with stages I-IV disease in relation to relative expression levels of DCLK1-S measured by qRT-PCR. n=92 patients. (b) = Kaplan-Meier overall survival curves of CRC patients with stages I-III disease, in relation to relative expression levels of DCLK1-S measured by qRT-PCR n=71 patients. (c) = Kaplan-Meier disease free survival curves of CRC patients with stages I-III disease, in relation to relative expression levels of DCLK1-S measured by qRT-PCR. n=67 patients. The cutoff threshold values were defined by using the median values of DCLK1-S expression of each cohort in cancer tissues.

**Table 2.1: Oligonucleotide (Primer) Sequences Used for qRT-PCR/RT-PCR/ChIP/Promoter-methylation Assays**

**Table 2.1**
**Primer Sequences Used for RT-PCR/qRT-PCR And Other Assays**

| Target cDNA/gDNA | Species | Primer Sequence | Assay |
|---|---|---|---|
| DCLK1-Long (cDNA) | Human | F:GGAGTGGTGAAACGCCTGTAC | RT-PCR & qRT-PCR |
| | | R:GGTTCCATTAACTGAGCTGG | |
| DCLK1-Short (cDNA) | Human | F:ACACTAAGACTGTGTCCATGTTAGAACTC | RT-PCR & qRT-PCR |
| | | R:AAGCCTTCCTCCGACACTTCT | |
| DCLK1-Long (cDNA) | Mouse | F:TCAATGAGGACCAGCTCCAG | RT-PCR & qRT-PCR |
| | | R:TCCGAGAGAGTTCGGGTCA | |
| DCLK1-Short (cDNA) | Mouse | F:AAGACGTCAGCCTTACGCAG | RT-PCR & qRT-PCR |
| | | R:GAGAGATCCTCTGCTTCCGC | |
| -1443 TCF *cis* element in 5′ promoter (gDNA) | Human | F:AGAGCTGTGTCTGCTTGG | ChIP PCR |
| | | R:GTTCATTCCAGGGCAGCTTA | |
| -1141 TCF *cis* element in 5′ promoter (gDNA) | Human | F:TAAGCTGCCCTGGAATGAAC | ChIP PCR |
| | | R:CCCAAGCTATGCACTCTGGT | |
| NF-κB *cis* element in intron V promoter (gDNA) | Human | F:CTGTATCCACTGCCCTCTGT | ChIP PCR |
| | | R:GCAAAGCTATCTTCAGGAGG | |
| DCLK1-5′ promoter(-1067/-650) (gDNA) | Human | F:TTTAGGGGTGTAGTTAAGTTAGATG | DNA Methylation of CpG sites |
| | | R:AACCTCTCTCTCCAAAAAAAAA | |
| DCLK1-L-Luc (-2234/-503) (gDNA) | Human | F:ACATGACTGTGGGCAAATGA | Promoter Reporter Construct |
| | | R:CCCAAGCTATGCACTCTGGT | |
| DCLK1-S-Luc1(-2503/-771) | Human | F:GGTGCTTCCGTTCAAAGTGT | Promoter Reporter Construct |
| | | R:CAGTCTCAGGAATACCTTGC | |
| DCLK1-S-Luc2(-1348/-771) | Human | F:CCTCCTGAAGATAGCTTTGC | Promoter Reporter Construct |
| | | R:CAGTCTCAGGAATACCTTGC | |
| Primer 1-Adaptor | Non-Human | F:GAGAACCGCGTATCAACCCC | LM-PCR |
| Primer 2-DCLK1 common | Human | R:GTGACGTAGAGGAGCCGCCA | LM-PCR |

The forward (F) and reverse (R) primer sequences that were designed and used for amplifying the indicated target cDNA/gDNA for conducting the different assays are shown.

**Table 2.2: Relative Expression of DCLK1-L/S In Normal Colonic Mucosa Samples From 22 Patients By Western Blot Analysis**

**Table 2.2**

Relative Expression Of DCLK1-L/S In Normal Colonic Mucosa Samples From a total of22 Patients By Western Blot Analysis

| DCLK1-L/S Expression | # of Patients |
|---|---|
| DCLK1-L High Expression | 16/22 |
| DCLK1-L Low Expression | 5/22 |
| DCLK1-L No Expression | 1/22 |
| DCLK1-S High Expression | 1/22 |
| DCLK1-S Low Expression | 6/22 |
| DCLK1-S No Expression | 15/22 |

Normal colonic mucosa samples were collected from a total of 22 patients, free of adenocarcinomas, as described under methods. Relative band density in the western blots of normal colonic mucosa samples was analyzed using Image J, as described in Methods. Samples which expressed similar concentrations as HEK293 cells, used as positive control, were arbitrarily grouped under DCLK1-L high expression; samples which expressed less than 50% of that in HEK293 cells were arbitrarily grouped as DCLK1-L low expression; samples with no detectable expression, similar to that in HCT116 cells were labeled DCLK1-L No expression. Levels of DCLK1-S expression were quantified similarly, but HCT116 cells were used as a positive control, and HEK293 ce4lls were used as a negative control. Only one normal colon mucosal sample from patient 262, appeared to be negative for both S/L isoforms, which could be due to possible degradation of the sample, since samples after endoscopic collection, are usually flash frozen within 5min, but due to logistics can remain at room temperature for longer than 10 min, before flash freezing, as described.

**Table 2.3: RT-PCR Analysis of Long and Short Transcripts of DCLK1 in Human Colon Cancer Cell Lines**

**Table2.3**

RT-PCR analysis of long and short transcript of DCLK1 in human colon cancer cell lines

| Cell Line | ATCC # | DCLK1 LONG | DCLK1 SHORT | Mutant Gene(s) |
|---|---|---|---|---|
| LOVO | CCL-229 | - | + | APC, $KRAS^{13}$, MSH2 |
| SW1116 | CCL-233 | - | + | APC, $KRAS^{12}$, TP53 |
| SW837 | CCL-235 | - | + | APC, $KRAS^{12}$, TP53 |
| SW948 | CCL-237 | - | + | APC, APC, $KRAS^{61}$, PIK3CA |
| HCT116 | CCL-247 | - | + | $KRAS^{13}$, PIK3CA |
| SW-480 | CCL-228 | - | + | APC, $KRAS^{12}$, SMAD4 |
| DLD1 | CCL-221 | - | + | APC, $KRAS^{13}$, PIK3CA, TP53 |
| COLO205 | CCL-222 | - | | APC, BRAF, SMAD4, TP53 |
| RKO | CRL-2577 | - | + | BRAF, PIK3CA |
| LS411N | CRL2159 | - | + | APC, BRAF, TP53 |
| SW1417 | CCL-238 | - | | APC, BRAF, PIK3R1, TP53 |
| HT29 | HTB-38 | - | + | APC, BRAF, PIK3CA, SMAD4, TP53 |
| NCIH508 | CCL-253 | - | + | BRAF, PIK3CA, TP53 |
| Caco2 | HTB-37 | - | + | APC, SMAD4, TP53 |
| COLO320 | CCL-320 | - | + | APC, TP53 |

DCLK1-L and S primers were used to identify the isoforms being expressed by 15 colon cancer cell lines. The cell line name, ATCC catalog number, and mutational status of each cell line is provided. Most of these cell lines were purchased from ATCC in January of 2015. Cells positive for either DCLK1-L or S are represented by + sign, while cells negative for DCLK1-L or S are represented by - sign.

**Table 2.4: Clinicopathological Variables and DCLK1-S Expression in 92 Colorectal Cancer Patients**

**Table 2.4**

**Clinicopathological Variables and DCLK1-S Expression In 92 Patients with CRCs**

| Variable | | n | High (n=46) | Low (n=46) | P Value |
|---|---|---|---|---|---|
| Gender | Male | 57 | 29 | 28 | 1.000 |
| | Female | 35 | 17 | 18 | |
| Age (years) | <68 (median) | 47 | 20 | 27 | 0.211 |
| | ≧68 | 45 | 26 | 19 | |
| Tumor Size | ≧4.1cm (median) | 47 | 22 | 25 | 0.677 |
| | < 4.1cm | 45 | 24 | 21 | |
| Histological Type | Differentiated | 82 | 40 | 42 | 0.738 |
| | Undifferentiated | 10 | 6 | 4 | |
| Pathological T Category | pT1 | 11 | 3 | 8 | **0.019*** |
| | pT2 | 12 | 4 | 8 | |
| | pT3 | 59 | 32 | 27 | |
| | pT4 | 10 | 7 | 3 | |
| Vessel Involvment | Positive | 42 | 25 | 17 | 0.143 |
| | Negative | 50 | 21 | 29 | |
| Lymphatic Vessel Involvement | Positive | 70 | 41 | 29 | **0.007*** |
| | Negative | 22 | 5 | 17 | |
| Lymph Node Metastasis | N0 | 51 | 21 | 30 | 0.093 |
| | N1 | 41 | 25 | 16 | |
| Distant Metastasis | M0 | 71 | 35 | 36 | 1.000 |
| | M1 | 21 | 11 | 10 | |
| TNM Stage | Stage I | 19 | 5 | 14 | 0.061 |
| | Stage II | 30 | 15 | 15 | |
| | Stage III | 22 | 15 | 7 | |
| | Stage IV | 21 | 11 | 10 | |

**#Pearson's chi-square-test; *p<0.05**

Samples were obtained from patients with colonic adenocarcinomas at CRC stages of I-IV, from 92 patients in Japan, as described in Methods. The relative expression levels of DCLK1-S were analyzed by qRT-PCR, and high/low expression groups were classified by the median expression values in cancer tissues.

**Table 2.5: Multivariate Analysis for Predictors of Overall Survival**

**Table 2.5**

**Multivariate Analysis for Predictors of Overall Survival**

| Variables | Univariate | | | Multivariate | | |
|---|---|---|---|---|---|---|
| | *HR* | *95%Cl* | *p value* | *HR* | *95%Cl* | *p value* |
| Gender (Male vs. Female) | 1.2 | 0.52-2.77 | 0.66 | 1.53 | 0.57-4.13 | 0.41 |
| Age (≧68 (median) vs. <68) | 1.26 | 0.58-2.75 | 0.56 | 0.77 | 0.29-2.05 | 0.6 |
| Histological type (Undifferentiated/differentiated) | 3.49 | 1.39-8.77 | **0.008*** | 4.46 | 1.54-12.9 | **0.006*** |
| Tumor Size (≧4.1cm (median) vs. <4.1cm ) | 1.33 | 0.62-2.87 | 0.47 | 1.22 | 0.48-3.11 | 0.68 |
| Lymph Node metastasis(present/absent) | 13 | 3.90-43.1 | **<0.001*** | 4.70 | 1.17-18.8 | **0.03*** |
| Distant metastasis(present/ absent) | 9.67 | 4.35-21.5 | **<0.001*** | 11.2 | 3.65-34.6 | **<0.001*** |
| DCLK1-S expression(high/low) | 3.55 | 1.41-8.99 | **0.008*** | 7.93 | 2.25-27.9 | **0.0014*** |

**HR=hazard ratio** **Cl=confidence level** ***p<0.05**

Cox's proportional hazards models were used to estimate hazard ratios (HRs) for overall survival. In multivariate analysis, undifferentiated histological type, lymph node metastasis, distant metastasis, and high DCLK1-S expression were independent prognostic factors in the cohort of 92 CRC patients. Cl=confidence level; *p<0.05 for the indicated variables.

## 2.4 DISCUSSION

A clinically important discovery of our studies to address my Aim 1, was that an alternate-promoter (β) within IntronV of *DCLK1* gene is used by human colon cancer cell lines (hCCCs) and hCRCs to express a short-transcript of DCLK1 (DCLK1-S) (termed Isoform 2 in NCBI data base). In a cohort of 92 patients, we found that high-expressers of DCLK1-S had an overall worse survival and disease free survival than low-expressers (**Fig 2.14**). DCLK1-S expression was determined to be an independent prognostic factor for patients with CRCs (**Table 2.5**). Another important finding was that epigenetic silencing of 5'(α)-promoter and loss of expression of DCLK1-L during adenoma-carcinoma sequence of colon-carcinogenesis was chronologically followed by activation

of IntronV(β)-promoter of h*DCLK1*-gene, even though the two events are probably independent and not connected mechanistically.

We did not observe DNA-methylation of 5'(α)-promoter in HEKmGAS cells, suggesting that epigenetic silencing of 5(α)'-promoter is not a prerequisite for activating IntronV(β)-promoter. Sustained activation of NF-κB, downstream of autocrine PG, may play an important role as well, as suggested by data in **Figure 2.12**. Overexpression of PG in normal intestinal epithelial cells was ineffective towards imparting tumorigenic potential to the cells (Singh et al., 2010), suggesting that overexpression of PG and activation of NF-κB pathway, in the context of human embryonic cells, up-regulates tumorigenic pathway which appears to include activation of IntronV(β)-promoter of h*DCLK1*-gene. Inflammatory microenvironment of tumors, potentially leading to sustained activation of NF-κB pathway, may also play a role in elevated levels of DCLK1-S in Ads/AdCAs, in situ, (**Fig 2.3, 2.5**), as suggested in literature (Schwitalla et al., 2013). Thus, factors up-stream of activation of DCLK1-S expression, such as an inflammatory-microenvironment/progastrins/activation of oncogenic-pathways, likely play an important role in the expression of DCLK1-S in hCRCs.

A critical role of DCLK1 expression in maintaining tumorigenic/metastatic potential of hCCCs/CSCs was previously reported (Kantara et al., 2014; Sureban et al., 2011a). In the current studies, DCLK1-S was identified as the major isoform in hCCCs/hCRCs, with a few exceptions (**Figs 2.3, 2.5**), suggesting that DCLK1-S likely supports the previously reported tumorigenic/metastatic potential of hCCCs (Kantara et al., 2014; Sarkar et al., 2012). However, in mouse models of colon-carcinogenesis, high levels of DCLK-L in the absence of DCLK-S are expressed (**Fig 2.5e**). Co-expression of diphtheria-toxin in DCLK1+cells in small-intestines/colons, results in loss of tumorigenesis in mouse models of colon carcinogenesis (Nakanishi et al., 2013; Westphalen et al., 2014). These findings suggest that DCLK-L expression is required for colon tumorigenesis in mice. Metastatic spread of mouse colon tumors, however, has not

been reported in $Apc^{Min/+}$ mice or in mice treated with AOM±DSS (Cobb et al., 2004; Nakanishi et al., 2013; Singh et al., 2000a; Westphalen et al., 2014). Epithelial-mesenchymal-transition by hCCCs requires DCLK1 expression (Chandrakesan et al., 2014), suggesting that metastatic spread of colon cancer cells may require the expression of DCLK1-S by hCCCs, which only express DCLK1-S (**Table 2.3**). We recently reported expression of DCLK1-S by circulating cancer-stem-cells in hCRC patients (Kantara et al., 2015), providing further evidence that DCLK1-S may be required for imparting metastatic potential to hCCCs. The latter possibility is further supported by the fact that, HEKmGAS cells overexpressing DCLK1-S (**Figs 2.3, 2.5**), implanted in the cecum of athymic nude mice and metastasized to the liver (Sarkar et al., 2012). Thus, metastasis of colon tumors is possible in mice, but absence of DCLK-S expression by mouse tumors may impede metastasis. This intriguing possibility needs to be examined in future.

As discussed in introduction, DNA methylation and epigenetic-silencing of 5'(α)-promoters has been documented for many genes during tumorigenesis. Multiple promoters are methylated in both mouse tumors and hCRCs (Grimm et al., 2013). However, in a recent report (Borinstein et al., 2010), it was confirmed that 5'(α)-promoter of some genes (including DCLK1) are methylated and silenced in human colon tumors, but not in mouse colon tumors. Reports in literature (as discussed in introduction) confirm that 5'(α)-promoter of mouse *DCLK1*-gene does not get silenced during tumorigenesis, as confirmed by us (**Fig 2.5**). In the current studies, we further confirm that loss of DCLK1-L in hCCCs is due to DNA methylation and can be reversed with de-methylating agents (**Fig 2.7d,e**). Normal human colon cell line and hNCs, on the other hand, continue to express DCLK1-L from 5'(α)-promoter. This important difference in hNCs and hCCCs was confirmed by primer-extension analysis (**Fig 2.7a-c**). Majority of the hCCCs/CRCs up-regulate expression of DCLK1-S from an alternate (β)-promoter within IntronV, while mouse colon tumors do not (**Fig 2.5**), for unknown reasons.

The activation of (β)-promoter for transcribing DCLK1-S isoform was recently described in mouse cerebellum (Pal et al., 2011). The use of alternate-promoters for transcribing shorter isoforms, especially for genes which have hypermethylated 5'-promoters, is a dominant phenomenon and more common than transcription of splice-variants during development and disease progression (Archey et al., 1999; Hoivik et al., 2013; Pal et al., 2011). There is thus accumulating evidence in recent literature which strongly supports our novel findings regarding the use of an alternate-(β) promoter within IntronV for expressing shorter isoforms of DCLK1 in hCCCs/hCRCs. More recently, shorter isoforms of DCLK1 (47KDa) were reported in KRAS mutant hCCCs (Hammond et al., 2015), which further supports our findings; however, we did not observe a specific correlation between expression of DCLK1-S and mutant phenotype of hCCCs (**Table 2.3**).

By *in silico* analysis, we discovered that while the 5'(α)-promoter was positive for functional TCF4/LEF binding sites and a few NF-κB binding sites (**Figs 2.8, 2.9, 2.11**), the IntronV(β)-promoter was positive for a functional NF-κB binding site, upstream of a TATA box (**Figs 2.8, 2.11**). We therefore examined the role of NF-κB/β-catenin signaling pathways in regulating the activity of α/β promoters. Since progastrins activate NF-κB/β-catenin signaling pathways (Rengifo-Cam et al., 2007; Sarkar et al., 2011; Umar et al., 2008; Umar et al., 2009), resulting in increased expression of stem cell markers, including DCLK1 in normal colon crypts and transformed cells (Sarkar et al., 2012; Sarkar et al., 2011), we used progastrin for activating NF-κB/β-catenin in HEK293/HEKC cells, and examined their role in activating 5'(α)-promoter for DCLK1-L expression. Since tumorigenic/metastatic potential of HCT116/HEKmGAS cells is dependent on autocrine PG (Sarkar et al., 2012; Singh et al., 2007), we used these cell lines to examine the role of NF-κBp65 in mediating transcriptional activation of intronV(β)-promoter for expressing DCLK1-S. Experiments with Promoter-reporter constructs along with ChIP assays, in the presence or absence of siRNAs against the two

transcriptional factors (**Figs 2.8-2.13**), confirmed that TCF4/LEF binding sites, in response to activated β-catenin, activates 5'(α)-promoter of Dclk1-L (in tissues such as mouse colons/tumors (Jin et al., 2009; Sarkar et al., 2011), while NF-κB binding site, in response to activated NF-κBp65 and its partners, activates IntronV(β)-promoter (thus up-regulating DCLK1-S expression in hCCCs, **Figs 2.3, 2.5, Table2.3**). NF-κB binding sites in the 5'(α)-promoter, on the other hand, did not appear to be playing any role in activating the (α)-promoter and/or the expression of DCLK1-L (**Fig 2.9**). Both the 5'(α) and IntronV(β) promoters are positive for several other binding sites, which likely play synergistic/antagonistic roles in dictating transcriptional activity of the promoters, which was not examined in Aim 1. However, in Aim 3, a negative regulator of DCLK1-S expression was discovered, and is described in detail in Chapter 4.

In summary, our findings from my aim 1 studies, suggests that the 5'(α)-promoter of *DCLK1*-gene becomes epigenetically silenced during colon-carcinogenesis at early stages, resulting in loss of expression of DCLK1-L in adenomas and hCRCs. Oncogenic and inflammatory pathways associated with colon-carcinogenesis may be involved in transcriptional-activation of the alternate-(β) promoter within IntronV, resulting in alternate expression of DCLK1-S. Usage of two separate promoters by normal vs. cancer cells in humans provides an opportunity for developing methods for specifically targeting DCLK1-S as an approach for eliminating colon cancer growths. Additionally, since high expressers of DCLK1-S had worse overall/disease free survival, DCLK1-S expression by colonic tumors may provide a useful diagnostic/prognostic tool.

# Chapter 3: DCLK1-S enhances the invasive potential of colon cancer cells via a novel NFATC2 mediated pathway, resulting in enhanced expression of extracellular matrix protein, COL3A1.

***This chapter is a copy of a manuscript to be submitted to Cancer Research (O'Connell et al., 2016c). Part of this work has also been selected to be presented as a Poster of Distinction at Digestive Disease Week, 2016 (O'Connell et al., 2016d).**

## 3.1 INTRODUCTION

Colorectal cancer is the third most prevalent and deadly cancer in the United States (Siegel et al., 2014a). Although many improvements have been made in screening and early detection of colonic growths, ~15-25% of colorectal cancer patients are currently diagnosed with advanced stages of colorectal cancer, and already have metastatic disease (Marques et al., 2014). Of the patients diagnosed with advanced stage colorectal cancer, ~80-90% have unresectable metastatic liver disease (Marques et al., 2014). Nearly 50% of all patients who are diagnosed with early stages of colorectal cancers, will eventually develop metastases in their lifetime, (Marques et al., 2014). Patients whose colorectal cancers are detected as primary cancers, localized to the colons (Stages I-II), have a 5-year survival rate of 90.1%. However, when the cancer has spread to lymph nodes or adjacent organs, the 5-year survival rate decreases to 69.2%, and when the cancer spreads to distant organs, the 5-year survival rate steeply decreases to 11.7% (Siegel et al., 2012).

Cancer stem cells maintain their capacity to self-renew and can potentially differentiate into various cell types, however, they can also give rise to malignant growths and maintain tumorous growths (Abetov et al., 2015; Kozovska et al., 2014). Cancer stem cells are believed to be resistant to currently used chemo and radiation therapies (Cherciu et al., 2014; Kantara et al., 2014; Wang et al., 2015b). Although the

bulk of the colonic tumor mass is reduced in response to the currently used therapies, a small population of cancer stem cells can survive treatment and are capable of re-growing as primary/metastatic tumors, resulting in relapse of the disease (Cherciu et al., 2014; Kantara et al., 2014; Wang et al., 2015a). Thus targeting cancer stem cells along with conventional therapy could provide a more comprehensive treatment strategy for cancer patients, as suggested by the results of our recent findings (Kantara et al., 2014), and as emphasized in recent review articles (Cherciu et al., 2014; Wang et al., 2015b). Several putative stem cell markers, including LGR5, CD44, and DCLK1, have been reported to identify normal colonic stem cells; however, we recently reported (Sarkar et al., 2012), that colon cancer stem cells express many of the same markers as intestinal normal stem cells, as confirmed by others (Barker, 2014; Cherciu et al., 2014; Hirsch et al., 2014; Nakanishi et al., 2013). Therefore targeting cancer stem cells, while sparing normal stem cells, remains a challenge, and was discussed in our recent publication (and presented here in Chapter 2) (O'Connell et al., 2015)..

An important role of DCLK1 has been implicated in colon tumorigenesis in mice (Bailey et al., 2014; Nakanishi et al., 2013; Westphalen et al., 2014) and in maintaining the proliferative potential of human colon cancer cells (Kantara et al., 2014; Sarkar et al., 2012; Sureban et al., 2011b). In a recent report from our laboratory, we described that a subset of DCLK1+ cancer stem cells were resistant to inhibitory effects of chemopreventive/chemotherapeutic agents, and down-regulation of DCLK1 combined with chemoprevention was required for eliminating cancer stem cells, in vitro and *in vivo*, and for avoiding relapse (in terms of re-formation of tumorospheres from treated cells) (Kantara et al., 2014). These findings highlighted a possible critical role of DCLK1 in maintaining the *in vitro* and *in vivo* growth of human colon cancer cell lines. We also recently reported that 2 isoforms of DCLK1 (DCLK1-L/DCLK1-S) are transcribed by two different promoters (5'(α) and IntronV(β)) (O'Connell et al., 2015). The DCLK1-L isoform is silenced by DNA methylation in human colon adenocarcinomas, while the

DCLK1-S isoform is upregulated by many fold in colonic tumors (O'Connell et al., 2015). Our novel findings regarding alternate promoter usage by human normal colons vs. colorectal cancers suggest that one can develop strategies for specifically targeting DCLK1-S to eliminate colon cancer stem cells, while sparing DCLK1-L functions in the brain and other normal cells.

The loss of DCLK1 expression in cancer cells has been reported to result in the loss of proliferative/tumorigenic/metastatic potential of colon cancer cells (Kantara et al., 2014; Sureban et al., 2011b). However, RNAi methods used so far, target both isoforms of DCLK1. In the current studies we used shRNA knockdown methods to specifically target DCLK1-S isoform in human colon cancer cell lines, in order to delineate the biological role of cancer specific DCLK1-S isoform. Isogenic clones of a representative human colon cancer cell line (HCT116 cells) were generated to either express control shRNA (HCT-C) or DCLK1-shRNA (HCT-D). Western Blot analysis and RT-PCR analysis confirmed 80-90% knockdown of DCLK1-S expression in HCT-D clones compared to HCT-C clones. The goal of my Aim 2 studies was to evaluate molecular/genetic pathways mediating effects of DCLK1-S. In order to achieve this goal, isogenic clones of HCT116 cells (HCT-C/HCT-D) were subjected to next generation sequencing.

Many pathways were identified to be altered in response to DCLK1-S downregulation in HCT-D vs. HCT-C clones, as described in results. The pathways/molecules associated with cell movement/invasion appeared to be one of the most significantly affected. While I was in the process of completing my Aim 2 studies, a recent study was published, which implicated DCLK1 to be critically involved in accelerating tumor invasion and metastasis of pancreatic cancer cells (Ito et al., 2016). Ito et al. demonstrated that DCLK1 was predominantly expressed in cancer stem cells, in agreement of our previous findings (Kantara et al., 2014), and that DCLK1 was involved in imparting invasive and metastatic potential to cancer cells (Ito et al., 2016).

Overexpression of DCLK1 resulted in an enhanced metastatic phenotype, while knockdown of DCLK1 suppressed metastasis of pancreatic cancer cells both *in vitro* and *in vivo* (Ito et al., 2016). Ito et al. suggested that DCLK1 was essential for the invasive/metastatic phenotype of cancer stem cells (Ito et al., 2016). Therefore, for my Aim 2 studies, I investigated the genes/pathways, downstream of DCLK1-S expression, which may be mediating the invasive potential of colon cancer cells. Of the genes identified by RNAseq analysis, downstream of DCLK1-S expression, SPARC and COL3A1 emerged as two candidate genes/proteins, which were increased by many fold in response to DCLK1-S, and which have been previously reported to play a critical role in enhancing the invasive potential of cancer cells (Arnold and Brekken, 2009; Basso et al., 2001; Ewald et al., 2013; Nagaraju et al., 2014; Su et al., 2014; Turashvili et al., 2007; Xiong et al., 2014). Hence the role of DCLK1-S in mediating the expression of SPARC and COL3A1, and their role in increasing the invasive potential of DCLK1-S expressing colon cancer cells was evaluated as part of my Aim 2 studies.

### 3.1.1 SPARC

SPARC (secreted protein, acidic, cysteine-rich), a secreted glycoprotein, is a member of the matricellular family of proteins. Matricellular proteins are nonstructural extracellular matrix (ECM) proteins that contribute to the structure and composition of the ECM, and mediate cellular interactions with the adjacent microenvironment (Alford and Hankenson, 2006; Bornstein, 2009; Bornstein and Sage, 2002). SPARC plays a key role in regulating matrix organization and modulating cell behavior (Bornstein, 2009).

The *SPARC* gene is located on the long arm of chromosome 5 at position 31-33 (5q31-33). Previous names of SPARC include Osteonectin (ON) and Basement-Membrane Protein 40 (BM-40). Three transcript variants of SPARC have been identified. The full length predominant transcript (NM_003118.3) is 3604 bp, contains 9 exons, and

results in a 303 aa peptide with a molecular mass of 34.632 kDa (NP_003109.1) (as described in the NCBI database). SPARC isoform 2 (NM_001309443.1) is 3601 bp and utilizes an alternate in-frame splice junction. The resulting transcript contains 9 exons and results in a 302 aa peptide (NP_001296372.1), that has the same N and C terminus as compared to isoform 1. SPARC isoform 3 (NM_001309444.1) is 3621 bp and utilizes an alternate splice junction located at the 5' end of exon 9. The resulting transcript contains 10 exons and results in a 341 aa peptide (NP_001296373.1) that has a longer C-terminus as compared to isoforms 1 and 2.

The predominant SPARC mature peptide is composed of an N-terminal acidic domain, a follistatin-like domain, and an extracellular C-terminal domain as described in **Figure 3.1**. The N-terminal acidic domain, rich in Asp and Glu, functions to binds calcium and has chemosensitizing properties (Kos and Wilding, 2010; Lane and Sage, 1990). A possible role of the N-terminal acidic domain in inducing apoptosis has also been reported (Rahman et al., 2011). The follistatin-like N terminal domain contains cysteine-rich residues and was reported to inhibit cell proliferation in earlier studies (Funk and Sage, 1991), and to bind both activin and inhibin in later studies (Kos and Wilding, 2010). Opposing effects of the N terminal domain of SPARC have been reported on angiogenesis, where in both stimulation of angiogenesis (Lane et al., 1994), and inhibition of endothelial cell migration (Chlenski et al., 2004; Funk and Sage, 1991), have been reported. The C-terminal extracellular domain is a calcium binding domain that binds calcium (Pottgiesser et al., 1994), fibular collagens (Mayer et al., 1991; Pottgiesser et al., 1994; Sasaki et al., 1998), and PDGF (Platelet-Derived Growth Factor) (Kupprion et al., 1998; Sage and Vernon, 1994). A possible role of the extracellular domain in anti-angiogenesis (Chlenski et al., 2004; Lane and Sage, 1990), inhibition of cellular proliferation (Sage et al., 1989), and induction of MMPs (Matrix Metalloproteinases) (Sasaki et al., 1997; Sasaki et al., 1998) has been reported, making it difficult to predict the specific functions of this protein. It is possible that the function of

SPARC will likely be dictated by the cell type and microenvironment of the cells, and may be quite contextual. The receptor for SPARC, if any, has yet to be identified, and it is not thought that SPARC competes with any other ligands (Bradshaw and Sage, 2001).

**Figure 3.1: Diagrammatic Representation of SPARC Protein Domains**

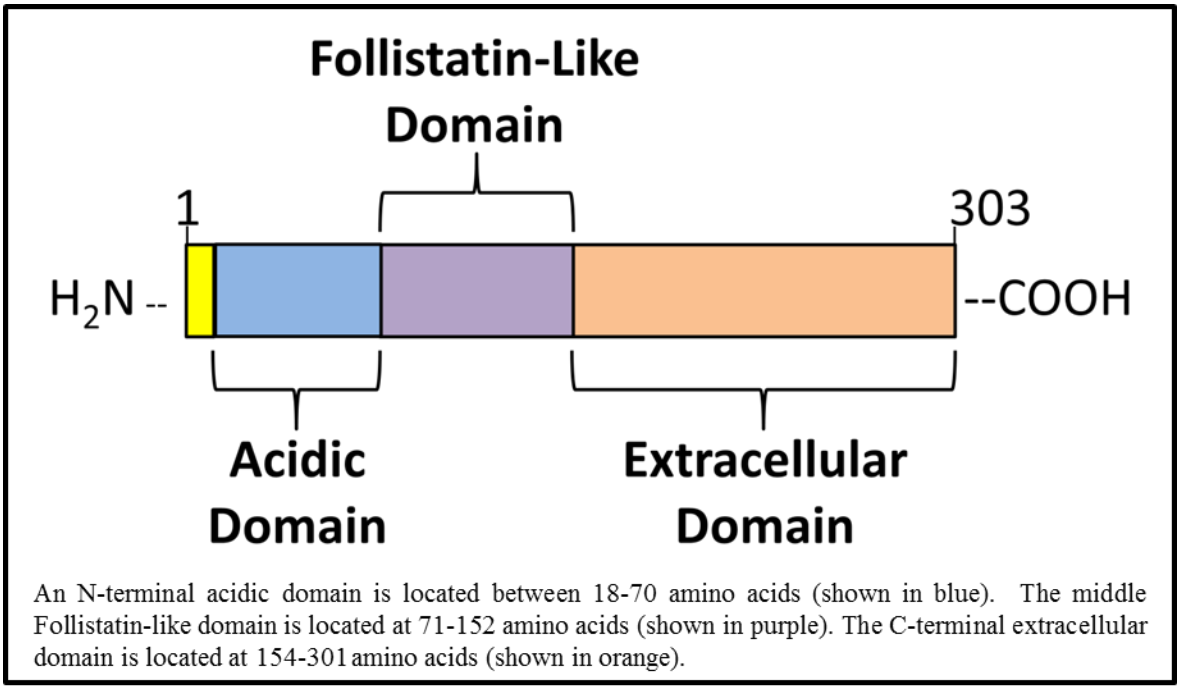


An N-terminal acidic domain is located between 18-70 amino acids (shown in blue). The middle Follistatin-like domain is located at 71-152 amino acids (shown in purple). The C-terminal extracellular domain is located at 154-301 amino acids (shown in orange).

Although SPARC plays a critical role in maintenance of the ECM in tissue development and normal tissue homeostasis (Bradshaw, 2009), the role of SPARC in cancer remains highly controversial, for all the reasons described above. The role of SPARC in cancer has been extensively studied and reviewed (Arnold and Brekken, 2009; Chlenski and Cohn, 2010; Nagaraju et al., 2014; Said and Theodorescu, 2013; Tai and Tang, 2008), however it appears that the activity of SPARC is both context and tissue type dependent, as discussed above. Recently, SPARC's role in different tumor types including prostate cancer, urothelial cancer, colorectal cancer, pancreatic cancer, esophageal cancer, gastric cancer, hepatocellular carcinoma, ovarian cancer, cervical

cancer, endometrial cancer, breast cancer, skin cancer, lung cancer, meningioma, glioma, medulloblastoma, and neuroblastoma was reviewed (Chlenski and Cohn, 2010; Said and Theodorescu, 2013; Tai and Tang, 2008). In each tumor type, SPARC was found to be differentially expressed, and its expression was found to relate to variable patient outcomes. In some tumors, high expression of SPARC was found to correlate to overall worse patient survival, while in other cancers low expression of SPARC was found to correlate with overall worse patient survival (Chlenski and Cohn, 2010; Said and Theodorescu, 2013; Tai and Tang, 2008). However, the pattern of expression of SPARC (whether enhanced or decreased in tumor tissues as compared to normal tissues) is contextual, and dependent on type of cancer (Chlenski and Cohn, 2010; Said and Theodorescu, 2013; Tai and Tang, 2008). Many different and sometimes opposite functions of SPARC have been described in the cancerous growths in different organs, and include modulation of ECM, cell adhesion, migration, cell survival, apoptosis, tumor growth, and even response to chemotherapy and radiation,, as detailed in recent reviews (Arnold and Brekken, 2009; Nagaraju et al., 2014). Thus SPARC may function either as a pro-invasive factor or even a tumor suppressor, which is tumor specific, and could also be contextual, in relation to many other factors (including study design and isoform-specificity), which require further investigation.

As in other tissue types, the role of SPARC in colorectal cancer remains poorly understood (Said and Theodorescu, 2013; Tai and Tang, 2008). It was initially reported that SPARC expression was localized to the basement membrane (Wewer et al., 1988) and SPARC was detected in multiple cases of colorectal cancers (Porter et al., 1995). It was also reported that SPARC expression in colorectal cancer patients was upregulated in the stroma of resected colorectal tumors as compared to non-diseased colon (Lussier et al., 2001). A microarray gene expression study demonstrated high levels of SPARC in bulk-undissected colorectal tumors as compared to normal colonic tissues (Chan et al., 2008). Using microscopic fine-needle dissection of bulk colorectal

tumors, SPARC expression was found to be increased by six fold in malignant colorectal epithelial cells as compared to normal epithelial cells (Wiese et al., 2007). However, using both colon cancer cell lines and human colorectal tumors, Yang et al., demonstrated that SPARC expression was suppressed in both cancer cell lines and tumors as compared to normal mucosa (Yang et al., 2007). The methylation status of the SPARC promoter was evaluated and 6 of the 7 cell lines and all 20 primary colon cancers demonstrated hypermethylation of the promoter (Yang et al., 2007). SPARC expression was examined in a cohort of 292 CRC patients and it was found that patients lacking SPARC expression had significantly worse overall survival compared to patients with normal expression (Yang et al., 2007). Yang et al., concluded that SPARC was epigenetically silenced in colorectal tumors and that silencing of SPARC resulted in worse overall survival (Yang et al., 2007). In tumors resistant to chemotherapy, SPARC expression was found to be lower than in tumors sensitive to chemotherapy (Tai et al., 2005). When SPARC was overexpressed in resistant tumors, SPARC increased the sensitivity of colon cancer cells to chemotherapy and radiation suggesting that treatment of resistant colorectal tumors with addition of SPARC could increase survival of patients with low levels of SPARC expression (Tai et al., 2005). The findings of Yang et al and Tai et al., as described above, however, appear to be the exception, rather than the rule, since overwhelming literature in the colorectal cancer area, suggests a promotional role of SPARC in colorectal cancers. Further studies are therefore necessary in order to fully understand the role of SPARC in colorectal cancer.

### 3.1.2 COL3A1

The *COL3A1* (collagen, type III, alpha 1) gene is located on the long arm of chromosome 2 at position 31 (2q31). The COL3A1 transcript (NM_000090.3) is 5490 bps, contains 51 exons and results in a 1466 aa preprocollagen polypeptide

(NP_000081.1) (as described in the NCBI database). The COL3A1 polypeptide is composed of two propeptide domains, two non-helical regions, a triple helical region and an N-terminal signaling domain, as shown in **Figure 3.2**.

**Figure 3.2: Diagrammatic Representation of COL3A1 Protein Domains**

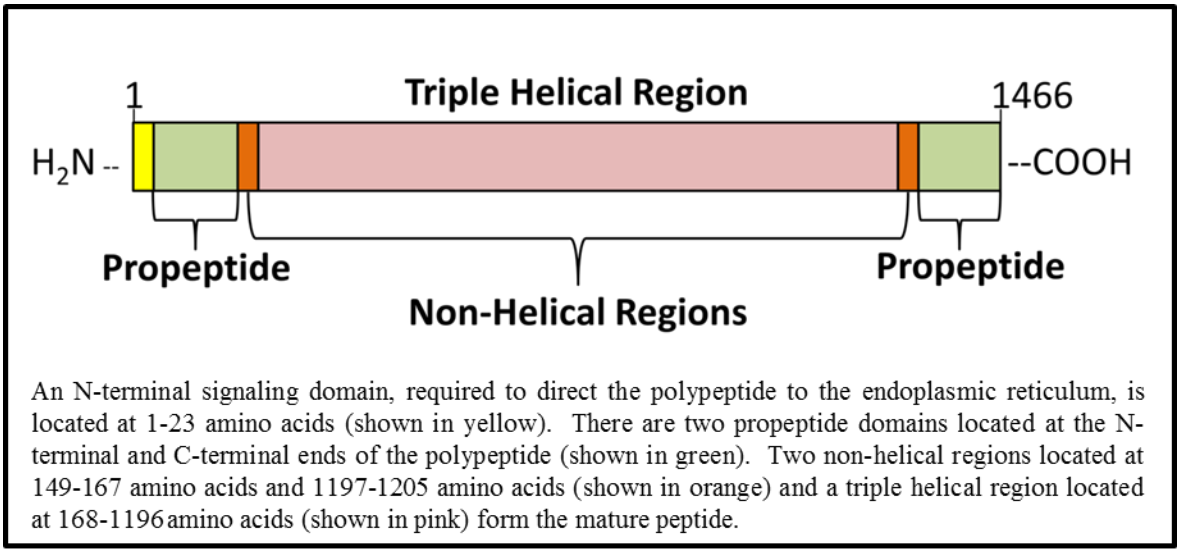


An N-terminal signaling domain, required to direct the polypeptide to the endoplasmic reticulum, is located at 1-23 amino acids (shown in yellow). There are two propeptide domains located at the N-terminal and C-terminal ends of the polypeptide (shown in green). Two non-helical regions located at 149-167 amino acids and 1197-1205 amino acids (shown in orange) and a triple helical region located at 168-1196 amino acids (shown in pink) form the mature peptide.

The polypeptide of COL3A1 is further processed into Type III collagen. Type III collagen synthesis is described in **Figure 3.3**. Briefly, the preprocollagen polypeptide is hydroxylated and glycosylated within the rough endoplasmic reticulum and a triple-helix is assembled from three preprocollagen polypeptides to form procollagen. Propeptides are cleaved to form the collagen molecule, and assembled into larger collagen fibrils which eventually aggregate to form a collagen fiber, described as Type III collagen ($[\alpha1(III)]_3$). Type III collagen is distributed throughout skin, internal organs, and blood vessels (Bustin, 2015).

**Figure 3.3: Type III Collagen Synthesis**

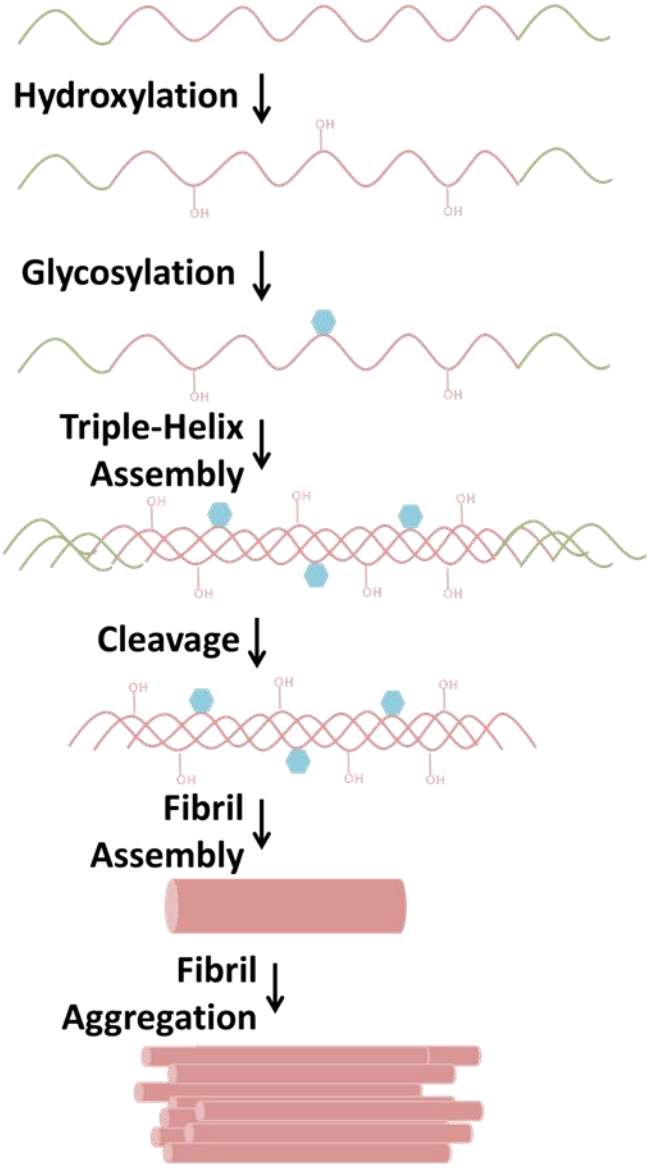


Type III collagen is composed of 3 α1(III) polypeptide chains. Polypeptide chains, called preprocollagen, are synthesized on membrane-bound ribosomes and then migrate to the lumen of the Rough Endoplasmic Reticulum. In the lumen of the ER, the peptide is hydroxylated at select prolines (by P4H and P43 proyl-hydroxylases) and lysines (by LH1, LH2, and LH3 lysine-hydroxylases). Following hydroxylation, hydroxylysines are glycosylated (by LH3). Three preprocollagen peptides combine to form procollagen, a triple stranded helical molecule stabilized by hydrogen bonds. The procollagen molecules are then packaged and secreted from the Golgi Apparatus. Once secreted, propeptides (shown in green), are cleaved to form collagen molecules (by metalloproteinases). Collagen molecules then assemble in the extracellular space to form larger collagen fibrils. Collagen fibrils then aggregate to form a collagen fiber.

Multiple mutations of COL3A1 have been reported (Kuivaniemi et al., 1991), and most result in Ehlers-Danlos syndrome type IV (EDS type IV). EDH type IV is a devastating inherited connective tissue disorder that results in acrogeria (sunken face), translucent skin, and severe obstetrical, arterial, and digestive complications (Germain, 2007).

Throughout literature, COL3A1 has been reported to be upregulated in a large number of tumor types. Using a meta-analytical approach, Wu et al, mined the NCBI dbEST database for differentially expressed genes (DEGs) between normal and cancer tissues from different tumor types (Wu et al., 2012a). COL3A1was identified as a DEG between normal and cancer tissues from multiple organs, including breast, liver, prostate, and thyroid, demonstrating that COL3A1 is a potential biomarker of cancer in many different tissues (Wu et al., 2012a). Serum levels of PIIP (N-terminal peptide cleaved from the type III collagen precursor molecule) have been reported to be elevated in patients with ovarian cancer (Kauppila et al., 1989), liver cancer (Hatahara et al., 1984), breast cancer (Hatahara et al., 1984), colon cancer (Hatahara et al., 1984), pancreatic cancer (Hatahara et al., 1984), stomach cancer (Hatahara et al., 1984), lung cancer (Hatahara et al., 1984), uterine cancer (Hatahara et al., 1984), soft tissue sarcomas (Wiklund et al., 1992), and metastatic bone tumors (Yudoh et al., 1994).

Several Microarray studies have demonstrated that COL3A1 is enhanced in gastric cancer tumors as compared to normal gastric tissues (Hippo et al., 2002; Oue et al., 2004). Using cluster analysis, Hu et al., demonstrated that COL3A1 was involved in ECM-receptor mediated interactions and focal adhesion pathways, both of which are enriched in gastric cancers (Hu and Chen, 2012).

By analyzing 36, publicly available patient databases, Ewald et. al. reported that COL3A1 was specifically associated with muscle invasive bladder transition cell carcinomas, and detected COL3A1 in patients with advanced stages of muscle invasive

bladder tumors (T2 and T3 tumors), with minimal expression of COL3A1 in T1 tumors (Ewald et al., 2013).

An important tumor suppressive role of let-7d was demonstrated in renal cell carcinoma (RCC) in which COL3A1 was identified as a direct target of let-7d. Su et al. identified an inverse correlation between let-7d levels and COL3A1 expression in malignant RCC clinical samples. Downregulation of let-7d resulted in an increased expression of COL3A1 and an increase in the metastatic potential of RCC cells demonstrating that let-7d suppresses metastasis of RCC cells by directly targeting COL3A1 (Su et al., 2014).

In breast cancer, COL3A1 was determined to be significantly correlated with increased expression of P4HA2 (Prolyl 4-Hydroxylase, Alpha Polypeptide II), an enzyme required for collagen triple helix formation and stabilization. Inhibition of P4HA2 activity resulted in inhibition of tumor growth and metastasis and reduction of collagen deposition, suggesting that P4HA2 enhances collagen deposition resulting in invasion (Xiong et al., 2014). Microarray analysis of invasive ductal and lobular carcinomas (IDC and ILC) indicate that COL3A1 is upregulated in IDC and ILC but not in normal breast tissues (Turashvili et al., 2007).

Deep sequencing of human colorectal cancer and normal colonic tissue samples identified COL3A1 as a DEG (Wu et al., 2012b). Expression levels of COL3A1 were confirmed to be upregulated in additional colorectal cancer samples as compared to normal samples by qRT-PCR. By functional enrichment analysis, the ECM receptor interaction pathway was identified as the most commonly affected pathway between colorectal cancer and normal samples, demonstrating a critical role of COL3A1 and ECM in colorectal cancer (Wu et al., 2012b). In the serum of colorectal patients, PIIP levels were determined to be significantly increased in patients with distant metastasis (Basso et al., 2001). High levels of PIIP in the serum was reported to be prognostic for patients' overall survival (Basso et al., 2001). In patients with early stage colorectal cancer (stages

I-II), high levels of PIIP in the serum was reported to be predictive for death from recurrence of the disease (Basso et al., 2001). Basso et al. suggested that the association between advanced tumor stage and increased serum levels of PIIP, may be due to enhanced collagen synthesis by metastatic cancer cells, resulting in collagen acting as a guide for the migrating cancer cells (Basso et al., 2001).

Throughout literature, fibular collagens, such as collagen III, have been implicated in aiding the invasion of cancer cells (Basso et al., 2001; Ewald et al., 2013; Su et al., 2014; Turashvili et al., 2007; Xiong et al., 2014). Although the exact role of COL3A1 in invasion has yet to be elucidated, it is speculated that collagen remodels the ECM by providing the necessary "tracks" needed for invasion of migrating cancer cells (Gritsenko et al., 2012; Lu et al., 2011). These speculations are supported by the fact that most malignant tumors are enriched in COL3A1 (Ewald et al., 2013; Hippo et al., 2002; Oue et al., 2004; Turashvili et al., 2007; Wu et al., 2012a; Wu et al., 2012b; Xiong et al., 2014), as described above. Surprisingly, increased ECM stiffness, resulting from increased collagen deposition, has been reported to promote cancer cell invasion (Levental et al., 2009). A stiff collagen matrix allows cancer cells to invade into healthy tissues by providing a track of least resistance (Gritsenko et al., 2012). This process is best described in the invasion of breast cancer cells, in which an increased expression of collagen results in collagen fiber bundling and straightening, causing collagen fibers to become thicker and start aligning perpendicularly to the tumor boundary (Conklin et al., 2011). The perpendicularly aligned collagen bundles provide contact guidance and an unhindered track of least resistance (Goetz et al., 2011). An illustration of this speculated process is provided in **Figure 3.4**.

**Figure 3.4: Remodeling of Collagen Fibers Promotes Invasion**

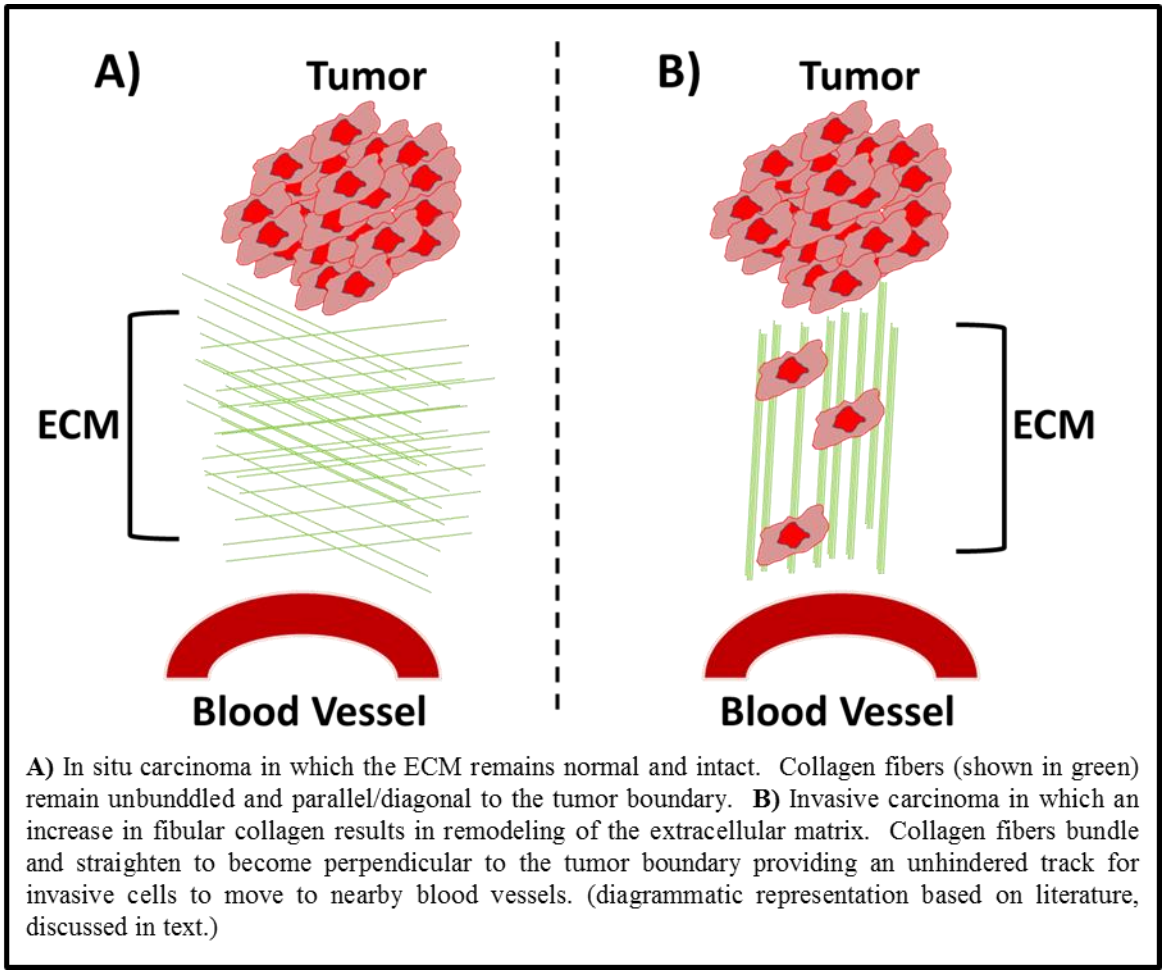


**A)** In situ carcinoma in which the ECM remains normal and intact. Collagen fibers (shown in green) remain unbunddled and parallel/diagonal to the tumor boundary. **B)** Invasive carcinoma in which an increase in fibular collagen results in remodeling of the extracellular matrix. Collagen fibers bundle and straighten to become perpendicular to the tumor boundary providing an unhindered track for invasive cells to move to nearby blood vessels. (diagrammatic representation based on literature, discussed in text.)

The results of my Aim 2 studies, suggest for the first time, that the expression of SPARC and COL3A1 is downstream of enhanced expression of DCLK1-S in colorectal cancers, and the mediatory mechanisms were further investigated as part of my Aim 2 studies. In order to understand the mediatory mechanisms, I conducted *in silico* analysis of both the SPARC and the COL3A1 promoters, in order to identify the presence of possible common *cis* elements in the two promoters, for binding known transcription factors. Several potential binding sites for NFATC2 were identified in both of the promoters, which led me to examine potential role of NFATC2 in DCLK1-S mediated upregulation of SPARC and COL3A1 in colon cancer cells, as part of my Aim 2 studies.

### 3.1.3 NFATC2

NFATC2 (nuclear factor of activated T-cells, cytoplasmic, calcineurin-dependent 2) is a member of the NFAT (nuclear factor of activated T cells) family of proteins. The NFAT family of proteins function as transcriptional factors and often cooperate with other transcription factors such as FOXP3 (Forkhead Box P3), GATA4 (GATA Binding Protein 4), and AP1 (Activator-Protein 1) (Chen et al., 1998; Jain et al., 1992; Wu et al., 2006). The NFAT family is comprised of 5 known proteins: NFATC2 (NFAT1), NFATC1 (NFAT2), NFATC4 (NFAT3), NFATC3 (NFAT4), and NFAT5 (tonicity enhancer binding protein) (Chuvpilo et al., 1999; Hogan et al., 2003; Shou et al., 2015). Each protein is composed of a C-terminal domain (C-TERM) and a conserved RHR (Rel-homology region) domain. The RHR domain comprises the DNA binding domain of the NFAT proteins and is structurally similar to the binding domain of the Rel family (also described as the NF-κB family) (Chytil and Verdine, 1996; Nolan, 1994). The recognition sites for transcriptional binding partners (as described above) are located within the RHR (Qin et al., 2014). NFATC1-4 contain an additional NHD (NFAT homology Domain) which includes the domains for TAD (transactivation domain), CDS (calcineurin docking site), NLS (nuclear localization signal), and NES (nuclear export signal) (Hogan et al., 2003; Qin et al., 2014; Shou et al., 2015). As a result of the presence of CDS domain, NFATC1-4 proteins are also calcium/calcineurin sensitive. NFAT5 lacks an NHD domain containing the CDS domain, resulting in insensitivity of NFAT5 to calcium/calcineruin; instead NFAT5 is sensitive to extracellular tonicity (Lopez-Rodríguez et al., 1999; Miyakawa et al., 1999; Trama et al., 2002).

The *NFATC2* gene is located on the long arm of chromosome 20 at position 13 (20q13). Previously NFATC2 was referred to as NFAT1 or NFATp. Eight transcript variants of NFATC2 have been identified. The full length predominant isoform (NM_173091, transcript variant 2) encodes for the longest isoform and is 7442 bps long,

contains 10 exons, and results in a 925 aa peptide with a molecular mass of 100.146 kDa (NP_775114.1) (as described in the NCBI database). NFATC2 transcript variant 1 (NM_012340.4) is 7442 bps and contains an alternate exon in the 3' end that causes a frameshift. The resulting transcript contains 11 exons and results in a 921 aa peptide (NP_036472.2) and has a shorter and distinct C-terminus compared to variant 2. NFATC2 transcript variant 3 (NM_001136021.2) is 7452 bps and uses an alternate first exon and contains an alternate exon at the 3' end. The resulting transcript contains 11 exons and results in a 901 aa peptide (NP_001129493.1) with a shorter and distinct N- and C-termini compared to variant 2. NFATC2 variant 4 (NM_001258292.1) is 7364 bps and uses an alternate first exon. The resulting transcript contains 10 exons and transcribes for 905 aa peptide (NP_001245221) that has a shorter and distinct N-terminus compared to variant 2. NFATC2 variant 5 (NM_001258294.1) is 6938 bps and has an alternate first exon, an alternate exon at the 3' end, and uses an alternate splice junction at the 5' end. The resulting transcript contains 10 exons and results in a 702 aa peptide (NP_001245223.1) that is shorter at the N-terminus and has a shorter and distinct C-terminus compared to variant 2. NFATC2 transcript variant 6 (NM_001258295.1) is 6850 bps and has an alternate first exon and uses an alternate splice junction at the 5' end. The resulting transcript is 10 exons and results in a 706 aa peptide (NP_001245224.1) that is shorter at the N-terminus. NFATC2 transcript variant 7 (NM_001258296.1) is 7016 bps and has an alternate splice junction at the 5' end of a coding exon and contains an alternate exon at the 3' end. The resulting transcript is 11 exons and results in a 702 aa peptide (NP_001245225.1) that is shorter at the N-terminus compared to variant 2. NFATC2 transcript variant 8 (NM_001258297.1) is 6928 bps and has an alternate splice junction at the 5' end of a coding exon. The resulting transcript is 10 exons and results in a 706 aa peptide (NP_001245226.1) that is shorter at the N-terminus compared to variant 2. As discussed above, the predominant NFATC2 protein is composed of an N-terminal NHD, a RHR domain, and a C-terminal domain, as shown in **Figure 3.5** (Macian, 2005;

Szuhai et al., 2009). The regulatory NHD is composed of a TAD, a CDS, 2 SRR motifs, 3 SPXX motifs, and an N-terminal NLS. The C-Terminal domain contains a C-terminal NLS and NES. The DNA-binding RHR facilitates binding of NFATC2 to the consensus sequence of 5'-GGAAAA-3' and contains the point of contact for multiple binding partners such as FOS and JUN.

**Figure 3.5: Diagrammatic Representation of NFATC2 Protein Domains**

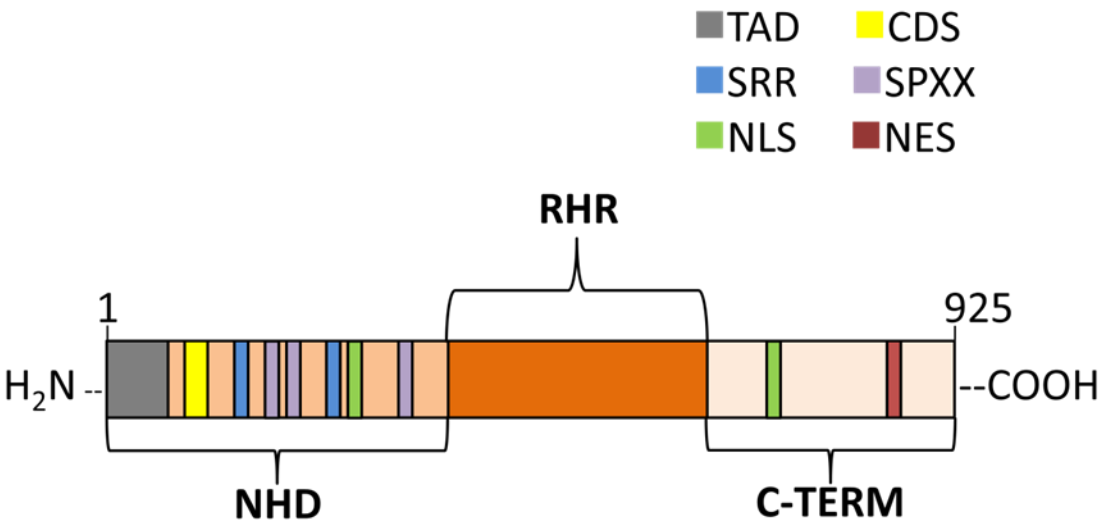


An N-terminal NFAT Homology domain (NHD) is located between 1-407 amino acids. The NHD contains TAD (transactivation domain) located at 1-100 amino acids and is shown in grey, 2 SRR (serine rich regions) shown in blue, 3 SPXX (serine-prolineXX-repeat motifs) shown in purple, a CDS (calcineurin docking site) shown in yellow, and an N-terminal NLS (nuclear localization signal) shown in lime green. A middle Rel-homology region (RHR) is located between 407-677 amino acids. A C-terminal domain (C-TERM) is located at 677-925 amino acids. The C-TERM contains a C-terminal NLS shown in lime green and NES (nuclear export signal) shown in red.

The activation of NFATC2 and other calcineurin dependent NFAT family members (NFATC1-4) has been extensively studied and reviewed (Hogan et al., 2003; Müller and Rao, 2010; Pan et al., 2013; Qin et al., 2014; Shou et al., 2015). In resting cells, NFATC2 is present in the cytosol in an inactive, hyperphosphorylated state (Luo et al., 1996; Okamura et al., 2000; Qin et al., 2014). Serine residues are heavily

phosphorylated within the SRR and SPXX motifs (Luo et al., 1996; Shou et al., 2015). NFATC2 activation is calcineurin-mediated and tightly controlled. A detailed description of the activation of NFATC2 is illustrated in **Figure 3.6**.

**Figure 3.6: Diagrammatic Representation of Pathways Reported to be Involved in the Activation of NFATC2**

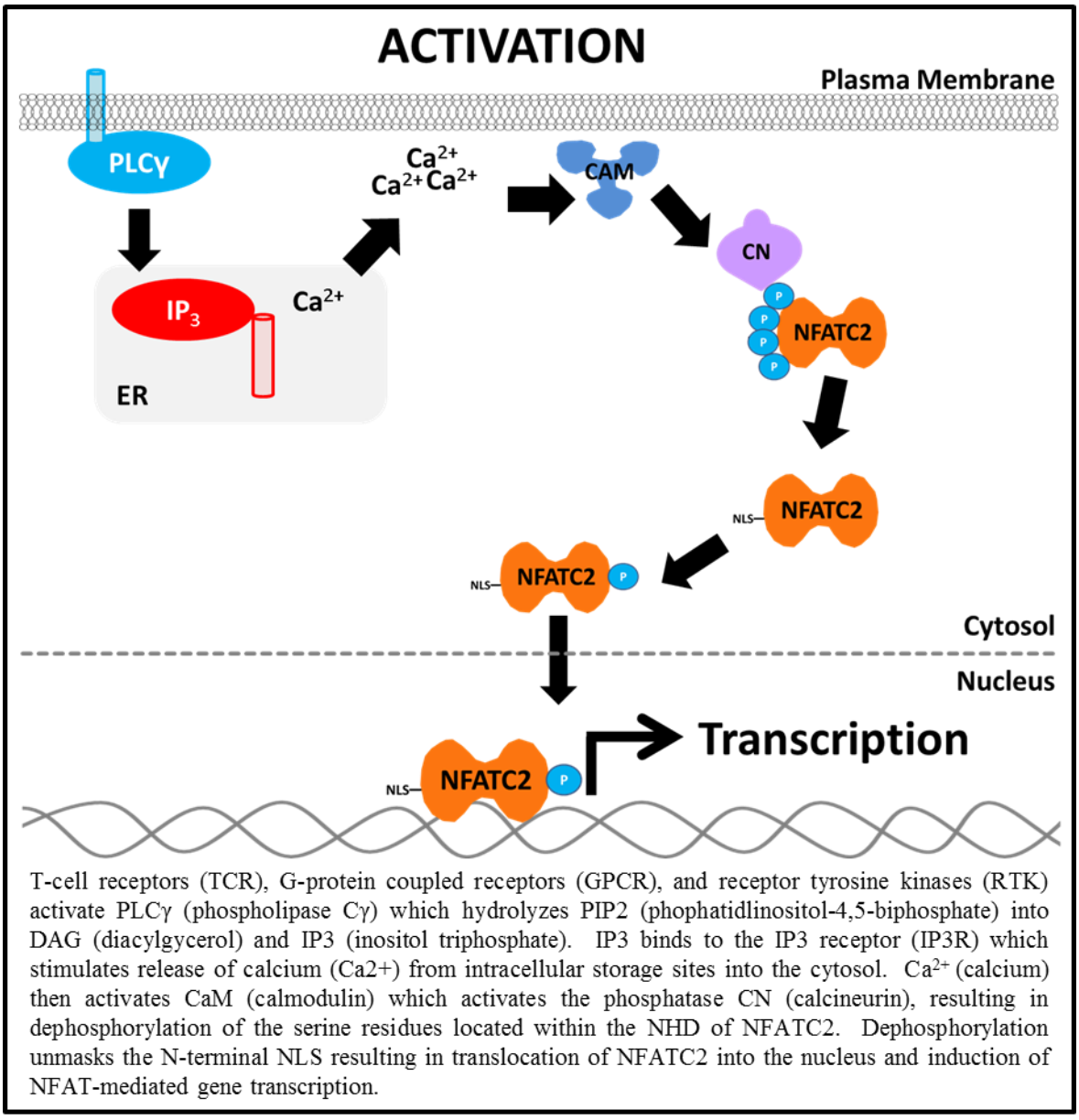

In brief, PLCγ (phospholipase Cγ) hydrolyzes $IP_3$ (inositol triphosphate) resulting in the release of calcium into the cytosol which activates calmodulin, which in turn activates calcineurin. Calcineurin then dephosphorylates the serine residues in the NHD resulting in unmasking of the N-terminal NLS. NFATC2 is then free to translocate to the nucleus and induce transcription (Hogan et al., 2003; Müller and Rao, 2010; Qin et al., 2014; Shou et al., 2015).

Deactivation of NFATC2 is also tightly regulated and controlled (Hogan et al., 2003; Müller and Rao, 2010; Pan et al., 2013; Qin et al., 2014; Shou et al., 2015). Deactivation is primarily coordinated by three classes of kinases: priming, export, and maintenance kinases. When intracellular $Ca^{2+}$ levels are low, DYRK1 and DYRK2 (dual-specificity tyrosine-phosphorylation regulated kinases 1 and 2) (priming kinases) phosphorylate NFATC2 at the SPXX-3 motif, priming NFATC2 for further phosphorylation (Gwack et al., 2006; Okamura et al., 2004; Pan et al., 2013). Export kinases GSK3 (glycogen-synthase kinase 3β) and CK1 (casein kinase 1) then operate to rephosphorylate NFATC2 at the SPXX motifs and the SRR1 motif which facilities its export out of the nucleus and into the cytoplasm (Gwack et al., 2006; Okamura et al., 2004; Pan et al., 2013). Importantly, it has been shown that CK1 phosphorylation of the SRR1 motif regulates the exposure of the NLS while the GSK3 phosphorylation of the SPXX motifs regulates DNA binding affinity (Okamura et al., 2004). CK1 can also operate as a maintenance kinase functioning to keep NFATC2 hyperphosphorylated and in an inactive state (Gwack et al., 2006; Okamura et al., 2004; Pan et al., 2013). A diagrammatic description of the deactivation of NFATC2 is provided in **Figure 3.7**.

**Figure 3.7: Diagrammatic Representation of Pathways Reported to be Involved if the De-activation of NFATC2**

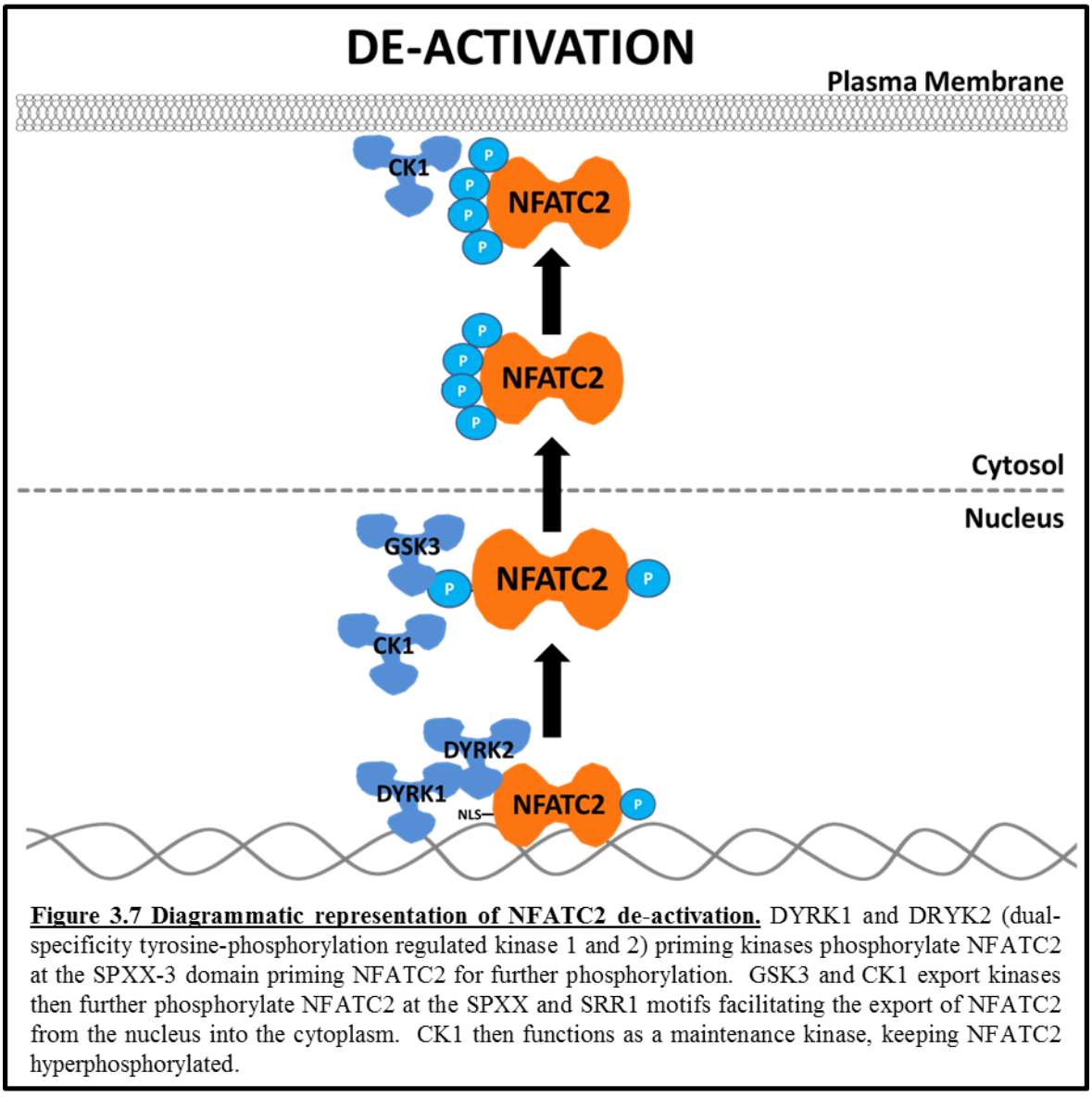


**Figure 3.7 Diagrammatic representation of NFATC2 de-activation.** DYRK1 and DRYK2 (dual-specificity tyrosine-phosphorylation regulated kinase 1 and 2) priming kinases phosphorylate NFATC2 at the SPXX-3 domain priming NFATC2 for further phosphorylation. GSK3 and CK1 export kinases then further phosphorylate NFATC2 at the SPXX and SRR1 motifs facilitating the export of NFATC2 from the nucleus into the cytoplasm. CK1 then functions as a maintenance kinase, keeping NFATC2 hyperphosphorylated.

Recently an additional level of regulation has been identified for NFATC2. It has been well described that phosphatases activate NFATC2 by dephosphorylating residues within the NHD and kinases deactivate NFATC2 by re-phosphorylating these same residues (as described above). However, recent reports have demonstrated that phosphorylation of specific residues results in enhanced transcriptional activity of NFATC2 (Gómez-Casero et al., 2007; Okamura et al., 2000; Ortega-Pérez et al., 2005;

Vázquez-Cedeira and Lazo, 2012). The first report of this phenomenon came in 2000. By mass spectrometry, Okamura et al., demonstrated that there are 14 conserved phosphoserine residues within the NHD. To expose the NLS and mask the NES, 13 residues are required to be dephosphorylated; however a single novel Ser residue (located between residues 45-61), is capable of promoting transcriptional activity upon phosphorylation (Okamura et al., 2000). Later studies demonstrated that mutation of the $^{53}$SPSS$^{56}$ motif resulted in diminished transactivating functions of NFATC2, suggesting that phosphorylation of these residues is critical for activation of NFATC2 (Gómez-Casero et al., 2007). Gomez-Casero et al. were able to demonstrate that Cot/Tpl2 and PKCζ (protein kinase C ζ) cooperate to enhance transcriptional activity of NFATC2 by PKCζ mediated phosphorylation of the $^{53}$SPSS$^{56}$ motif (Gómez-Casero et al., 2007). Similarly, other kinases have been implicated in enhancing NFATC2 transcriptional activity. These kinases include JNK (c-jun N-terminal kinases), which can phosphorylate T$^{116}$ and S$^{170}$ (Ortega-Pérez et al., 2005), and VRK2 (vaccinia-related kinase 2), which phosphorylates S$^{32}$ (Vázquez-Cedeira and Lazo, 2012); each of these described phosphorylations enhances transcriptional activity of NFATC2. The above studies demonstrate the complexity of NFATC2 regulation and suggest that additional kinases may be involved in promoting NFATC2 mediated transcription.

The NFAT family of proteins has been shown to play a critical role in regulation of cancer initiation and progression through involvement in angiogenesis, migration, and invasion (Mancini and Toker, 2009; Müller and Rao, 2010; Shou et al., 2015). NFATC2 has been reported to play an enhancing role in a variety of different cancers, including melanoma (Werneck et al., 2011), glioblastoma (Tie et al., 2013), hepatocellular (Zhang et al., 2012), breast (Gaudineau et al., 2012; Jauliac et al., 2002; Singh et al., 2011; Vázquez-Cedeira and Lazo, 2012; Yiu and Toker, 2006; Yoeli-Lerner et al., 2009; Yoeli-Lerner et al., 2005), pancreas (Singh et al., 2011), and colon (Duque et al., 2005; Gerlach et al., 2012; Hong et al., 2010; Masuo et al., 2009; Tripathi et al., 2014). Additionally a

vast amount of evidence suggests that NFATC2 may mediate cancer progression through enhancing the invasive capability of cancer cells, as described below.

An important role of NFATC2 in cancer was initially reported in breast carcinoma (Jauliac et al., 2002). Jauliac et al. reported a functional role of NFATC2 in promoting the invasive capability of breast carcinoma cells (Jauliac et al., 2002). NFATC2 was found to be expressed in both normal breast tissues and tissues derived from invasive breast carcinomas; however, co-localization of NFATC2 and $\alpha_6\beta_4$ integrin (previously shown to be highly expressed in breast carcinomas, but not in normal breast tissues) was only detected in invasive breast carcinoma samples (Jauliac et al., 2002). Importantly, Jauliac et al. demonstrated that expression of NFATC2 induced both the migratory and invasive capability of MDA-MB-435 breast carcinoma cells, unlike NFAT5 which was only capable of inducing migration of the cancer cells, without invasion (Jauliac et al., 2002). Jauliac et al. concluded that NFATC2 was expressed in both normal and breast carcinomas in human patients, and unlike other NFAT family of proteins, NFATC2 played a critical role in mediating the invasive capability of breast carcinoma cells (Jauliac et al., 2002). However, unique gene signatures involved in invasion, that are perhaps induced by NFATC2 (but not other members of NFAT family) remain to be identified (Jauliac et al., 2002). It was later reported that NFATC2 mediated breast cancer cell motility and invasiveness which could be blocked by AKT (Yoeli-Lerner et al., 2005). AKT was shown to blunt NFATC2 transcriptional activity by reducing nuclear translocation of NFATC2, due to the ubiquitination and degradation of NFATC2 by AKT (Yoeli-Lerner et al., 2005). AKT mediated NFATC2 loss of function resulted in an inhibition of both motility and invasion (Yoeli-Lerner et al., 2005). In a subsequent report, Yoeli-Lerner et al. reported that the loss of NFATC2 function (due to AKT blunting) was mediated by inactivation of GSK-3β (which was previously shown to deactivate NFATC2 by phosphorylation resulting in nuclear export of NFATC2) which resulted in degradation of NFATC2 and subsequent inhibition of invasion (Yoeli-Lerner

et al., 2009). The surprising relationship between GSK-3β and NFATC2 was later evaluated and it was determined that GSK-3β played a critical role in stabilizing the activated form of NFATC2 via phosphorylation of the SP2 domain, protecting NFATC2 from ubiquitin degradation (Singh et al., 2011). Role of GSK-3β in maintaining NFATC2 activity, demonstrates the complexity of regulation of NFATC2 activation/deactivation. In order to determine genes downstream of NFATC2, NFATC2 overexpressing MDA-MB-435 isogenic clones were derived and subjected to microarray analysis (Yiu and Toker, 2006). Gene expression profiling revealed that COX-2 was one of the most upregulated genes in response to NFATC2 overexpression (Yiu and Toker, 2006). COX-2 was confirmed to be transcriptionally upregulated via NFATC2 and downregulation of either NFATC2 or COX-2 resulted in a decrease in the invasive capability of breast cancer cells, suggesting that breast cancer invasion was promoted by NFATC2, due to possible up-regulation of COX-2 expression (Yiu, 2006). NFATC2 was confirmed to bind and activate the COX-2 promoter, resulting in increased invasive capability of breast cancer cells (Vázquez-Cedeira and Lazo, 2012). Vazquez-Cedeira and Lazo also described that NFATC2 was activated by phosphorylation of VRK2 (as described above), and inhibition of VRK2 resulted in decreased COX-2 expression and invasive capability of breast cancer cells, due to loss of binding of NFATC2 to the COX-2 promoter (Vázquez-Cedeira and Lazo, 2012). NFATC2 was reported to bind and promote activation of LCN2 (lipocalin 2) promoter, which in turn upregulates TNF-like receptor, TWEAKR, and its ligand TWEAK, resulting in an increased invasive capability of breast cancer cells (Gaudineau et al., 2012).

Although the majority of research on NFATC2 and its role in cancer cell invasion has focused on breast cancer, an important role of NFATC2 in colon cancer cell invasion has also been reported (Duque et al., 2005; Hong et al., 2010). Expression of NFATC2 in colon cancer cell lines was first reported in 2005 (Duque et al., 2005). Duque et al. demonstrated that NFATC2 is activated via $Ca^{2+}$/Cn activation in colon cancer cells, as in

other cell types (as described above) and activation of NFATC2 resulted in activation of COX-2 expression, which was later shown to mediate the invasive capability of breast cancer cells, as described above (Duque et al., 2005). In an attempt to define a molecular signature for early stage colorectal cancer patients that can predict the development of metastatic disease, NFATC2 was identified as one of 53 genes, which represented a unique set of genes capable of distinguishing cancer cells which will likely develop metastatic/invasive characteristics (Hong et al., 2010). Based on my studies so far, and on available literature in the area of breast and colon carcinomas, NFATC2 appears to play a critical role in mediating the invasive capability of cancer cells.

Based on the results of my Aim 2 studies, it is likely that significant increases in the expression of DCLK1-S in colon cancer cells, mediates increased transcriptional activity of NFATC2, by functioning as a specific kinase for phosphorylating the NFATC2 $^{53}$SPPS$^{56}$ motif. Increased transcriptional activation of NFATC2 likely results in increased expression of COL3A1 and other target genes. Overall our findings suggest that DCLK1-S may play a critical role in mediating the invasive potential of colon cancer cells by transcriptional activation of NFATC2, resulting in up-regulation of invasion associated proteins (such as COL3A1), causing re-modeling of extracellular matrix for unhindered invasion by colon cancer cells.

## 3.2 MATERIALS AND METHODS

### 3.2.1 Reagents Used

Antibodies used in these studies included: anti-β-actin (total) (Sigma, St. Louis, MO); anti-DCLK1, anti-NFATC2, anti-collagen III (Abcam, Cambridge, MA); anti-SPARC (Cell Signaling Technology, Danvers, MA), anti-GFP (Novus Biologicals LLC,

Littleton, CO), Anti-Flag (ThermoFischer Scientific, Waltham, MA). Smart Pool of target specific small interfering RNA (siRNA) (DCLK1 and NFATC2) and non-targeting (control) siRNA Pool were purchased from Dharmacon (Lafayette, CO). Sepharose beads and all other chemical reagents were purchased from Sigma. cDNA synthesis master mix was purchased from GeneDEPOT (Baker, TX). Syber green qRT-PCR kit was purchased from Bio-Rad (Hercule, CA). Promega GoTaq®green Master Mix (Maddison, WI) was used for PCR amplification, using a Thermal Cycler from Eppendorf (Hauppauge, NY). Restriction enzymes and competent cells were purchased from New England BioLabs (Ipswich, MA). Transfection reagent, FuGENE®6 was bought from Roche (Branford, CT), and all primers used were synthesized by Sigma (St. Louis, MO) (as described in **Table 3.1**).

### 3.2.2 Cell Culture

HCT116 and HEK293 cell lines were obtained from ATCC (Manassas, VA), and have been maintained in the laboratory for several years. COLO-205, RKO, COLO-320 and SW1417 were purchased from ATCC within the past two years and were confirmed by ATCC. All cell lines were monitored regularly for absence of mycoplasma. HCT116 and HEK293 cell lines were confirmed within the past 3 years to represent human epithelial cell lines with the help of Biosynthesis Company (Lewisville, TX). All cell lines were cultured in DMEMF12 medium (Invitrogen, Grand Island, NY), supplemented with 10% FCS containing 1% penicillin/streptomycin in a humid atmosphere at 37°C with 5% CO2. The stable clones of HCT116, and COLO205 cells were cultured in the same medium supplemented with 100µg/mL Geneticin (Invitrogen, Grand Island, NY) under similar conditions.

### 3.2.3 Generation of HCT116 clones, stably transfected with DCLK1-shRNA for downregulation of endogenous DCLK1-S

Initially, HCT116 cells were transiently transfected with seven hDCLK1-lentiviral-shRNA plasmids (V2LS library) (Dharmacon, Lafayette, CO); non-silencing shRNA-pGIPZ lentiviral-plasmid was used as a control (Dharmacon, Lafayette, CO), as per manufacturer's instructions. Down-regulation of DCLK1 expression by >70% was measured by WB analysis in cells transfected with V2LS_36413 and V2LHS_36415 plasmids. These plasmids were transfected into HCT116 cells to produce stably expressing clones that expressed either DCLK1-shRNA-413/415 (HCT-D) or pGIPZ-vector only clones (HCT-C). The downregulation of DCLK1 was confirmed by qRT-PCR and western blot analysis, as shown under results.

### 3.2.4 Generation of COLO205 clones, stably over-expressing full length GFP-DCLK1-L/S

Eukaryotic expression plasmids expressing N-terminally GFP tagged full length coding sequence of DCLK1-Long and DCLK1-Short were purchased (GeneCopoeia, Rockville, MD). COLO205 cells were chosen for over-expressing either the L or the S isoforms of DCLK1, because COLO205 cells, unlike >80% of available colon cancer cell lines, were reported by us to lack the expression of both L/S isoforms of DCLK1 (O'Connell et al., 2015). COLO205 clones, stably expressing full length DCLK1-Long (205-L) or DCLK1-Short (205-S) were generated as previously described (Sarkar et al., 2011). Vector Transfected clones (205-C) expressing only GFP served as controls. GPF and DCLK1 expression was confirmed by qRT-PCR, western blot analysis and immunofluorescence, and is shown in results.

### 3.2.5 Transient-transfection of cells with oligonucleotides and expression plasmids

Cell lines were transfected with either target specific (DCLK1 or NFATC2)/control siRNA, or expression/control plasmids as indicated, using LipofectamineTM 2000 (Invitrogen, Grand Island, NY) according to manufacturer's instructions, as previously described (Kantara et al., 2014; O'Connell et al., 2015; Sarkar et al., 2011). Transfected cells were propagated in normal growth medium containing 10% FCS, and processed for RT-PCR analysis after 48h of transfection for confirming down-regulation of the target genes (DCLK1 and NFATC2) or expression of indicated expression plasmids.

### 3.2.6 Analysis of cell lines/isogenic clones/tissue samples by RT-PCR/qRT-PCR

Total RNA was isolated from cell lines (isogenic clones and treated/control cells) in monolayer cultures at 60-70% confluency, or from human patient tissues (described below) using Trizol Reagent (Invitrogen), as previously described (O'Connell et al., 2015). For qRT-PCR, the iTaq Universal SYBR Green Supermix (Bio-Rad, CA) was used as per the manufacturer's instructions, as previously described (O'Connell et al., 2015). The primer sequences used for PCR amplification of cDNA for both RT-PCR/qRT-PCR analysis are provided in **Table 3.1**. Electrophoresis gels presented were cropped to present all the bands observed within the range covered by the molecular markers used (between 100 bp and 1000 bp for RT-PCR data), in order to avoid primer dimers seen towards the end of the run. Processing of the electrophoresis blots was applied equally across the entire image. Touch-up tools were not used to manipulate data.

### 3.2.7 Western Immunoblot (WB) analysis

Cell lines (isogenic clones and treated/control cells) growing as mono-layer cultures, were harvested and processed for preparing cellular lysates, followed by electrophoresis, and transferred to PVDF-membranes as previously described (Kantara et al., 2014; O'Connell et al., 2015). Frozen tissue samples obtained from patients as described below were homogenized and processed for preparation of tissue lysates in RIPA buffer as described previously (Kantara et al., 2014; O'Connell et al., 2015). Samples containing 30-50 µg of proteins were subjected to electrophoresis and transferred to PVDF-membranes as previously described (Kantara et al., 2014; O'Connell et al., 2015). Blots were cut into horizontal strips containing target or loading-control proteins (β-actin), and processed for WB, as described previously (Kantara et al., 2014; O'Connell et al., 2015). Antigen-antibody complexes were detected with a chemiluminescence-reagent kit (Thermoscientific, IL or GE Healthcare, UK). Membrane-strips containing either target or loading control proteins were simultaneously exposed for equal time to autoradiographic films. Western blots presented were cropped to exclude bands beyond the range of the molecular markers, at the running end and at the loading end. Processing of films was applied equally across the entire image. Touch-up tools were not used to manipulate data.

### 3.2.8 *In Vitro* Growth Assays

*In vitro* proliferation of cells (isogenic clones) was quantified in an MTT assay as previously described (Sarkar et al., 2012). Briefly cells were plated at equal concentrations (5000 cells per well) in 96-well plates. After plating, cells were serum starved for 24 hours before addition of 0-12% FCS containing media for 48 hrs. The total number of viable cells was determined in an MTT (3–4,5-Dimethylthiazol-2-yl) assay. The *in vitro* tumorigenic potential was measured in a soft agar clonogenic assay as

previously described (Sarkar et al., 2011). Briefly, cells were seeded at equal concentrations, (10,000 cells per well) in 6-well culture plates in 0.5% agar in growth media containing 0-12% FCS. The total number of colonies per well were counted and graphed.

### 3.2.9 *In Vitro* Invasion Assay

Transwell chambers, precoated with Matrigel, were purchased from Corning Inc (Corning, NY). Isogenic clones were seeded and allowed to attach to a 10 cm plate. After 24 hours, isogenic clones were serum starved for 24 hours. After an additional 24 hours, cells were removed from the plate and washed 3 times with serum free media. Cell were resuspended in 0.5 mL of serum free media and transferred to the top of transwell chambers. Chambers were placed in a 24 well plate with 0.5 mL media containing variable levels of FCS. HCT isogenic clones were placed in media containing 20% serum, and COLO205 isogenic clones were placed in media containing 5% serum. After 12 hours, cells that had invaded through the matrigel to the lower surface of the chamber were stained with crystal violet and allowed to dry. The cells that had invaded through the transwell membrane, were counted and % cells that had invaded, compared to total number of cells plated, were graphed.

### 3.2.10 *In Vitro* growth of cells as spheroids

Isogenic clones were grown as spheroids as previously described (Kantara et al., 2014). In brief, cells were plated at a density of 5000 cells/well into 24-well ultra low-attachment plates (Costar, Corning NY). Cells were suspended in serum-free media containing DMEM/F12 (1:1) + 1% Anti-Anti Antibiotic-Antimycotic supplemented with B-27 (50X) (all from Invitrogen, Grand Island, NY), epidermal growth factor (EGF)

20ng/ml and fibroblast growth factor (bFGF) (10ng/ml) (both from Sigma-Aldrich, St Louis, MO). Media was changed every 2-3 days and the formation of spheroids (tumorospheres/spheres) monitored daily. Spheres were imaged at 4x, 10x and 40x using white light microscopy (Nikon, NY).

### 3.2.11 *In vivo* tumorigenic/metastatic assays

Cells were inoculated in athymic (Nude) mice to grow either sub-dermal xenografts or metastatic growths in liver/lung after intrasplenic-inoculations as previously described (Kantara et al., 2014; Sarkar et al., 2012). To prepare cells for inoculation into the athymic (Nude) mice, sub-confluent cells in cultures were scraped and re-suspended in phosphate buffered saline (PBS) as single cell suspensions. For subdermal xenograft injections, 5x106 cells/100µL PBS were inoculated on right and left flanks of female athymic mice, 4 weeks of age (Envigo, United Kingdom) (as per our approved IACUC protocols-IRB#01-12-054B). After 3–6wks from time of inoculation, tumors were harvested, dissected free of host tissue, patted dry and weighed. For intrasplenic inoculations, $2x10^6$ cells/50µl PBS were inoculated in the tip of the spleens, after making a <1cm incision on the dorsal side (left of center, right below the ribs) of the female athymic mice, 4 weeks of age (Envigo, United Kingdom) (as per our approved IACUC protocols-IRB#01-12-054B). The incision was followed by suturing the dermis and clipping the skin with wound clips. Mice receiving intrasplenic inoculations were subjected to splenectomy after 24h of inoculation to avoid splenic/peritoneal growths. After 3-6 weeks from time of inoculation, liver and lungs were harvested. Both subdermal xenografts and lung and livers from intrasplenic inoculated mice, were washed with tissue wash buffer and fixed overnight using 10% formalin, followed by 70% ethanol. Embedding and sectioning was performed with the help of Vel-Lab (Houston,

TX), and the sections were processed for H&E, IHC and IF staining for specific protein markers (as published previously (Kantara et al., 2014; Sarkar et al., 2012).

### 3.2.12 Immunostaining

For IF staining of cells, cells were grown on coverslips in 24-well plates and at 70% confluency, cells were fixed using a 1:1 ratio of acetone:methanol solution at -20◦ for 30 minutes as previously described (Kantara et al., 2014; Sarkar et al., 2012). In brief, cells were washed 3X with PBS, blocked with 5% goat serum for 1 hour. Cells were then stained with either anti-DCLK1 antibody (1:200), anti-GFP (1:200) or anti-NFATC2 antibody (1:200). Excess antibody was washed off and cells were incubated with either goat anti-rabbit-IgG coupled to Alexa Flour 488 or goat anti-mouse-IgG coupled to Alexa Flour 594. Excess antibody was washed off and cells were incubated with 4', 6-diamidino-2-phenylindole (DAPI) for 2 minutes. Cover slips were then mounted onto glass slides using FluorSaveTM Reagent (CALBIOCHEM, La Jolla, CA). Images were acquired using Zeiss Axioplan epifluorescent microscope (META). Images were analyzed using METAMORPH, v6.0 software (Molecular Devices). To quantitate % cells positive for GFP expression, cells expressing GFP were counted in 15-20 fields of view per well for each cell line.

For IHC staining of liver/lung samples obtained from nude mice, slides containing tissue sections were deparaffinized and hydrated using xylene and ethanol. Slides were unmasked for antigen by boiling in sodium citrate buffer, pH 6.0. Endogenous peroxidase was neutralized by incubating in 3% $H_2O_2$ for 20min and washed in PBS. 5% goat serum was used to block non-specific binding. Rabbit polyclonal primary antibody against GFP was used at 1:250 dilution, rabbit polyclonal primary antibody against SPARC was used at 1:200 dilution, and mouse monoclonal primary antibody against COL3A1 was used at 1:800 dilution at 4˚C overnight. Incubated sections were washed and incubated at room

temperature for 2h with HRP conjugated anti-rabbit or anti-mouse antibody at 1:200 dilution. Sections were further incubated for 30min at RT, using biotinylated secondary anti-rabbit or anti-mouse antibodies (1:200) followed by washing with PBS and incubated with DAB (Dako Inc.). Images from the tissue sections were captured by a Nikon microscope (TS100) equipped with a camera at 20X and 40X magnifications, after mounting the sections with coverslips, as previously described (Sarkar et al., 2012).

### 3.2.13 Differential Gene Expression by RNAseq Analysis

Total RNA was isolated (as described above) from biological triplicates of HCT-C and HCT-D isogenic clones. Library construction and RNA sequencing was performed at the UTMB Next Generation Sequencing Core Facility. RNA was fragmented by incubation at 94◦ for 8 minutes in 19.5 μL fragmentation buffer (Illumina, San Diego, CA). First and second strand synthesis, adapter ligation, and library amplification were performed according to manufacturer's instructions using the TruSeq RNA Sample Preparation kit (Illumina, San Diego, CA). Using an Illumina Truseq RNA v2 Kit (Illumina, San Diego, CA), a sequencing library was prepared according to the manufacturer's instructions. Paired end, 50-base sequencing was performed on an Illumina HiSeq 1000 using a TruSeq SBS kit v3 (Illumina, San Diego, CA) according to the manufacturer's instructions. Reads were mapped to the human hg19 reference (https://support.illumina.com/sequencing/sequencing_software/igenome.html) using the STAR version 2.3.1a alignment program. Differential gene expression was analyzed with the Cuffdiff function of the Cufflinks software suite, version 2.2.1. The molecular functions and Biological processes changed in response to DCLK1-S were analyzed by the PANTHER (Protein Analysis Through Evolutionary Relationships) Classification System version 9.0 (http://pantherdb.org/). Ingenuity Pathway Analysis (IPA) was used

to identify the top pathways changed in response to downregulation of DCLK1-S and heat maps were constructed based on genes involved in top pathways.

### 3.2.14 Procurement of samples from normal colonic mucosa and colonic tumors of patients

Samples of normal colonic mucosa and primary colonic tumors, were obtained as discarded samples (as per our approved UTMB IRB protocol #91-310) from the Tissue Core Facility at Cancer Center, University of Alabama, as part of CHTN Program funded by NIH. All samples were collected and flash-frozen and stored in liquid nitrogen or -80°C until analyzed. Pathology of all samples was confirmed.

### 3.2.15 Generation of SPARC and COL3A1 promoter-reporter (luciferase) constructs

Based on the published promoter sequences of SPARC and COL3A1, primer sets were designed to amplify promoter segments of the SPARC promoter from -125 through -2059 nucleotides and the COL3A1 promoter from +48 through -1348 nucleotides using genomic DNA from HCT116 cells. The primers were synthesized with the restriction sites Xho1 at 5'-end and HindIII at 3' end, in order to clone into PcLUC vector (New England Biosciences, MD) (as shown in **Table 3.1**). The PCR products were purified using QIAquick PCR Purification kit (Qiagen, CA), cloned into luciferase expression vector (PcLUC vector) and amplified in DH5α competent cells (New England Biosciences, MD). Positive colonies were processed for purifying the promoter-reporter expression plasmids; control plasmids lacked SPARC and COL3A1 promoter sequences.

### 3.2.16 Promoter-Reporter assays

Cells were transiently transfected with the indicated promoter-reporter constructs using FuGENE6 for 24-48h, as per manufacturer's instructions; control cells were transfected with empty PcLUC vector, lacking promoter sequences. Media was collected from transfected cells and luciferin was added according to instructions of the manufacturer (New England Biosciences, MD). Luciferase activity was measured using a luminometer (Dynex Technologies, VA) after 10sec of addition of substrate, as previously described (O'Connell et al., 2015; Sarkar et al., 2011).

### 3.2.17 Chromatin Immunoprecipitation Assays (ChIP)

ChIP assays were performed as previously described (O'Connell et al., 2015). In brief, cells were fixed in 1% formaldehyde to crosslink DNA to bound proteins, and reaction stopped by adding 0.125M glycine. Cells were washed with cold PBS, pelleted, and resuspended in ChIP sonication buffer, followed by sonication and centrifugation of fragments (600-700bp long). The crosslinked chromatin supernatant was immunopreciptated using target-specific antibody (2-5 µg purified IgG) at 4℃, overnight. Control samples contained no antibody. For obtaining input levels of the corresponding proteins, equivalent numbers of cells were also processed for Western Immunoblot analysis. Protein A/G Sepharose beads, pre-absorbed by Herring sperm DNA (100µg/ml) was added to the chromatin-antibody complex and centrifuged to sediment the beads. DNA was eluted from the beads with elution buffer and DNA was precipitated using a high salt method (as previously described (Ishizawa et al., 1991). The extracted DNA was purified and used for PCR amplification of the immunoprecipitated DNA with specific NFATC2 primers. The primer sequences used for this purpose are listed in **Table 3.1**.

### 3.2.18 Immunoprecipitation

Immunoprecipitation of DCLK1 and NFATC2 was performed as previously described (Sarkar et al., 2011). Cellular lysates of cells/transfected cells were prepared as described above. The lysates were pre cleared for nonspecific binding by incubating with 5µg of normal rabbit serum for 2h at 4°C, followed by incubating with 50µl sepharose H/C beads for 1 hour. The lysate was then incubated at 4°C overnight with 5µg of anti-DCLK1 polyclonal antibody (as described above). The bound complex was pulled down with Protein A sepharose beads for 6h at 4°C followed by washing the beads with RIPA buffer. The beads were suspended in 2X SDS sample buffer, boiled and processed for Western Blot analysis for NFATC2, irrespective of phosphorylation status.

### 3.2.19 Generation of WT and MUT NFATC2-FLAG expression plasmids

Eukaryotic expression plasmids expressing C-terminally FLAG tagged full length coding sequence of WT NFATC2 or MUT NFATC2 were purchased (GeneCopoeia, Rockville, MD). In MUT NFATC2 expression plasmids, serine$^{53}$ was mutated to alanine$^{53}$ and serine$^{56}$ was mutated to alanine$^{56}$. The mutant plasmid was confirmed by sequencing and used for transfections as described above.

### 3.2.20 Statistical analysis

Data are presented as mean±SEM of values obtained from indicated number of patient samples or experiments. To test for significant differences between means, nonparametric Mann Whitney test was employed using STAT view 4.1 (Abacus Concepts, Inc, Berkley, CA).

## 3.3 RESULTS

### 3.3.1 Biological Effects of Down-Regulating the Expression of DCLK1-S in Colon Cancer Cells

HCT116 cells, previously shown to express high levels of DCLK1-S, with undetectable levels of DCLK1-L expression (due to methylation of the 5'(α)-promoter) (O'Connell et al., 2015), were used to generate isogenic clones stably expressing either empty vector (HCT-C) or DCLK1-shRNA (HCT-D). HCT-D clones were confirmed to be significantly downregulated for the expression of DCLK1-S (**Fig 3.8A,B**). Transcript levels of DCLK1-S were downregulated by ~2.25 fold in HCT-D vs. HCT-C clones, by qRT-PCR analysis (**Fig 3.8A**). DCLK1-S protein levels, measured by western blot analysis, were also attenuated in HCT-D vs. HCT-C clones (**Fig 3.8B**). Growth rate of HCT-D clones was ~2 fold lower than that of HCT-C clones, in response to increasing concentrations of fetal calf serum (**Fig 3.8C**). The colonogenicity of HCT-D vs. HCT-C clones was also decreased by ~5 fold, in a soft agar assay (**Fig 3.8D**). The invasive potential of HCT-D clones was attenuated by ~4 fold as compared to that of HCT-C cells, measured in a transwell assay, as described in methods (**Fig 3.8E**). Tumorigenic potential of clones was examined *in vivo*, by evaluating the growth of an equal number of cells as subdermal xenografts in athymic nude mice, as described in methods. Mice inoculated with HCT-D cells failed to generate palpable tumors, while all mice inoculated with HCT-C clones formed tumors with tumor volumes similar to those previously published with HCT116 cells (Kantara et al., 2014), as presented in **Figure 3.8F**. HCT-C and HCT-D clones were also subjected to a functional stem cell assay, by growing the cells in 3D, *in vitro*, in low attachment plates (spheroidal assays), by our published methods (Kantara et al., 2014), as described in methods. HCT-C clones formed well defined spheroids, as previously described (Kantara et al., 2014), while HCT-D

clones failed to form spheroidal structures (**Fig 3.8G**). In summary, proliferative/tumorigenic/invasive and spheroid formation potential of HCT-D clones was significantly attenuated, due to loss of DCLK1-S expression. Loss of tumorigenic potential of HCT-D clones was perhaps the most severe, which may reflect a significant loss in the population of cancer stem cells in the HCT-D clones, further supported by the absence of spheroid formation by the downregulated cells.

### 3.3.2 Transcriptional changes in response to DCLK1-S downregulation

To evaluate the transcriptional differences between HCT-C and HCT-D clones, RNAseq analysis of biological triplicates was performed, as described in methods. A total number of 2999 genes were found to be significantly different in HCT-C vs. HCT-D clones. A total of 227 genes were significantly upregulated by >2 fold (as shown in **Appendix 1**), while 213 genes were significantly downregulated by >-2 fold (as shown in **Appendix 2**) (**Fig 3.9A**). DCLK1 expression was downregulated by an average of -1.87 fold in HCT-D clones vs. HCT-C clones. To evaluate the biological processes and molecular functions disrupted by DCLK1-S downregulation, genes downregulated by more than 3 fold were subjected to PANTHER analysis, as described in methods. The various biological processes and molecular functions disrupted by DCLK1-S downregulation are presented in **Figure 3.9B,C**. Prominent biological processes that were disrupted, included adhesion, response to stimulus, and apoptosis (**Fig 3.9B**). Some of the prominent molecular functions disrupted, included catalytic activity, binding, and receptor activity (**Fig 3.9C**). To evaluate the specific cellular pathways disrupted by DCLK1-S silencing, Ingenuity Pathway Analysis (IPA) of genes up/downregulated >3 fold was conducted. The top 5 pathways affected by DCLK1-S downregulation included cellular growth (**Fig3.10A**), tumor development (**Fig3.10B**), cellular movement (**Fig3.10C**), cellular death (**Fig3.10D**), and apoptosis (**Fig3.10E**), as presented in **Figure**

**3.10**. Heat maps of up/down regulated genes, involved in each specific pathway, are shown (**Fig 3.10**). Based on PANTHER analysis, IPA, and recent reports (Ito et al., 2016), two specific genes, known to play a significant role in enhancing the invasive potential of colon cancer cells, were identified as SPARC and COL3A. These two molecules were further evaluated in relation to DCLK1-S expression, as part of my Aim 2 studies.

### 3.3.3 SPARC and COL3A1 are expressed downstream of DCLK1-S

Both SPARC and COL3A1 were confirmed to be significantly downregulated in HCT-D clones, compared to that in HCT-C clones, by qRT-PCR (**Fig 3.11A**) and western blot analysis (**Fig 3.11B**). Relative transcript levels of SPARC were down regulated by ~-12 fold while transcript levels of COL3A1 were down regulated by ~-14 fold in HCT-D vs. HCT-C clones (**Fig 3.11A**). Relative protein levels of SPARC and COL3A1 were similarly attenuated in HCT-D vs. HCT-C clones (**Fig 3.11B**). Colon cancer cell lines, positive for significant expression of DCLK1-S (RKO, SW1116), were also positive for significant expression of SPARC and COL3A1, while colon cancer cell lines, negative for DCLK1-S expression (COLO205, SW1417), were also negative for SPARC and COL3A1 expression (**Fig 3.11C**). We have previously reported that normal colonic patient samples are generally negative for the expression of DCLK1-S, while colonic adenocarcinomas from patients are generally positive for significant levels of DCLK1-S expression (O'Connell et al., 2015), as summarized in **Fig 3.11F**. Some of these samples were examined for the expression of SPARC/COL3A1. Normal colonic mucosal samples from patients, negative for DCLK1-S expression, were found to express null to low levels of SPARC and COL3A1 (**Fig3.11D**), while primary colon adenocarcinoma samples from patients, were positive for high levels of DCLK1-S and SPARC/COL3A1 (**Fig3.11E**). Thus, the relative expression levels of SPARC and

COL3A1 strongly correlated with the expression levels of DCLK1-S in normal colons and colon cancer cells/adenocarcinomas, providing further evidence that SPARC/COL3A1 are likely down stream of DCLK1-S expression in colon cancers.

### 3.3.4 Isoform specific effects of DCLK1 on SPARC/COL3A1 and the invasive potential of colon cancer cells

COLO205 cells (205), were previously reported to be negative for the expression of both DCLK1-L and DCLK1-S isoforms (O'Connell et al., 2015). We therefore used these cells to generate isogenic clones of stably expressing cells, which either expressed the empty GFP vector (205-C), GFP tagged DCLK1-L (205-L), or the GFP tagged DCLK1-S (205-S); the GFP tag in both the L and S vectors was located at the N-terminal end. The 205-L and 205-S clones were confirmed to overexpress DCLK1-L/DCLK1-S at the transcript (**Fig 3.12A**) and protein levels (**Fig 3.12B**), respectively. GFP expression of all three isogenic clones was confirmed by IF analysis (**Fig 3.12C**). Percentage of cells positive for GFP in the three isogenic clones was quantified, as described in methods (**Figure 3.12D)**. For reasons unknown, GFP expression was lower in both 205-L and 205-S clones as compared to that in 205-C, however GFP expression levels were comparable in 205-L vs. 205-S clones (**Fig 3.12D**).

The three isogenic 205 clones were used for evaluating isoform specific effects of DCLK1 on the expression of SPARC/COL3A1, and used for examining differences, if any, in the invasive potential of the control vs. L/S expressing 205 colon cancer cells. The expression of SPARC and COL3A1 was significantly upregulated, at the transcript (**Fig 3.13A**) and protein (**Fig 3.13B**) levels, in 205-S clones, overexpressing DCLK1-S. However, expression levels of SPARC and COL3A1 remained unchanged in 205-C and 205-L clones, overexpressing DCLK1-L, suggesting for the first time that at least some of the pathways, downstream of the two isoforms maybe significantly different. The

transcriptional activity of the promoters for SPARC and COL3A1, was next examined. Promoter reporter constructs were constructed (as described in methods) (**Fig 3.13C**). The transcriptional activity of SPARC and COL3A1 promoters was significantly increased in the 205-S clones, compared to that of the 205-C and 205-L clones (**Fig 3.13D**). These results provide additional evidence that SPARC and COL3A1 are expressed downstream of DCLK1-S, but not DCLK1-L.

The invasive potential of the isogenic clones was next examined in an *in vitro* invasion assay, as described in methods. The invasive potential of 205-S cells, was ~7 fold higher compared to that of either 205-C or 205-L cells, based on the number of invasive cells detected by crystal violet staining of the transwell membrane inserts (**Fig 3.13E**).

To examine the invasive potential of 205 isogenic clones *in vivo*, an equal number of cells from the three clones were inoculated in the spleens of athymic nude mice, intrasplenically (as described in methods). Within 3 weeks of inoculation, mice inoculated with 205-S clones developed visually apparent metastatic lesions in the livers, unlike mice inoculated with 205-C or 205-L clones; livers from representative mice are presented in **Figure 3.14A**. Livers from mice in all three groups were processed for H&E staining (**Fig 3.14B**). As can be seen, metastatic lesions were only seen in the livers of 205-S mice, while livers of 205-C or 205-L mice appeared to be free of metastatic lesions (**Fig 3.14B**). Liver samples from all three groups were also processed by RT-PCR for measuring relative expression levels of DCLK1-L/S in the livers, as a reflection of presence of invasive cells from the three clones (**Fig 3.14C**). We have previously reported the expression of DCLK1-L, but no DCLK1-S expression, in the hepatocytes of normal mouse livers (O'Connell, 2015). The relative levels of DCLK1-L were not significantly different in the liver samples of mice inoculated with the three 205 clones. However, DCLK1-S expression was detected only in the livers of the mice inoculated with 205-S clones, further confirming that while the 205-S clones had

metastasized to the livers, the other two clones likely lacked metastatic potential, and had not invaded the livers from the spleen (**Fig 3.14C**). The relative expression levels of GFP were also evaluated in the livers of mice inoculated with 205 clones, by western blot analysis (**3.14D**). GFP expression was only detected in the livers of mice injected with 205-S clones, once again demonstrating that only the 205-S clones had developed invasive potential, and become metastatic (**3.14D**), in agreement with *in vitro* findings, presented in **Figure 3.13E**. Next the protein levels of GFP/SPARC/COL3A1 in the livers of mice inoculated with 205 isogenic clones was examined by IHC of liver sections. The metastatic lesions in the livers of mice injected with 205-S clones were positive for GFP/SPARC/COL3A1 staining (**Fig 3.15**), while the livers of mice inoculated with 205-C or 205-L clones were relatively negative for GFP/SPARC/COL3A1 staining (**Fig 3.15)**. Based on the results presented in **figures 3.13** to **3.15**, from the *in vitro* and *in vivo* assays, it appears likely that DCLK1-S (but not DCLK1-L) expression in colon cancer cells, significantly enhances the invasive potential of the cells. It is also strongly indicated that SPARC and COL3A1 expression are upregulated several fold in response to DCLK1-S expression, but not DCLK1-L expression, in colon cancer cells, which may mediate the increase in the invasive potential of the cells.

### 3.3.5 Role of NFATC2 in upregulating transcriptional activity of SPARC and COL3A1

In order to understand the mechanisms by which DCLK1-S may be mediating the increased expression of SPARC/COL3A1, I conducted *in silico* analysis of both the SPARC and COL3A1 promoters to identify the presence of a possible common *cis* element in the two promoters. Several potential binding sites for NFATC2 were identified in both the promoters (as described in **Figures 3.16 and 3.17**). There were 6

potential NFATC2 binding sites within 3 kb of the start site of the SPARC promoter (**Fig 3.16**) and 9 potential NFATC2 binding sites within 3 kb of the start site of the COL3A1 promoter (**Fig3.17**). NFATC2 binding, *in situ*, to the potential NFATC2 binding sites was examined in ChIP assays. The -1470/-1339 binding site in the SPARC promoter (**Fig 3.18A**) and the -728 binding site in the COL3A1 promoter (**Fig 3.18B**) were determined to be the only functional NFATC2 binding sites in HCT116 cells, of the several sites examined in this study. I next examined the role of DCLK1-S expression on the binding of NFATC2 to the promoters of SPARC and COL3A1, by conducting ChIP assays in HCT-C/HCT-D clones. Results of ChIP assays confirmed that binding of NFATC2 to either the -1470/-1339 binding site in the SPARC promoter (**Fig 3.18C**) or the -728 binding site in the COL3A1 promoter (**Fig 3.18D**) was significantly downregulated in HCT-D clones compared to that in HCT-C clones. Relative binding of NFATC2 to the indicated NFATC2 binding sites, from several experiments, is presented as % of total NFATC2 binding (input) in the cells (**Fig 3.18E**). To confirm a role of DCLK1-S and NFATC2 in the transcriptional regulation of SPARC and COL3A1, wild type HCT116 cells were transiently transfected with siRNAs against either DCLK1 or NFATC2 (as described in methods). In cells transfected with either DCLK1 or NFATC2 siRNA, COL3A1 expression was significantly downregulated, compared to that in cells transfected with the respective control siRNA (**Fig 3.18F**). However, surprisingly, SPARC expression was significantly downregulated only in cells transfected with DCLK1 siRNA, but not in cells transfected with NFATC2 siRNA (**Fig 3.18F**). These results suggest that NFATC2 is required for upregulating the expression of COL3A1 in response to DCLK1-S, while NFATC2 may not be required for upregulating the expression of SPARC in response to DCLK1-S.

### 3.3.6 Association of DCLK1-S with NFATC2

DCLK1-S retains the calmodulin like kinase domain as discussed in chapter 1. Previous reports have suggested that DCLK1 proteins can potentially function like a kinase (Shang et al., 2003), and in at least one report, a kinase inhibitor (LRRK2-IN-1) was reported to inhibit the biological effects of DCLK1 protein (Weygant et al., 2014). Since my results suggest that a potent transcription factor, NFATC2, binds the promoters of SPARC and COL3A1, downstream of DCLK1-S, I hypothesized that NFATC2 may become activated/phosphorylated at critical Ser/Thr sites, by possibly associating with DCLK1-S in colon cancer cells. The latter intriguing possibility was evaluated in the next set of experiments. To investigate if DCLK1-S co-localizes with NFATC2, HCT-C and HCT-D clones were used to co-IP NFATC2 with DCLK1-S. As can be seen in **Figure 3.19A**, DCLK1-S co-imunoprecipitated with NFATC2 in HCT-C cells, but not in HCT-D cells. The co-localization of DCLK1-S and NFATC2 in HCT-C/D clones was further evaluated by IF staining of the cells (**Fig 3.19B**). In HCT-C clones, strong co-localization of DCLK1-S and NFATC2 was evident (highlighted by arrows in the merged images), while HCT-D clones did not demonstrate any co-localization of NFATC2 with DCLK1-S, since S isoform is nearly absent in HCT-D clones (**Fig 3.19B**). To examine if association of NFATC2 with DCLK1 protein is isoform specific, 205 isogenic clones were also subjected to IF staining for the two proteins (**Fig 3.19C**). The 205-C and 205-L clones did not demonstrate co-localization of NFATC2 with DCLK1, to any significant level; however NFATC2 was strongly co-localized with DCLK1 in 205-S clones (as highlighted by arrows in the merged images) (**Fig 3.19C**).

### 3.3.6 Role of phosphorylation at the NFATC2 $^{53}$SPPS$^{56}$ enhancement motif, in mediating downstream effects of DCLK1-S in colon cancer cells

As described in the introduction of this chapter, activity of NFATC2 can be regulated at many different levels (Gómez-Casero et al., 2007; Okamura et al., 2000). A large amount of literature describes deactivation of NFATC2 by several kinases (summarized in **Figure 3.7**). However, a class of kinases has also been identified, which are implicated in enhancing the activity of NFATC2 by phosphorylation at the $^{53}$SPPS$^{56}$ motif, located within the NHD (Gómez-Casero et al., 2007; Okamura et al., 2000). We therefore evaluated if the $^{53}$SPPS$^{56}$ motif of NFATC2 was necessary to activate COL3A1. To evaluate the importance of the $^{53}$SPPS$^{56}$ motif, mutant NFATC2 was generated as described in methods, where in Ser53 and Ser56 were mutated to Ala53 and Ala56, as shown in **Figure 3.20A**. Plasmids expressing either the WT or MUT NFATC2 cDNA were transiently transfected into HCT116 cells, and the resultant expression of COL3A1 was monitored at the RNA and protein levels, after 48 hrs of transfection. Relative levels of COL3A1 were significantly downregulated, at both the transcript (**Fig 3.20B**) and protein (**Fig 3.20C**) levels in the cells transfected with MUT plasmid compared to levels in cells transfected with the WT plasmid. To further confirm these important findings, HCT116 cells were co-transfected with COL3A1 promoter-reporter constructs (described above), along with plasmids expressing either the MUT or WT NFATC2. The transcriptional activity of COL3A1 promoter-reporter construct was significantly lower in HCT116 cells co-transfected with the MUT vs. the WT plasmid (**Fig 3.20D**). In HCT116 cells, transfected with either the MUT or WT NFATC2 plasmid, the binding of MUT NFATC2 to the -728 NFATC2 binding site in the COL3A1 promoter, was significantly reduced compared to that of WT NFATC2, in ChIP assays (representative ChIP data from one of three similar experiments, are shown in **Fig 3.20E**; relative binding of MUT/WT NFATC2 from all three experiments is shown in **Fig 3.20F**).

My results with NFATC2 and SPARC, presented above in **Figure 3.18F**, suggested that NFATC2 does not have any significant role in regulating the transcriptional activity of SPARC promoter. To confirm that NFATC2, with or without phosphorylation at the $^{53}$SPPS$^{56}$ motif, was not involved in the transcriptional regulation of SPARC, HCT116 cells were transfected with either the WT or MUT NFATC2 cDNA plasmids, and the relative expression levels of SPARC measured. The expression of SPARC remained unchanged, at both the transcript (**Fig 3.21B**) and protein (**Fig 3.21C**) levels, in cells transfected with either WT or MUT NFATC2. Similarly, the transcriptional activity of the SPARC promoter-reporter construct (described above), remained unchanged in HCT116 cells, transfected with either WT or MUT NFATC2 (**Fig 3.21D**). The binding of NFATC2 to the -1470/-1339 NFATC2 binding site in the SPARC promoter, also remained unchanged in cells transfected with either WT or MUT NFATC2, in ChIP assays (representative ChIP data are shown in **Fig 3.21E,** while relative binding of WT/MUT NFATC2 from all three experiments is shown in **Fig 3.21F**). The results of the above experiments demonstrate for the first time that phosphorylation of NFATC2 at the $^{53}$SPPS$^{56}$ motif, in response to possible direct interaction with the DCLK1-S kinase, is required for transcriptional activation of COL3A1, resulting in the expression of elevated levels of COL3A1 in colon cancer cells. However, elevated levels of SPARC, in response increased expression of DCLK1-S in colon cancer cells, appears to be independent of NFATC2 binding to its promoter.

**Figure 3.8: Downregulation of DCLK1-S Inhibits Proliferative/Clonogenic/Invasive/Spheroidal Formation Potential of HCT116 Colon Cancer Cells**

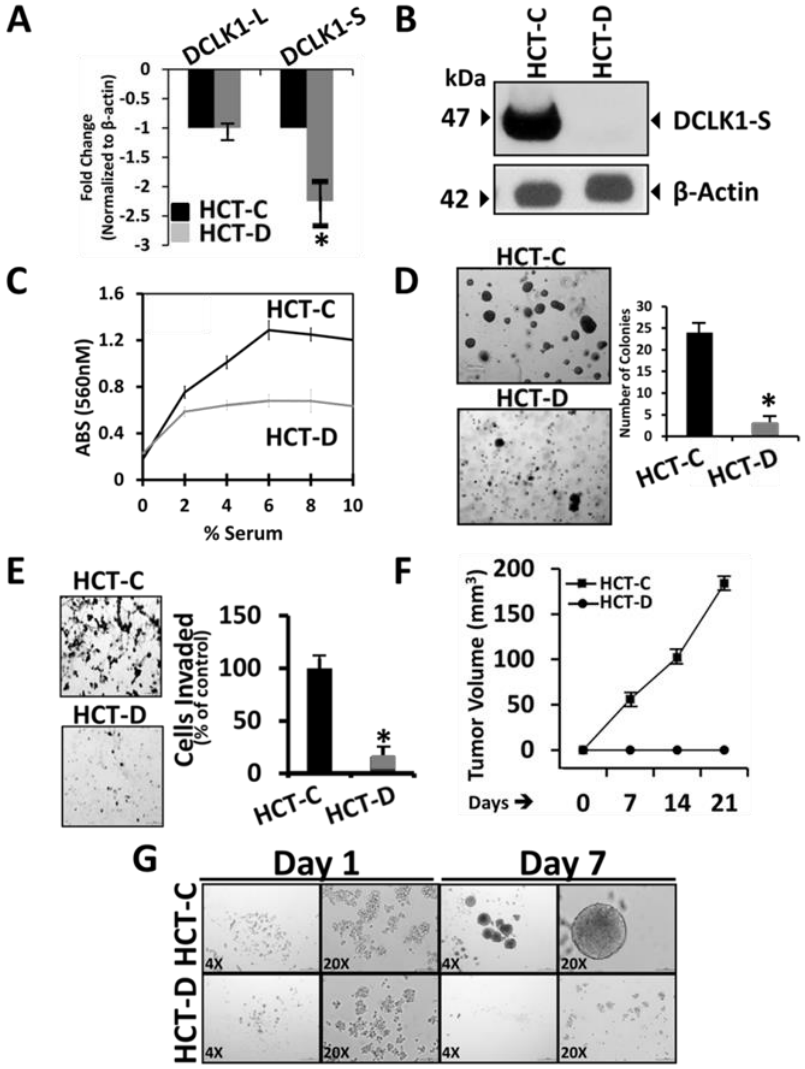


**A)** DCLK1 L/S expression in HCT-C/HCT-D isogenic clones by qRTPCR. Each value represents Mean±SEM of 3 separate experiments. **B)** DCLK1-S expression in HCT-C/HCT-D isogenic clones by western blot analysis. Blot presented is representative of 3 separate experiments. **C)** Growth rate of an equal number of HCT-C and HCT-D cells in response to increasing concentrations of serum, measured in an MTT assay. Absorbance values are plotted against serum concentration. Each value represents data from 8 separate wells/experiment, from a representative of 3 similar experiments. **D)** Representative Images of clonogenic growth of HCT-C and HCT-D clones on soft agar in response to 10% serum are shown; bar graphs = Mean±SEM of number of colonies/5 wells from indicated clones . **E)** Invasive potential of an equal number of HCT-C and HCT-D cells in Transwells in response to 10% serum. Represntative images are shown; Bar graphs = Mean±SEM of % cells (of control), which had invaded the transwell inserts (stained with crystal violet) per 3 wells from indicated clones. **F)** Tumor Volume of HCT-C and HCT-D clones, grown as subdermal tumors, presented as Mean±SEM of 6 tumors from 3 mice, at indicated time points, after inoculation of equal # of cells. **G)** Spheroid assays with cells from the HCT-C/D clones, grown in non-adherent stem cell cultures, after indicated time-points. Representative images of spheroids from 6 wells/clone from two separate experiments are shown. *=P<0.05 vs HCT-C values

**Figure 3.9: Molecular Functions and Biological Processes Disrupted in Response to DCLK-S Downregulation**

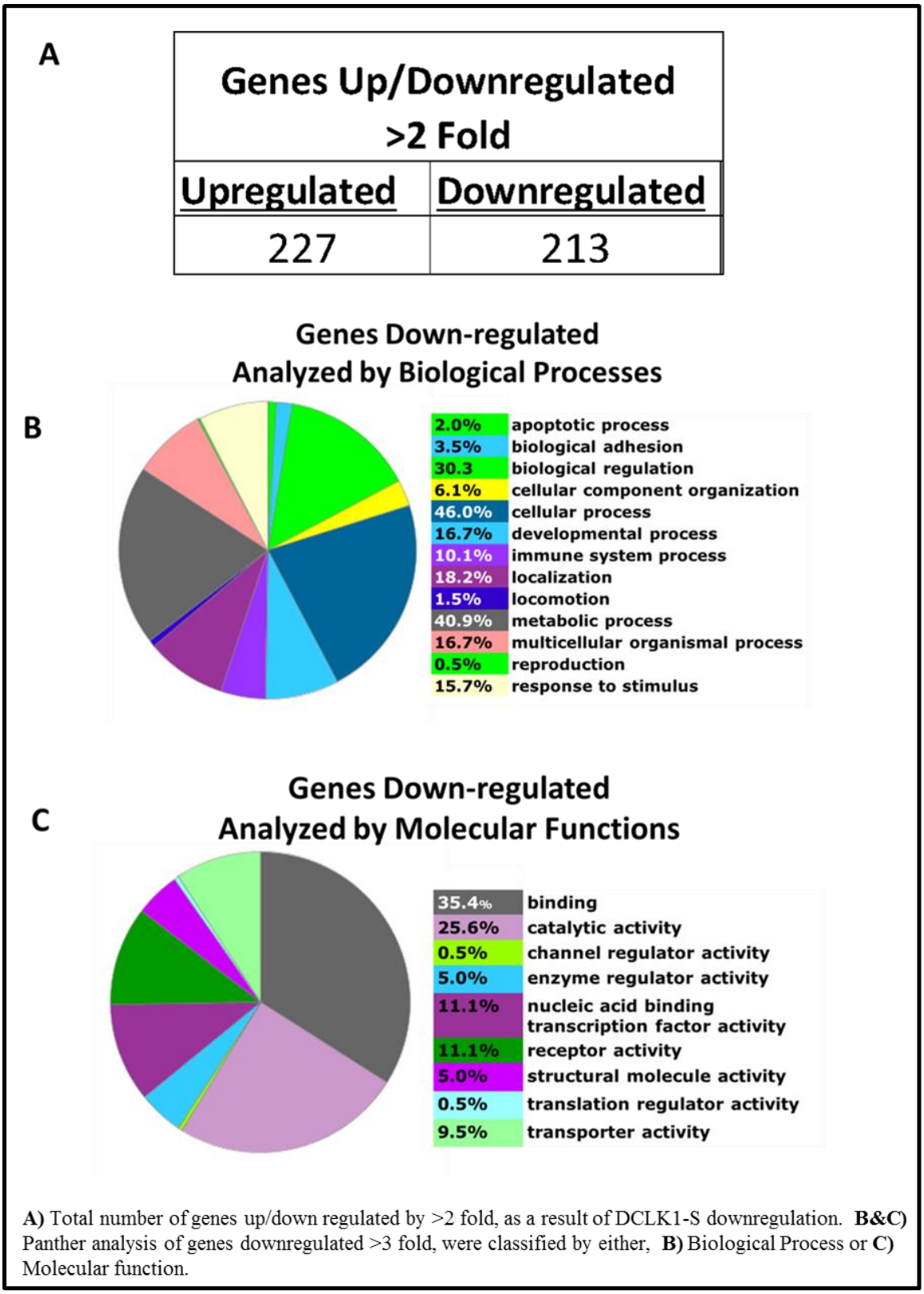


**A)** Total number of genes up/down regulated by >2 fold, as a result of DCLK1-S downregulation. **B&C)** Panther analysis of genes downregulated >3 fold, were classified by either, **B)** Biological Process or **C)** Molecular function.

**Figure 3.10: Cellular Pathways Disrupted in HCT116 Cells in Response to DCLK1-S Downregulation**

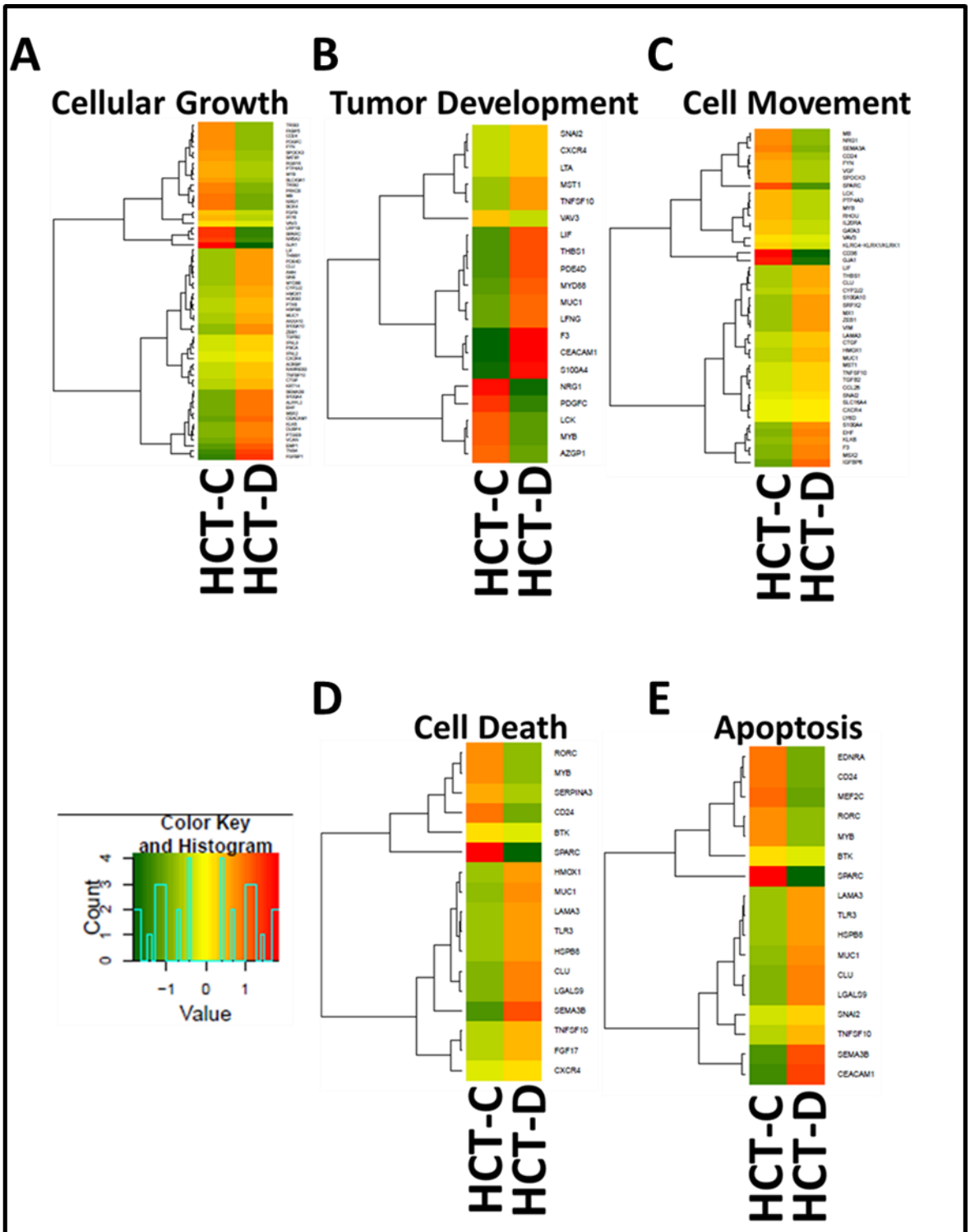


Heat maps generated from top cellular pathways disrupted in response to DCLK1-S downregulation, were identified by IPA analysis. Top pathways included **A)** Cellular Growth, **B)** Tumor Development, **C)** Cell Movement, **D)** Cell Death, and **E)** Apoptosis. A color key and histogram are provided for reference.

**Figure 3.11: Expression of DCLK1-S and Downstream Targets SPARC/COL3A1**

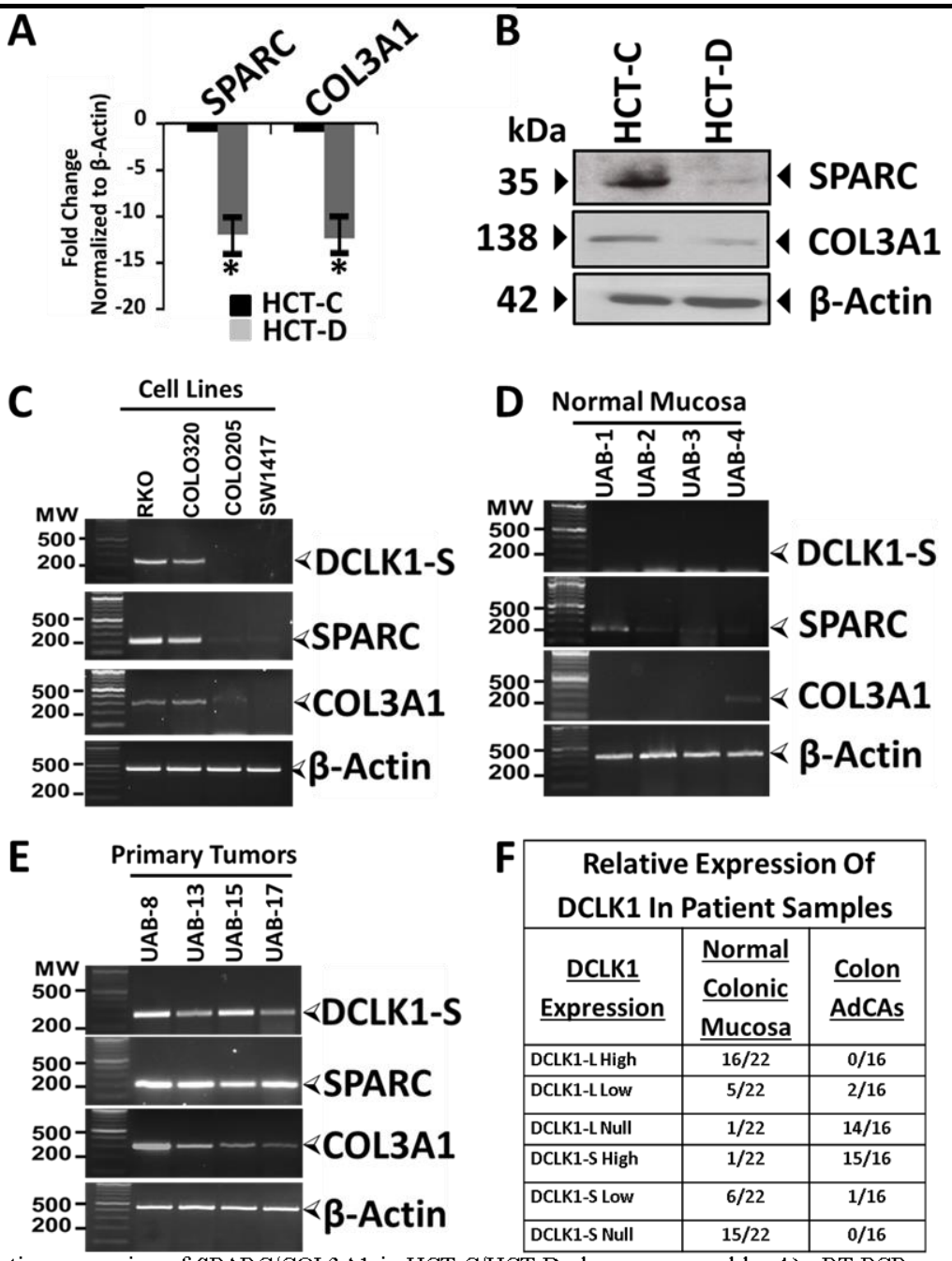


**F**

| Relative Expression Of DCLK1 In Patient Samples | | |
|---|---|---|
| DCLK1 Expression | Normal Colonic Mucosa | Colon AdCAs |
| DCLK1-L High | 16/22 | 0/16 |
| DCLK1-L Low | 5/22 | 2/16 |
| DCLK1-L Null | 1/22 | 14/16 |
| DCLK1-S High | 1/22 | 15/16 |
| DCLK1-S Low | 6/22 | 1/16 |
| DCLK1-S Null | 15/22 | 0/16 |

Relative expression of SPARC/COL3A1 in HCT-C/HCT-D clones measured by **A)** qRT-PCR and **B)** western blot analysis. Representative RT-PCR data for the 3 transcripts from: **C)** human colon cancer cell lines; **D)** human normal colonic mucosa; and **E)** primary colon adenocarcinomas from patients. **F)** DCLK1-L/S levels in normal colonic mucosa and colon AdCAs of patients, previously reported (O'Connell et al., 2015). For A-E, β-actin was run as internal controls. In A, each value represents Mean±SEM of 3 separate biological clones. All data presented in B-E are representative of 2-3 separate experiments. Molecular weight (MW) in terms of bps and molecular mass in terms of kDa are shown on left-hand side of each image. D and E are representative of 5–10 patient samples, analyzed in duplicate.

*=P<0.05 vs HCT-C values

**Figure 3.12: Confirmation of COLO205 (205) Clones, Overexpressing Control GFP or GFP Tagged DCLK1-L/S**

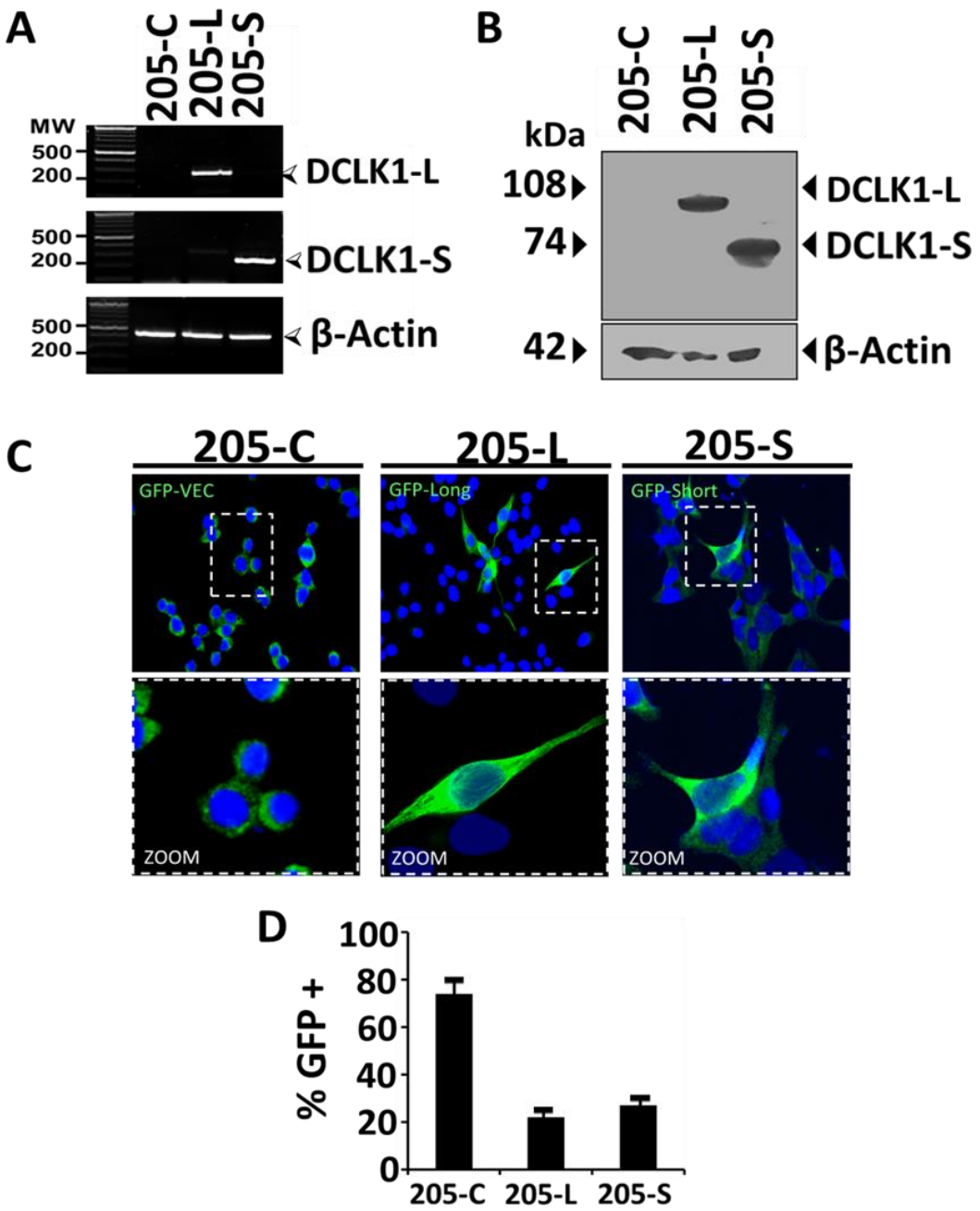


**A)** Relative expression of DCLK1 L/S in 205-C/205-L/205-S isogenic clones by RT-PCR **B)** Relative expression of GFP tagged DCLK1-L/S expression in 205-C/205-L/205-S clones by western blot analysis. **C)** Representative Images of GFP expression in 205-C/205-L/205-S cells grown on coverslips. **A**-**C** = representative data from 2-3 separate experiments. The molecular weight (MW) in terms of bps and molecular mass in terms of kDa is shown on left-hand side of each image. **D)** % cells positive for GFP expression in 205-C/205-L/205-S clones, growing on cover slips. Each value in **D** represents Mean±SEM of 15-20 fields of view from 4 separate wells in 2 experiments. Images in **C,** suggests differences in morphology of control vs L and S cells, which may reflect biological impact of the isoform expression, and needs further investigation.

**Figure 3.13: DCLK1 Isoform Specific Expression of SPARC/COL3A1 in 205 Clones: Effect on Invasion**

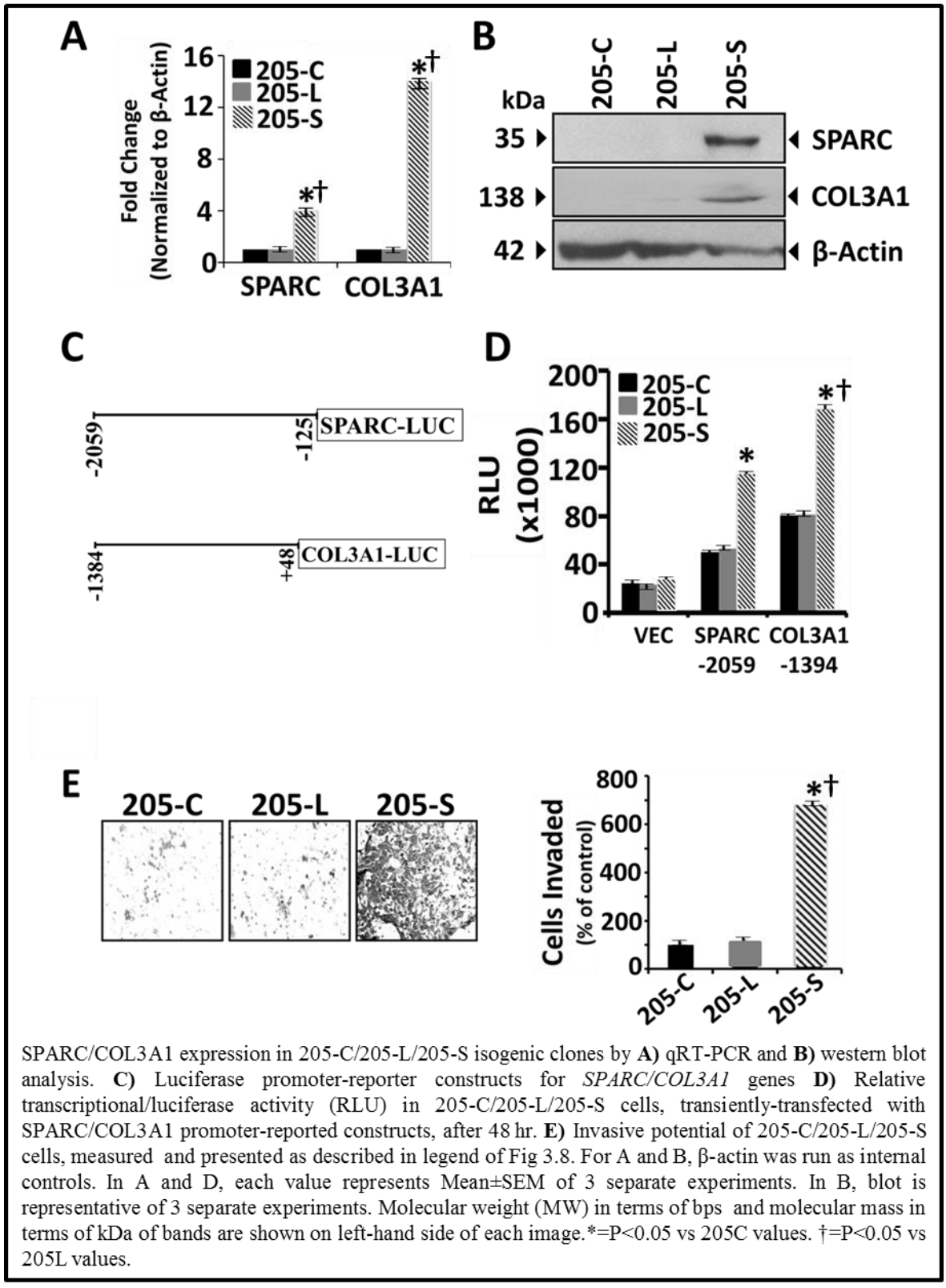


SPARC/COL3A1 expression in 205-C/205-L/205-S isogenic clones by **A)** qRT-PCR and **B)** western blot analysis. **C)** Luciferase promoter-reporter constructs for *SPARC/COL3A1* genes **D)** Relative transcriptional/luciferase activity (RLU) in 205-C/205-L/205-S cells, transiently-transfected with SPARC/COL3A1 promoter-reported constructs, after 48 hr. **E)** Invasive potential of 205-C/205-L/205-S cells, measured and presented as described in legend of Fig 3.8. For A and B, β-actin was run as internal controls. In A and D, each value represents Mean±SEM of 3 separate experiments. In B, blot is representative of 3 separate experiments. Molecular weight (MW) in terms of bps and molecular mass in terms of kDa of bands are shown on left-hand side of each image.*=P<0.05 vs 205C values. †=P<0.05 vs 205L values.

**Figure 3.14: Metastatic Potential of DCLK1 L vs. S Isogenic Clones**

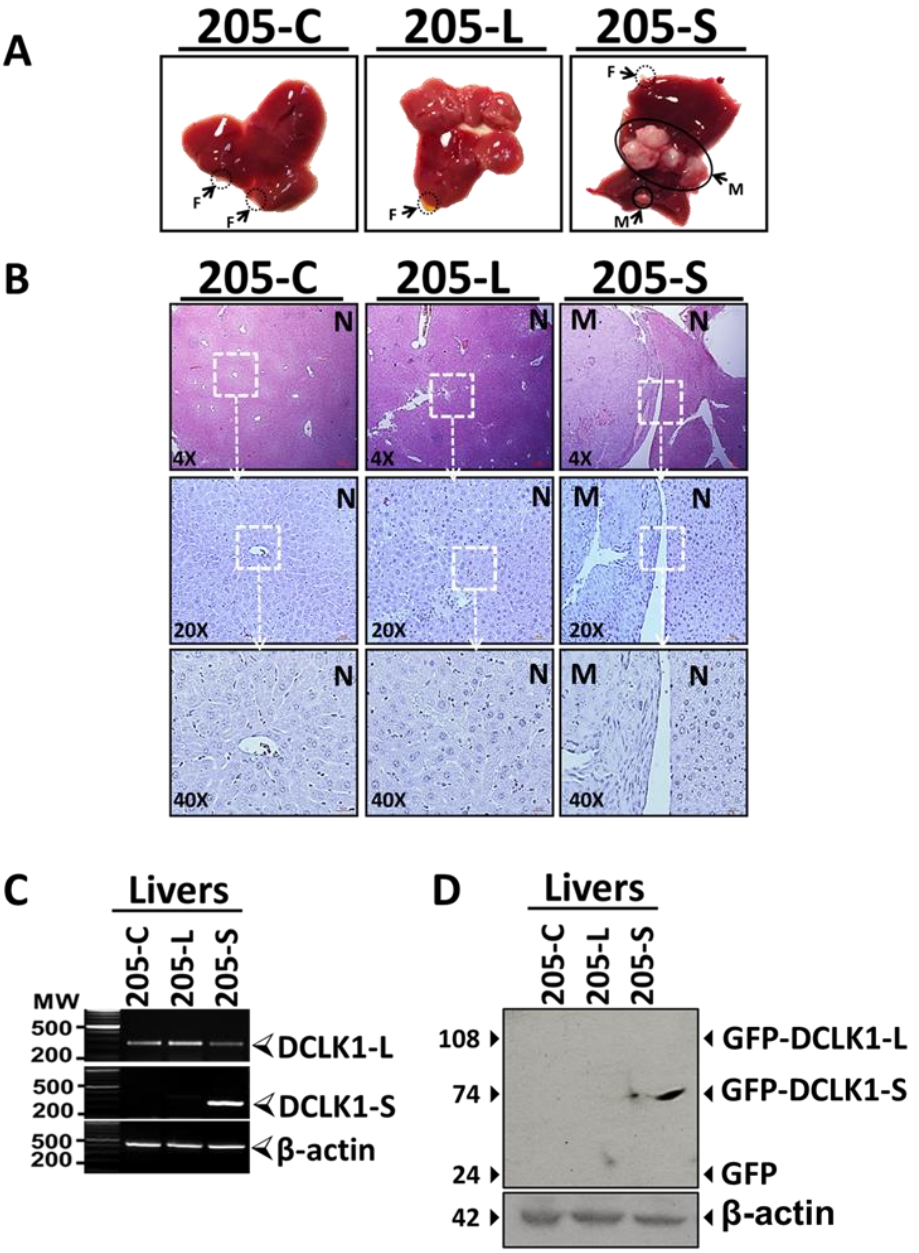


Liver tissues were removed 3 wks after intrasplenic incoulation of mice with equal # of 205-C/205-L/205-S isogenic clones. **A)** Representative images of liver metastasis from mice inoculated intrasplenically with 205-C/205-L/205-S clones. F=Fat and M=Met Tumor. Tissue sections were flash frozen as described in methods. B) H&E staining of liver sections from the mice. Representative sections of livers from the three groups of mice, which were either devoid of met lesions (C/L clones) or were positive for met lesions (S clones). (N= normal looking liver, M=met tumor cells in liver). Relative expression levels of GFP-DCLK1-L/S in the livers of mice inoculated intrasplenically with 205-C/205-L/205-S clones by **C)** RT-PCR and **D)** Western blot analysis (anti-GFP antibody used for WB). B-C) Data presented in A-D are representative of livers obtained from 4 mice per group. The molecular weight (MW) in terms of bps and molecular mass in terms of kDa are shown on left-hand side of each image.

**Figure 3.15: Metastatic Tumors in Liver, Obtained Only from Mice Inoculated with 205-S clones, are Positive for SPARC and COL3A1**

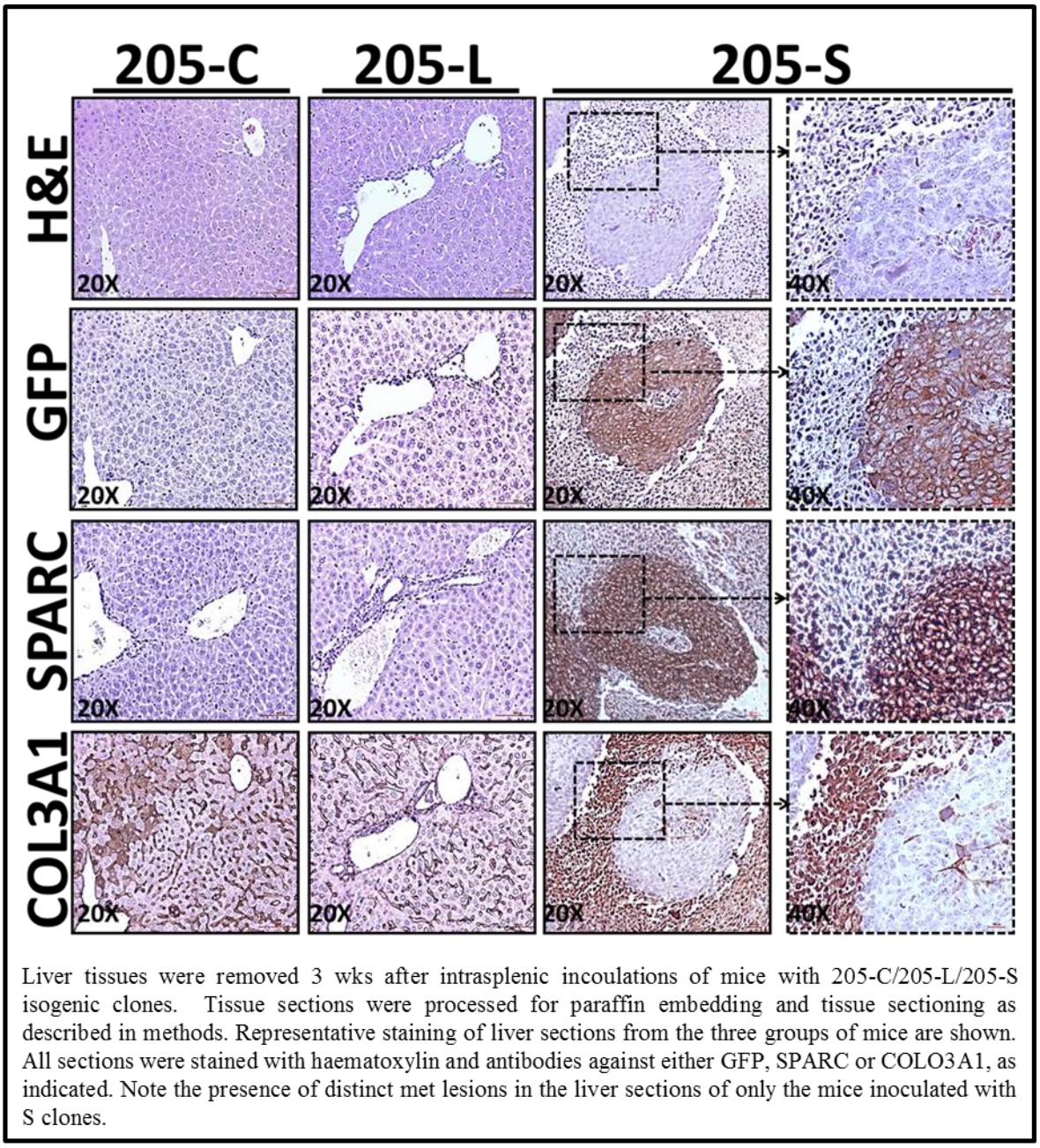


Liver tissues were removed 3 wks after intrasplenic incoulations of mice with 205-C/205-L/205-S isogenic clones. Tissue sections were processed for paraffin embedding and tissue sectioning as described in methods. Representative staining of liver sections from the three groups of mice are shown. All sections were stained with haematoxylin and antibodies against either GFP, SPARC or COLO3A1, as indicated. Note the presence of distinct met lesions in the liver sections of only the mice inoculated with S clones.

**Figure 3.16: NFATC2 Binding Sites on SPARC Promoter**

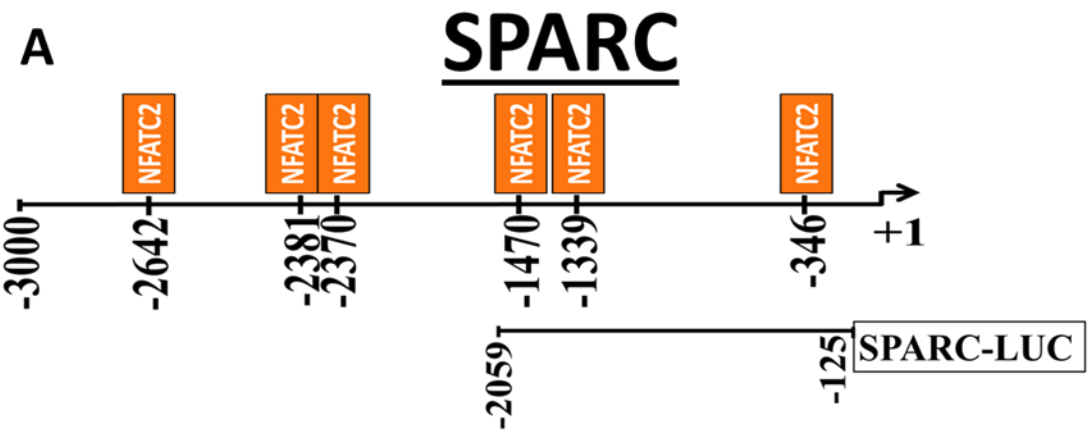


B

**NFATC2 Consensus Site**
**5'-GGAAAA-3'**

| NFATC2 Consensus Sites on the SPARC promoter | | |
|---|---|---|
| **Location** | **Sequence** | **% Similarity to Consensus Sequence** |
| -2642 | CCCAAAGG | 95.0% |
| -2381 | CCTTTAGG | 90.5% |
| -2370 | TCAAAAG | 91.9% |
| -1470 | CCTTTCCA | 92.3% |
| -1339 | CCTTTCAG | 91.8% |
| -346 | CCTTTGTG | 90.8% |

**A)** *In silico* analysis of ~3 kb of SPARC promoter, identified several binding sites for NFATC2, with >90% similarity with the consensus sequence **(shown on top of B).** The SPARC luciferase promoter reporter construct used is diagrammatically shown below the mapped promoter in A. The location and sequence of each NFATC2 binding site, in the SPARC promoter is tabulated in **B**.

**Figure 3.17: NFATC2 Binding Sites on COL3A1 Promoter**

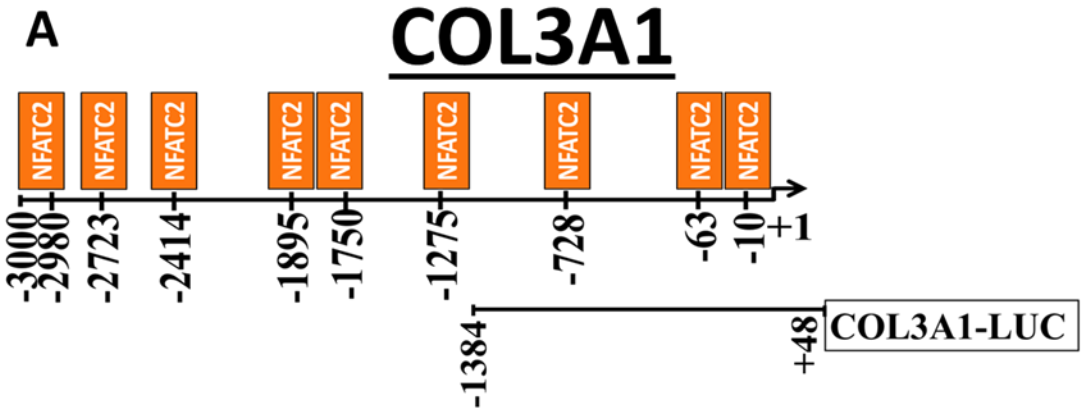


B

**NFATC2 Consensus Site**
**5'-GGAAAA-3'**

| NFATC2 Consensus Sites on the COL3A1 promoter | | |
|---|---|---|
| **Location** | **Sequence** | **% Similarity to Consensus Sequence** |
| -2980 | CAACAAAGG | 91.3% |
| -2723 | TGTTAAGG | 84.8% |
| -2414 | ATGCAAAGG | 90.3% |
| -1895 | CCTTTCCCC | 90.2% |
| -1750 | CCTTTCCTG | 91.2% |
| -1275 | GTTTAAAGG | 91.0% |
| -728 | ATGAAAAGG | 92.9% |
| -63 | TCAGAAAGG | 98.9% |
| -10 | AAGCAAAGG | 99.3% |

**A)** *In silico* analysis of ~3 kb of COL3A1 promoter, identified several binding sites for NFATC2, with >90% similarity with the consensus sequence **(shown on top of B).** The COL3A1 luciferase promoter reporter construct used is diagrammatically shown below the mapped promoter in A. The location and sequence of each NFATC2 binding site, in the COL3A1 promoter is tabulated in **B**.

**Figure 3.18: Role of NFATC2 Binding Sites in Activation of SPARC and COL3A1 Promoters**

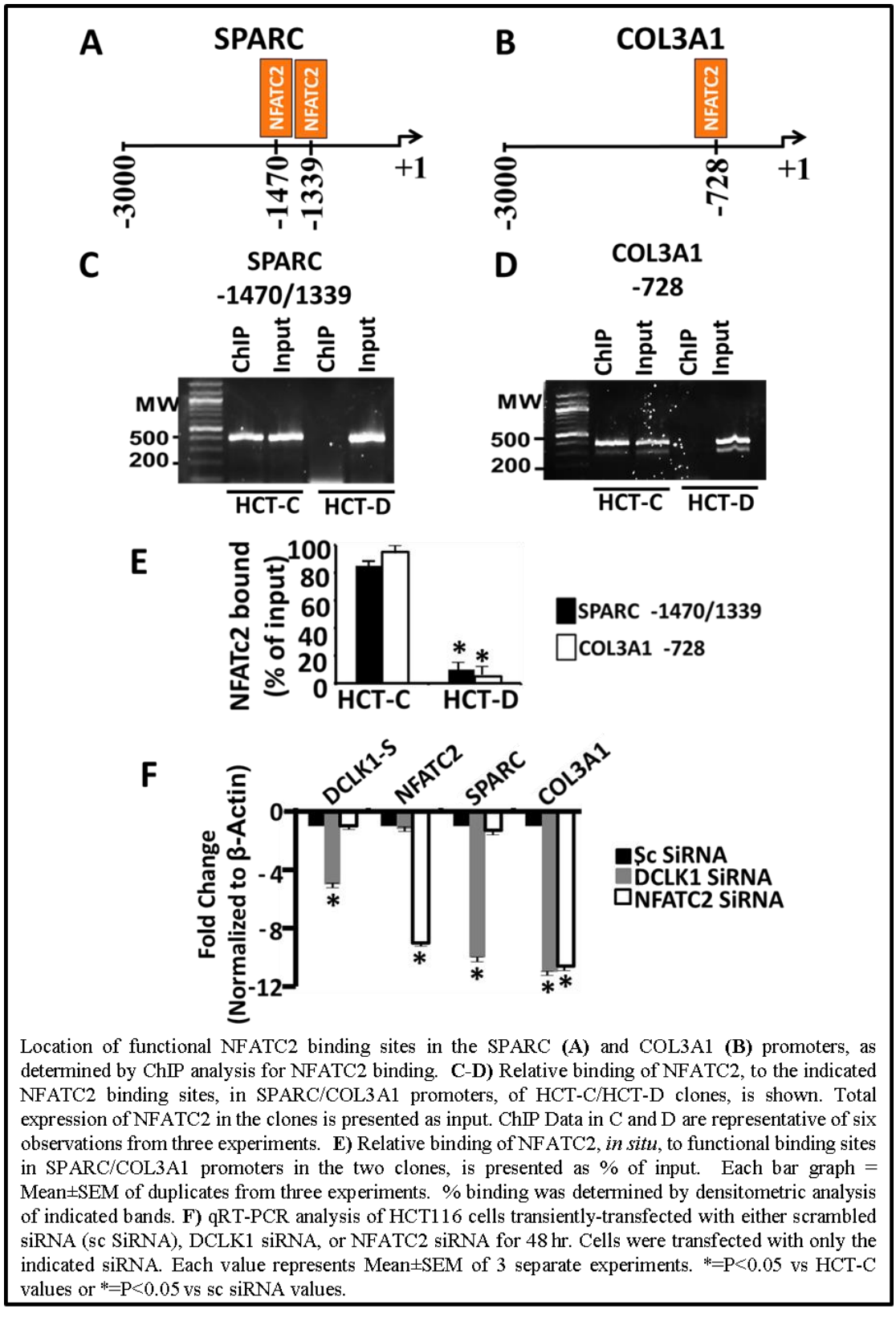


Location of functional NFATC2 binding sites in the SPARC **(A)** and COL3A1 **(B)** promoters, as determined by ChIP analysis for NFATC2 binding. **C-D)** Relative binding of NFATC2, to the indicated NFATC2 binding sites, in SPARC/COL3A1 promoters, of HCT-C/HCT-D clones, is shown. Total expression of NFATC2 in the clones is presented as input. ChIP Data in C and D are representative of six observations from three experiments. **E)** Relative binding of NFATC2, *in situ*, to functional binding sites in SPARC/COL3A1 promoters in the two clones, is presented as % of input. Each bar graph = Mean±SEM of duplicates from three experiments. % binding was determined by densitometric analysis of indicated bands. **F)** qRT-PCR analysis of HCT116 cells transiently-transfected with either scrambled siRNA (sc SiRNA), DCLK1 siRNA, or NFATC2 siRNA for 48 hr. Cells were transfected with only the indicated siRNA. Each value represents Mean±SEM of 3 separate experiments. *=P<0.05 vs HCT-C values or *=P<0.05 vs sc siRNA values.

**Figure 3.19: Co-Localization of DCLK1-S with NFATC2**

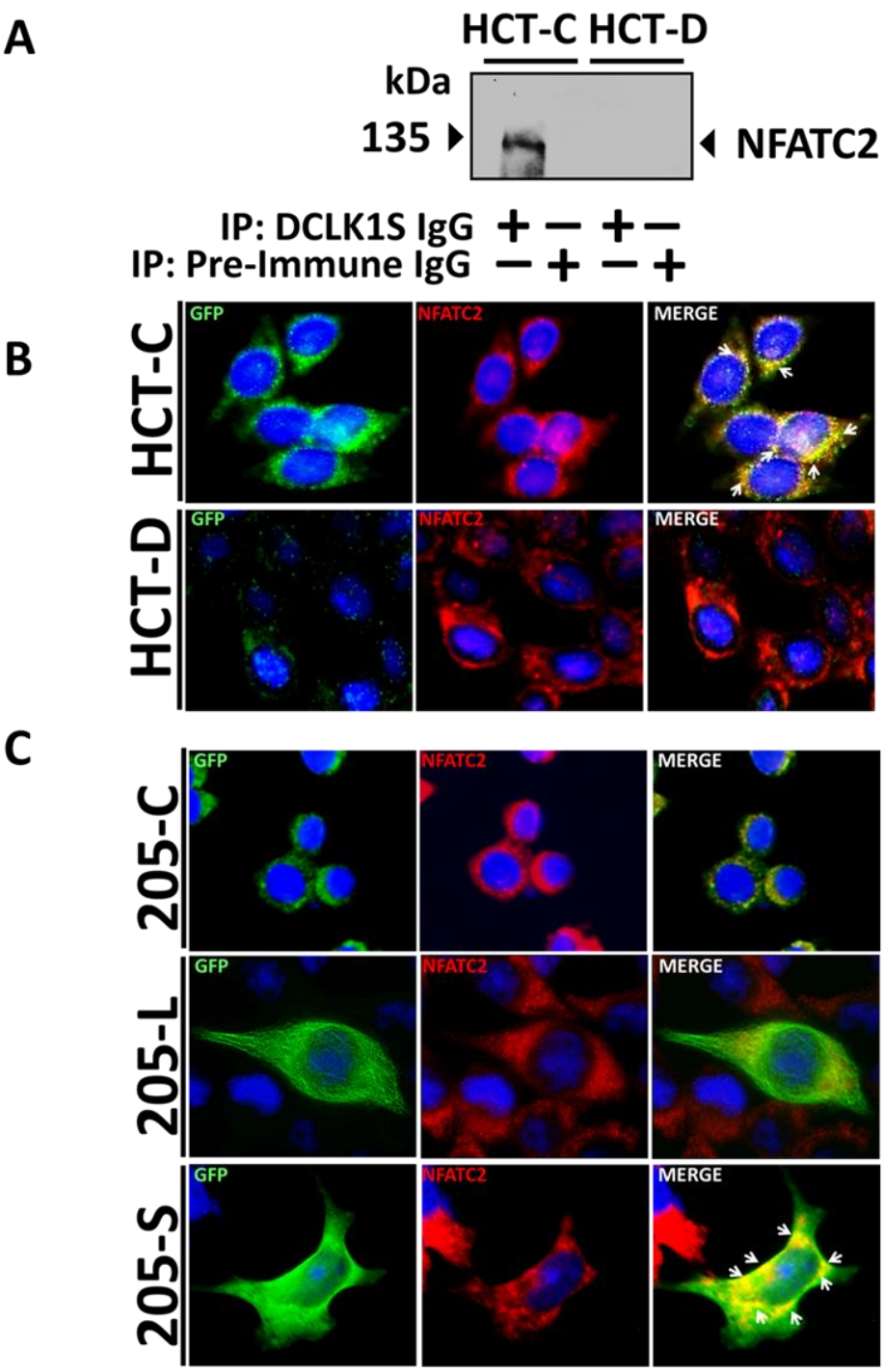


**A)** Cellular lysates of HCT-C /D were processed for CO-IP with either preimmune control IgG or anti-DCLK1-S-Abs and probed for NFATC2 by western blot analysis. Representative IF images of HCT-C/HCT-D (**B**) and 205-C/205-L/205-S (**C**) cells grown on coverslips, stained with Abs against the indicated proteins, as described in methods. Co-localization of the indicated proteins is depicted in yellow color in merged images. A-C, representative data from 3 separate experiments.

**Figure 3.20: Effect of Mutated NFATC2 (at the $^{53}$SPPS$^{56}$ Motif ) on COL3A1 Promoter activity and on Expression of COL3A1.**

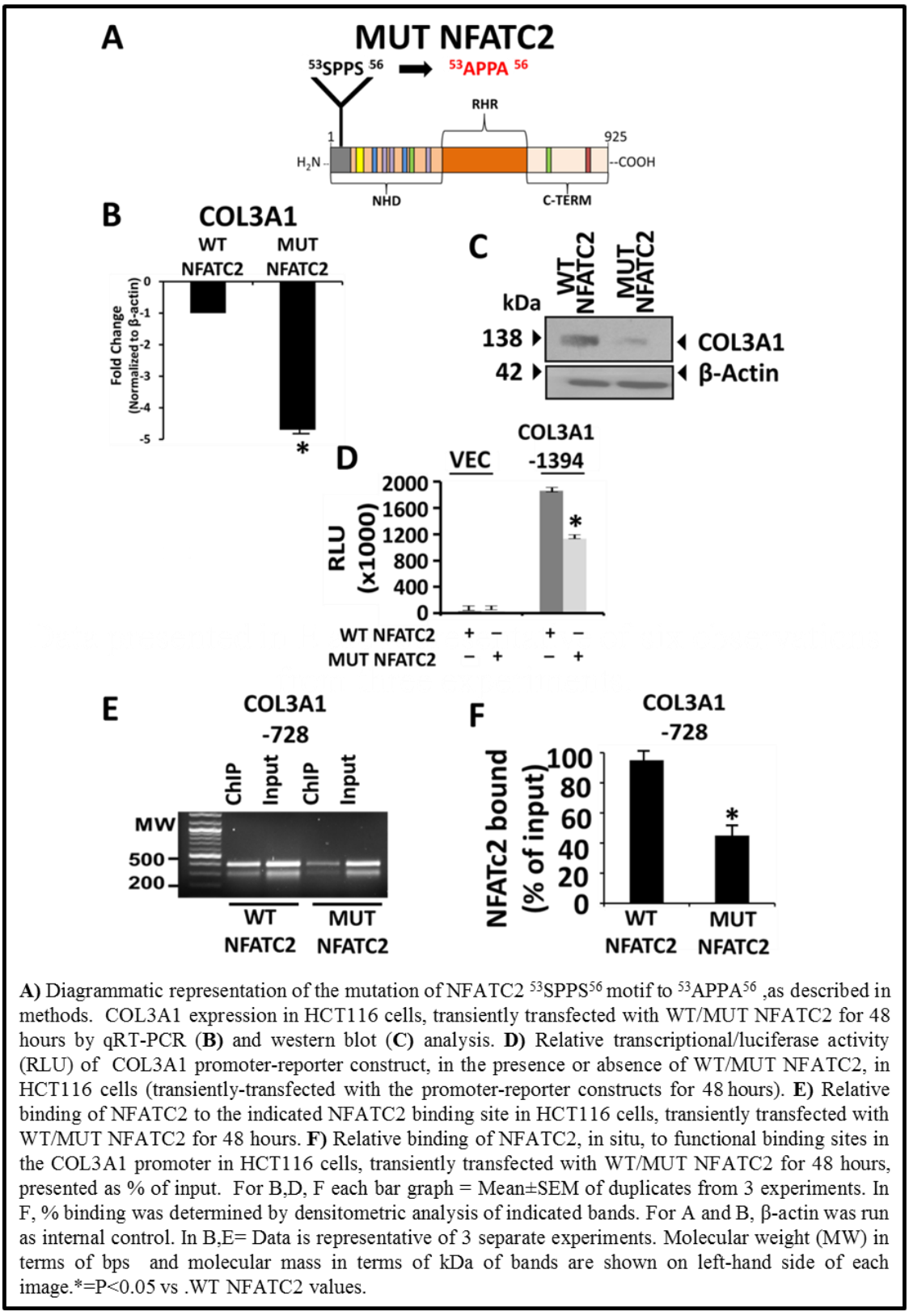


**A)** Diagrammatic representation of the mutation of NFATC2 $^{53}$SPPS$^{56}$ motif to $^{53}$APPA$^{56}$ ,as described in methods. COL3A1 expression in HCT116 cells, transiently transfected with WT/MUT NFATC2 for 48 hours by qRT-PCR (**B)** and western blot (**C)** analysis. **D)** Relative transcriptional/luciferase activity (RLU) of COL3A1 promoter-reporter construct, in the presence or absence of WT/MUT NFATC2, in HCT116 cells (transiently-transfected with the promoter-reporter constructs for 48 hours). **E)** Relative binding of NFATC2 to the indicated NFATC2 binding site in HCT116 cells, transiently transfected with WT/MUT NFATC2 for 48 hours. **F)** Relative binding of NFATC2, in situ, to functional binding sites in the COL3A1 promoter in HCT116 cells, transiently transfected with WT/MUT NFATC2 for 48 hours, presented as % of input. For B,D, F each bar graph = Mean±SEM of duplicates from 3 experiments. In F, % binding was determined by densitometric analysis of indicated bands. For A and B, β-actin was run as internal control. In B,E= Data is representative of 3 separate experiments. Molecular weight (MW) in terms of bps and molecular mass in terms of kDa of bands are shown on left-hand side of each image.*=P<0.05 vs .WT NFATC2 values.

**Figure 3.21: Effect of Mutated NFATC2 (at the $^{53}$SPPS$^{56}$ Motif) on SPARC Promoter activity and on Expression of SPARC.**

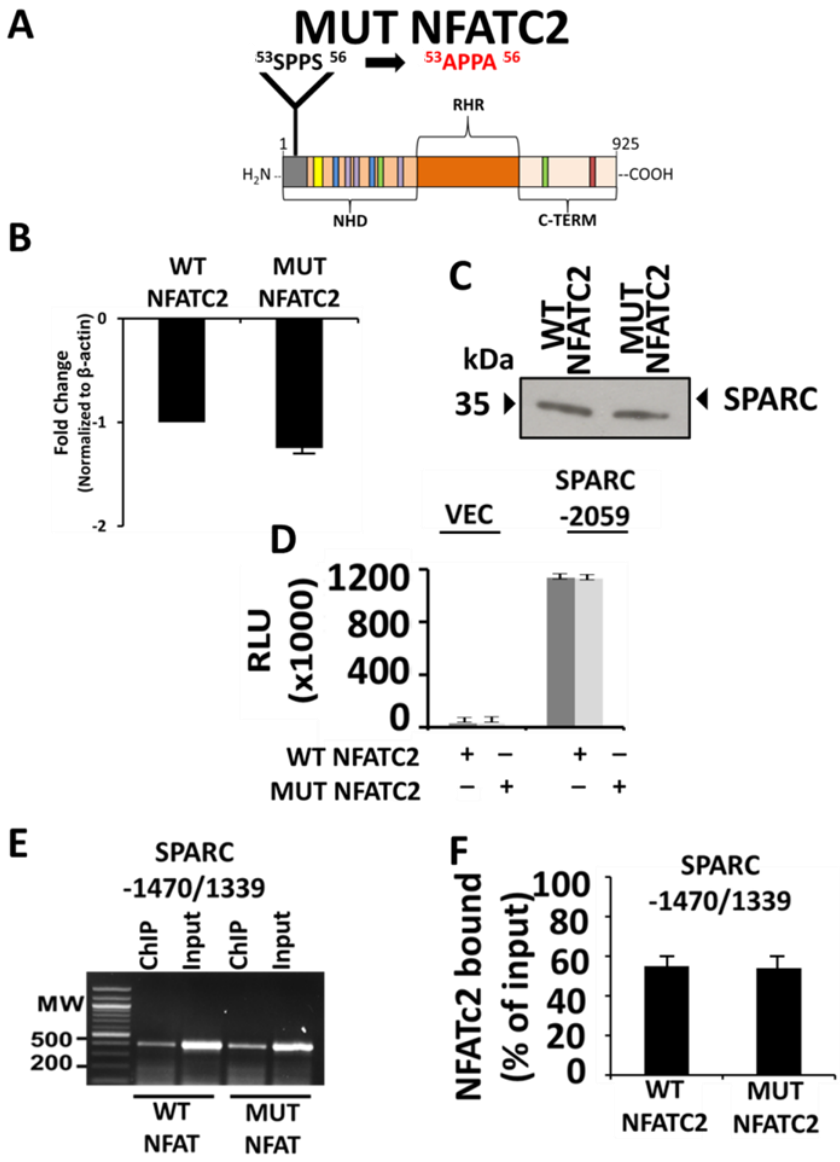


**A)** Diagrammatic representation of the mutation of NFATC2 $^{53}$SPPS$^{56}$ motif to $^{53}$APPA$^{56}$ ,as described in methods. SPARC expression in HCT116 cells, transiently transfected with WT/MUT NFATC2 for 48 hours by qRT-PCR (**B)** and western blot (**C)** analysis. **D)** Relative transcriptional/luciferase activity (RLU) of SPARC promoter-reporter construct, in the presence or absence of WT/MUT NFATC2, in HCT116 cells (transiently-transfected with the promoter-reporter constructs for 48 hours). **E)** Relative binding of NFATC2 to the indicated NFATC2 binding site in HCT116 cells, transiently transfected with WT/MUT NFATC2 for 48 hours. **F)** Relative binding of NFATC2*, in situ*, to functional binding sites in the SPARC promoter in HCT116 cells, transiently transfected with WT/MUT NFATC2 for 48 hours, presented as % of input. For B,D, F each bar graph = Mean±SEM of duplicates from 3 experiments. In F, % binding was determined by densitometric analysis of indicated bands. For A and B, β-actin was run as internal control. In B,E= Data is representative of 3 separate experiments. Molecular weight (MW) in terms of bps and molecular mass in terms of kDa of bands are shown on left-hand side of each image.*=P<0.05 vs. WT NFATC2 values.

**Figure 3.22: Co-Localization of DCLK1-S with WT/MUT NFATC2**

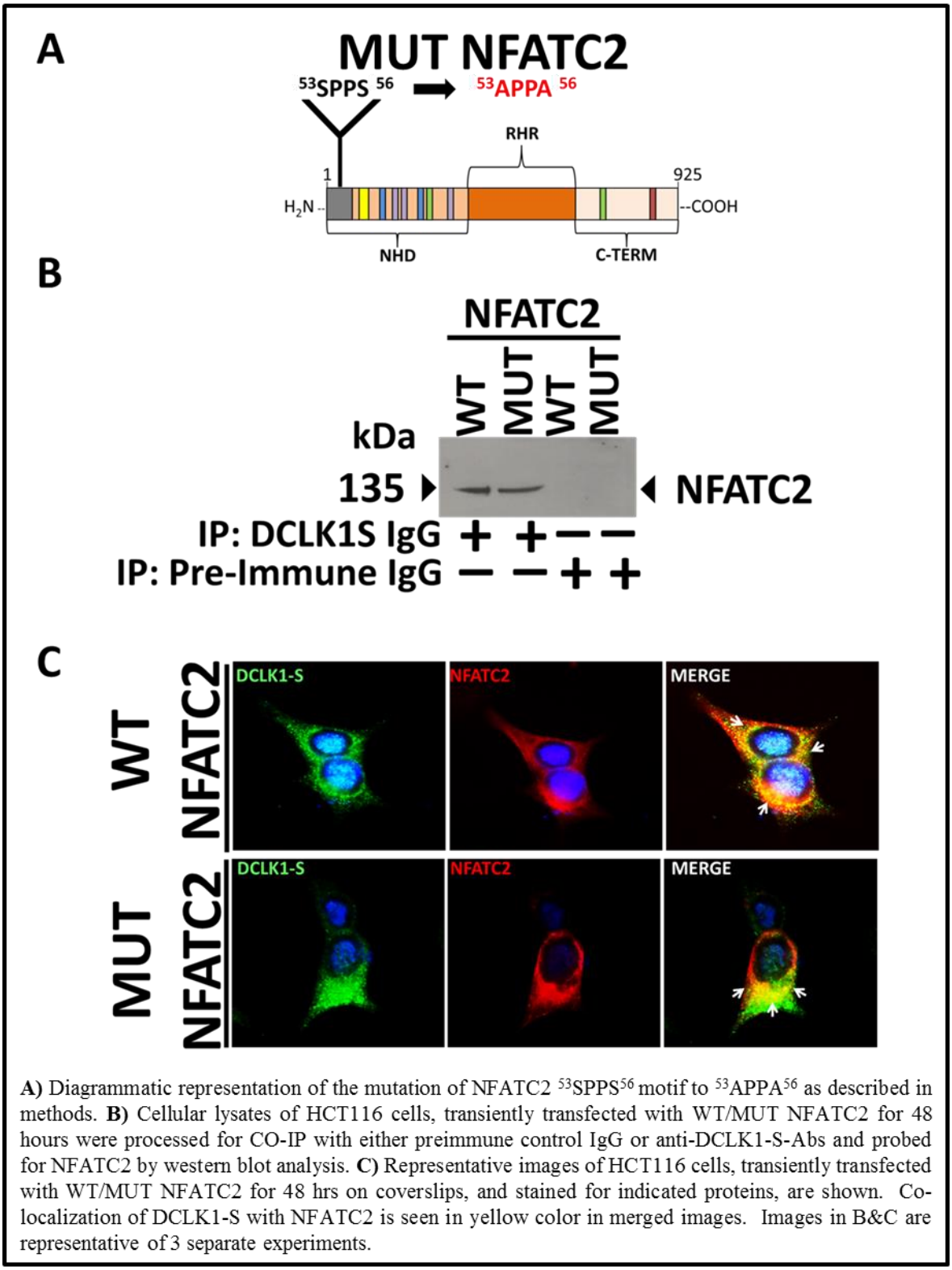


**A)** Diagrammatic representation of the mutation of NFATC2 $^{53}$SPPS$^{56}$ motif to $^{53}$APPA$^{56}$ as described in methods. **B)** Cellular lysates of HCT116 cells, transiently transfected with WT/MUT NFATC2 for 48 hours were processed for CO-IP with either preimmune control IgG or anti-DCLK1-S-Abs and probed for NFATC2 by western blot analysis. **C)** Representative images of HCT116 cells, transiently transfected with WT/MUT NFATC2 for 48 hrs on coverslips, and stained for indicated proteins, are shown. Co-localization of DCLK1-S with NFATC2 is seen in yellow color in merged images. Images in B&C are representative of 3 separate experiments.

**Table 3.1: Oligonucleotide (primer) Sequences Used for qRT-PCR/RT-PCR/ChIP for Aim 3 Experiments**

**Table 3.1**

| Target cDNA/gDNA | Species | Primer Sequence | Assay |
|---|---|---|---|
| DCLK1-Long (cDNA) | Human | F:GGAGTGGTGAAACGCCTGTAC | RT-PCR & qRT-PCR |
| | | R:GGTTCCATTAACTGAGCTGG | |
| DCLK1-Short (cDNA) | Human | F:ACACTAAGACTGTGTCCATGTTAGAACTC | RT-PCR & qRT-PCR |
| | | R:AAGCCTTCCTCCGACACTTCT | |
| SPARC (cDNA) | Human | F:GTGCAGAGGAAACCGAAGAG | RT-PCR & qRT-PCR |
| | | R:AAGGGCAGGAAGAGTCGAA | |
| COL3A1 (cDNA) | Human | F:AAACCTAAGGAAACTTCACG | RT-PCR & qRT-PCR |
| | | R:GCTATTCATGTGTCTAAATATGAATATTG | |
| NFATC2 (cDNA) | Human | F:GCCATCAACAGCTGCTTCCA | RT-PCR & qRT-PCR |
| | | R:CACACCCCGCACCTTAATGA | |
| -1470/-1339 NFATC2 *cis* element in SPARC promoter(gDNA) | Human | F:ATGGCAAGAGAGACAGGGGC | ChIP PCR |
| | | R:GAATGCCTTGGCTTCCCAAA | |
| -728 NFATC2 cis element in COL3A1 promoter (gDNA) | Human | F:TGTGCACAGGCATAGAGACGGA | ChIP PCR |
| | | R:GCAAAGCTATCTTCAGGAGG | |
| SPARC-LUC (-2059/-125) (gDNA) | Human | F:CCAAGCTTGACAGGTGAGGGGAGGAAA | Promoter Reporter Construct |
| | | R:AACCTAGGTGCCTAAACCGACTCACAGA | |
| COL3A1-LUC (-1384/+48) (gDNA) | Human | F:CCCTCGAGTTTGCCACTGTCCATGCTTA | Promoter Reporter Construct |
| | | R:CCCCCTAGGGTTCAAAGTAGCCACCATCAA | |

The forward (F) and reverse (R) primer sequences that were designed and used for amplifying the indicated target cDNA/gDNA for conducting the different assays are shown.

## 3.3 DISCUSSION

Accumulating evidence suggests that cancer stem cells are capable of surviving radiation/chemotherapy and are able to regrow as primary or metastatic tumors, resulting in relapse of the disease (Cherciu et al., 2014; Kantara et al., 2014; Wang et al., 2015b). We and others have therefore proposed that targeting cancer stem cells, in conjunction with conventional or other therapies, may provide a more comprehensive strategy for

treating cancers. Therefore identification of cancer stem cells with reliable markers remains an important goal in the field (Cherciu et al., 2014; Kantara et al., 2014; Kantara et al., 2015; Wang et al., 2015a). Several putative stem cell markers have been identified, however colon cancer cells express many of the same markers as intestinal stem cells (including DCLK1) (Barker, 2014; Cherciu et al., 2014; Hirsch et al., 2014; Nakanishi et al., 2013; Sarkar et al., 2012); therefore targeting cancer stem cells, while sparing normal stem cells, remains a challenge. We recently reported that an alternate promoter within the Intron V of the *DCLK1* gene is utilized by colon cancer cells to express a shorter transcript of DCLK1 (DCLK1-S), while the 5'(α)-promoter is utilized by normal colonic cells to express the full length DCLK1 transcript (DCLK1-L) (O'Connell et al., 2015), as described in detail in Chapter 2. The 5'(α)-promoter of *DCLK1* becomes methylated in colon adenocarcinomas resulting in silencing of DCLK1-L expression (O'Connell et al., 2015). The two promoters appear to be regulated independently, and the expression of one does not appear to be connected to the expression of the other. Therefore an opportunity exists to specifically target DCLK1-S as an approach for eliminating colon cancer stem cells while preserving normal colonic stem cells.

The presence of multiple isoforms of DCLK1 within the brain has been extensively reported (Burgess and Reiner, 2002; Engels et al., 2004; Omori et al., 1998; Pal et al., 2011; Shang et al., 2003; Silverman et al., 1999; Vreugdenhil et al., 1999); however the specific biological functions of each isoform have remained undefined. DCLK1-S lacks both N-terminal DCX doublecortin domains as compared to DCLK1-L, therefore differences in the 3D structure of the isoforms can be expected. To date, the crystal structure of either the full length DCLK1-L isoform or the shorter DCLK1-S isoform have not been resolved (Kim et al., 2003b). The substrates and regulators of both isoforms of DCLK1 have also remained elusive (Shang et al., 2003), and DCLK1 has been termed an "orphan kinase". Due to likely differences in the 3D structures of the long and short isoforms, it is speculated that the biological functions and activities of the

isoforms will likely be different. In my Aim 2 studies, I used shRNA knockdown method to downregulate the expression of DCLK1-S isoform in a representative colon cancer cell line, (which only expressed the short isoform, due to hypermethylation and silencing of the 5' promoter), in order to delineate biological role of the cancer specific DCLK1-S isoform. Based on my studies, I discovered that NFATC2 may represent a novel substrate for the kinase domain of DCLK1-S, which allows activation of the potent transcriptional factor and results in significantly enhancing the expression of COL3A1 and the invasive potential of the colon cancer cells, *in vitro* and *in vivo* (**Fig 3.19**). Most importantly, my studies suggest that overexpression of the S isoform by colon cancer cells imparts a potent invasive phenotype to the cells, strongly suggesting that targeting the kinase domain or the downstream functions of the S isoform may allow us to specifically target cancer stem cells.

In here we report for the first time that DCLK1-S binds (and most likely activates) NFATC2 via the NFATC2 $^{53}$SPPS$^{56}$ motif. The activation/de-activation of NFATC2 has been well described throughout literature. NFATC2 is activated via calcineurin/calmodulin mediated de-phosphorylation of multiple serine residues, resulting in the unmasking of the NLS. NFATC2 is then free to translocate to the nucleus and induce transcription (Hogan et al., 2003; Müller and Rao, 2010; Qin et al., 2014; Shou et al., 2015). The de-activation of NFATC2 is coordinated through several kinases that function to phosphorylate serine residues resulting in re-masking of the NLS and maintaining a hyper-phosphorylated state so that NFATC2 remains inactive (Hogan et al., 2003; Müller and Rao, 2010; Pan et al., 2013; Qin et al., 2014; Shou et al., 2015). An additional level of NFATC2 regulation has been reported, in which certain kinases function to enhance the transcriptional activity of NFATC2 via phosphorylation of the NFATC2 $^{53}$SPPS$^{56}$ motif (Gómez-Casero et al., 2007; Okamura et al., 2000). By mutating the NFATC2 $^{53}$SPPS$^{56}$ motif, we were able to demonstrate that NFATC2 was no longer able to upregulate the expression of COL3A1, suggesting that the NFATC2 $^{53}$SPPS$^{56}$

motif is critical for measuring DCLK1-S mediated overexpression of COL3A1 in colon cancer cells (**Fig 3.20**). Importantly, the binding of DCLK1-S (by IP analysis), or the translocation of NFATC2 into the nucleus (by IF analysis), was not affected by mutation of the NFATC2 $^{53}$SPPS$^{56}$ motif, suggesting that phosphorylation of NFATC2 $^{53}$SPPS$^{56}$ motif needs to be inhibited by either engineering a mutation of this site or by discovering a specific inhibitor of phosphorylation at this site. In future studies an important role of DCLK1-S is phosphorylating/activating NFATC2 at the $^{53}$SPPS$^{56}$ motif needs to be confirmed, using recombinant proteins and *in vitro* kinase assays. However based on my results so far, it is speculated that DCLK1-S plays a critical role in enhancing the activation of NFATC2 via phosphorylation of the NFATC2 $^{53}$SPPS$^{56}$ motif, resulting in the increased expression/secretion of COL3A1, which likely imparts an invasive potential to the cells.

Both SPARC (Arnold and Brekken, 2009; Nagaraju et al., 2014) and COL3A1 (Basso et al., 2001; Ewald et al., 2013; Su et al., 2014; Turashvili et al., 2007; Xiong et al., 2014) have been implicated in playing a critical role in mediating the invasive potential of cancer cells via rearrangement of the extracellular matrix. ECM stiffness from increased collagen deposition has been reported to promote cell invasion by providing a track of least resistance for invasive cells (Conklin et al., 2011; Goetz et al., 2011; Gritsenko et al., 2012; Levental et al., 2009). During invasion, collagen fibers bundle and straighten out, causing the fibers to become thick and align perpendicularly to the tumor boundary. The perpendicularly aligned collagen bundles provide contact guidance for cells and an unhindered track for invasion with least resistance.

In my Aim 2 studies, I have confirmed that DCLK1-S (but not DCLK1-L) mediates the expression of SPARC and COL3A1 (**Fig 3.11 & 3.13**). Therefore the role of DCLK1-S in enhancing the invasive potential of DCLK1 was evaluated both *in vitro* and *in vivo* (**Fig 3.13 & 3.14).** Our results demonstrate that the increased invasive potential of cells due to expression of DCLK1-S is isoform specific (**Fig 3.14**). Using the well-

established *in vivo* model for invasion studies (Sarkar et al., 2012), we learned that mice inoculated with DCLK1-S overexpressing, but not DCLK1-L overexpressing, isogenic colon cancer cells, developed visible metastatic lesions in the livers within 3 weeks of inoculation. The latter results suggested the novel possibility that DCLK1-S (but not DCLK1-L) enhanced the invasive potential of colon cancer cells (**Fig 3.14**). Importantly, high levels of SPARC and COL3A1 were detected in the metastatic lesions of mice inoculated with DCLK1-S expressing cells (**Fig 3.15**), confirming my *in vitro* findings (shown in **Figure 3.13**), and demonstrating increased expression of SPARC and COL3A1, in response to DCLK1-S expression in colon cancer cells. It is speculated that the increased expression of SPARC and/or COL3A1, downstream of DCLK1-S, may facilitate ECM remodeling around the colon cancer cells/tumors to facilitate invasion, as described in literature.

In my Aim 2 studies, I concentrated on examining a role of DCLK1-S in enhancing the invasive potential of colon cancer cells. However multiple pathways are significantly disrupted in colon cancer cells, down regulated for the expression of DCLK1-S expression (**Fig 3.9 & 3.10**). These pathways include cellular growth, tumor development, cell death, and apoptosis (**Fig 3.9 & 3.10**). Our experiments thus far demonstrate that downregulation of DCLK1-S results in the inhibition of the proliferative/tumorigenic/invasive potential of HCT116 colon cancer cells, which likely reflects the loss of cancer stem cells measured in spheroidal assays (**Fig 3**.). Thus, attenuation of DCLK1-S expression results in significant changes in the biology of cancer cells, both *in vitro* and *in vivo* (**Fig 3.8**). To better understand the role DCLK1-S in colon carcinogenesis, especially in humans, additional studies are required to evaluate the role of DCLK1-S in each of the molecular pathways, discovered to be significantly altered in cells in which DCLK1-S has been downregulated.

A clinically important discovery of the current studies is the identification of genes activated downstream of DCLK1-S (**Appendix 2**). Since the L/S transcripts of

DCLK1 are >99% homologous (O'Connell et al., 2015), 3' of the doublecortin domains, specifically targeting DCLK1-S remains an issue. In order to avoid toxicity, it may be significantly more difficult to only target S-isoform, while sparing the L-isoform. Therefore identifying isoform specific targets, downstream of DCLK1-S, as conducted in my studies, may have significant translational value, in terms of prevention and treatment of colorectal cancers, in the absence of side effects to normal tissues.

In summary, our findings suggest that DCLK1-S is required for maintaining proliferative/tumorigenic/metastatic potential of colon cancer cells, both *in vitro* and *in vivo*, probably by maintaining the viability of cancer stem cells (measured in spheroid assay). My studies have established, with some confidence, the critical role of DCLK1-S (but not DCLK1-L) in enhancing the invasive potential of colon cancer cells. DCLK1-S functions to bind and activate the NFATC2 $^{53}$SPPS$^{56}$ motif resulting in enhanced activation of NFATC2. NFATC2 then translocates from the cytosol to the nucleus and transcriptionally upregulates the expression of COL3A1, resulting in remodeling of the extracellular matrix in order to enhance the invasive capacity of colon cancer cells, as diagrammatically presented in **Figure 3.23**. The identification of genes activated downstream of DCLK1-S provides an opportunity for developing methods that can specifically target downstream effects of DCLK1-S, without disrupting the function of DCLK1-L in normal cells.

**Figure 3.23: Diagrammatic Representation of Mechanisms by which DCLK1-S is Speculated to Mediate Downstream Effects, based on my Aim 2 Findings**

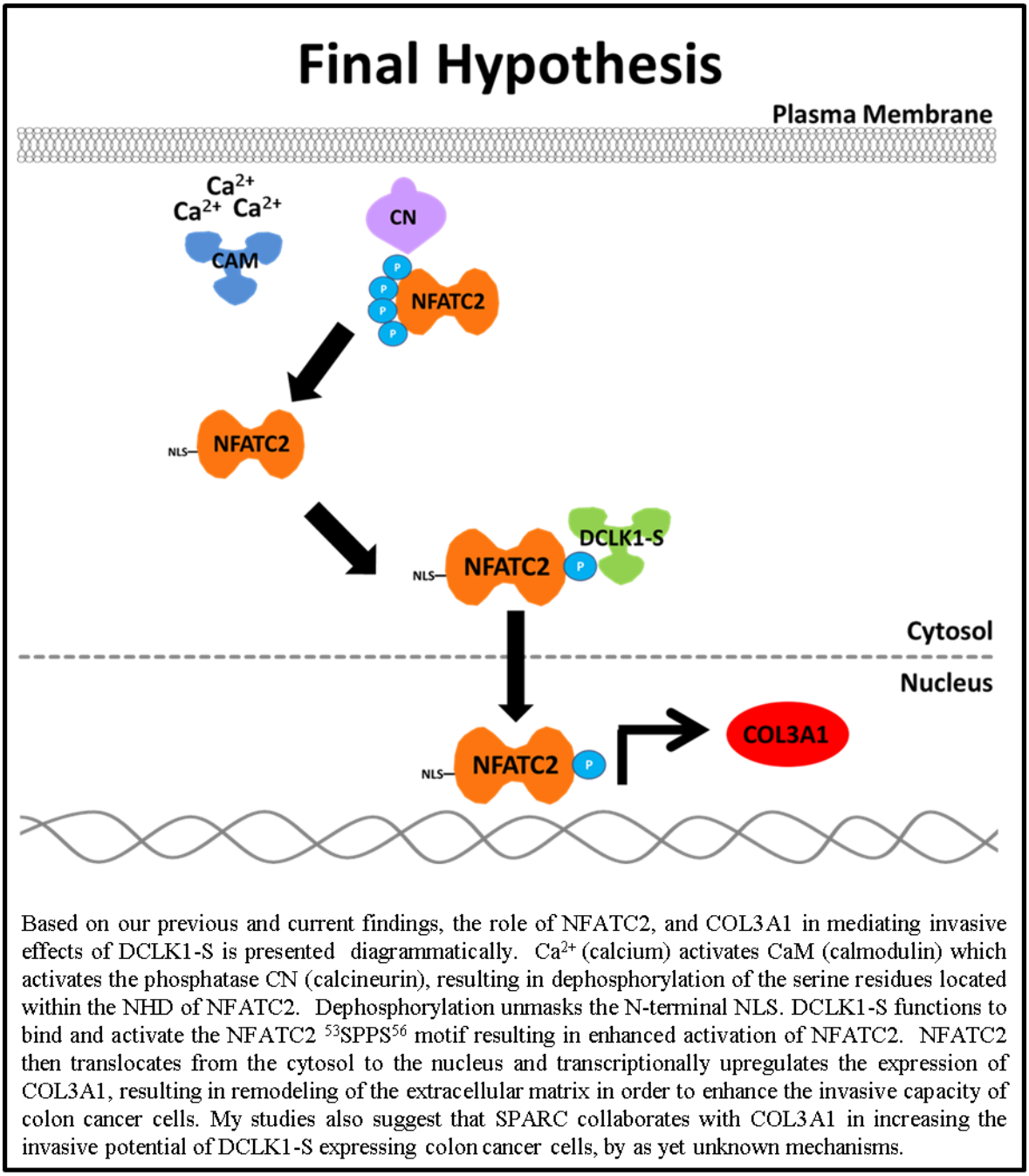


Based on our previous and current findings, the role of NFATC2, and COL3A1 in mediating invasive effects of DCLK1-S is presented diagrammatically. $Ca^{2+}$ (calcium) activates CaM (calmodulin) which activates the phosphatase CN (calcineurin), resulting in dephosphorylation of the serine residues located within the NHD of NFATC2. Dephosphorylation unmasks the N-terminal NLS. DCLK1-S functions to bind and activate the NFATC2 $^{53}$SPPS$^{56}$ motif resulting in enhanced activation of NFATC2. NFATC2 then translocates from the cytosol to the nucleus and transcriptionally upregulates the expression of COL3A1, resulting in remodeling of the extracellular matrix in order to enhance the invasive capacity of colon cancer cells. My studies also suggest that SPARC collaborates with COL3A1 in increasing the invasive potential of DCLK1-S expressing colon cancer cells, by as yet unknown mechanisms.

# Chapter 4: FOXD3 is a novel repressor of the expression of short isoform of DCLK1 (DCLK1-S) from IntronV(β)-promoter of human DCLK1 gene, and is epigenetically silenced in human colorectal cancers: Prognostic/Diagnostic implications of FOXD3/DCLK1-S expression in human colorectal cancers.

***This chapter is a copy of a manuscript to be submitted to Oncotarget (O'Connell et al., 2016a). This work has also been selected to be presented as a Poster of Distinction at Digestive Disease Week, 2016 (O'Connell et al., 2016b).**

## 4.1 INTRODUCTION

DCLK1 is a specific marker of colon and pancreatic cancers in mice (Bailey et al., 2014; Nakanishi et al., 2013; Westphalen et al., 2014), and is elevated in human colon adenocarcinomas (Gagliardi et al., 2012a; Kantara et al., 2014; O'Connell et al., 2015). Downregulation of DCLK1, results in loss of cancer stem cell markers and tumorigenic potential of human colon cancer cells (Kantara et al., 2014; Sureban et al., 2011b). We recently reported a novel finding that human colorectal cancers express short transcripts of DCLK1 (DCLK1-S) from an alternate promoter located within the intron V of the *DCLK1* gene, while normal human colons express the canonical long transcript (DCLK1-L) from the 5'(α)-promoter of the gene (O'Connell et al., 2015). We and others have demonstrated that the 5'(α)-promoter is hypermethylated in human colorectal cancers, resulting in epigenetic silencing and loss of expression of DCLK1-L (Marie Vedeld et al., 2014; O'Connell et al., 2015; Vedeld et al., 2014). Although the 5'(α)-promoter is differentially methylated in normal human colons vs. human colorectal cancers, methylation status of the IntronV(β)-promoter does not change (O'Connell et al., 2015). We therefore hypothesized that differential expression of DCLK1-S in normal colons vs.

human colorectal cancers is perhaps due to differences in the transcriptional activity of the promoter in normal vs. cancer cells. To test our hypothesis, we conducted *in silico* analysis of the IntronV(β)-promoter and found several potential binding sites for FOXD3 within 3 kb of the transcriptional start site of the IntronV(β)-promoter (as described in **Figure 4.1**). Therefore the role of FOXD3 in regulating the IntronV(β)-promoter was further evaluated.

**Figure 4.1: FOXD3 Binding Sites on DCLK1 IntronV-β-promoter**

**A**

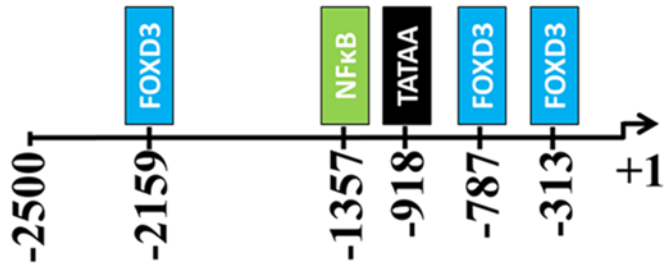


**B**

**FOXD3 Consensus Site**
**5-A[AT]T[AG]TTTGTTT-3**

| FOXD3 Consensus Sites on the IntronV-(β)-promoter of DCLK1 | | |
|---|---|---|
| **Location** | **Sequence** | **% Similarity to Consensus Sequence** |
| -2159 | TTGTTTTTGT | 92.0% |
| -728 | TTTTATTGTTT | 93.5% |
| -313 | AAACAAACAAA | 98.5% |

**A)** *In silico* analysis of ~3 kb of IntronV(β)-promoter of *DCLK1*, identified several binding sites for FOXD3, with >90% similarity with the consensus sequence **(shown on top of B).** The location and sequence of each FOXD3 binding site, in the IntronV(β)-promoter is tabulated in **B**.

### 4.1.1 FOXD3

FOXD3 (Forkhead Box D3) is a member of the forkhead box (FOX) family of transcription factors which is characterized by a distinct FH (forkhead) domain (Weigel and Jäckle, 1990) . The FH domain is a helix-turn-helix DNA binding motif (Wijchers et al., 2006). In humans there are 17 FOX gene subfamilies (FOXA-R) in which 41 genes have been identified (Myatt and Lam, 2007). FOX protein family members have been found to be important in a number of biological processes including development, differentiation, metabolism, proliferation, migration, and invasion (Myatt and Lam, 2007; Wijchers et al., 2006).

The *FOXD3* gene is located on the short arm of chromosome 1 at position 31 (1p31). Previous names of FOXD3 include HNF3, VAMAS2, AIS1, HFH2, and Genesis. The FOXD3 transcript (NM_012183.2) is 2078 bps, contains 1 exon and transcribes a 478 aa protein with molecular mass of 47.630 kDa (NP_036315.1) (as described in the NCBI database). The distinctive FH domain (also known as winged helix domain) is located at 141-218 aa, as shown in **Figure 4.2**.

**Figure 4.2: Diagrammatic Representation of FOXD3 Protein Domains**

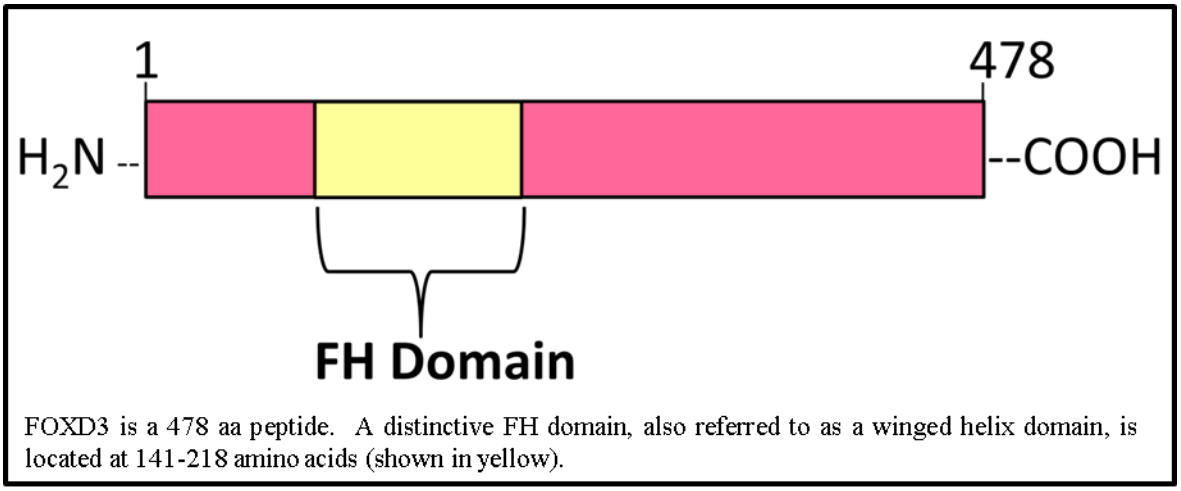


FOXD3 is a 478 aa peptide. A distinctive FH domain, also referred to as a winged helix domain, is located at 141-218 amino acids (shown in yellow).

A role of FOXD3 in development is well established (Hanna et al., 2002; Kos et al., 2001; Liu and Labosky, 2008; Pan et al., 2006; Sutton et al., 1996; Teng et al., 2008; Tompers et al., 2005). FOXD3 was first identified in embryonic stem cells (Sutton et al., 1996) and has been shown to play a critical role in the early mouse embryo where it functions to maintain pluripotent cells within the neural crest (Teng et al., 2008), inner cell mass (Hanna et al., 2002), and trophoblast progenitors (Tompers et al., 2005). It has also been demonstrated that FOXD3 is required to establish murine embryonic stem cell lines *in vitro* (Liu and Labosky, 2008; Pan et al., 2006), and knockdown of FOXD3 is embryonically lethal in mice (Hanna et al., 2002; Tompers et al., 2005). An important role in later development has also been reported in which FOXD3 plays a key role in migrating neuronal crest cells and repression of melanogenesis in the avian embryo (Kos et al., 2001). FOXD3 functions primarily as a transcriptional repressor (Sutton et al., 1996). However, it can also act as a transcriptional activator of a number of genes including ERBB3 (Erb-B2 Receptor Tyrosine Kinase 3) (Abel et al., 2013), OCT4 (Pan et al., 2006), and NANOG (Pan et al., 2006), many of which are required for suppressing differentiation of stem cells. The consensus DNA binding sequence for FOXD3 has been identified as 5'-A[A/T]T[A/G]TTTGTTT-3', which is comprised of two overlapping forkhead binding sites (Sutton et al., 1996).

The role of FOXD3 in repression of melanogenesis led investigators to examine if FOXD3 played a role in melanomas (Abel and Aplin, 2010; Basile et al., 2012; Katiyar and Aplin, 2011; Kubic et al., 2015; Weiss et al., 2014). Initial reports demonstrated that FOXD3 was suppressed by B-RAF and that ectopic expression of FOXD3 inhibited cell growth of melanoma cells by upregulating p21expression, resulting in cell cycle arrest at the G1 phase (Abel and Aplin, 2010). In subsequent reports it was demonstrated that ectopic expression of FOXD3 resulted in inhibition of spheroidal growths, migration, and invasion of melanoma cells, which was shown to be mediated via binding of FOXD3 to the Rnd3 (Rho Family GTPase 3) promoter (Katiyar and Aplin,

2011). The role of FOXD3 in adaptive resistance of melanoma to targeted therapies was also evaluated; it was reported that RAF/MEK inhibitors up regulate FOXD3 expression, resulting in FOXD3 mediated up regulation of ERBB3 (Erb-B2 Receptor Tyrosine Kinase 3) (Abel et al., 2013; Basile et al., 2012). FOXD3 has been reported to inhibit migration of melanoma cells through repression of TWIST1 (Twist Family BHLH Transcription Factor 1) (Weiss et al., 2014). At the same time, FOXD3 was reported to enhance migration of melanoma cells, by co-activating expression of CXCR4 (Chemokine (C-X-C Motif) Receptor 4) and PAX3 (Paired Box 3) (Kubic et al., 2015).

The role of FOXD3 in neural crest cells led investigators to examine if FOXD3 was involved in the generation of neuroblastomas, an embryonal tumor, derived from the neural crest (Li et al., 2013). The investigators reported that FOXD3 transactivates the expression of NDRG, by directly binding its promoter, resulting in the suppression of growth, angiogenesis, invasion, and metastasis of neuroblastoma cells (Li et al., 2013). The Li et al., additionally reported that expression levels of FOXD3 were significantly down regulated in neuroblastoma cell lines and tumors, and overall survival of neuroblastoma patients was significantly higher in patients expressing higher levels of FOXD3 (Li et al., 2013). Based on the above findings, Li et al. concluded that FOXD3 is a novel tumor suppressor of neuroblastomas, and suppresses growth and aggressiveness of the cells (Li et al., 2013). A possible inhibitory role of FOXD3 was similarly reported in breast and lung cancers (Chu et al., 2014; Wang et al., 2015a; Yan et al., 2015; Zhao et al., 2014). Zhao et al., reported that low levels of FOXD3 were inversely associated with metastatic status of invasive ductal carcinomas of the breast (Zhao et al., 2014). Chu et al., reported down regulation of FOXD3 expression in breast tumors vs. normal breasts; low levels of FOXD3 in breast cancers was found to be associated with shorter disease free survival of the patients (Chu et al., 2014). Chu et al. additionally reported that down regulation of FOXD3 caused increased cell proliferation/invasion of breast cancer cells, while over expression of FOXD3 inhibited tumor growth and metastasis, suggesting a

critical tumor suppressive role for FOXD3 (Chu et al., 2014). Reports also demonstrated that FOXD3 was down regulated in lung cancers (Wang et al., 2015a; Yan et al., 2015). Over expression of FOXD3 resulted in the inhibition of cell/tumor growth *in vitro* and *in vivo*, and reduced angiogenesis *in vivo* (Yan et al., 2015). FOXD3 has also been reported to bind and activate miR-137, resulting in suppression of cell growth, migration and invasion of hepatocellular carcinoma cells (Liu et al., 2014).

Methylation of the *FOXD3* promoter has been reported in recent years in gastric and colon cancers (Cheng et al., 2013; van Roon et al., 2013), which likely mediates epigenetic silencing of the gene, and loss of expression of FOXD3 in many cancers. Using integrative genome wide scans, FOXD3 was reported to be hypermethylated in gastric tissues of H pylori infected patients, and in patients with gastric cancers, who had short-term survival (Cheng et al., 2013). Overexpression of FOXD3 in gastric cancer cell lines resulted in inhibition of cell growth and invasion of cells, *in vitro,* and also reduced the growth of tumors/xenografts in mice; Cheng et al. believed that the inhibitory effects of FOXD3 were mediated by its binding/activating proapototic target genes, CYFIP2 and RARB (Cheng et al., 2013). Relative levels of FOXD3, CYFIP2 (Cytoplasmic FMR1 Interacting Protein 2) and RARB (Retinoic Acid Receptor, Beta) were down regulated in human gastric tumor tissues compared to that in normal tissues, suggesting that methylation of FOXD3 results in enhanced gastric carcinogenesis in patients with H Pylori infection (Cheng et al., 2013). Using the method of differential methylation hybridization, BRAF mutation-specific hypermethylation of FOXD3 was reported (van Roon et al., 2013). Van Roon et al. also reported high levels of FOXD3 in normal colonic tissue and in tumors with wtBRAF; on the other hand, FOXD3 was not detected in colonic tumors positive for mutBRAF (van Roon et al., 2013). The results from the above described studies strongly suggest that FOXD3 is a tumor suppressor, and may represent a novel therapeutic target for a large number of tumor types.

The results of my Aim 3 studies confirm an inhibitory role of FOXD3 in colon cancers. Our studies demonstrate for the first time that FOXD3 is a potent transcriptional inhibitor of IntronV(β)-promoter, resulting in the absence of DCLK1-S expression in normal human colons. We also evaluated the pathophysiological relevance of DCLK1-S and FOXD3 expression in overall survival of colorectal cancer patients in a cohort of 92 patients, and determined that patients expressing relatively high levels of DCLK1-S and low levels of FOXD3 had significantly worse overall survival as compared to patients expressing relatively low levels of DCLK1-S and high levels of FOXD3 suggesting that measuring relative levels of DCLK1-S and FOXD3 will likely have diagnostic/prognostic significance.

## 4.2 MATERIALS AND METHODS

### 4.2.1 Reagents Used

Antibodies used in these studies included: anti-β-actin (total) (Sigma, St. Louis, MO); anti-DCLK1 antibody (Abcam, Cambridge, MA); anti-FOXD3 antibody (Abcam, Cambridge, MA). Smart Pool of target-specific small interfering RNA (siRNA) and non-targeting (control) siRNA Pool were purchased from Dharmacon (Lafayette, CO). Sepharose beads and all other chemical reagents were purchased from Sigma. cDNA synthesis master mix was purchased from GeneDEPOT (Baker, TX). Syber green qRT-PCR kit was purchased from Bio-Rad (Hercule, CA). Promega GoTaq®green Master Mix (Maddison, WI) was used for PCR amplification, using a Thermal Cycler from Eppendorf (Hauppauge, NY). Cloning vector pGL2 was from Promega, and TOPO-TA cloning vector was purchased from Invitrogen (Grand Island, NY). Restriction enzymes and competent cells were purchased from New England BioLabs (Ipswich, MA). Transfection reagent FuGENE6 was bought from Roche (Branford, CT), and all primers used were synthesized by Sigma.

### 4.2.2 Cell culture

HEK293 and HCT116 cell lines were obtained from ATCC, and have been maintained in the laboratory for several years. COLO-205, RKO, COLO-320 and SW1417 were purchased from ATCC within the past two years and confirmed by ATCC. CCD841 were generously gifted to our laboratory from Dr. Carla Kantara (Department of BMB, UTMB). CCD841 cells were purchased from ATCC within the past two years, and confirmed by ATCC. All cell lines were monitored regularly for absence of mycoplasma, and HEK293 and HCT116 cell lines were confirmed to represent human epithelial cell lines with the help of Biosynthesis Company (Lewisville, TX).

### 4.2.3 Procurement of samples from normal colonic mucosa and colonic tumors of patients for RT-PCR analysis

Samples of normal colonic mucosa and primary colonic tumors were obtained as discarded samples (as per our approved UTMB IRB protocol #91-310) from the Tissue Core Facility at Cancer Center, University of Alabama, as part of CHTN Program funded by NIH. All samples were collected and flash-frozen and stored in liquid nitrogen or at -80°C until analyzed. Pathology of all samples was confirmed.

### 4.2.4 Analysis of cell lines/tissue samples by RT-PCR/qRT-PCR

Total RNA was isolated from cell lines (isogenic clones and treated/control cells) in monolayer cultures at 60-70% confluency, or from human patient tissues using Trizol Reagent (Invitrogen), as previously described (O'Connell et al., 2015). For qRT-PCR, the iTaq Universal SYBR Green Supermix (Bio-Rad, CA) was used as per the manufacturer's instructions, as previously described (O'Connell et al., 2015). The primer sequences used for PCR amplification of cDNA for both RT-PCR/qRT-PCR analysis are

provided in **Table 4.1**. Electrophoresis gels presented were cropped to present all the bands observed within the range covered by the molecular markers used (between 100 bp and 1000 bp for RT-PCR data), in order to avoid primer dimers seen towards the end of the run. Processing of the electrophoresis blots was applied equally across the entire image. Touch-up tools were not used to manipulate data.

### 4.2.5 Western Immunoblot (WB) analysis

Cell lines (isogenic clones and treated/control cells) growing as mono-layer cultures, were harvested and processed for preparing cellular lysates, followed by electrophoresis and transferred to PVDF-membranes as previously described (Kantara et al., 2014; O'Connell et al., 2015). Samples containing 30-50 µg of proteins were subjected to electrophoresis and transferred to PVDF-membranes as previously described (Kantara et al., 2014; O'Connell et al., 2015). Blots were cut into horizontal strips containing target or loading-control proteins (β-actin), and processed for WB, as described previously (Kantara et al., 2014; O'Connell et al., 2015). Antigen antibody complexes were detected with a chemiluminescence-reagent kit (Thermoscientific, IL or GE Healthcare, UK). Membrane-strips containing either target or loading control proteins were simultaneously exposed for equal time to autoradiographic films. Western blots presented were cropped to exclude bands beyond the range of the molecular markers, at the running end and at the loading end. Processing of films was applied equally across the entire image. Touch-up tools were not used to manipulate data.

### 4.2.6 Western Immunoblot (WB) analysis

Cells were treated with 5-azacytidine as previously described (O'Connell et al., 2015). In brief, HCT116 cells were seeded in 100 mm dishes at a density of $5x10^6$

cells/dish, one day prior to drug treatment. The cells were treated with 10 μM 5-aza-2′-deoxycytidine (5-Azacytidine) on days 2 and 5 of culture. The cells were harvested on day 6 of culture and total RNA isolated. RNA was processed for measuring relative levels of DCLK1-S and FOXD3 by RT-PCR.

### 4.2.7 Generation of promoter-reporter constructs for IntronV-(β)promoter of *DCLK1*-gene

The short isoform of DCLK1 (isoform 2) (NM_001195415.1 in NCBI data base) is transcribed from a promoter within IntronV, as recently reported (O'Connell et al., 2015). Promoter-reporter constructs were generated as previously described (O'Connell et al., 2015). In brief, promoter fragments within IntronV (-2503/-771) were amplified using genomic DNA and cloned into PGL2 basic vector at XhoI and HindIII sites. The purified IntronV-promoter-reporter constructs, were confirmed by DNA sequencing. Primer sequences used for PCR amplification of the promoter segments are listed in **Table 4.1**.

### 4.2.8 Transient-transfection of cells with oligonucleotides and expression plasmids

Cell lines were transfected with either target specific FOXD3/control siRNA, or expression/control plasmids as indicated, using LipofectamineTM 2000 (Invitrogen, Grand Island, NY) according to manufacturer's instructions, as previously described (Kantara et al., 2014; O'Connell et al., 2015; Sarkar et al., 2011). Transfected cells were propagated in normal growth medium containing 10% FCS, and processed for RT-PCR analysis after 48h of transfection for confirming downregulation of the target gene (DCLK1 and FOXD3) or expression of indicated expression plasmids.

### 4.2.9 Promoter-Reporter assays

Promoter reporter assays were performed as previously described (O'Connell et al., 2015). In brief, cells were transiently transfected with the indicated promoter reporter constructs using FuGENE6 for 24-48h, as per manufacturer's instructions; control cells were transfected with empty PGL2 vector, lacking promoter sequences. Transfected cells were lysed in luciferase assay lysis buffer and luciferin was added according to instructions of the manufacturer (Promega, WI). Luciferase activity was measured using a luminometer (Dynex Technologies, VA) after 10sec of addition of substrate, as previously described (O'Connell et al., 2015; Sarkar et al., 2011).

### 4.2.10 Chromatin Immunoprecipitation Assays (ChIP)

ChIP assays were performed as previously described (O'Connell et al., 2015). In brief, cells were fixed in 1% formaldehyde to crosslink DNA to bound proteins, and reaction stopped by adding 0.125M glycine. Cells were washed with cold PBS, pelleted, and resuspended in ChIP sonication buffer, followed by sonication and centrifugation of fragments (600-700bp long). The crosslinked chromatin supernatant was immunopreciptated using target specific antibody (2-5 µg purified IgG) at 4°C, overnight. Control samples contained no antibody. For obtaining input levels of the corresponding proteins, equivalent numbers of cells were also processed for Western Immunoblot analysis. Protein A/G Sepharose beads, pre-absorbed by Herring sperm DNA (100µg/ml) was added to the chromatin-antibody complex and centrifuged to sediment the beads. DNA was eluted from the beads with elution buffer and DNA was precipitated using a high salt method (as previously described (Ishizawa et al., 1991). The extracted DNA was purified and purified DNA was used for PCR amplification of the immunoprecipitated DNA with specific primers designed around the FOXD3 binding sites. The primer sequences used for this purpose are listed in **Table4.1**.

### 4.2.11 Procurement of samples from colonic tumors of patients for Kaplan-Meier survival curves

Sixty-seven colorectal carcinoma tissues were used for clinical validation of DCLK1-S and/or FOXD3 expression from an independent cohort as previously described (O'Connell et al., 2015). These specimens were preserved immediately after surgical resection in RNA later (QIAGEN, Chartsworth, CA) and stored at -80°C until RNA extraction. The surgical samples were obtained from the Mie University Hospital, Japan, from patients enrolled during 2005 to 2011. Written informed consent was obtained from each patient (as per approved BCM IRB protocol #005-134). **All tissues were collected in accordance with the approved guidelines set forth by UTMB and BCM for the IRB protocols.**

### 4.2.12 Statistical analysis

Data are presented as mean±SEM of values obtained from indicated number of patient samples or experiments. To test for significant differences between means, nonparametric Mann Whitney test was employed using STAT view 4.1 (Abacus Concepts, Inc, Berkley, CA). Chi-square tests were used to analyze the relationship between DCLK1-S expression and clinicopathological factors. Overall survival curves were analyzed using Kaplan-Meier method, and comparisons were made using the log-rank test. The cut off threshold between high and low expression group for DCLK1-S and FOXD3 transcripts was defined by the median values of the gene's expression in cancerous tissue. All p values were two-sided and differences were considered to be statistically significant if $<0.05$.

## 4.3 RESULTS

### 4.3.1 FOXD3 expression inversely correlates with DCLK1-S expression in human cell lines and human patient samples

We have previously reported that human normal colonic patient samples and cell lines mainly expressed DCLK1-L while human colonic adenocarcinomas and colon cancer cell lines mainly expressed DCLK1-S, downstream of an IntronV(β)-promoter (O'Connell et al., 2015). An important role of NF-κB was reported for activating the IntronV(β)-promoter (O'Connell et al., 2015). Further *in silico* analysis revealed several additional *cis* elements (as shown in **Figure 4.1A**), which likely play an important role in regulating transcriptional activity of IntronV(β)-promoter. Amongst the additional *cis* elements identified, FOXD3 was chosen for further evaluation, as a potential transcriptional inhibitor of the IntronV(β)-promoter, based on the literature in the field (as described above). FOXD3 expression was evaluated in relation to the expression of DCLK1-S. As previously reported, HCT116 colon cancer cells were positive for significant DCLK1-S expression, while HEK293 and CCD841 cells (normal human epithelial/colon mucosal cells) were negative for DCLK1-S expression (O'Connell et al., 2015) (**Fig 4.3A,B**). HEK293 and CCD841 cells, positive for DCLK1-L expression from the 5'(α)promoter, were found to be positive for FOXD3 expression; HCT116 colon cancer cells, on the other hand, were relatively negative for FOXD3 expression (**Fig 4.3A,B**). I next evaluated a panel of colon cancer cell lines. Cells positive for DCLK1-S expression were negative for FOXD3 expression (RKO, SW1116), and cells negative for DCLK1-S expression were positive for FOXD3 expression (COLO205, SW1417) (**Fig4.3C**). Normal colonic mucosal samples from patients, negative for DCLK1-S expression, were positive for high levels of FOXD3 (**Fig4.3.D**) while primary colon adenocarcinoma samples from patients, positive for high levels of DCLK1-S expression, did not express detectable levels of FOXD3 **(Fig4.3E)**. Thus, the relative expression

levels of FOXD3 inversely correlated with the expression levels of DCLK1-S, in normal colonic cell lines/normal colons and in colon cancer cells/adenocarcinomas.

### 4.3.2 FOXD3 promoter is epigenetically silenced in HCT116 colon cancer cells.

The promoter of FOXD3 has previously been reported to be hypermethylated in various cancers including colorectal cancers (Cheng et al., 2013; Li et al., 2013; van Roon et al., 2013). Because colon cancer cell lines and human colorectal adenocarcinomas were void of FOXD3 expression, hypermethylation of the FOXD3 promoter was evaluated. HCT116 cells were treated with 5-Azacytidine. We have previously reported that DCLK1-S expression is decreased in response to treatment with 5-Azacytidine (O'Connell et al., 2015) **(Fig 4.3F).** However, FOXD3 was re-expressed in HCT116 cells treated with 5-Azacytidine (**Fig 4.3F**). Re-expression of FOXD3 in response to treatment, confirms that the FOXD3 promoter is epigenetically silenced in colorectal cancer cells, due to hypermethylation, as previously reported (van Roon et al., 2013) **(Fig 4.3F)**.

### 4.3.3 FOXD3 binding to the Intron V(β) promoter in DCLK1 gene, as a potential transcriptional regulator of DCLK1-S expression

As described above, *in silico* analysis of the IntronV(β)-promoter revealed several potential binding sites for FOXD3 within 3 kb of the start site **(Fig 4.1A)**. FOXD3 binding, *in situ,* to the potential FOXD3 binding sites was examined in ChIP assays. The -2159 and -787 binding sites were determined to be the only functional FOXD3 binding sites in HEK293 cells, of the many sites examined in this study. HEK293, non-transformed embryonic epithelial cells were used for the remainder of the studies, since CCD841 cells are difficult to transfect. Similar to CCD841cells, HEK293 cells were also

null for DCLK1-S expression, but expressed relatively high levels of FOXD3, at both the transcript and protein levels **(Fig4.3A,B)**. Results of ChIP assays demonstrated that non-tumorigenic HEK293 cells were positive for FOXD3 binding to both the -2159 and -787 sites, while tumorigenic HCT116 cells were negative for FOXD3 binding to both sites **(Fig 4.4B,C)**. Relative binding of FOXD3 to the indicated FOXD3 binding sites, from several experiments is presented as % of total FOXD3 (input) in the cells **(Fig 4.4D)**. These results suggest that the FOXD3 *cis* elements likely play an important role in the transcriptional regulation of the IntronV(β)-promoter, and likely dictate the absence of DCLK1-S expression in non-transformed/normal cells. For reasons unknown, relative binding of FOXD3 was significantly higher to the -787 site, compared to that with the -2159 site in HCT116 cells.

### 4.3.4 Role of FOXD3 binding sites in down regulating transcriptional activity of IntronV-β-promoter

To evaluate the role of FOXD3 in transcriptional regulation of DCLK1-S, HCT116 cells were transiently transfected with FOXD3 or control cDNA (Vec) (as described in methods). In cells transfected with FOXD3 cDNA, DCLK1-S expression was significantly downregulated at both the transcript **(Fig 4.5B)** and protein levels **(Fig 4.5C).** Using a IntronV(β)-promoter-reporter constructs, previously described (O'Connell et al., 2015) (as shown in **Figure 4.5A**), a possible role of FOXD3 in regulating the transcriptional activity of IntronV(β)-promoter was examined. HCT116 cells were transiently co-transfected with FOXD3/Vec cDNA and DCLK1-S-LUC1/LUCVec promoter-reporter constructs. The transcriptional activity of the IntronV(β)-promoter-reporter constructs was significantly decreased in cells co-transfected with FOXD3 cDNA containing plasmid **(Fig 4.5D)**. To further confirm a role of FOXD3 in regulating the expression of DCLK1-S, HEK293 cells were transiently transfected with

Con/FOXD3 siRNA. In cells transfected with FOXD3 siRNA, DCLK1-S expression levels were significantly upregulated at both the transcript **(Fig 4.6B)** and protein levels in HEK293 cells **(Fig 4.6C),** confirming an important inhibitory role of FOXD3 on the expression of the S-isoform, but not the L-isoform (as the 5'(α)promoter of *DCLK1* gene lacks FOXD3 binding sites)**.** Using DCLK1-S-LUC1 promoter-reporter construct, HEK293 cells were transiently co-transfected with Con/FOXD3 siRNA and DCLK1-S-LUC1/LUC Vec promoter-reporter constructs. The transcriptional activity of the IntronV(β)-promoter was significantly increased in HEK293 cells, transfected with FOXD3 siRNA, compared to that of cells transfected with the control siRNA **(Fig4.6D)**. These results suggest that the FOXD3, and its *cis* elements, play an important role in down regulating transcriptional activity of the IntronV(β)-promoter. Interestingly, even after down regulating FOXD3 expression in HEK293 cells, transcriptional activity of IntronV(β)-promoter remained significantly lower than that in HCT116 cells (**Fig4.5D and Fig4.6D**), suggesting that besides loss of FOXD3, up-regulation of oncogenic pathways, such as activated NF-κB, are required for optimally activating the expression of IntronV(β)-promoter in cells, as previously reported/discussed (O'Connell et al., 2015).

### 4.3.5 High expression of DCLK1-S and low expression of FOXD3 in AdCA samples from colorectal cancer patients is associated with poor patient survival

The expression patterns of DCLK1-S and FOXD3 transcripts, in relation to clinicopathological parameters, were analyzed using an independent cohort of patient specimens, as described in methods. As previously described (O'Connell et al., 2015), high expression of DCLK1-S significantly correlated with overall poor patient survival in patients with Stages I-III disease (**Fig 4.7A**). We now report that low expression of FOXD3 similarly correlates with overall poor patient survival in patients with Stages I-III

disease, although the correlation was not statistically significant (**Fig 4.7B**). However, on evaluating the expression of both DCLK1-S and FOXD3, in relation to patient survival, we found that high-DCLK1-S/low-FOXD3 patients had the worst overall survival, compared with low-DCLK1-S/high-FOXD3 patients (**Fig4.7C**). The latter findings demonstrates that high expression of DCLK1-S, in conjunction with low expression of FOXD3, was a stronger independent prognostic factor than expression of high levels of DCLK1-S alone.

**Figure 4.3: Expression of DCLK1-S and FOXD3 in Human Cell Lines Patient Samples**

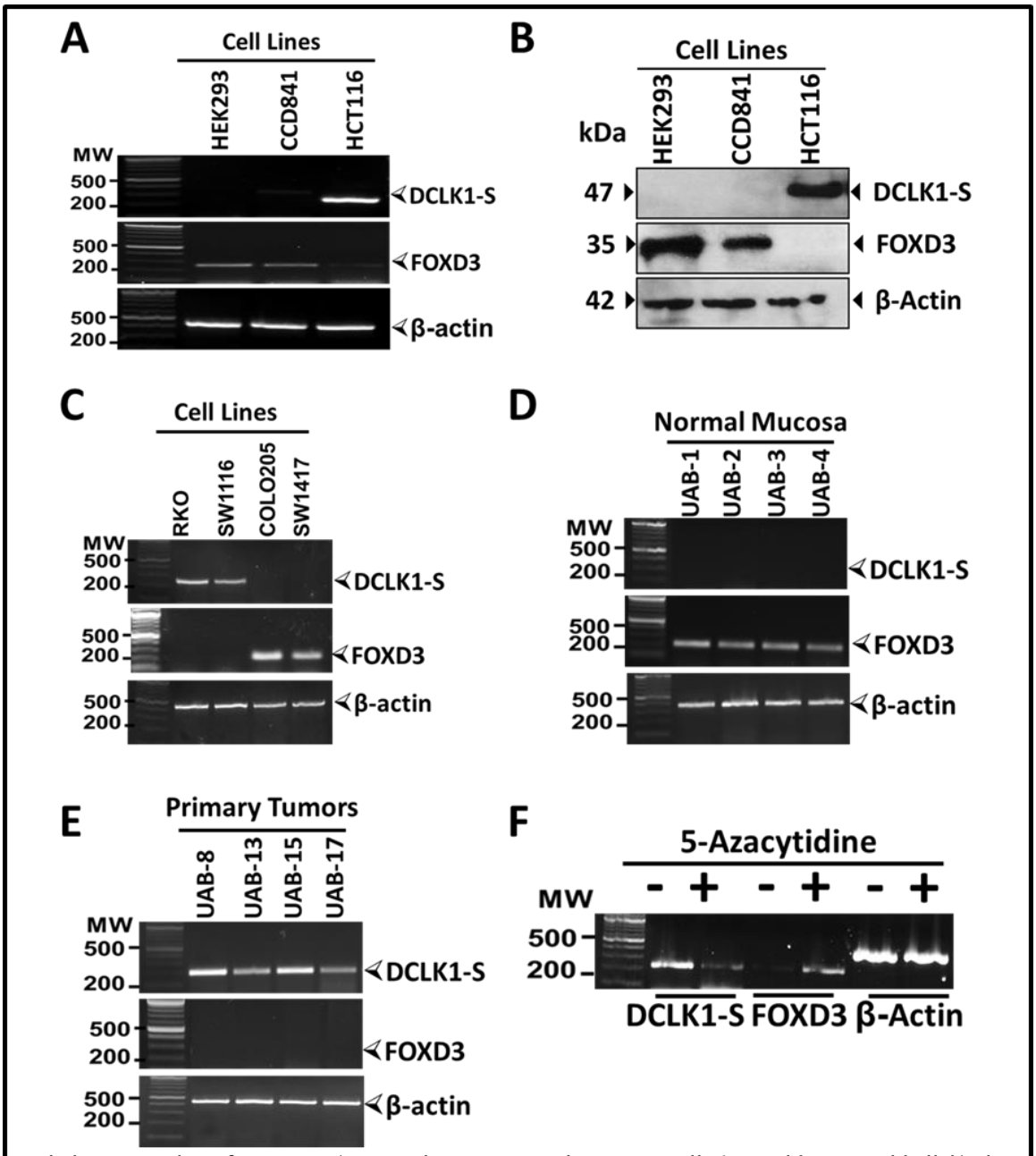


Relative expression of DCLK1-S/FOXD3 in HEK293 and CCD841 cells (normal human epithelial/colon mucosal cells) and HCT116 colon cancer cell line measured by **A)** RT-PCR and **B)** western blot analysis. Representative RT-PCR data for DCLK1-S and FOXD3 from **C)** colon cancer cell lines; **D)** human normal colonic mucosa; and **E)** primary colon adenocarcinomas from patients. **F)** Relative expression (RT-PCR) of DCLK1-S and FOXD3 in HCT116 cells, in presence or absence of treatment with 5-aza-2′-deoxycytidine (5-azacytidine) is shown. For A-F, β-actin was run as internal control. All data presented are representative of 2-3 experiments. The molecular weight (MW) in terms of bps and molecular mass in terms of kDa are shown on left-hand side of each image. D and E are representative of 5–10 separate patient samples, analyzed in duplicate. F is representative of 3 separate experiments run in duplicate.

**Figure 4.4: Role of FOXD3 Binding Sites in Activation of the IntronV-(β)-promoter of *DCLK1***

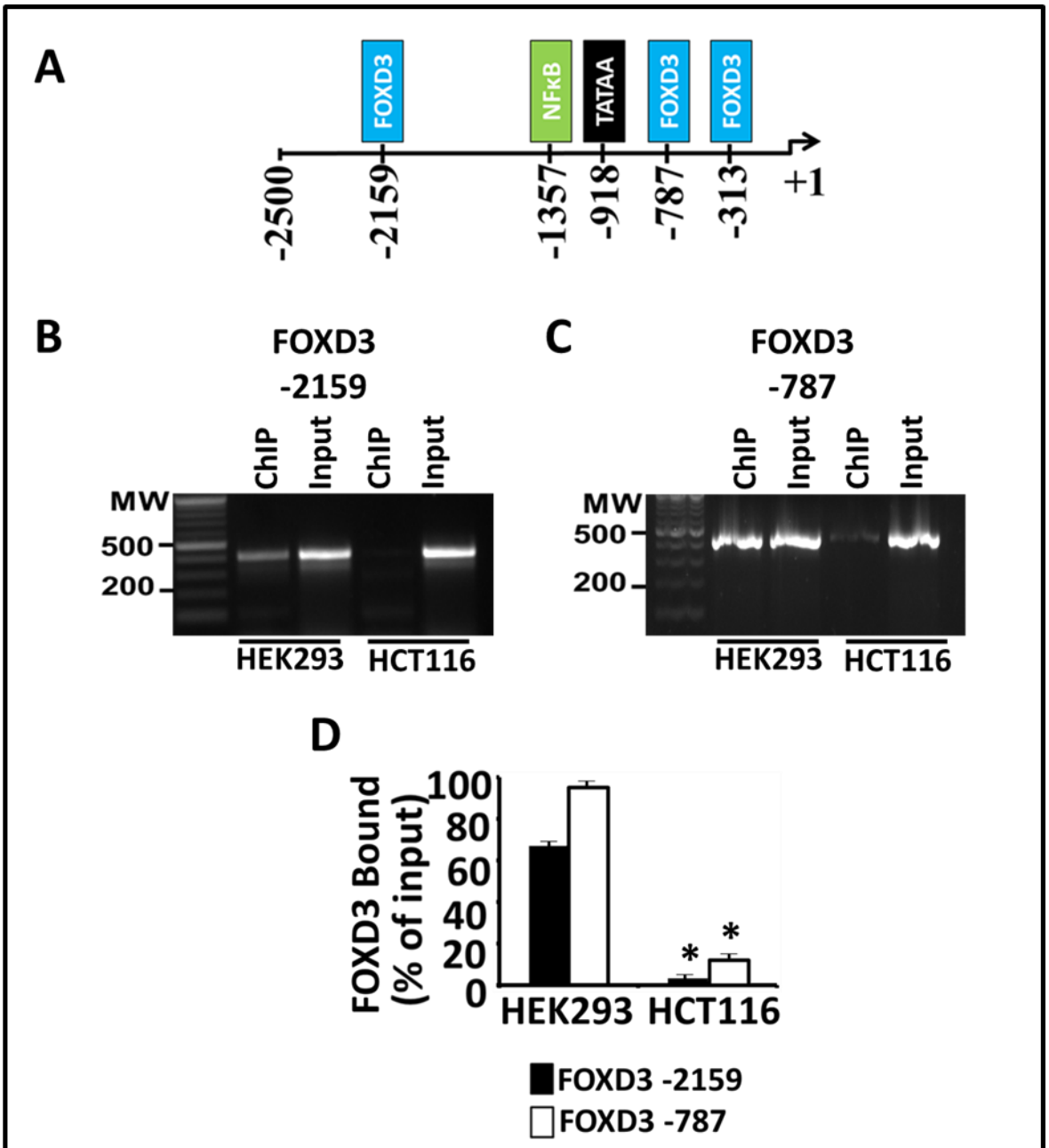


**A)** Map of functional FOXD3 binding sites on the IntronV-β-promoter, as determined by ChIP analysis. **B-C)** Relative binding of FOXD3 to the indicated FOXD3 binding sites located within the IntronV-β-promoter of HEK293 and HCT116 cells. Data presented in B and C are representative of six observations from three experiments. **D)** Relative binding of FOXD3, *in situ*, to functional binding sites in the IntronV-β-promoter in HEK293 and HCT116 cells, presented as a % of input. Each bar graph = Mean±SEM of duplicates from three experiments. % binding was determined by densitometric analysis of indicated bands. *=P<0.05 vs values presented for HEK293 cells.

**Figure 4.5: Overexpression of FOXD3 Results in Inhibition of the IntronV-(β)-promoter of *DCLK1***

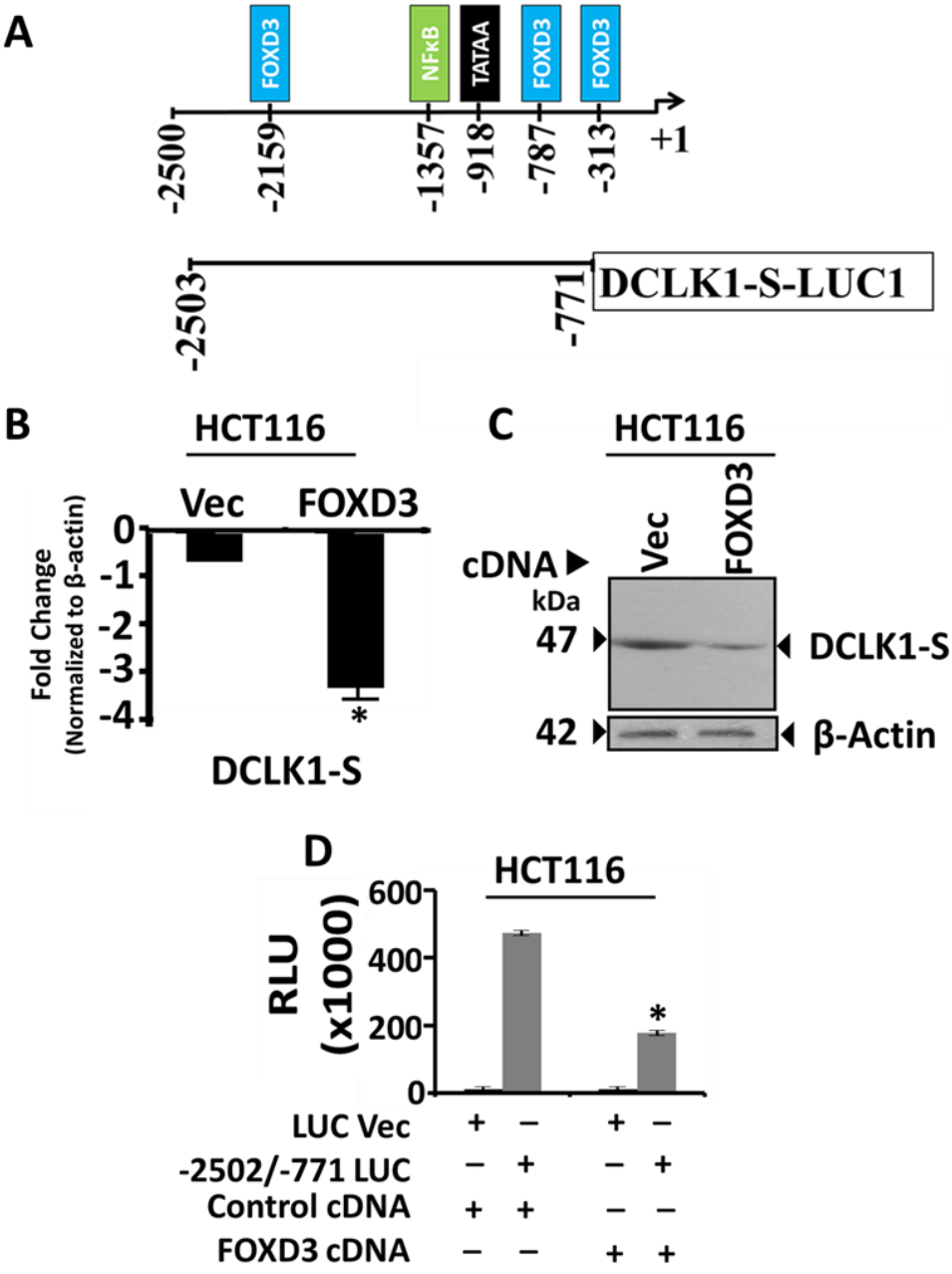


**A)** Diagrammatic representation of the FOXD3 binding sites on the DCLK1 IntronV-β-promoter and the construct (DCLK1-S-LUC1) used for the promoter reporter assays is diagrammatically shown below the mapped promoter. DCLK1-S expression in HCT116 cells, transiently transfected with Vector or FOXD3 cDNA plasmids for 48 hours measured by **B)** qRT-PCR and **C)** western blot analysis. **D)** Relative transcriptional/luciferase activity (RLU) of HCT-116 cells, transiently-transfected with the Vector or FOXD3 cDNA plasmids and DCLK1-S-LUC1 promoter construct for 48 hours. Data presented in C is representative of 3 experiments. The molecular weight (MW) in terms of kDa is shown on left-hand side of image. Each bar graph = Mean±SEM of duplicates from three experiments. *=P<0.05 vs. Vec transfected cells.

**Figure 4.6: Downregulation of FOXD3 Results in Activation of the IntronV-(β)-promoter of *DCLK1***

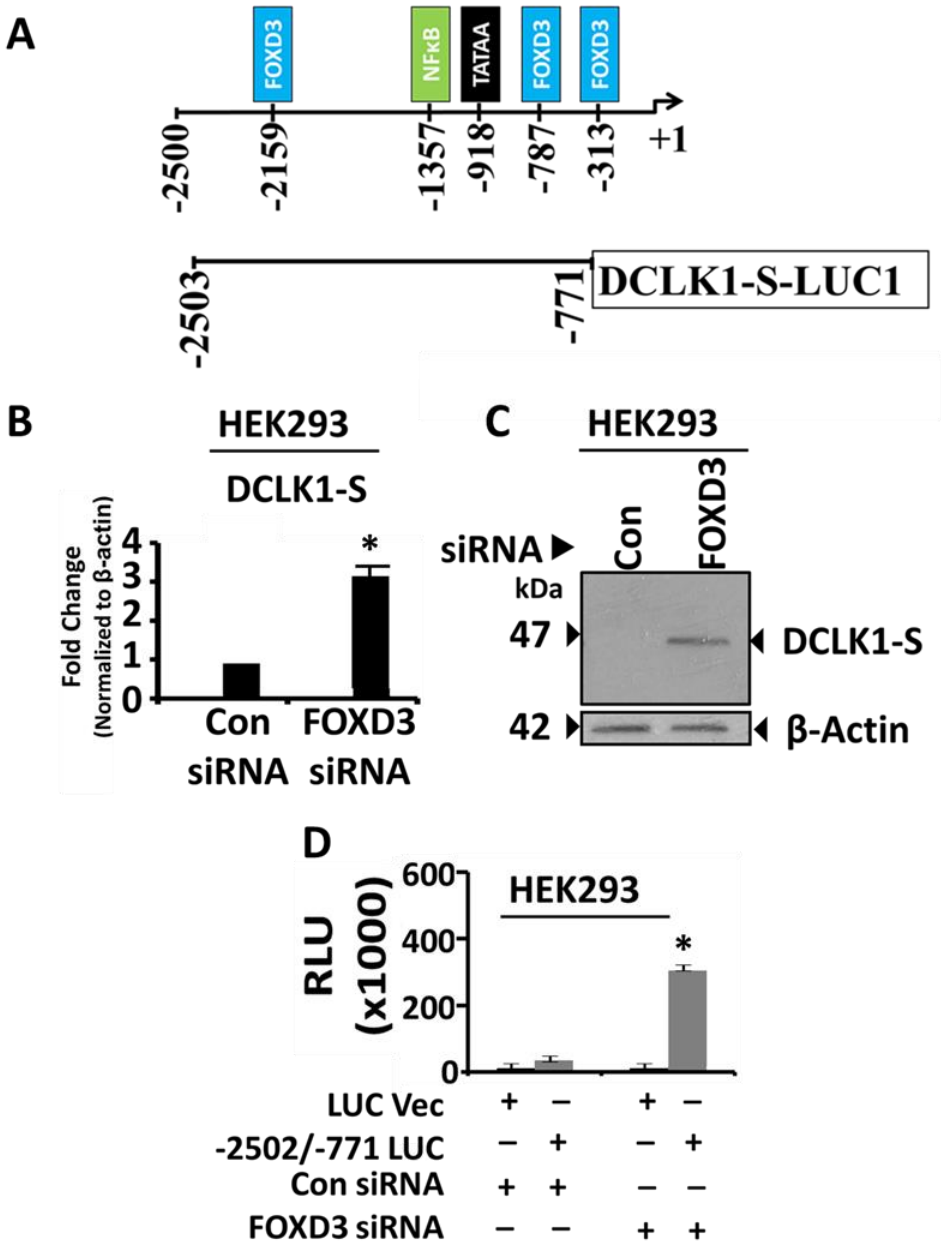


**A)** Diagrammatic representation of the FOXD3 binding sites on the DCLK1 IntronV-β-promoter and the construct (DCLK1-S-LUC1) used for the promoter reporter assays is diagrammatically shown below the mapped promoter. DCLK1-S expression in HEK293 cells, transiently transfected with con siRNA or FOXD3 siRNA for 48 hours measured by **B)** qRT-PCR and **C)** western blot analysis. **D)** Relative transcriptional/luciferase activity (RLU) of HEK293 cells, transiently-transfected with the con siRNA or FOXD3 siRNA and DCLK1-S-LUC1 promoter construct for 48 hours. Data presented in C is representative of 3 experiments. The molecular weight (MW) in terms of kDa is shown on left-hand side of image. Each bar graph = Mean±SEM of duplicates from three experiments. *=P<0.05 vs. Con transfected cells.

**Figure 4.7: Overall Survival of Patients with CRC, in Relation to Low or High Expression of DCLK1-S and/or FOXD3**

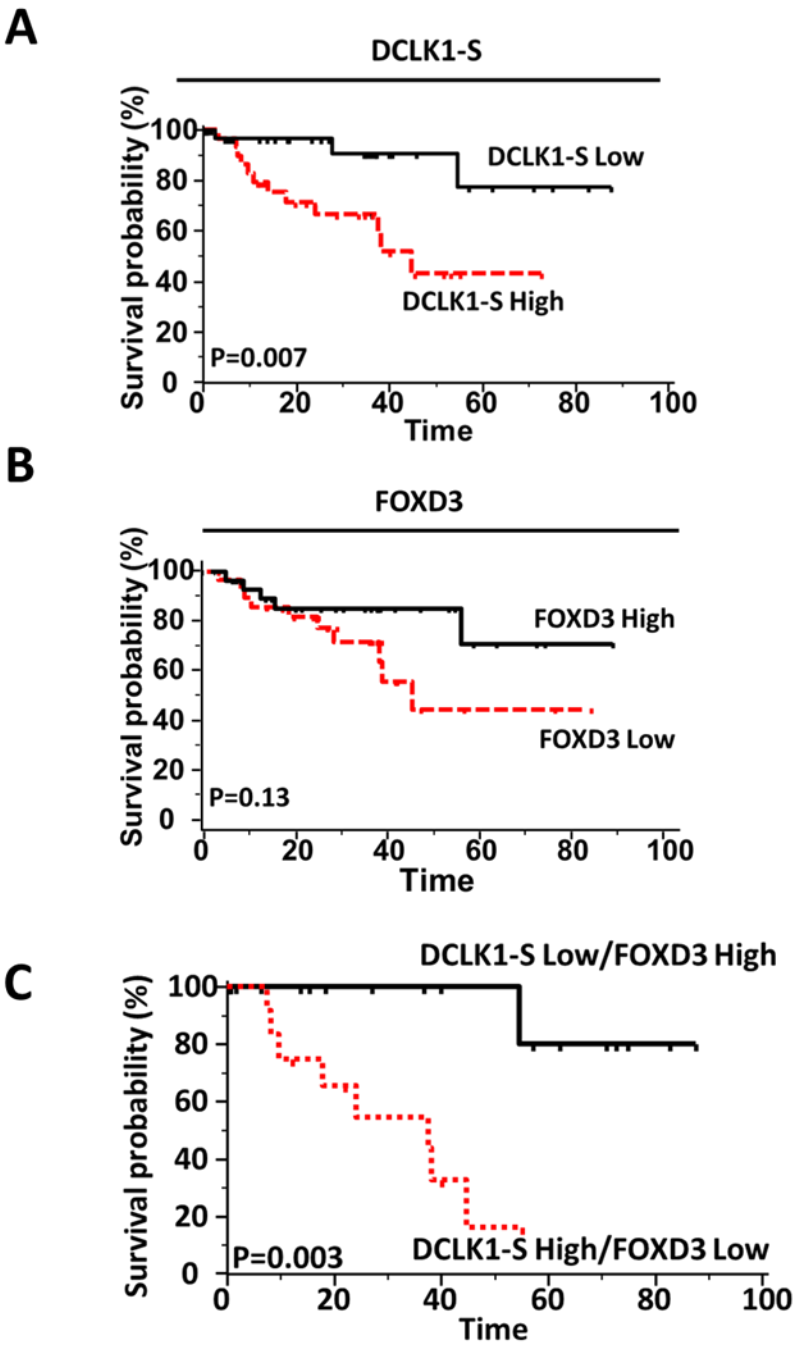


**A)** Kaplan-Meier overall survival curves of CRC patients with stages I-III disease, in relation to relative expression levels of DCLK1-S measured by qRT-PCR; n = 67 patients. **B)** Kaplan-Meier overall survival curves of CRC patients with stages I-III disease, in relation to relative expression levels of FOXD3. **C)** Kaplan-Meier overall survival curves of CRC patients with stages I-III disease, in relation to relative expression levels of DCLK1-S and FOXD3 expression. The cutoff threshold values were defined by using the median values of DCLK1-S expression of each cohort in cancer tissues.

**Table 4.1: Oligonucleotide (primer) Sequences Used for qRT-PCR/RT-PCR/ChIP Assays for Aim 3 Studies.**

**Table 4.1**

| Target cDNA/gDNA | Species | Primer Sequence | Assay |
|---|---|---|---|
| DCLK1-Short (cDNA) | Human | F:ACACTAAGACTGTGTCCATGTTAGAACTC | RT-PCR & qRT-PCR |
| | | R:AAGCCTTCCTCCGACACTTCT | |
| FOXD3 (cDNA) | Human | F:GTGCAGAGGAAACCGAAGAG | RT-PCR & qRT-PCR |
| | | R:AAGGGCAGGAAGAGTCGAA | |
| -2159 FOXD3 *cis* element in DCLK1 IntronV-β-promoter gDNA) | Human | F: AGGGCAAGAGCTGGAGAGCA | ChIP PCR |
| | | R: TGGCCTACGCCCTTCACAGAGGG | |
| -787 FOXD3 cis element in DCLK1 IntronV-β-promoter gDNA) | Human | F: GGGCTGGCACAGTAAGGCAAG | ChIP PCR |
| | | R: GAGCAAATAGGGAAGCAAACACAGT | |
| DCLK1-S-Luc1(-2503/-771) (gDNA) | Human | F:GGTGCTTCCGTTCAAAGTGT | Promoter Reporter Construct |
| | | R:CAGTCTCAGGAATACCTTGC | |

The forward (F) and reverse (R) primer sequences that were designed and used for amplifying the indicated target cDNA/gDNA for conducting the different assays are shown.

## 4.3 DISCUSSION

By *in silico* analysis, I identified several FOXD3 binding sited in the IntronV(β)-promoter of the *DCLK1* gene, and confirmed at least two of these sites to be functional FOXD3 binding sites, by ChIP analysis. We therefore examined the role of FOXD3 in regulating the activity of the IntronV(β)-promoter. Our results for the first time demonstrate that FOXD3 functions to bind and repress activity of the IntronV(β)-promoter in normal cells. As described above, FOXD3 functions primarily as a transcriptional repressor (Sutton et al., 1996) and has been shown to be a novel tumor suppressor in number of cancers (Chu et al., 2014; Katiyar and Aplin, 2011; Li et al., 2013). As part of my Aim 3 studies, I discovered that relative expression levels of

FOXD3 are inversely related to the expression of DCLK1-S in normal and colon cancer cells/adenocarcinomas, strongly suggesting that loss of FOXD3 expression may allow colon cancer cells to express DCLK1-S. Overexpression of exogenous FOXD3 in colon cancer cells resulted in significantly down regulated expression of DCLK1-S in the cancer cells (**Fig 4.5**), while down regulation of endogenous FOXD3 in normal cells, caused transcriptional activation of the IntronV(β)-promoter with an increase in the relative levels of DCLK1-S in the cells (**Fig 4.6**). The latter findings suggest that FOXD3 may indeed be acting as a tumor suppressor by repressing the transcriptional activity of the β promoter, resulting in the loss of DCLK1-S expression. Our results in chapters 2 and 3 strongly suggest that DCLK1-S expression enhances metastatic potential of colon cancer cells. Therefore FOXD3 may play a critical role in hindering the metastatic phenotype of colon cancer cells. Future studies will allow us to confirm if re-expression of FOXD3 in colon cancer cells/tumors can be used as an approach for preventing metastatic spread of colorectal cancers.

Multiple reports demonstrate that FOXD3 is downregulated in several tumor types, compared to its expression levels in the corresponding normal tissues (Chu et al., 2014; Li et al., 2013; Zhao et al., 2014). My Aim 3 studies demonstrate that FOXD3 levels are significantly lower in human colorectal cancers (**Fig4.3E**), compared to that in normal colonic mucosa (**Fig4.3D**). Thus an important finding of my Aim 3 studies is that FOXD3 expression inversely correlates with the expression of DCLK1-S, in both normal/cancer cell lines (**Fig4.3A,B,C**) and in normal/adenocarcinoma samples from human patients (**Fig4.3D,E**).

FOXD3 has been reported to be epigenetically silenced during the progression and formation of cancerous tumors from normal cells in many organs (Cheng et al., 2013; van Roon et al., 2013). Our results suggest that the *FOXD3* gene becomes methylated during colon carcinogenesis, causing loss of FOXD3 expression, and results in the expression of DCLK1-S in human colorectal cancers. In order to confirm methylation of

FOXD3 promoter, one needs to conduct methylation analysis of the promoter in normal and cancer cells. However, the FOXD3 promoter is highly C-G rich, which makes the methylation analysis of the FOXD3 promoter/introns challenging, as reported by other groups as well (Cheng et al., 2013; van Roon et al., 2013). Therefore it remains to be determined if methylation status of the FOXD3 promoter can be used for prognostic/diagnostic purposes, as currently suggested for 5'(α) promoter of *DCLK1*-gene (O'Connell et al., 2015; Vedeld et al., 2014). We were, however, able to determine that patients expressing high-DCLK1-S/low-FOXD3 had significantly worse overall survival compared to patients expressing low-DCLK1-S/high-FOXD3. A clinically important finding was that high expression of DCLK1-S, in conjunction with low expression of FOXD3, is a stronger independent prognostic factor than expression of high levels of DCLK1-S alone.

In summary, we report for the first time that FOXD3 is a potent repressor of the IntronV(β)-promoter of the human *DCLK1* gene in normal cells. Out results strongly suggest that loss of FOXD3 expression during colon carcinogenesis likely occurs due to hypermethylation and silencing of the *FOXD3* gene, resulting in the expression of DCLK1-S in human colorectal cancers. Our findings also suggest a prognostic/diagnostic value of measuring relative expression levels of DCLK1-S/FOXD3 in tumors of colorectal cancer patients. It is speculated that loss of expression of both DCLK1-L and FOXD3, associated with increased expression of DCLK1-S, can be used as an early diagnostic marker of epigenetic changes, associated with colon carcinogenesis in humans.

# Chapter 5: Conclusions

The major goal of my dissertation was to examine the mechanism by which DCLK1 supports the growth characteristics/functions of cancer cells, with a long term goal of developing novel diagnostic markers and treatment strategies for targeting cancer stem cells, while sparing normal stem cells. To achieve my major goals, studies were conducted in three aims to examine the following: 1) Possible expression of an alternate isoform of DCLK1 from an alternate promoter in colorectal cancers; 2) Biological role of cancer specific DCLK1-S isoform, 3) Underlying mechanisms dictating differential expression of DCLK1-S in normal colons vs. human colorectal cancers, speculated to be due to differences in transcriptional activity of the β promoter in normal vs. cancer cells.

## 5.1 Alternate isoform of DCLK1 from and alternate promoter in colorectal cancers

In Chapter Two we examined the epigenetic changes and alternative promoter usage by human colon cancers for expressing DCLK1-isoforms. Recent reports have demonstrated that the 5' promoter of human *DCLK1*-gene is hypermethylated in human colorectal cancers (Marie Vedeld et al., 2014; Vedeld et al., 2014), suggesting the possibility that the 5' promoter of human *DCLK1*-gene may be epigenetically silenced in human colorectal cancers. Our findings suggest that the hypermethylation of the human *DCLK1*-gene is an early event during adenoma-carcinoma sequence of colon carcinogenesis in humans (O'Connell et al., 2015). Our data also suggests an absence of expression of long transcripts/isoforms in all 15 human colon cancer cell lines screened to date, suggesting epigenetic silencing of the 5'(α)-promoter due to its hypermethylation in human colorectal cancers (O'Connell et al., 2015). Although the 5'(α)-promoter is

epigenetically silenced in human colon cancer cell lines and colorectal cancers, high levels of DCLK1 protein have been reported in human colon cancer cell lines and colorectal cancers (Gagliardi et al., 2012a; Gagliardi et al., 2012b; Kantara et al., 2014; Singh et al., 2012). The discrepancy between the reported presence of DCLK1 protein in human colon cancer cell lines and colorectal cancers, and hypermethylation/epigenetic silencing of 5'(α)-promoter, suggests the possibility that human colon cancer cell lines and colorectal cancers may be utilizing an alternate promoter for expressing alternate isoforms of DCLK1. To examine this novel possibility we conducted *in silico* analysis of the human *DCLK1*-gene, which led us to confirm the presence of a canonical TATA box within the β promoter located within IntronV. In Chapter Two we describe that the IntronV-(β)-promoter is used as an alternate-promoter by human colon cancer cell lines and colorectal cancers for expressing a short transcript. Based on sequence homology, the long (L) and short (S) transcripts of DCLK1, found in normal human colon cell lines/normal human colons vs. human colon cancer cell lines and colorectal cancers, respectively, were determined to be identical to isoforms 1 (NM_004734.4) and 2 (NM_001195415.1) in the NCBI data base. For the purpose of our studies we have termed the isoform 1 as DCLK1-L and the isoform 2 as DCLK1-S, to clearly differentiate between the molecular sizes of the two isoforms. Colon tumors and normal colons from mice, on the other hand, were confirmed to only express the long isoform(s).

Transcriptional regulation of the α/β promoters in the human *DCLK1*-gene in epithelial cells remains largely unknown. Activation of β-catenin and NF-κBp65 was reported to be critically required for upregulating DCLK1 protein in response to autocrine and endocrine progastrins (Sarkar et al., 2011). We therefore conducted *in silico* analysis of the two promoters followed by promoter-reporter/ChIP assays, in the presence or absence of the known activator (progastrin), and we identified an important role of β-catenin binding to TCF4/LEF binding-sites for activating 5'(α)-promoter, and an important role of NF-κB binding-site for activating IntronV-(β)promoter.

In order to define pathophysiological relevance of DCLK1-S expression by human colorectal cancers, the overall-survival of a cohort of 92 CRC patients was examined in relation to high/low expression of DCLK1-S. A clinically important finding was that high-expressers of DCLK1-S had significantly worse overall-survival, and disease free interval. DCLK1-S expression represented an independent diagnostic/prognostic marker for CRC patients.

### 5.2 BIOLOGICAL ROLE OF CANCER SPECIFIC DCLK1-S ISOFORM

In Chapter 3 studies we investigated the cellular mechanisms by which DCLK1-S supports the growth of cancer stem cells. An important role of DCLK1 has been implicated in colon tumorigenesis in mice (Bailey et al., 2014; Nakanishi et al., 2013; Westphalen et al., 2014) and in maintaining the proliferative potential of human colon cancer cells (Kantara et al., 2014; Sarkar et al., 2012; Sureban et al., 2011b). In a recent report from our laboratory, we described that a subset of DCLK1+ cancer stem cells were resistant to inhibitory effects of chemopreventive/chemotherapeutic agents, and down-regulation of DCLK1 combined with chemoprevention was required for eliminating cancer stem cells, in vitro and *in vivo*, and for avoiding relapse (in terms of re-formation of tumorospheres from treated cells) (Kantara et al., 2014). These findings highlighted a possible critical role of DCLK1 in maintaining the *in vitro* and *in vivo* growth of human colon cancer cell lines. The loss of DCLK1 expression in cancer cells has been reported to result in the loss of proliferative/tumorigenic/metastatic potential of colon cancer cells (Kantara et al., 2014; Sureban et al., 2011b). However, RNAi methods used so far, target both isoforms of DCLK1.

In Chapter 3 studies we used shRNA knockdown methods to specifically target DCLK1-S isoform in a human colon cancer cell line, in order to delineate the biological role of cancer specific DCLK1-S isoform. Isogenic clones of a representative human

colon cancer cell line (HCT116 cells) were generated to either express control shRNA (HCT-C) or DCLK1-shRNA (HCT-D). Using these clones, we determined that DCLK1-S is required for maintaining proliferative/tumorigenic/metastatic potential of colon cancer cells, both in vitro and in vivo. From these studies we also established a critical role of DCLK1-S (but not DCLK1-L) in enhancing the invasive potential of colon cancer cells. To evaluate molecular/genetic pathways mediating effects of DCLK1-S, isogenic clones of HCT116 cells (HCT-C/HCT-D) were subjected to next generation sequencing. Although many pathways were identified to be altered in response to DCLK1-S downregulation in HCT-D vs. HCT-C clones, the pathways/molecules associated with cell movement/invasion appeared to be one of the most significantly affected. Therefore, I investigated the genes/pathways, downstream of DCLK1-S expression, which may be mediating the invasive potential of colon cancer cells. Of the genes identified by RNAseq analysis, downstream of DCLK1-S expression, SPARC and COL3A1 emerged as two candidate genes/proteins, which were increased by many fold in response to DCLK1-S, and which have been previously reported to play a critical role in enhancing the invasive potential of cancer cells (Arnold and Brekken, 2009; Basso et al., 2001; Ewald et al., 2013; Nagaraju et al., 2014; Su et al., 2014; Turashvili et al., 2007; Xiong et al., 2014). Hence the role of DCLK1-S in mediating the expression of SPARC and COL3A1, and their role in increasing the invasive potential of DCLK1-S expressing colon cancer cells was evaluated.

The results of my Chapter 3 studies suggest for the first time, that the expression of SPARC and COL3A1 is downstream of enhanced expression of DCLK1-S in colorectal cancers. In order to understand the mediatory mechanisms, I conducted *in silico* analysis of both the SPARC and the COL3A1 promoters, in order to identify the presence of possible common *cis* elements in the two promoters, for binding known transcription factors. Several potential binding sites for NFATC2 were identified in both of the promoters, which led me to examine potential role of NFATC2 in DCLK1-S

mediated upregulation of SPARC and COL3A1 in colon cancer cells. Based on the results of my Chapter 3 studies, it is likely that significant increases in the expression of DCLK1-S in colon cancer cells, mediates increased transcriptional activity of NFATC2, by functioning as a specific kinase for phosphorylating the NFATC2 $^{53}$SPPS$^{56}$ motif. Increased transcriptional activation of NFATC2 likely results in increased expression of COL3A1 and other target genes. Overall our findings suggest that DCLK1-S may play a critical role in mediating the invasive potential of colon cancer cells by transcriptional activation of NFATC2, resulting in up-regulation of invasion associated proteins (such as COL3A1), causing re-modeling of extracellular matrix for unhindered invasion by colon cancer cells.

### 5.3 UNDERLYING MECHANISMS DICTATING DIFFERENTIAL EXPRESSION OF DCLK1-S IN NORMAL COLONS VS. HUMAN COLORECTAL CANCERS

We recently reported a novel finding that human colorectal cancers express short transcripts of DCLK1 (DCLK1-S) from an alternate promoter located within the intron V of the *DCLK1* gene, while normal human colons express the canonical long transcript (DCLK1-L) from the 5'(α)-promoter of the gene (O'Connell et al., 2015). We and others have demonstrated that the 5'(α)-promoter is hypermethylated in human colorectal cancers, resulting in epigenetic silencing and loss of expression of DCLK1-L (Marie Vedeld et al., 2014; O'Connell et al., 2015; Vedeld et al., 2014). Although the 5'(α)-promoter is differentially methylated in normal human colons vs. human colorectal cancers, methylation status of the IntronV(β)-promoter does not change (O'Connell et al., 2015). We therefore hypothesized that differential expression of DCLK1-S in normal colons vs. human colorectal cancers is perhaps due to differences in the transcriptional activity of the promoter in normal vs. cancer cells. To test our hypothesis, we conducted *in silico* analysis of the IntronV(β)-promoter and found several potential binding sites for

FOXD3 within the IntronV(β)-promoter. Therefore the role of FOXD3 in regulating the IntronV(β)-promoter was further evaluated.

The results of my Chapter 4 studies confirm an inhibitory role of FOXD3 in colon cancers. Our studies demonstrate for the first time that FOXD3 is a potent transcriptional inhibitor of IntronV(β)-promoter, resulting in the absence of DCLK1-S expression in normal human colons. We also evaluated the pathophysiological relevance of DCLK1-S and FOXD3 expression in overall survival of colorectal cancer patients in a cohort of 92 patients, and determined that patients expressing relatively high levels of DCLK1-S and low levels of FOXD3 had significantly worse overall survival as compared to patients expressing relatively low levels of DCLK1-S and high levels of FOXD3 suggesting that measuring relative levels of DCLK1-S and FOXD3 will likely have diagnostic/prognostic significance.

## 5.4 SUMMARY

Overall my results revealed that: 1) DCLK1-S is expressed in colon cancer cells and in human adenocarcinomas, downstream of an IntronV(β)-promoter, while DCLK1-L is primarily expressed in normal colons, downstream of the 5'(α)promoter, 2) DCLK1-S functions as a kinase and binds NFATC2, resulting in activation/phosphorylation of NFATC2 at the $^{53}$SPPS$^{56}$ motif, and upregulation of COL3A1 expression, which likely mediates the observed increase in invasive potential of DCLK1-S expressing colon cancer cells, 3) FOXD3 is a potent transcriptional inhibitor of the IntronV(β)-promoter, resulting in the absence of DCLK1-S expression in normal human colons and patients expressing high-DCLK1-S/low-FOXD3 have worse overall survival compared to patients expressing low-DCLK1-S/high-FOXD3. An overall summary of my results is presented in **Figure 5.1**.

**Figure 5.1: Diagrammatic Representation of the Role of DCLK1-S in Normal and Colon Cancer Cells**

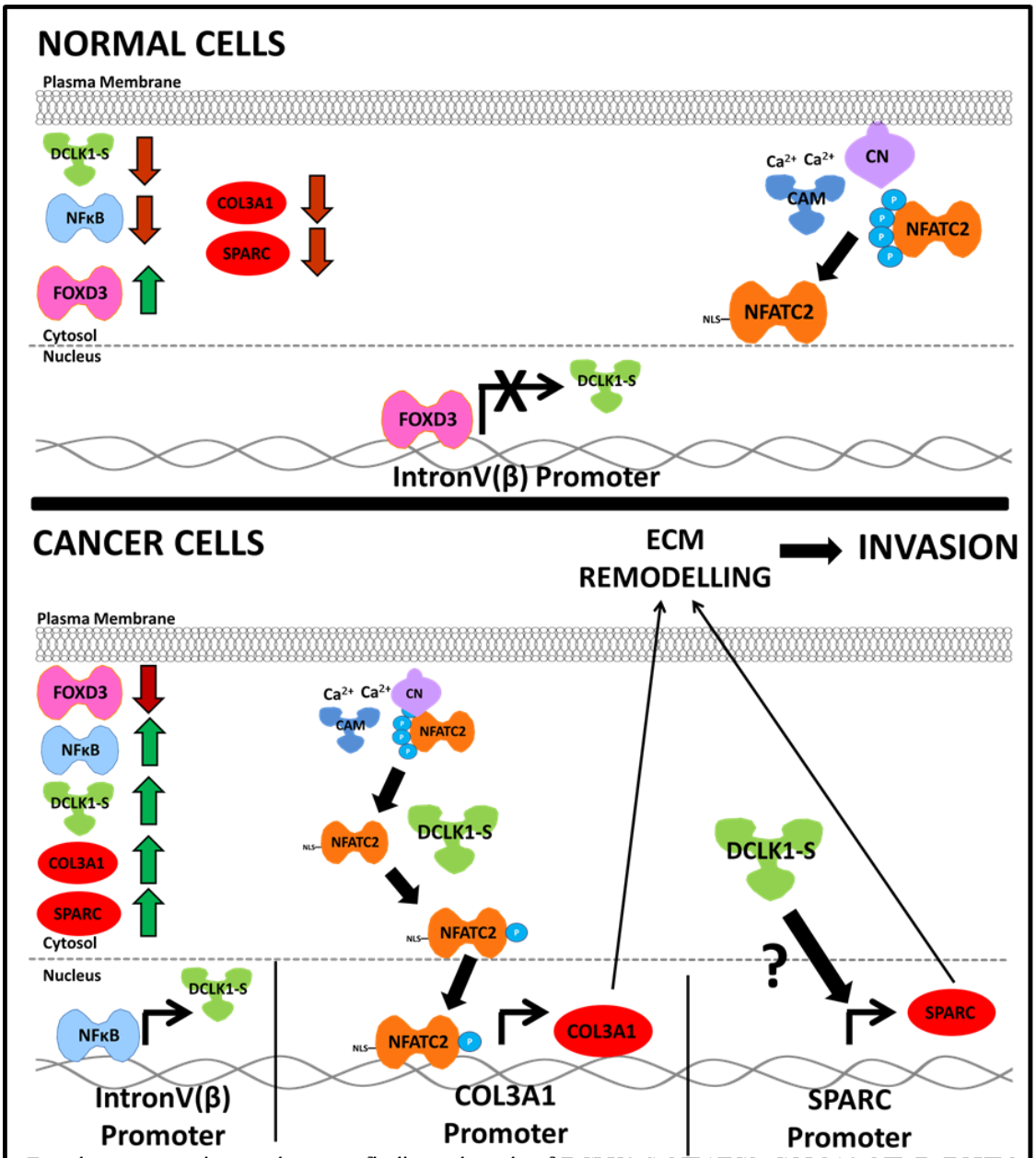


Based on our previous and current findings, the role of DCLK1-S, NFATC2, COL3A1, NFκB, FOXD3 is presented diagrammatically. In normal cells, FOXD3 acts a transcriptional inhibitor of the IntronV(β)-promoter. Therefore DCLK1-S expression remains suppressed in normal cells, and NFATC2 remains in an inactive state within the cytosol. In colon cancer cells, FOXD3 promoter is methylated resulting in the removal of the suppression and transcriptional activation of DCLK1-S in response to several oncogenic pathways, including presence of activated NFκB. Elevated levels of DCLK1-S then enhance expression of COL3A1 and SPARC. COL3A1 expression appears to be mediated via the phosphorylation of NFATC2 $^{53}$SPPS$^{56}$ Motif, resulting in translocation of NFATC2 into the nucleus and activation of the COL3A1 promoter. However the role of DCLK1-S in enhancing the expression of SPARC remains to be elucidated. SPARC and COL3A1are then secreted from the cell in order to facilitate ECM remodeling resulting in invasion.

## 5.5 CLINICAL RELEVANCE

Our novel findings regarding alternative usage of promoters by normal vs. cancer stem cells, suggests that specifically targeting DCLK1-S may eliminate cancer stem cells, while sparing DCLK1-L functions in normal colons. Now that we have identified signaling pathways/molecules, downstream of DCLK1-S, we have developed a high throughput screening (HTS) bioassay to help us identify small molecules/chemicals from available libraries, which can potentially downregulate biological effects of DCLK1-S in cancer cells, without inhibiting functions of DCLK1-L in normal cells. The significant fold decrease in the expression of *COL3A1* gene was exploited and COL3A1 luciferase activity was used as a readout for the loss of DCLK1-S expression/function. These experiments are currently on going in our laboratory.

Since high expressers of DCLK-S had significantly worse overall/disease free survival, DCLK1-S may have significant diagnostic/prognostic significance. Therefore, we have generated a specific DCLK1-S Ab which does not cross react with DCLK1-L, but specifically detects the S-isoform in human colorectal cancers, with little or no background. We hypothesize that patients whose Hps/Ads at baseline colonoscopy are positive for DCLK1-S staining, will likely develop recurrent growths at shorter time intervals. To assess the predictive value of DCLK1-S staining in resected patient polyps, at the time of baseline colonoscopy, we have designed a retrospective study, in which archived FFPE (Formalin-fixed, paraffin-embedded) samples from Department of Pathology, UTMB, will be used. These studies are also currently ongoing in our laboratory.

Therefore based on my studies, it may be possible to eliminate cancer stem cells while preserving normal stem cell function by specifically targeting DCLK1-S. My studies also suggest that DCLK1-S and FOXD3 can be utilized as diagnostic/prognostic markers.

### 5.6 FUTURE GOALS

Immediate goals: My results raise several important questions that will need to be evaluated in the future, in order to obtain a more complete understanding of DCLK1-S functions. For example, it remains to be confirmed if DCLK1-S functions to phosphorylate serine residues within the NFATC2 $^{53}$SPPS$^{56}$ motif. Our studies suggest that the NFATC2 $^{53}$SPPS$^{56}$ motif is important in DCLK1-S mediated activation of NFATC2, resulting in the increased transcriptional activation of the COL3A1 promoter. However, it remains to be confirmed if DCLK1-S actually phosphorylates NFATC2 at the $s^{53}$ and $s^{56}$ sites. The mechanisms mediating increased expression of SPARC, downstream of DCLK1-S, also remain to be investigated. We have now established a role of DCLK1-S in enhancing the invasive potential of colon cancer cells. We had, however, identified several additional pathways that were significantly altered on downregulation of DCLK1-S expression in colon cancer cells; the role of these pathways in mediating the biological effects of DCLK1-s remain to be elucidated. The IntronV(β)-promoter was positive for several other binding sites, besides NF-κB and FOXD3. It remains to be determined if these *cis* elements and their binding partners play an important role in the expression of DCLK1-S in colon cancer cells.

Long term goal: The long term goal of these studies is to understand the functions and molecular and cellular biology of the short and long isoforms of the stem cell marker, DCLK1, in normal and colon cancer cells.

**Appendix 1 Upregulated Genes >2 Fold Identified by RNAseq Analysis**

| Upregulated Genes >2 Fold Identified by RNAseq Analysis | | |
|---|---|---|
| **Gene ID** | **Fold Change** | **p_Value** |
| DDX60L | 2.00228 | 0.00005 |
| GPRC5A | 2.00817 | 0.00005 |
| MST1 | 2.01124 | 0.00065 |
| LAG3 | 2.01207 | 0.00275 |
| SLC7A9 | 2.01474 | 0.004 |
| LOC100289019 | 2.01628 | 0.00005 |
| C10orf107 | 2.01696 | 0.0026 |
| ERAP2 | 2.01881 | 0.00005 |
| ADAM21 | 2.02701 | 0.00005 |
| MYD88 | 2.02809 | 0.00005 |
| XRCC4 | 2.0402 | 0.00005 |
| TGFB2 | 2.04176 | 0.00005 |
| LAMA3 | 2.04499 | 0.00005 |
| PRSS3 | 2.0469 | 0.00005 |
| C10orf54 | 2.05465 | 0.00005 |
| HOXB4 | 2.05487 | 0.00005 |
| MARK2P9 | 2.05769 | 0.0026 |
| CFB | 2.059 | 0.00005 |
| HMOX1 | 2.06236 | 0.00005 |
| YJEFN3 | 2.06275 | 0.00045 |
| PLK2 | 2.07007 | 0.00005 |
| PHYHIP | 2.07692 | 0.00015 |
| CLU | 2.0779 | 0.00005 |
| C6orf165 | 2.08046 | 0.00235 |
| LRRC48 | 2.08495 | 0.0006 |
| HOXB6 | 2.08681 | 0.00005 |

| | | |
|---|---|---|
| PTRF | 2.08713 | 0.00005 |
| NMI | 2.09192 | 0.00005 |
| MUC1 | 2.09489 | 0.00005 |
| C15orf52 | 2.10688 | 0.00005 |
| PTK6 | 2.11199 | 0.00005 |
| AVPI1 | 2.11396 | 0.00005 |
| MDGA1 | 2.1157 | 0.00005 |
| COL7A1 | 2.11743 | 0.00005 |
| CTGF | 2.12532 | 0.00005 |
| AMH | 2.12548 | 0.00005 |
| CPT1B | 2.13021 | 0.00005 |
| BTN3A3 | 2.13696 | 0.00005 |
| CASP4 | 2.14272 | 0.00005 |
| CD300C | 2.14369 | 0.00375 |
| APOBEC3F | 2.1462 | 0.00005 |
| ALOX15B | 2.1481 | 0.00095 |
| POU2F2 | 2.1619 | 0.00005 |
| HOXB8 | 2.16501 | 0.00005 |
| CORO6 | 2.16517 | 0.00195 |
| LGALS9 | 2.16668 | 0.00005 |
| NEBL | 2.16784 | 0.00005 |
| IFIT3 | 2.17064 | 0.00005 |
| ACRBP | 2.17362 | 0.00045 |
| ADAM19 | 2.17617 | 0.00005 |
| WFDC3 | 2.17903 | 0.0073 |
| LFNG | 2.1796 | 0.00005 |
| ZBTB38 | 2.1807 | 0.00005 |
| LIF | 2.18343 | 0.00005 |
| AXIN2 | 2.18924 | 0.00005 |
| APOBEC3H | 2.19132 | 0.00005 |
| COL4A6 | 2.192 | 0.00005 |
| ALDH3B1 | 2.19295 | 0.00005 |
| IL28B | 2.19826 | 0.00855 |

| | | |
|---|---|---|
| NMU | 2.19871 | 0.00005 |
| LY6D | 2.20664 | 0.00725 |
| DNER | 2.2127 | 0.00005 |
| SMPD1 | 2.21357 | 0.00005 |
| SCG2 | 2.21963 | 0.00005 |
| ADAMTS16 | 2.22391 | 0.00005 |
| GNE | 2.22894 | 0.00005 |
| SH3RF2 | 2.24008 | 0.00005 |
| HOXB3 | 2.24349 | 0.00005 |
| C12orf36 | 2.24877 | 0.00275 |
| GJB4 | 2.25345 | 0.00005 |
| ACCN3 | 2.25601 | 0.00005 |
| STX1A | 2.25923 | 0.00005 |
| LOC283663 | 2.26506 | 0.00025 |
| FN3K | 2.27322 | 0.00085 |
| DUSP10 | 2.27324 | 0.00005 |
| KRTAP3-1 | 2.27445 | 0.00005 |
| LGI4 | 2.28236 | 0.00105 |
| LRRC66 | 2.28261 | 0.00125 |
| LRRC37A3 | 2.28726 | 0.00005 |
| LTA | 2.29252 | 0.0024 |
| PSMB9 | 2.29459 | 0.00005 |
| AQP3 | 2.29994 | 0.00005 |
| GRAMD1B | 2.30226 | 0.00005 |
| ARL4C | 2.31237 | 0.00005 |
| CNGA1 | 2.31419 | 0.0003 |
| DOK3 | 2.33404 | 0.00005 |
| SNAI2 | 2.35187 | 0.00215 |
| MMP28 | 2.35268 | 0.00025 |
| GBP1 | 2.35786 | 0.0001 |
| CXCR4 | 2.38282 | 0.0014 |
| KCNAB3 | 2.39246 | 0.0002 |
| SLC16A4 | 2.39474 | 0.00115 |

| | | |
|---|---|---|
| SECTM1 | 2.4025 | 0.00005 |
| S100A10 | 2.40767 | 0.00005 |
| CNTNAP3B | 2.41211 | 0.00005 |
| PRKCDBP | 2.42127 | 0.00005 |
| PCSK9 | 2.42208 | 0.00005 |
| S100A3 | 2.4277 | 0.00005 |
| GBP2 | 2.42843 | 0.00015 |
| ANXA10 | 2.43609 | 0.00005 |
| IL28A | 2.45152 | 0.00265 |
| PDE4D | 2.45163 | 0.00005 |
| RAB19 | 2.456 | 0.0043 |
| TBC1D2 | 2.46489 | 0.00005 |
| KRT86 | 2.46678 | 0.00005 |
| MGAT5B | 2.47959 | 0.00005 |
| PSCA | 2.48264 | 0.0002 |
| CCDC17 | 2.48725 | 0.0011 |
| EFR3B | 2.49219 | 0.00005 |
| HSPB8 | 2.49235 | 0.00005 |
| TINAGL1 | 2.52668 | 0.00005 |
| GLYCTK | 2.53175 | 0.00005 |
| THBS1 | 2.54035 | 0.00005 |
| MYEOV | 2.54153 | 0.00005 |
| ANO1 | 2.54867 | 0.00005 |
| HERC5 | 2.55708 | 0.00005 |
| HOXB2 | 2.5576 | 0.00025 |
| FXYD3 | 2.56173 | 0.00005 |
| FAM71F2 | 2.57089 | 0.01005 |
| CATSPERG | 2.57391 | 0.00005 |
| ZNF488 | 2.57412 | 0.00005 |
| CYB5A | 2.58026 | 0.00005 |
| CMYA5 | 2.60155 | 0.00005 |
| UCN2 | 2.60282 | 0.00075 |
| SPEF1 | 2.60293 | 0.00415 |

| | | |
|---|---|---|
| FLRT3 | 2.61266 | 0.00955 |
| PLVAP | 2.63312 | 0.0022 |
| PODXL2 | 2.63863 | 0.00005 |
| CYP4F3 | 2.64648 | 0.00005 |
| GLIS3 | 2.65401 | 0.00005 |
| MRGPRF | 2.66153 | 0.0029 |
| CASS4 | 2.66347 | 0.0003 |
| NPM2 | 2.66997 | 0.00055 |
| KLK6 | 2.67287 | 0.00005 |
| VILL | 2.67629 | 0.00005 |
| SAMD9 | 2.69146 | 0.00005 |
| FAM46B | 2.71508 | 0.00005 |
| ADAM32 | 2.73029 | 0.00105 |
| APOBEC3D | 2.732 | 0.00005 |
| GCHFR | 2.73317 | 0.00005 |
| RNF224 | 2.7603 | 0.00845 |
| LOXL4 | 2.76452 | 0.00005 |
| MX1 | 2.78986 | 0.00005 |
| SEMA3B | 2.79033 | 0.00005 |
| CCDC106 | 2.79274 | 0.00005 |
| LINC00511 | 2.80921 | 0.00005 |
| CYP24A1 | 2.81201 | 0.00005 |
| SLC25A34 | 2.81901 | 0.00035 |
| DUSP4 | 2.82068 | 0.00005 |
| ANKRD2 | 2.82409 | 0.0014 |
| APOBEC3G | 2.82504 | 0.00005 |
| INHBB | 2.83287 | 0.00005 |
| PTGES | 2.83786 | 0.00005 |
| LOC100505633 | 2.83983 | 0.00015 |
| MYO15B | 2.84 | 0.00015 |
| GABRR2 | 2.84534 | 0.00335 |
| LY6G6C | 2.85175 | 0.00225 |
| KRT20 | 2.85731 | 0.00005 |

| | | |
|---|---|---|
| S100A5 | 2.86192 | 0.00005 |
| SLC22A20 | 2.86261 | 0.00175 |
| S100A4 | 2.882 | 0.00005 |
| FAM83E | 2.88508 | 0.00005 |
| MAMDC4 | 2.88717 | 0.00005 |
| LOC283404 | 2.90953 | 0.0021 |
| C9orf172 | 2.91264 | 0.00015 |
| LAT | 2.94667 | 0.00005 |
| SH3TC2 | 2.95399 | 0.00005 |
| PGM5P2 | 2.95476 | 0.0001 |
| ITGB2 | 2.97582 | 0.00125 |
| MILR1 | 2.97751 | 0.00785 |
| TNFSF10 | 3.00491 | 0.00005 |
| TLR3 | 3.02485 | 0.00005 |
| FRZB | 3.02915 | 0.0058 |
| LOC100505918 | 3.03462 | 0.0008 |
| MIR31HG | 3.06265 | 0.00005 |
| KLK10 | 3.06535 | 0.00005 |
| LOC100134259 | 3.08396 | 0.00075 |
| AMIGO2 | 3.08889 | 0.00005 |
| RARRES3 | 3.0893 | 0.0002 |
| TRANK1 | 3.1066 | 0.00005 |
| ZEB1 | 3.10827 | 0.00005 |
| CYP3A5 | 3.1276 | 0.00005 |
| TRIML2 | 3.12821 | 0.00005 |
| F3 | 3.16718 | 0.00005 |
| B3GALT5 | 3.20114 | 0.00005 |
| AURKC | 3.21644 | 0.00265 |
| CPA4 | 3.26045 | 0.00005 |
| MSX2 | 3.27429 | 0.00005 |
| ZNF614 | 3.29281 | 0.00005 |
| EMP1 | 3.31448 | 0.00005 |
| KRT15 | 3.32016 | 0.00005 |

| | | |
|---|---|---|
| SLC16A6 | 3.32601 | 0.00005 |
| VIM | 3.36752 | 0.00005 |
| KRT32 | 3.39577 | 0.0105 |
| CCL25 | 3.40338 | 0.00305 |
| ZNF83 | 3.40911 | 0.00005 |
| IFNE | 3.41095 | 0.00145 |
| ECM1 | 3.42659 | 0.00005 |
| HIF3A | 3.42998 | 0.00005 |
| COL13A1 | 3.45615 | 0.00005 |
| SRPX2 | 3.51614 | 0.00005 |
| CEACAM1 | 3.52483 | 0.00005 |
| CYP26A1 | 3.52923 | 0.00045 |
| GDA | 3.56845 | 0.00005 |
| FGF17 | 3.57775 | 0.0067 |
| SYTL5 | 3.58324 | 0.00005 |
| HSD17B3 | 3.59632 | 0.0065 |
| APOL1 | 3.60281 | 0.00005 |
| NWD1 | 3.6142 | 0.00005 |
| VCAN | 3.6195 | 0.00005 |
| RAET1L | 3.63284 | 0.00005 |
| EHF | 3.6369 | 0.00005 |
| LOC100507127 | 3.65318 | 0.0064 |
| TCN1 | 3.65707 | 0.00005 |
| CYP4F12 | 3.65823 | 0.00005 |
| CNTNAP3 | 3.70116 | 0.00005 |
| NHS | 3.75365 | 0.00005 |
| C11orf86 | 3.77074 | 0.00975 |
| OTOP1 | 3.78536 | 0.0089 |
| RAB27B | 3.80431 | 0.00005 |
| RIMKLB | 3.81987 | 0.00015 |
| FBP1 | 3.8201 | 0.0001 |
| LOC100124692 | 3.86692 | 0.00025 |
| ITPKB | 3.87829 | 0.0004 |

| | | |
|---|---|---|
| ATP6V0A4 | 3.92557 | 0.00005 |
| EDAR | 3.93462 | 0.00005 |
| KLK5 | 3.99169 | 0.00005 |
| IGFBP6 | 4.05637 | 0.00005 |
| UPK3B | 4.11672 | 0.00005 |
| CYP2J2 | 4.17399 | 0.0002 |
| CLIC3 | 4.22156 | 0.00005 |
| TNS4 | 4.42904 | 0.00005 |
| TRIM29 | 4.4306 | 0.00005 |
| KRT14 | 4.43284 | 0.0034 |
| COL17A1 | 4.44732 | 0.00005 |
| ZBED2 | 4.58501 | 0.00005 |
| ANKRD1 | 4.63351 | 0.0001 |
| ITGB7 | 4.71538 | 0.0002 |
| FGFBP1 | 4.7447 | 0.00005 |
| C1orf116 | 5.10721 | 0.00005 |
| KRT81 | 5.57619 | 0.00005 |
| ALPPL2 | 5.65978 | 0.00005 |
| CFH | 5.88831 | 0.0003 |
| ALPP | 6.00826 | 0.00015 |
| KRT13 | 6.26633 | 0.0018 |
| ALDH3A1 | 6.63267 | 0.00005 |
| PRSS33 | 6.83437 | 0.0086 |
| C10orf81 | 7.19009 | 0.0004 |

**Appendix 2 Downregulated Genes <-2 Fold Identified by RNAseq Analysis**

| Downregulated Genes <-2 Fold Identified by RNAseq Analysis | | |
|---|---|---|
| **Gene ID** | **Fold Change** | **p_Value** |
| CD36 | -9.76117 | 0.00005 |
| PBX1 | -9.46431 | 0.00035 |
| RANBP3L | -9.00691 | 0.00475 |
| RERG | -8.93372 | 0.0032 |
| MGP | -7.371 | 0.00005 |
| GJA1 | -7.07952 | 0.00005 |
| INHBE | -6.77088 | 0.0003 |
| GGT5 | -6.70891 | 0.00005 |
| RMRP | -6.53885 | 0.00015 |
| ERP27 | -5.88645 | 0.00085 |
| NR5A2 | -5.6828 | 0.00005 |
| SDPR | -5.65671 | 0.00005 |
| FAM198B | -5.4928 | 0.00005 |
| SPOCK1 | -5.24691 | 0.0066 |
| FAM49A | -5.21585 | 0.0001 |
| RPPH1 | -5.16664 | 0.0001 |
| SLC1A3 | -5.13449 | 0.00005 |
| MB | -5.05339 | 0.00005 |
| LGSN | -4.97391 | 0.00005 |
| CNTNAP2 | -4.87825 | 0.00005 |
| DPYSL3 | -4.87714 | 0.00005 |
| CAPN13 | -4.75338 | 0.0009 |
| COL3A1 | -4.69698 | 0.00005 |

| | | |
|---|---|---|
| LRP1B | -4.66317 | 0.00005 |
| SPARC | -4.65235 | 0.00005 |
| ICAM1 | -4.62994 | 0.00005 |
| LOC100507003 | -4.62868 | 0.00005 |
| KLHDC7B | -4.53456 | 0.00005 |
| KIAA0226L | -4.45899 | 0.0017 |
| LCK | -4.35268 | 0.0002 |
| TRPV6 | -4.32484 | 0.00005 |
| ZNF493 | -4.28628 | 0.0013 |
| NUPR1 | -4.20832 | 0.00005 |
| PAH | -4.19237 | 0.00005 |
| SULT1C2 | -4.18117 | 0.0001 |
| TNFRSF9 | -4.15624 | 0.00005 |
| LOC100131138 | -4.0352 | 0.00005 |
| PRPH | -4.02136 | 0.00005 |
| NRG1 | -4.00947 | 0.00005 |
| HEPH | -3.99626 | 0.00005 |
| RAB34 | -3.98687 | 0.00005 |
| RFTN1 | -3.93257 | 0.00005 |
| SCN9A | -3.89358 | 0.00005 |
| CSDC2 | -3.88815 | 0.0089 |
| NEURL | -3.86526 | 0.0001 |
| ZNF516 | -3.76679 | 0.00005 |
| C12orf39 | -3.70144 | 0.0005 |
| EDA2R | -3.69735 | 0.00005 |
| DHRS2 | -3.68915 | 0.00005 |
| FCGRT | -3.62088 | 0.0028 |
| FCRLA | -3.61761 | 0.00135 |
| ATP2C2 | -3.58905 | 0.00005 |
| C15orf59 | -3.57796 | 0.00495 |
| IL21R | -3.54425 | 0.0035 |
| ANK3 | -3.5117 | 0.00005 |
| IL31RA | -3.48682 | 0.00055 |

| | | |
|---|---|---|
| MYOM3 | -3.45541 | 0.00005 |
| SLC7A2 | -3.45258 | 0.00005 |
| PNPLA1 | -3.42448 | 0.0002 |
| PPP1R1A | -3.41157 | 0.0003 |
| HLA-DOA | -3.39968 | 0.00005 |
| ALPL | -3.34929 | 0.00105 |
| LOC283050 | -3.34679 | 0.00005 |
| ZNF268 | -3.3457 | 0.00005 |
| ODAM | -3.33756 | 0.00005 |
| SPNS3 | -3.33005 | 0.00995 |
| OLFML3 | -3.25625 | 0.00185 |
| BIN2 | -3.21459 | 0.00205 |
| SNTB1 | -3.18142 | 0.00005 |
| IL20RA | -3.17901 | 0.0005 |
| CREB5 | -3.16859 | 0.00005 |
| VGF | -3.16289 | 0.00005 |
| BEND7 | -3.14247 | 0.00005 |
| ZNF648 | -3.13869 | 0.00055 |
| TRIB2 | -3.13381 | 0.00005 |
| LRG1 | -3.09177 | 0.0015 |
| NAV3 | -3.06679 | 0.00005 |
| KCND3 | -3.04819 | 0.00005 |
| KLF15 | -3.04002 | 0.00005 |
| FGF9 | -3.01323 | 0.00005 |
| EDNRA | -2.99621 | 0.00005 |
| FAM107B | -2.9931 | 0.00005 |
| PRKAA2 | -2.98449 | 0.00005 |
| FOXN4 | -2.9723 | 0.00005 |
| SPOCK3 | -2.96156 | 0.00005 |
| HIST2H2AC | -2.94994 | 0.0002 |
| PRKD3 | -2.93241 | 0.00005 |
| MYCL1 | -2.93217 | 0.00005 |
| WLS | -2.92655 | 0.00005 |

| | | |
|---|---|---|
| MEX3A | -2.92113 | 0.00005 |
| SYT5 | -2.91789 | 0.00005 |
| MAML3 | -2.89115 | 0.0009 |
| SHANK1 | -2.88981 | 0.00005 |
| SNCAIP | -2.88979 | 0.0006 |
| TRPV4 | -2.8897 | 0.00005 |
| SOX4 | -2.86604 | 0.00005 |
| PKIB | -2.86292 | 0.00005 |
| LOC643401 | -2.84602 | 0.001 |
| CHST1 | -2.84331 | 0.0001 |
| ALPK2 | -2.82418 | 0.0001 |
| TESC | -2.7895 | 0.00005 |
| NRSN2 | -2.78378 | 0.00005 |
| EIF4E3 | -2.78357 | 0.00005 |
| LOC100216001 | -2.7778 | 0.006 |
| RUNDC3B | -2.77517 | 0.00005 |
| UPP1 | -2.76175 | 0.00005 |
| DSC3 | -2.74874 | 0.00005 |
| SATB1 | -2.72436 | 0.00005 |
| TMPRSS13 | -2.71875 | 0.00005 |
| LMO4 | -2.6945 | 0.00005 |
| RENBP | -2.69213 | 0.0072 |
| RIMS2 | -2.688 | 0.00005 |
| KCNB1 | -2.68525 | 0.00115 |
| SERTAD4 | -2.67047 | 0.00395 |
| HIST1H1E | -2.66727 | 0.0015 |
| NCKAP5 | -2.64794 | 0.00005 |
| CECR2 | -2.64714 | 0.00005 |
| PDE3A | -2.63688 | 0.00005 |
| SYT3 | -2.61804 | 0.00005 |
| VAV3 | -2.61648 | 0.0051 |
| ZNF136 | -2.6104 | 0.0005 |
| C20orf151 | -2.61015 | 0.0003 |

| | | |
|---|---|---|
| IL18R1 | -2.60877 | 0.00115 |
| LINC00494 | -2.60785 | 0.00135 |
| SPTB | -2.60724 | 0.00005 |
| PELI2 | -2.60279 | 0.00005 |
| CABP1 | -2.59272 | 0.00015 |
| TEX19 | -2.59205 | 0.00005 |
| BHLHA15 | -2.56935 | 0.00005 |
| SH3BGRL2 | -2.56583 | 0.00005 |
| B3GALT1 | -2.55285 | 0.00035 |
| C6orf48 | -2.53556 | 0.00005 |
| TRIB3 | -2.50839 | 0.00005 |
| CD24 | -2.49692 | 0.00005 |
| OLAH | -2.49334 | 0.00525 |
| TOX2 | -2.48095 | 0.00005 |
| AZGP1 | -2.47732 | 0.00005 |
| PTPDC1 | -2.4632 | 0.00005 |
| GJC1 | -2.46224 | 0.00005 |
| ONECUT1 | -2.45547 | 0.00145 |
| IFI16 | -2.44907 | 0.001 |
| ELFN1 | -2.44385 | 0.00005 |
| NCKAP1L | -2.43918 | 0.0004 |
| PAGE4 | -2.42303 | 0.0059 |
| CPQ | -2.40616 | 0.00005 |
| FKBP5 | -2.39922 | 0.00005 |
| EFNA2 | -2.39818 | 0.00005 |
| LYPD6B | -2.396 | 0.00005 |
| SUN3 | -2.3935 | 0.00005 |
| MSI1 | -2.38438 | 0.00005 |
| ZNF804A | -2.36419 | 0.00005 |
| AKNA | -2.36279 | 0.00005 |
| HTR6 | -2.35842 | 0.00165 |
| C20orf160 | -2.34633 | 0.0005 |
| SLC43A1 | -2.34183 | 0.00005 |

| | | |
|---|---|---|
| CLMP | -2.34149 | 0.0004 |
| GXYLT2 | -2.33604 | 0.00035 |
| RORC | -2.33339 | 0.00005 |
| RGS16 | -2.3244 | 0.00005 |
| SEMA3A | -2.32362 | 0.00005 |
| LINGO1 | -2.32158 | 0.00005 |
| KLRK1 | -2.32055 | 0.00185 |
| NFIA | -2.28598 | 0.00005 |
| CHRM4 | -2.28551 | 0.00005 |
| NELL2 | -2.28267 | 0.0001 |
| CR2 | -2.28122 | 0.00005 |
| HPD | -2.27157 | 0.0046 |
| FXYD1 | -2.26014 | 0.00015 |
| PDE2A | -2.25632 | 0.00005 |
| EBF4 | -2.25092 | 0.00005 |
| FYN | -2.24392 | 0.00005 |
| FAM129A | -2.2438 | 0.00005 |
| ADAP1 | -2.23769 | 0.00005 |
| MEF2C | -2.236 | 0.00005 |
| SULF2 | -2.22466 | 0.00005 |
| HEY1 | -2.22343 | 0.00005 |
| PDGFC | -2.2219 | 0.00005 |
| SOX8 | -2.21734 | 0.00005 |
| ZNF586 | -2.21188 | 0.00025 |
| SERPINA3 | -2.19453 | 0.00085 |
| C4orf32 | -2.1944 | 0.00005 |
| SYT7 | -2.18612 | 0.00005 |
| C1orf21 | -2.18296 | 0.00005 |
| NRARP | -2.16038 | 0.00005 |
| ZNF469 | -2.15606 | 0.00005 |
| ARL4A | -2.14794 | 0.00005 |
| CLGN | -2.14692 | 0.00005 |
| DFNA5 | -2.14388 | 0.00005 |

| | | |
|---|---|---|
| LOC730091 | -2.14209 | 0.00005 |
| CCDC64B | -2.14172 | 0.00005 |
| PTP4A3 | -2.138 | 0.00005 |
| MYB | -2.12288 | 0.00005 |
| GAS7 | -2.12157 | 0.00005 |
| FOXP2 | -2.11161 | 0.00005 |
| ESRP1 | -2.10678 | 0.00005 |
| DOC2B | -2.10537 | 0.00005 |
| WNT2B | -2.09817 | 0.00015 |
| GATA3 | -2.09538 | 0.00005 |
| ARHGAP24 | -2.08864 | 0.00005 |
| TNNC1 | -2.08768 | 0.00025 |
| FSD1 | -2.07846 | 0.00005 |
| RPH3A | -2.07491 | 0.0012 |
| BTK | -2.07483 | 0.0056 |
| RPLP0P2 | -2.05864 | 0.0003 |
| KCNQ4 | -2.0488 | 0.00005 |
| ICA1 | -2.04119 | 0.00005 |
| C20orf96 | -2.02663 | 0.00005 |
| SCN4A | -2.02407 | 0.00005 |
| SH3GL3 | -2.01573 | 0.00125 |
| PHGDH | -2.01245 | 0.00005 |
| ITGAX | -2.01096 | 0.00025 |
| RHOU | -2.00959 | 0.00005 |
| EPB41L4A-AS1 | -2.0075 | 0.00005 |
| IGSF9 | -2.00507 | 0.00005 |

# Bibliography

Abdelsattar, Z. M., Wong, S. L., Regenbogen, S. E., Jomaa, D. M., Hardiman, K. M. and Hendren, S. (2016). Colorectal cancer outcomes and treatment patterns in patients too young for average-risk screening. *Cancer*.

Abel, E. V. and Aplin, A. E. (2010). FOXD3 is a mutant B-RAF-regulated inhibitor of G(1)-S progression in melanoma cells. *Cancer Res* 70, 2891-900.

Abel, E. V., Basile, K. J., Kugel, C. H., Witkiewicz, A. K., Le, K., Amaravadi, R. K., Karakousis, G. C., Xu, X., Xu, W., Schuchter, L. M. et al. (2013). Melanoma adapts to RAF/MEK inhibitors through FOXD3-mediated upregulation of ERBB3. *J Clin Invest* 123, 2155-68.

Abetov, D., Mustapova, Z., Saliev, T. and Bulanin, D. (2015). Biomarkers and signaling pathways of colorectal cancer stem cells. *Tumour Biol* 36, 1339-53.

Alford, A. I. and Hankenson, K. D. (2006). Matricellular proteins: Extracellular modulators of bone development, remodeling, and regeneration. *Bone* 38, 749-57.

Andresen, K., Boberg, K. M., Vedeld, H. M., Honne, H., Hektoen, M., Wadsworth, C. A., Clausen, O. P., Karlsen, T. H., Foss, A., Mathisen, O. et al. (2012). Novel target genes and a valid biomarker panel identified for cholangiocarcinoma. *Epigenetics* 7, 1249-57.

Archey, W. B., Sweet, M. P., Alig, G. C. and Arrick, B. A. (1999). Methylation of CpGs as a determinant of transcriptional activation at alternative promoters for transforming growth factor-beta3. *Cancer Res* 59, 2292-6.

Arnold, S. A. and Brekken, R. A. (2009). SPARC: a matricellular regulator of tumorigenesis. *J Cell Commun Signal* 3, 255-73.

Bailey, C. E., Hu, C. Y., You, Y. N., Bednarski, B. K., Rodriguez-Bigas, M. A., Skibber, J. M., Cantor, S. B. and Chang, G. J. (2015). Increasing disparities in the age-related incidences of colon and rectal cancers in the United States, 1975-2010. *JAMA Surg* 150, 17-22.

Bailey, J. M., Alsina, J., Rasheed, Z. A., McAllister, F. M., Fu, Y. Y., Plentz, R., Zhang, H., Pasricha, P. J., Bardeesy, N., Matsui, W. et al. (2013). DCLK1 Marks a Morphologically Distinct Subpopulation of Cells With Stem Cell Properties in Preinvasive Pancreatic Cancer. *Gastroenterology*.

Bailey, J. M., Alsina, J., Rasheed, Z. A., McAllister, F. M., Fu, Y. Y., Plentz, R., Zhang, H., Pasricha, P. J., Bardeesy, N., Matsui, W. et al. (2014). DCLK1 marks a morphologically distinct subpopulation of cells with stem cell properties in preinvasive pancreatic cancer. *Gastroenterology* 146, 245-56.

Barker, N. (2014). Adult intestinal stem cells: critical drivers of epithelial homeostasis and regeneration. *Nat Rev Mol Cell Biol* 15, 19-33.

Barker, N., van Es, J. H., Jaks, V., Kasper, M., Snippert, H., Toftgård, R. and Clevers, H. (2008). Very long-term self-renewal of small intestine, colon, and hair follicles from cycling Lgr5+ve stem cells. *Cold Spring Harb Symp Quant Biol* 73, 351-6.

Barker, N., van Es, J. H., Kuipers, J., Kujala, P., van den Born, M., Cozijnsen, M., Haegebarth, A., Korving, J., Begthel, H., Peters, P. J. et al. (2007). Identification of stem cells in small intestine and colon by marker gene Lgr5. *Nature* 449, 1003-7.

Basile, K. J., Abel, E. V. and Aplin, A. E. (2012). Adaptive upregulation of FOXD3 and resistance to PLX4032/4720-induced cell death in mutant B-RAF melanoma cells. *Oncogene* 31, 2471-9.

Basso, D., Belluco, C., Mazza, S., Greco, E., Della Rocca, F., Pauletto, P., Nitti, D., Lise, M. and Plebani, M. (2001). Colorectal cancer metastatic phenotype stimulates production by fibroblasts of N-terminal peptide of type III collagen: clinical implications for prognosis. *Clin Chim Acta* 312, 135-42.

Berg, M. and Soreide, K. (2012). EGFR and downstream genetic alterations in KRAS/BRAF and PI3K/AKT pathways in colorectal cancer: implications for targeted therapy. *Discov Med* 14, 207-14.

Berke, J. D., Paletzki, R. F., Aronson, G. J., Hyman, S. E. and Gerfen, C. R. (1998). A complex program of striatal gene expression induced by dopaminergic stimulation. *J Neurosci* 18, 5301-10.

Borinstein, S. C., Conerly, M., Dzieciatkowski, S., Biswas, S., Washington, M. K., Trobridge, P., Henikoff, S. and Grady, W. M. (2010). Aberrant DNA methylation occurs in colon neoplasms arising in the azoxymethane colon cancer model. *Mol Carcinog* 49, 94-103.

Bornstein, P. (2009). Matricellular proteins: an overview. *J Cell Commun Signal* 3, 163-5.

Bornstein, P. and Sage, E. H. (2002). Matricellular proteins: extracellular modulators of cell function. *Curr Opin Cell Biol* 14, 608-16.

Bradshaw, A. D. (2009). The role of SPARC in extracellular matrix assembly. *J Cell Commun Signal* 3, 239-46.

Bradshaw, A. D. and Sage, E. H. (2001). SPARC, a matricellular protein that functions in cellular differentiation and tissue response to injury. *J Clin Invest* 107, 1049-54.

Bu, Y. and Cao, D. (2012). The origin of cancer stem cells. *Front Biosci (Schol Ed)* 4, 819-30.

Burgess, H. A., Martinez, S. and Reiner, O. (1999). KIAA0369, doublecortin-like kinase, is expressed during brain development. *J Neurosci Res* 58, 567-75.

Burgess, H. A. and Reiner, O. (2000). Doublecortin-like kinase is associated with microtubules in neuronal growth cones. *Mol Cell Neurosci* 16, 529-41.

Burgess, H. A. and Reiner, O. (2001). Cleavage of doublecortin-like kinase by calpain releases an active kinase fragment from a microtubule anchorage domain. *J Biol Chem* 276, 36397-403.

Burgess, H. A. and Reiner, O. (2002). Alternative splice variants of doublecortin-like kinase are differentially expressed and have different kinase activities. *J Biol Chem* 277, 17696-705.

Bustin, S. (2015). Molecular Biology of the Cell, Sixth Edition; ISBN: 9780815344643; and Molecular Biology of the Cell, Sixth Edition, The Problems Book; ISBN 9780815344537. *Int J Mol Sci* 16, 28123-5.

Chan, S. K., Griffith, O. L., Tai, I. T. and Jones, S. J. (2008). Meta-analysis of colorectal cancer gene expression profiling studies identifies consistently reported candidate biomarkers. *Cancer Epidemiol Biomarkers Prev* 17, 543-52.

Chandrakesan, P., May, R., Qu, D., Weygant, N., Taylor, V. E., Li, J. D., Ali, N., Sureban, S. M., Qante, M., Wang, T. C. et al. (2015). Dclk1+ small intestinal epithelial tuft cells display the hallmarks of quiescence and self-renewal. *Oncotarget* 6, 30876-86.

Chandrakesan, P., Weygant, N., May, R., Qu, D., Chinthalapally, H. R., Sureban, S. M., Ali, N., Lightfoot, S. A., Umar, S. and Houchen, C. W. (2014). DCLK1 facilitates intestinal tumor growth via enhancing pluripotency and epithelial mesenchymal transition. *Oncotarget*.

Chen, L., Glover, J. N., Hogan, P. G., Rao, A. and Harrison, S. C. (1998). Structure of the DNA-binding domains from NFAT, Fos and Jun bound specifically to DNA. *Nature* 392, 42-8.

Cheng, A. S., Li, M. S., Kang, W., Cheng, V. Y., Chou, J. L., Lau, S. S., Go, M. Y., Lee, C. C., Ling, T. K., Ng, E. K. et al. (2013). Helicobacter pylori causes epigenetic dysregulation of FOXD3 to promote gastric carcinogenesis. *Gastroenterology* 144, 122-133.e9.

Cherciu, I., Bărbălan, A., Pirici, D., Mărgăritescu, C. and Săftoiu, A. (2014). Stem cells, colorectal cancer and cancer stem cell markers correlations. *Curr Health Sci J* 40, 153-61.

Chlenski, A. and Cohn, S. L. (2010). Modulation of matrix remodeling by SPARC in neoplastic progression. *Semin Cell Dev Biol* 21, 55-65.

Chlenski, A., Liu, S., Baker, L. J., Yang, Q., Tian, Y., Salwen, H. R. and Cohn, S. L. (2004). Neuroblastoma angiogenesis is inhibited with a folded synthetic molecule corresponding to the epidermal growth factor-like module of the follistatin domain of SPARC. *Cancer Res* 64, 7420-5.

Chu, T. L., Zhao, H. M., Li, Y., Chen, A. X., Sun, X. and Ge, J. (2014). FoxD3 deficiency promotes breast cancer progression by induction of epithelial-mesenchymal transition. *Biochem Biophys Res Commun* 446, 580-4.

Chuvpilo, S., Avots, A., Berberich-Siebelt, F., Glöckner, J., Fischer, C., Kerstan, A., Escher, C., Inashkina, I., Hlubek, F., Jankevics, E. et al. (1999). Multiple NF-ATc isoforms with individual transcriptional properties are synthesized in T lymphocytes. *J Immunol* 162, 7294-301.

Chytil, M. and Verdine, G. L. (1996). The Rel family of eukaryotic transcription factors. *Curr Opin Struct Biol* 6, 91-100.

Clark, S. J., Harrison, J., Paul, C. L. and Frommer, M. (1994). High sensitivity mapping of methylated cytosines. *Nucleic Acids Res* 22, 2990-7.

Cobb, S., Wood, T., Ceci, J., Varro, A., Velasco, M. and Singh, P. (2004). Intestinal expression of mutant and wild-type progastrin significantly increases colon carcinogenesis in response to azoxymethane in transgenic mice. *Cancer* 100, 1311-23.

Conklin, M. W., Eickhoff, J. C., Riching, K. M., Pehlke, C. A., Eliceiri, K. W., Provenzano, P. P., Friedl, A. and Keely, P. J. (2011). Aligned collagen is a prognostic signature for survival in human breast carcinoma. *Am J Pathol* 178, 1221-32.

D'Angelo, R. C. and Wicha, M. S. (2010). Stem cells in normal development and cancer. *Prog Mol Biol Transl Sci* 95, 113-58.

De Mey, J. R. and Freund, J. N. (2013). Understanding epithelial homeostasis in the intestine: An old battlefield of ideas, recent breakthroughs and remaining controversies. *Tissue Barriers* 1, e24965.

Delgiorno, K. E., Hall, J. C., Takeuchi, K. K., Pan, F. C., Halbrook, C. J., Washington, M. K., Olive, K. P., Spence, J. R., Sipos, B., Wright, C. V. et al. (2014). Identification and manipulation of biliary metaplasia in pancreatic tumors. *Gastroenterology* 146, 233-44.e5.

Do, C., Bertrand, C., Palasse, J., Delisle, M. B., Shulkes, A., Cohen-Jonathan-Moyal, E., Ferrand, A. and Seva, C. (2012). A new biomarker that predicts colonic neoplasia outcome in patients with hyperplastic colonic polyps. *Cancer Prev Res (Phila)* 5, 675-84.

Duckworth, C. A., Clyde, D., Worthley, D. L., Wang, T. C., Varro, A. and Pritchard, D. M. (2013). Progastrin-induced secretion of insulin-like growth factor 2 from colonic myofibroblasts stimulates colonic epithelial proliferation in mice. *Gastroenterology* 145, 197-208.e3.

Duque, J., Fresno, M. and Iñiguez, M. A. (2005). Expression and function of the nuclear factor of activated T cells in colon carcinoma cells: involvement in the regulation of cyclooxygenase-2. *J Biol Chem* 280, 8686-93.

Engels, B. M., Schouten, T. G., van Dullemen, J., Gosens, I. and Vreugdenhil, E. (2004). Functional differences between two DCLK splice variants. *Brain Res Mol Brain Res* 120, 103-14.

Ewald, J. A., Downs, T. M., Cetnar, J. P. and Ricke, W. A. (2013). Expression microarray meta-analysis identifies genes associated with Ras/MAPK and related pathways in progression of muscle-invasive bladder transition cell carcinoma. *PLoS One* 8, e55414.

Femia, A. P., Dolara, P., Salvadori, M. and Caderni, G. (2013). Expression of LGR-5, MSI-1 and DCAMKL-1, putative stem cell markers, in the early phases of 1,2-dimethylhydrazine-induced rat colon carcinogenesis: correlation with nuclear β-catenin. *BMC Cancer* 13, 48.

Friocourt, G., Liu, J. S., Antypa, M., Rakic, S., Walsh, C. A. and Parnavelas, J. G. (2007). Both doublecortin and doublecortin-like kinase play a role in cortical interneuron migration. *J Neurosci* 27, 3875-83.

Funk, S. E. and Sage, E. H. (1991). The Ca2(+)-binding glycoprotein SPARC modulates cell cycle progression in bovine aortic endothelial cells. *Proc Natl Acad Sci U S A* 88, 2648-52.

Gagliardi, G., Goswami, M., Passera, R. and Bellows, C. F. (2012a). DCLK1 immunoreactivity in colorectal neoplasia. *Clin Exp Gastroenterol* 5, 35-42.

Gagliardi, G., Moroz, K. and Bellows, C. F. (2012b). Immunolocalization of DCAMKL-1, a putative intestinal stem cell marker, in normal colonic tissue. *Pathol Res Pract* 208, 475-9.

Gaudineau, B., Fougère, M., Guaddachi, F., Lemoine, F., de la Grange, P. and Jauliac, S. (2012). Lipocalin 2, the TNF-like receptor TWEAKR and its ligand TWEAK act downstream of NFAT1 to regulate breast cancer cell invasion. *J Cell Sci* 125, 4475-86.

Gerbe, F., Brulin, B., Makrini, L., Legraverend, C. and Jay, P. (2009). DCAMKL-1 expression identifies Tuft cells rather than stem cells in the adult mouse intestinal epithelium. *Gastroenterology* 137, 2179-80; author reply 2180-1.

Gerbe, F., Legraverend, C. and Jay, P. (2012). The intestinal epithelium tuft cells: specification and function. *Cell Mol Life Sci* 69, 2907-17.

Gerbe, F., van Es, J. H., Makrini, L., Brulin, B., Mellitzer, G., Robine, S., Romagnolo, B., Shroyer, N. F., Bourgaux, J. F., Pignodel, C. et al. (2011). Distinct ATOH1 and Neurog3 requirements define tuft cells as a new secretory cell type in the intestinal epithelium. *J Cell Biol* 192, 767-80.

Gerlach, K., Daniel, C., Lehr, H. A., Nikolaev, A., Gerlach, T., Atreya, R., Rose-John, S., Neurath, M. F. and Weigmann, B. (2012). Transcription factor NFATc2 controls the emergence of colon cancer associated with IL-6-dependent colitis. *Cancer Res* 72, 4340-50.

Germain, D. P. (2007). Ehlers-Danlos syndrome type IV. *Orphanet J Rare Dis* 2, 32.

Giannakis, M., Stappenbeck, T. S., Mills, J. C., Leip, D. G., Lovett, M., Clifton, S. W., Ippolito, J. E., Glasscock, J. I., Arumugam, M., Brent, M. R. et al. (2006). Molecular properties of adult mouse gastric and intestinal epithelial progenitors in their niches. *J Biol Chem* 281, 11292-300.

Goel, A. (2015). MicroRNAs as Therapeutic Targets in Colitis and Colitis-Associated Cancer: Tiny Players With a Giant Impact. *Gastroenterology* 149, 859-61.

Goetz, J. G., Minguet, S., Navarro-Lérida, I., Lazcano, J. J., Samaniego, R., Calvo, E., Tello, M., Osteso-Ibáñez, T., Pellinen, T., Echarri, A. et al. (2011). Biomechanical remodeling of the microenvironment by stromal caveolin-1 favors tumor invasion and metastasis. *Cell* 146, 148-63.

Grady, W. M. and Pritchard, C. C. (2014). Molecular alterations and biomarkers in colorectal cancer. *Toxicol Pathol* 42, 124-39.

Grimm, C., Chavez, L., Vilardell, M., Farrall, A. L., Tierling, S., Böhm, J. W., Grote, P., Lienhard, M., Dietrich, J., Timmermann, B. et al. (2013). DNA-methylome analysis of mouse intestinal adenoma identifies a tumour-specific signature that is partly conserved in human colon cancer. *PLoS Genet* 9, e1003250.

Gritsenko, P. G., Ilina, O. and Friedl, P. (2012). Interstitial guidance of cancer invasion. *J Pathol* 226, 185-99.

Gwack, Y., Sharma, S., Nardone, J., Tanasa, B., Iuga, A., Srikanth, S., Okamura, H., Bolton, D., Feske, S., Hogan, P. G. et al. (2006). A genome-wide Drosophila RNAi screen identifies DYRK-family kinases as regulators of NFAT. *Nature* 441, 646-50.

Gómez-Casero, E., San-Antonio, B., Iñiguez, M. A. and Fresno, M. (2007). Cot/Tpl2 and PKCzeta cooperate in the regulation of the transcriptional activity of NFATc2 through the phosphorylation of its amino-terminal domain. *Cell Signal* 19, 1652-61.

Haakensen, V. D., Bjøro, T., Lüders, T., Riis, M., Bukholm, I. K., Kristensen, V. N., Troester, M. A., Homen, M. M., Ursin, G., Børresen-Dale, A. L. et al. (2011). Serum estradiol levels associated with specific gene expression patterns in normal breast tissue and in breast carcinomas. *BMC Cancer* 11, 332.

Hammond, D. E., Mageean, C. J., Rusilowicz, E. V., Wickenden, J. A., Clague, M. J. and Prior, I. A. (2015). Differential Reprogramming of Isogenic Colorectal Cancer Cells by Distinct Activating KRAS Mutations. *J Proteome Res* 14, 1535-46.

Hanna, L. A., Foreman, R. K., Tarasenko, I. A., Kessler, D. S. and Labosky, P. A. (2002). Requirement for Foxd3 in maintaining pluripotent cells of the early mouse embryo. *Genes Dev* 16, 2650-61.

Hatahara, T., Igarashi, S. and Funaki, N. (1984). High concentrations of N-terminal peptide of type III procollagen in the sera of patients with various cancers, with special reference to liver cancer. *Gan* 75, 130-5.

Hippo, Y., Taniguchi, H., Tsutsumi, S., Machida, N., Chong, J. M., Fukayama, M., Kodama, T. and Aburatani, H. (2002). Global gene expression analysis of gastric cancer by oligonucleotide microarrays. *Cancer Res* 62, 233-40.

Hirsch, D., Barker, N., McNeil, N., Hu, Y., Camps, J., McKinnon, K., Clevers, H., Ried, T. and Gaiser, T. (2014). LGR5 positivity defines stem-like cells in colorectal cancer. *Carcinogenesis* 35, 849-58.

Hogan, P. G., Chen, L., Nardone, J. and Rao, A. (2003). Transcriptional regulation by calcium, calcineurin, and NFAT. *Genes Dev* 17, 2205-32.

Hoivik, E. A., Witsoe, S. L., Bergheim, I. R., Xu, Y., Jakobsson, I., Tengholm, A., Doskeland, S. O. and Bakke, M. (2013). DNA methylation of alternative promoters directs tissue specific expression of Epac2 isoforms. *PLoS One* 8, e67925.

Hong, Y., Downey, T., Eu, K. W., Koh, P. K. and Cheah, P. Y. (2010). A 'metastasis-prone' signature for early-stage mismatch-repair proficient sporadic colorectal cancer patients and its implications for possible therapeutics. *Clin Exp Metastasis* 27, 83-90.

Hu, K. and Chen, F. (2012). Identification of significant pathways in gastric cancer based on protein-protein interaction networks and cluster analysis. *Genet Mol Biol* 35, 701-8.

Humphries, A. and Wright, N. A. (2008). Colonic crypt organization and tumorigenesis. *Nat Rev Cancer* 8, 415-24.

Hur, K., Cejas, P., Feliu, J., Moreno-Rubio, J., Burgos, E., Boland, C. R. and Goel, A. (2014). Hypomethylation of long interspersed nuclear element-1 (LINE-1) leads to activation of proto-oncogenes in human colorectal cancer metastasis. *Gut* 63, 635-46.

Ikezono, Y. U., Koga, H., Abe, M., Akiba, J., Kawahara, A., Yoshida, T., Nakamura, T., Iwamoto, H., Yano, H., Kage, M. et al. (2015). High expression of the putative cancer stem cell marker, DCLK1, in rectal neuroendocrine tumors. *Oncol Lett* 10, 2015-2020.

Ishizawa, M., Kobayashi, Y., Miyamura, T. and Matsuura, S. (1991). Simple procedure of DNA isolation from human serum. *Nucleic Acids Res* 19, 5792.

Ito, H., Tanaka, S., Akiyama, Y., Shimada, S., Adikrisna, R., Matsumura, S., Aihara, A., Mitsunori, Y., Ban, D., Ochiai, T. et al. (2016). Dominant Expression of DCLK1 in Human Pancreatic Cancer Stem Cells Accelerates Tumor Invasion and Metastasis. *PLoS One* 11, e0146564.

Jain, J., Valge-Archer, V. E., Sinskey, A. J. and Rao, A. (1992). The AP-1 site at -150 bp, but not the NF-kappa B site, is likely to represent the major target of protein kinase C in the interleukin 2 promoter. *J Exp Med* 175, 853-62.

Jauliac, S., López-Rodriguez, C., Shaw, L. M., Brown, L. F., Rao, A. and Toker, A. (2002). The role of NFAT transcription factors in integrin-mediated carcinoma invasion. *Nat Cell Biol* 4, 540-4.

Jin, G., Ramanathan, V., Quante, M., Baik, G. H., Yang, X., Wang, S. S., Tu, S., Gordon, S. A., Pritchard, D. M., Varro, A. et al. (2009). Inactivating cholecystokinin-2 receptor inhibits progastrin-dependent colonic crypt fission, proliferation, and colorectal cancer in mice. *J Clin Invest* 119, 2691-701.

Kantara, C., O'Connell, M., Sarkar, S., Moya, S., Ullrich, R. and Singh, P. (2014). Curcumin Promotes Autophagic Survival of a Subset of Colon Cancer Stem Cells, Which Are Ablated by DCLK1-siRNA. *Cancer Res* 74, 2487-98.

Kantara, C., O'Connell, M. R., Luthra, G., Gajjar, A., Sarkar, S., Ullrich, R. L. and Singh, P. (2015). Methods for detecting circulating cancer stem cells (CCSCs) as a novel approach for diagnosis of colon cancer relapse/metastasis. *Lab Invest* 95, 100-12.

Katiyar, P. and Aplin, A. E. (2011). FOXD3 regulates migration properties and Rnd3 expression in melanoma cells. *Mol Cancer Res* 9, 545-52.

Kauppila, A., Puistola, U., Risteli, J. and Risteli, L. (1989). Amino-terminal propeptide of type III procollagen: a new prognosis indicator in human ovarian cancer. *Cancer Res* 49, 1885-9.

Kemper, K., Prasetyanti, P. R., De Lau, W., Rodermond, H., Clevers, H. and Medema, J. P. (2012). Monoclonal antibodies against Lgr5 identify human colorectal cancer stem cells. *Stem Cells* 30, 2378-86.

Kikuchi, M., Nagata, H., Watanabe, N., Watanabe, H., Tatemichi, M. and Hibi, T. (2010). Altered expression of a putative progenitor cell marker DCAMKL1 in the rat gastric mucosa in regeneration, metaplasia and dysplasia. *BMC Gastroenterol* 10, 65.

Kim, J. H. and Kang, G. H. (2014). Molecular and prognostic heterogeneity of microsatellite-unstable colorectal cancer. *World J Gastroenterol* 20, 4230-43.

Kim, M. H., Cierpicki, T., Derewenda, U., Krowarsch, D., Feng, Y., Devedjiev, Y., Dauter, Z., Walsh, C. A., Otlewski, J., Bushweller, J. H. et al. (2003a). The DCX-domain tandems of doublecortin and doublecortin-like kinase. *Nat Struct Biol* 10, 324-33.

Kim, M. H., Derewenda, U., Devedjiev, Y., Dauter, Z. and Derewenda, Z. S. (2003b). Purification and crystallization of the N-terminal domain from the human doublecortin-like kinase. *Acta Crystallogr D Biol Crystallogr* 59, 502-5.

Koizumi, H., Tanaka, T. and Gleeson, J. G. (2006). Doublecortin-like kinase functions with doublecortin to mediate fiber tract decussation and neuronal migration. *Neuron* 49, 55-66.

Kos, K. and Wilding, J. P. (2010). SPARC: a key player in the pathologies associated with obesity and diabetes. *Nat Rev Endocrinol* 6, 225-35.

Kos, R., Reedy, M. V., Johnson, R. L. and Erickson, C. A. (2001). The winged-helix transcription factor FoxD3 is important for establishing the neural crest lineage and repressing melanogenesis in avian embryos. *Development* 128, 1467-79.

Kozovska, Z., Gabrisova, V. and Kucerova, L. (2014). Colon cancer: cancer stem cells markers, drug resistance and treatment. *Biomed Pharmacother* 68, 911-6.

Kubic, J. D., Lui, J. W., Little, E. C., Ludvik, A. E., Konda, S., Salgia, R., Aplin, A. E. and Lang, D. (2015). PAX3 and FOXD3 Promote CXCR4 Expression in Melanoma. *J Biol Chem* 290, 21901-14.

Kuipers, E. J., Grady, W. M., Lieberman, D., Seufferlein, T., Sung, J. J., Boelens, P. G., van de Velde, C. J. H. and Watanabe, T. (2015). Colorectal cancer. *Nature Reviews Disease Primers*, 15065.

Kuivaniemi, H., Tromp, G. and Prockop, D. J. (1991). Mutations in collagen genes: causes of rare and some common diseases in humans. *FASEB J* 5, 2052-60.

Kupprion, C., Motamed, K. and Sage, E. H. (1998). SPARC (BM-40, osteonectin) inhibits the mitogenic effect of vascular endothelial growth factor on microvascular endothelial cells. *J Biol Chem* 273, 29635-40.

Kwatra, D., Subramaniam, D., Ramamoorthy, P., Standing, D., Moran, E., Velayutham, R., Mitra, A., Umar, S. and Anant, S. (2013). Methanolic extracts of bitter melon inhibit colon cancer stem cells by affecting energy homeostasis and autophagy. *Evid Based Complement Alternat Med* 2013, 702869.

Lane, T. F., Iruela-Arispe, M. L., Johnson, R. S. and Sage, E. H. (1994). SPARC is a source of copper-binding peptides that stimulate angiogenesis. *J Cell Biol* 125, 929-43.

Lane, T. F. and Sage, E. H. (1990). Functional mapping of SPARC: peptides from two distinct Ca+(+)-binding sites modulate cell shape. *J Cell Biol* 111, 3065-76.

Le Hellard, S., Håvik, B., Espeseth, T., Breilid, H., Løvlie, R., Luciano, M., Gow, A. J., Harris, S. E., Starr, J. M., Wibrand, K. et al. (2009). Variants in doublecortin- and calmodulin kinase like 1, a gene up-regulated by BDNF, are associated with memory and general cognitive abilities. *PLoS One* 4, e7534.

Levental, K. R., Yu, H., Kass, L., Lakins, J. N., Egeblad, M., Erler, J. T., Fong, S. F., Csiszar, K., Giaccia, A., Weninger, W. et al. (2009). Matrix crosslinking forces tumor progression by enhancing integrin signaling. *Cell* 139, 891-906.

Li, D., Mei, H., Qi, M., Yang, D., Zhao, X., Xiang, X., Pu, J., Huang, K., Zheng, L. and Tong, Q. (2013). FOXD3 is a novel tumor suppressor that affects growth, invasion, metastasis and angiogenesis of neuroblastoma. *Oncotarget* 4, 2021-44.

Li, L. and Bellows, C. F. (2013). Doublecortin-like kinase 1 exhibits cancer stem cell-like characteristics in a human colon cancer cell line. *Chin J Cancer Res* 25, 134-42.

Li, X. L., Zhou, J., Chen, Z. R. and Chng, W. J. (2015). P53 mutations in colorectal cancer - molecular pathogenesis and pharmacological reactivation. *World J Gastroenterol* 21, 84-93.

Lin, P. T., Gleeson, J. G., Corbo, J. C., Flanagan, L. and Walsh, C. A. (2000). DCAMKL1 encodes a protein kinase with homology to doublecortin that regulates microtubule polymerization. *J Neurosci* 20, 9152-61.

Liu, L. L., Lu, S. X., Li, M., Li, L. Z., Fu, J., Hu, W., Yang, Y. Z., Luo, R. Z., Zhang, C. Z. and Yun, J. P. (2014). FoxD3-regulated microRNA-137 suppresses tumour growth and metastasis in human hepatocellular carcinoma by targeting AKT2. *Oncotarget* 5, 5113-24.

Liu, Y. and Labosky, P. A. (2008). Regulation of embryonic stem cell self-renewal and pluripotency by Foxd3. *Stem Cells* 26, 2475-84.

Liu, Y. H., Tsang, J. Y., Ni, Y. B., Hlaing, T., Chan, S. K., Chan, K. F., Ko, C. W., Mujtaba, S. S. and Tse, G. M. (2015). Doublecortin-like kinase 1 expression associates with breast cancer with neuroendocrine differentiation. *Oncotarget*.

Lopez-Rodríguez, C., Aramburu, J., Rakeman, A. S. and Rao, A. (1999). NFAT5, a constitutively nuclear NFAT protein that does not cooperate with Fos and Jun. *Proc Natl Acad Sci U S A* 96, 7214-9.

Lu, P., Takai, K., Weaver, V. M. and Werb, Z. (2011). Extracellular matrix degradation and remodeling in development and disease. *Cold Spring Harb Perspect Biol* 3.

Luo, C., Shaw, K. T., Raghavan, A., Aramburu, J., Garcia-Cozar, F., Perrino, B. A., Hogan, P. G. and Rao, A. (1996). Interaction of calcineurin with a domain of the transcription factor NFAT1 that controls nuclear import. *Proc Natl Acad Sci U S A* 93, 8907-12.

Lussier, C., Sodek, J. and Beaulieu, J. F. (2001). Expression of SPARC/osteonectin/BM4O in the human gut: predominance in the stroma of the remodeling distal intestine. *J Cell Biochem* 81, 463-76.

Macian, F. (2005). NFAT proteins: key regulators of T-cell development and function. *Nat Rev Immunol* 5, 472-84.

Mancini, M. and Toker, A. (2009). NFAT proteins: emerging roles in cancer progression. *Nat Rev Cancer* 9, 810-20.

Marie Vedeld, H., Andresen, K., Andrassy Eilertsen, I., Nesbakken, A., Seruca, R., Gladhaug, I. P., Thiis-Evensen, E., Rognum, T. O., Muri Boberg, K. and Lind, G. E. (2014). The novel colorectal cancer biomarkers CDO1, ZSCAN18 and ZNF331 are frequently methylated across gastrointestinal cancers. *Int J Cancer*.

Mariotto, A. B., Yabroff, K. R., Shao, Y., Feuer, E. J. and Brown, M. L. (2011). Projections of the cost of cancer care in the United States: 2010-2020. *J Natl Cancer Inst* 103, 117-28.

Marques, A. M., Turner, A. and de Mello, R. A. (2014). Personalizing medicine for metastatic colorectal cancer: current developments. *World J Gastroenterol* 20, 10425-31.

Masuo, T., Okamura, S., Zhang, Y. and Mori, M. (2009). Cyclosporine A inhibits colorectal cancer proliferation probably by regulating expression levels of c-Myc, p21(WAF1/CIP1) and proliferating cell nuclear antigen. *Cancer Lett* 285, 66-72.

Matsumoto, N., Pilz, D. T. and Ledbetter, D. H. (1999). Genomic structure, chromosomal mapping, and expression pattern of human DCAMKL1 (KIAA0369), a homologue of DCX (XLIS). *Genomics* 56, 179-83.

May, R., Qu, D., Weygant, N., Chandrakesan, P., Ali, N., Lightfoot, S. A., Li, L., Sureban, S. M. and Houchen, C. W. (2014). Brief report: Dclk1 deletion in tuft cells results in impaired epithelial repair after radiation injury. *Stem Cells* 32, 822-7.

May, R., Riehl, T. E., Hunt, C., Sureban, S. M., Anant, S. and Houchen, C. W. (2008). Identification of a novel putative gastrointestinal stem cell and adenoma stem cell marker, doublecortin and CaM kinase-like-1, following radiation injury and in adenomatous polyposis coli/multiple intestinal neoplasia mice. *Stem Cells* 26, 630-7.

May, R., Sureban, S. M., Hoang, N., Riehl, T. E., Lightfoot, S. A., Ramanujam, R., Wyche, J. H., Anant, S. and Houchen, C. W. (2009). Doublecortin and CaM kinase-like-1 and leucine-

rich-repeat-containing G-protein-coupled receptor mark quiescent and cycling intestinal stem cells, respectively. *Stem Cells* 27, 2571-9.

May, R., Sureban, S. M., Lightfoot, S. A., Hoskins, A. B., Brackett, D. J., Postier, R. G., Ramanujam, R., Rao, C. V., Wyche, J. H., Anant, S. et al. (2010). Identification of a novel putative pancreatic stem/progenitor cell marker DCAMKL-1 in normal mouse pancreas. *Am J Physiol Gastrointest Liver Physiol* 299, G303-10.

Mayer, U., Aumailley, M., Mann, K., Timpl, R. and Engel, J. (1991). Calcium-dependent binding of basement membrane protein BM-40 (osteonectin, SPARC) to basement membrane collagen type IV. *Eur J Biochem* 198, 141-50.

Milla, P. J. (2009). Advances in understanding colonic function. *J Pediatr Gastroenterol Nutr* 48 Suppl 2, S43-5.

Miyakawa, H., Woo, S. K., Dahl, S. C., Handler, J. S. and Kwon, H. M. (1999). Tonicity-responsive enhancer binding protein, a rel-like protein that stimulates transcription in response to hypertonicity. *Proc Natl Acad Sci U S A* 96, 2538-42.

Mizuguchi, M., Qin, J., Yamada, M., Ikeda, K. and Takashima, S. (1999). High expression of doublecortin and KIAA0369 protein in fetal brain suggests their specific role in neuronal migration. *Am J Pathol* 155, 1713-21.

Mohammed, A., Janakiram, N. B., Madka, V., Brewer, M., Ritchie, R. L., Lightfoot, S., Kumar, G., Sadeghi, M., Patlolla, J. M., Yamada, H. Y. et al. (2015). Targeting pancreatitis blocks tumor-initiating stem cells and pancreatic cancer progression. *Oncotarget* 6, 15524-39.

Mundade, R., Imperiale, T. F., Prabhu, L., Loehrer, P. J. and Lu, T. (2014). Genetic pathways, prevention, and treatment of sporadic colorectal cancer. *Oncoscience* 1, 400-6.

Myatt, S. S. and Lam, E. W. (2007). The emerging roles of forkhead box (Fox) proteins in cancer. *Nat Rev Cancer* 7, 847-59.

Müller, M. R. and Rao, A. (2010). NFAT, immunity and cancer: a transcription factor comes of age. *Nat Rev Immunol* 10, 645-56.

Nagaraju, G. P., Dontula, R., El-Rayes, B. F. and Lakka, S. S. (2014). Molecular mechanisms underlying the divergent roles of SPARC in human carcinogenesis. *Carcinogenesis* 35, 967-73.

Nakanishi, Y., Seno, H., Fukuoka, A., Ueo, T., Yamaga, Y., Maruno, T., Nakanishi, N., Kanda, K., Komekado, H., Kawada, M. et al. (2013). Dclk1 distinguishes between tumor and normal stem cells in the intestine. *Nat Genet* 45, 98-103.

Nazemalhosseini Mojarad, E., Kuppen, P. J., Aghdaei, H. A. and Zali, M. R. (2013). The CpG island methylator phenotype (CIMP) in colorectal cancer. *Gastroenterol Hepatol Bed Bench* 6, 120-8.

Neradugomma, N. K., Subramaniam, D., Tawfik, O. W., Goffin, V., Kumar, T. R., Jensen, R. A. and Anant, S. (2014). Prolactin signaling enhances colon cancer stemness by modulating Notch signaling in a Jak2-STAT3/ERK manner. *Carcinogenesis* 35, 795-806.

Ning, X., Shu, J., Du, Y., Ben, Q. and Li, Z. (2013). Therapeutic strategies targeting cancer stem cells. *Cancer Biol Ther* 14, 295-303.

Nolan, G. P. (1994). NF-AT-AP-1 and Rel-bZIP: hybrid vigor and binding under the influence. *Cell* 77, 795-8.

Nomura, A., Banerjee, S., Chugh, R., Dudeja, V., Yamamoto, M., Vickers, S. M. and Saluja, A. K. (2015). CD133 initiates tumors, induces epithelial-mesenchymal transition and increases metastasis in pancreatic cancer. *Oncotarget*.

O'Connell, M., Sarkar, S., Luthra, G., Okugawa, Y., Toiyama, Y., Goel, A. and Singh, P. (2016a). FOXD3 is a novel repressor of the expression of short isoform of DCLK1 (DCLK1-S) from IntronV(β)-promoter of hDCLK1-gene, and is epigenetically silenced in hCRCs: Prognostic/Diagnostic implications of FOXD3/DCLK1-S expression in hCRCs.

O'Connell, M., Sarkar, S., Luthra, G., Okugawa, Y., Toiyama, Y., Ward, D., Goel, A. and Singh, P. (2016b). FOXD3 is a Novel Negative Regulator of IntronV(β)-Promoter Within hDCLK1-Gene in Normal Colonic Cells, But Gets Epigenetically Silenced in hCRCs, Resulting in the Expression of a Short Isoform of DCLK1 (DCLK1-S): Prognostic/Diagnostic Implications of FOXD3/DCLK1-S Expression in hCRCs. Proceedings of Digestive Disease Week.

O'Connell, M., Sarkar, S., Luthra, G., Spratt, H., Widen, S., Wood, T. and Singh, P. (2016c). DCLK1-S enhances the invasive potential of colon cancer cells via a novel NFATC2 mediated pathway, resulting in enhanced expression of extracellular matrix protein, COL3A1.

O'Connell, M., Sarkar, S., Ward, D. and Singh, P. (2016d). Short (S) Isoform of Cancer-Stem-Cell Marker, DCLK1, Is Critically Required for Maintaining Proliferative/Tumorigenic/Potenial of Human Colon Cancer Cells (hCCCs) Independent of DCLK1-L Isoform. .

Okamura, H., Aramburu, J., García-Rodríguez, C., Viola, J. P., Raghavan, A., Tahiliani, M., Zhang, X., Qin, J., Hogan, P. G. and Rao, A. (2000). Concerted dephosphorylation of the transcription factor NFAT1 induces a conformational switch that regulates transcriptional activity. *Mol Cell* 6, 539-50.

Okamura, H., Garcia-Rodriguez, C., Martinson, H., Qin, J., Virshup, D. M. and Rao, A. (2004). A conserved docking motif for CK1 binding controls the nuclear localization of NFAT1. *Mol Cell Biol* 24, 4184-95.

Okugawa, Y., Grady, W. M. and Goel, A. (2015). Epigenetic Alterations in Colorectal Cancer: Emerging Biomarkers. *Gastroenterology* 149, 1204-1225.e12.

Oliveras-Ferraros, C., Vazquez-Martin, A., Cuyàs, E., Corominas-Faja, B., Rodríguez-Gallego, E., Fernández-Arroyo, S., Martin-Castillo, B., Joven, J. and Menendez, J. A. (2014). Acquired resistance to metformin in breast cancer cells triggers transcriptome reprogramming toward a degradome-related metastatic stem-like profile. *Cell Cycle* 13, 1132-44.

Omori, Y., Suzuki, M., Ozaki, K., Harada, Y., Nakamura, Y., Takahashi, E. and Fujiwara, T. (1998). Expression and chromosomal localization of KIAA0369, a putative kinase structurally related to Doublecortin. *J Hum Genet* 43, 169-77.

Ong, B. A., Vega, K. J. and Houchen, C. W. (2014). Intestinal stem cells and the colorectal cancer microenvironment. *World J Gastroenterol* 20, 1898-909.

Ortega-Pérez, I., Cano, E., Were, F., Villar, M., Vázquez, J. and Redondo, J. M. (2005). c-Jun N-terminal kinase (JNK) positively regulates NFATc2 transactivation through phosphorylation within the N-terminal regulatory domain. *J Biol Chem* 280, 20867-78.

Oue, N., Hamai, Y., Mitani, Y., Matsumura, S., Oshimo, Y., Aung, P. P., Kuraoka, K., Nakayama, H. and Yasui, W. (2004). Gene expression profile of gastric carcinoma: identification of genes and tags potentially involved in invasion, metastasis, and carcinogenesis by serial analysis of gene expression. *Cancer Res* 64, 2397-405.

O'Connell, M. R., Sarkar, S., Luthra, G. K., Okugawa, Y., Toiyama, Y., Gajjar, A. H., Qiu, S., Goel, A. and Singh, P. (2015). Epigenetic changes and alternate promoter usage by human colon cancers for expressing DCLK1-isoforms: Clinical Implications. *Scientific Reports* 5, 14983.

Pal, S., Gupta, R., Kim, H., Wickramasinghe, P., Baubet, V., Showe, L. C., Dahmane, N. and Davuluri, R. V. (2011). Alternative transcription exceeds alternative splicing in generating the transcriptome diversity of cerebellar development. *Genome Res* 21, 1260-72.

Pan, G., Li, J., Zhou, Y., Zheng, H. and Pei, D. (2006). A negative feedback loop of transcription factors that controls stem cell pluripotency and self-renewal. *FASEB J* 20, 1730-2.

Pan, M. G., Xiong, Y. and Chen, F. (2013). NFAT gene family in inflammation and cancer. *Curr Mol Med* 13, 543-54.

Park, Y. S., Huh, J. W., Lee, J. H. and Kim, H. R. (2012). shRNA against CD44 inhibits cell proliferation, invasion and migration, and promotes apoptosis of colon carcinoma cells. *Oncol Rep* 27, 339-46.

Peterson, L. W. and Artis, D. (2014). Intestinal epithelial cells: regulators of barrier function and immune homeostasis. *Nat Rev Immunol* 14, 141-53.

Pino, M. S. and Chung, D. C. (2010). The chromosomal instability pathway in colon cancer. *Gastroenterology* 138, 2059-72.

Ponnurangam, S., Dandawate, P. R., Dhar, A., Tawfik, O. W., Parab, R. R., Mishra, P. D., Ranadive, P., Sharma, R., Mahajan, G., Umar, S. et al. (2015). Quinomycin A targets Notch signaling pathway in pancreatic cancer stem cells. *Oncotarget*.

Ponnurangam, S., Mammen, J. M., Ramalingam, S., He, Z., Zhang, Y., Umar, S., Subramaniam, D. and Anant, S. (2012). Honokiol in combination with radiation targets notch signaling to inhibit colon cancer stem cells. *Mol Cancer Ther* 11, 963-72.

Porter, P. L., Sage, E. H., Lane, T. F., Funk, S. E. and Gown, A. M. (1995). Distribution of SPARC in normal and neoplastic human tissue. *J Histochem Cytochem* 43, 791-800.

Pottgiesser, J., Maurer, P., Mayer, U., Nischt, R., Mann, K., Timpl, R., Krieg, T. and Engel, J. (1994). Changes in calcium and collagen IV binding caused by mutations in the EF hand

and other domains of extracellular matrix protein BM-40 (SPARC, osteonectin). *J Mol Biol* 238, 563-74.

Powrózek, T., Krawczyk, P., Nicoś, M., Kuźnar-Kamińska, B., Batura-Gabryel, H. and Milanowski, J. (2015). Methylation of the DCLK1 promoter region in circulating free DNA and its prognostic value in lung cancer patients. *Clin Transl Oncol*.

Qin, J. J., Nag, S., Wang, W., Zhou, J., Zhang, W. D., Wang, H. and Zhang, R. (2014). NFAT as cancer target: mission possible? *Biochim Biophys Acta* 1846, 297-311.

Qu, D., Johnson, J., Chandrakesan, P., Weygant, N., May, R., Aiello, N., Rhim, A., Zhao, L., Zheng, W., Lightfoot, S. et al. (2015). Doublecortin-like kinase 1 is elevated serologically in pancreatic ductal adenocarcinoma and widely expressed on circulating tumor cells. *PLoS One* 10, e0118933.

Rahman, M., Chan, A. P., Tang, M. and Tai, I. T. (2011). A peptide of SPARC interferes with the interaction between caspase8 and Bcl2 to resensitize chemoresistant tumors and enhance their regression in vivo. *PLoS One* 6, e26390.

Rao, C. V., Janakiram, N. B., Madka, V., Devarkonda, V., Brewer, M., Biddick, L., Lightfoot, S., Steele, V. E. and Mohammed, A. (2015). Simultaneous targeting of 5-LOX-COX and EGFR blocks progression of pancreatic ductal adenocarcinoma. *Oncotarget* 6, 33290-305.

Rengifo-Cam, W., Umar, S., Sarkar, S. and Singh, P. (2007). Antiapoptotic effects of progastrin on pancreatic cancer cells are mediated by sustained activation of nuclear factor-{kappa}B. *Cancer Res* 67, 7266-74.

Sabatino, S. A., White, M. C., Thompson, T. D., Klabunde, C. N. and (CDC), C. f. D. C. a. P. (2015). Cancer screening test use - United States, 2013. *MMWR Morb Mortal Wkly Rep* 64, 464-8.

Sage, E. H. and Vernon, R. B. (1994). Regulation of angiogenesis by extracellular matrix: the growth and the glue. *J Hypertens Suppl* 12, S145-52.

Sage, H., Vernon, R. B., Funk, S. E., Everitt, E. A. and Angello, J. (1989). SPARC, a secreted protein associated with cellular proliferation, inhibits cell spreading in vitro and exhibits Ca+2-dependent binding to the extracellular matrix. *J Cell Biol* 109, 341-56.

Said, N. and Theodorescu, D. (2013). Secreted Protein Acidic and Rich in Cysteine (Sparc) in Cancer. *Journal of Carcinogenesis & Mutagenesis* 4, 151.

Sancho, R., Cremona, C. A. and Behrens, A. (2015). Stem cell and progenitor fate in the mammalian intestine: Notch and lateral inhibition in homeostasis and disease. *EMBO Rep* 16, 571-81.

Sarkar, S., Kantara, C., Ortiz, I., Swiercz, R., Kuo, J., Davey, R., Escobar, K., Ullrich, R. and Singh, P. (2012). Progastrin overexpression imparts tumorigenic/metastatic potential to embryonic epithelial cells: phenotypic differences between transformed and nontransformed stem cells. *Int J Cancer* 131, E1088-99.

Sarkar, S., Swiercz, R., Kantara, C., Hajjar, K. A. and Singh, P. (2011). Annexin A2 mediates up-regulation of NF-κB, β-catenin, and stem cell in response to progastrin in mice and HEK-293 cells. *Gastroenterology* 140, 583-595.e4.

Sasaki, T., Göhring, W., Mann, K., Maurer, P., Hohenester, E., Knäuper, V., Murphy, G. and Timpl, R. (1997). Limited cleavage of extracellular matrix protein BM-40 by matrix metalloproteinases increases its affinity for collagens. *J Biol Chem* 272, 9237-43.

Sasaki, T., Hohenester, E., Göhring, W. and Timpl, R. (1998). Crystal structure and mapping by site-directed mutagenesis of the collagen-binding epitope of an activated form of BM-40/SPARC/osteonectin. *EMBO J* 17, 1625-34.

Schenk, G. J., Veldhuisen, B., Wedemeier, O., McGown, C. C., Schouten, T. G., Oitzl, M., de Kloet, E. R. and Vreugdenhil, E. (2010). Over-expression of δC-DCLK-short in mouse brain results in a more anxious behavioral phenotype. *Physiol Behav* 101, 541-8.

Schepers, A. G., Snippert, H. J., Stange, D. E., van den Born, M., van Es, J. H., van de Wetering, M. and Clevers, H. (2012). Lineage tracing reveals Lgr5+ stem cell activity in mouse intestinal adenomas. *Science* 337, 730-5.

Schwitalla, S., Fingerle, A. A., Cammareri, P., Nebelsiek, T., Göktuna, S. I., Ziegler, P. K., Canli, O., Heijmans, J., Huels, D. J., Moreaux, G. et al. (2013). Intestinal tumorigenesis initiated by dedifferentiation and acquisition of stem-cell-like properties. *Cell* 152, 25-38.

Shang, L., Kwon, Y. G., Nandy, S., Lawrence, D. S. and Edelman, A. M. (2003). Catalytic and regulatory domains of doublecortin kinase-1. *Biochemistry* 42, 2185-94.

Shin, E., Kashiwagi, Y., Kuriu, T., Iwasaki, H., Tanaka, T., Koizumi, H., Gleeson, J. G. and Okabe, S. (2013). Doublecortin-like kinase enhances dendritic remodelling and negatively regulates synapse maturation. *Nat Commun* 4, 1440.

Shou, J., Jing, J., Xie, J., You, L., Jing, Z., Yao, J., Han, W. and Pan, H. (2015). Nuclear factor of activated T cells in cancer development and treatment. *Cancer Lett* 361, 174-84.

Shu, T., Tseng, H. C., Sapir, T., Stern, P., Zhou, Y., Sanada, K., Fischer, A., Coquelle, F. M., Reiner, O. and Tsai, L. H. (2006). Doublecortin-like kinase controls neurogenesis by regulating mitotic spindles and M phase progression. *Neuron* 49, 25-39.

Siddheshwar, R. K., Gray, J. C. and Kelly, S. B. (2001). Plasma levels of progastrin but not amidated gastrin or glycine extended gastrin are elevated in patients with colorectal carcinoma. *Gut* 48, 47-52.

Siegel, R., Desantis, C. and Jemal, A. (2014a). Colorectal cancer statistics, 2014. *CA Cancer J Clin* 64, 104-17.

Siegel, R., DeSantis, C., Virgo, K., Stein, K., Mariotto, A., Smith, T., Cooper, D., Gansler, T., Lerro, C., Fedewa, S. et al. (2012). Cancer treatment and survivorship statistics, 2012. *CA Cancer J Clin* 62, 220-41.

Siegel, R., Ma, J., Zou, Z. and Jemal, A. (2014b). Cancer statistics, 2014. *CA Cancer J Clin* 64, 9-29.

Silverman, M. A., Benard, O., Jaaro, H., Rattner, A., Citri, Y. and Seger, R. (1999). CPG16, a novel protein serine/threonine kinase downstream of cAMP-dependent protein kinase. *J Biol Chem* 274, 2631-6.

Singh, P., Owlia, A., Varro, A., Dai, B., Rajaraman, S. and Wood, T. (1996). Gastrin gene expression is required for the proliferation and tumorigenicity of human colon cancer cells. *Cancer Res* 56, 4111-5.

Singh, P., Sarkar, S., Kantara, C. and Maxwell, C. (2012). Progastrin Peptides Increase the Risk of Developing Colonic Tumors: Impact on Colonic Stem Cells. *Curr Colorectal Cancer Rep* 8, 277-289.

Singh, P., Sarkar, S., Umar, S., Rengifo-Cam, W., Singh, A. P. and Wood, T. G. (2010). Insulin-like growth factors are more effective than progastrin in reversing proapoptotic effects of curcumin: critical role of p38MAPK. *Am J Physiol Gastrointest Liver Physiol* 298, G551-62.

Singh, P., Velasco, M., Given, R., Varro, A. and Wang, T. C. (2000a). Progastrin expression predisposes mice to colon carcinomas and adenomas in response to a chemical carcinogen. *Gastroenterology* 119, 162-71.

Singh, P., Velasco, M., Given, R., Wargovich, M., Varro, A. and Wang, T. C. (2000b). Mice overexpressing progastrin are predisposed for developing aberrant colonic crypt foci in response to AOM. *Am J Physiol Gastrointest Liver Physiol* 278, G390-9.

Singh, P., Wu, H., Clark, C. and Owlia, A. (2007). Annexin II binds progastrin and gastrin-like peptides, and mediates growth factor effects of autocrine and exogenous gastrins on colon cancer and intestinal epithelial cells. *Oncogene* 26, 425-40.

Singh, S. K., Baumgart, S., Singh, G., König, A. O., Reutlinger, K., Hofbauer, L. C., Barth, P., Gress, T. M., Lomberk, G., Urrutia, R. et al. (2011). Disruption of a nuclear NFATc2

protein stabilization loop confers breast and pancreatic cancer growth suppression by zoledronic acid. *J Biol Chem* 286, 28761-71.

Sipos, F. and Galamb, O. (2012). Epithelial-to-mesenchymal and mesenchymal-to-epithelial transitions in the colon. *World J Gastroenterol* 18, 601-8.

Sossey-Alaoui, K. and Srivastava, A. K. (1999). DCAMKL1, a brain-specific transmembrane protein on 13q12.3 that is similar to doublecortin (DCX). *Genomics* 56, 121-6.

Souza, R. F., Krishnan, K. and Spechler, S. J. (2008). Acid, bile, and CDX: the ABCs of making Barrett's metaplasia. *Am J Physiol Gastrointest Liver Physiol* 295, G211-8.

Su, B., Zhao, W., Shi, B., Zhang, Z., Yu, X., Xie, F., Guo, Z., Zhang, X., Liu, J., Shen, Q. et al. (2014). Let-7d suppresses growth, metastasis, and tumor macrophage infiltration in renal cell carcinoma by targeting COL3A1 and CCL7. *Mol Cancer* 13, 206.

Sureban, S. M., Madhoun, M. F., May, R., Qu, D., Ali, N., Fazili, J., Weygant, N., Chandrakesan, P., Ding, K., Lightfoot, S. A. et al. (2015). Plasma DCLK1 is a marker of hepatocellular carcinoma (HCC): Targeting DCLK1 prevents HCC tumor xenograft growth via a microRNA-dependent mechanism. *Oncotarget* 6, 37200-15.

Sureban, S. M., May, R., Lightfoot, S. A., Hoskins, A. B., Lerner, M., Brackett, D. J., Postier, R. G., Ramanujam, R., Mohammed, A., Rao, C. V. et al. (2011a). DCAMKL-1 regulates

epithelial-mesenchymal transition in human pancreatic cells through a miR-200a-dependent mechanism. *Cancer Res* 71, 2328-38.

Sureban, S. M., May, R., Mondalek, F. G., Qu, D., Ponnurangam, S., Pantazis, P., Anant, S., Ramanujam, R. P. and Houchen, C. W. (2011b). Nanoparticle-based delivery of siDCAMKL-1 increases microRNA-144 and inhibits colorectal cancer tumor growth via a Notch-1 dependent mechanism. *J Nanobiotechnology* 9, 40.

Sureban, S. M., May, R., Qu, D., Weygant, N., Chandrakesan, P., Ali, N., Lightfoot, S. A., Pantazis, P., Rao, C. V., Postier, R. G. et al. (2013). DCLK1 regulates pluripotency and angiogenic factors via microRNA-dependent mechanisms in pancreatic cancer. *PLoS One* 8, e73940.

Sureban, S. M., May, R., Ramalingam, S., Subramaniam, D., Natarajan, G., Anant, S. and Houchen, C. W. (2009). Selective blockade of DCAMKL-1 results in tumor growth arrest by a Let-7a MicroRNA-dependent mechanism. *Gastroenterology* 137, 649-59, 659.e1-2.

Sureban, S. M., May, R., Weygant, N., Qu, D., Chandrakesan, P., Bannerman-Menson, E., Ali, N., Pantazis, P., Westphalen, C. B., Wang, T. C. et al. (2014). XMD8-92 inhibits pancreatic tumor xenograft growth via a DCLK1-dependent mechanism. *Cancer Lett* 351, 151-61.

Sutton, J., Costa, R., Klug, M., Field, L., Xu, D., Largaespada, D. A., Fletcher, C. F., Jenkins, N. A., Copeland, N. G., Klemsz, M. et al. (1996). Genesis, a winged helix transcriptional repressor with expression restricted to embryonic stem cells. *J Biol Chem* 271, 23126-33.

Szuhai, K., Ijszenga, M., de Jong, D., Karseladze, A., Tanke, H. J. and Hogendoorn, P. C. (2009). The NFATc2 gene is involved in a novel cloned translocation in a Ewing sarcoma variant that couples its function in immunology to oncology. *Clin Cancer Res* 15, 2259-68.

Tai, I. T., Dai, M., Owen, D. A. and Chen, L. B. (2005). Genome-wide expression analysis of therapy-resistant tumors reveals SPARC as a novel target for cancer therapy. *J Clin Invest* 115, 1492-502.

Tai, I. T. and Tang, M. J. (2008). SPARC in cancer biology: its role in cancer progression and potential for therapy. *Drug Resist Updat* 11, 231-46.

Teng, L., Mundell, N. A., Frist, A. Y., Wang, Q. and Labosky, P. A. (2008). Requirement for Foxd3 in the maintenance of neural crest progenitors. *Development* 135, 1615-24.

Tie, X., Han, S., Meng, L., Wang, Y. and Wu, A. (2013). NFAT1 is highly expressed in, and regulates the invasion of, glioblastoma multiforme cells. *PLoS One* 8, e66008.

Tompers, D. M., Foreman, R. K., Wang, Q., Kumanova, M. and Labosky, P. A. (2005). Foxd3 is required in the trophoblast progenitor cell lineage of the mouse embryo. *Dev Biol* 285, 126-37.

Trama, J., Go, W. Y. and Ho, S. N. (2002). The osmoprotective function of the NFAT5 transcription factor in T cell development and activation. *J Immunol* 169, 5477-88.

Tripathi, M. K., Deane, N. G., Zhu, J., An, H., Mima, S., Wang, X., Padmanabhan, S., Shi, Z., Prodduturi, N., Ciombor, K. K. et al. (2014). Nuclear factor of activated T-cell activity is associated with metastatic capacity in colon cancer. *Cancer Res* 74, 6947-57.

Turashvili, G., Bouchal, J., Baumforth, K., Wei, W., Dziechciarkova, M., Ehrmann, J., Klein, J., Fridman, E., Skarda, J., Srovnal, J. et al. (2007). Novel markers for differentiation of lobular and ductal invasive breast carcinomas by laser microdissection and microarray analysis. *BMC Cancer* 7, 55.

Tuy, F. P., Saillour, Y., Kappeler, C., Chelly, J. and Francis, F. (2008). Alternative transcripts of Dclk1 and Dclk2 and their expression in doublecortin knockout mice. *Dev Neurosci* 30, 171-86.

Umar, S., Sarkar, S., Cowey, S. and Singh, P. (2008). Activation of NF-kappaB is required for mediating proliferative and antiapoptotic effects of progastrin on proximal colonic crypts of mice, in vivo. *Oncogene* 27, 5599-611.

Umar, S., Sarkar, S., Wang, Y. and Singh, P. (2009). Functional cross-talk between beta-catenin and NFkappaB signaling pathways in colonic crypts of mice in response to progastrin. *J Biol Chem* 284, 22274-84.

van Geel, R. M., Beijnen, J. H., Bernards, R. and Schellens, J. H. (2015). Treatment Individualization in Colorectal Cancer. *Curr Colorectal Cancer Rep* 11, 335-344.

van Roon, E. H., Boot, A., Dihal, A. A., Ernst, R. F., van Wezel, T., Morreau, H. and Boer, J. M. (2013). BRAF mutation-specific promoter methylation of FOX genes in colorectal cancer. *Clin Epigenetics* 5, 2.

Vasen, H. F., Tomlinson, I. and Castells, A. (2015). Clinical management of hereditary colorectal cancer syndromes. *Nat Rev Gastroenterol Hepatol* 12, 88-97.

Vedeld, H. M., Skotheim, R. I., Lothe, R. A. and Lind, G. E. (2014). The recently suggested intestinal cancer stem cell marker DCLK1 is an epigenetic biomarker for colorectal cancer. *Epigenetics* 9, 346-50.

Vega, K. J., May, R., Sureban, S. M., Lightfoot, S. A., Qu, D., Reed, A., Weygant, N., Ramanujam, R., Souza, R., Madhoun, M. et al. (2012). Identification of the putative intestinal stem cell marker doublecortin and CaM kinase-like-1 in Barrett's esophagus and esophageal adenocarcinoma. *J Gastroenterol Hepatol* 27, 773-80.

Verissimo, C. S., Cheng, S., Puigvert, J. C., Qin, Y., Vroon, A., van Deutekom, J., Price, L. S., Danen, E. H., van de Water, B., Fitzsimons, C. P. et al. (2012). Combining doublecortin-like kinase silencing and vinca alkaloids results in a synergistic apoptotic effect in neuroblastoma cells. *J Pharmacol Exp Ther* 342, 119-30.

Verissimo, C. S., Elands, R., Cheng, S., Saaltink, D. J., ter Horst, J. P., Alme, M. N., Pont, C., van de Water, B., Håvik, B., Fitzsimons, C. P. et al. (2013). Silencing of doublecortin-like (DCL) results in decreased mitochondrial activity and delayed neuroblastoma tumor growth. *PLoS One* 8, e75752.

Verissimo, C. S., Molenaar, J. J., Fitzsimons, C. P. and Vreugdenhil, E. (2011). Neuroblastoma therapy: what is in the pipeline? *Endocr Relat Cancer* 18, R213-31.

Verissimo, C. S., Molenaar, J. J., Meerman, J., Puigvert, J. C., Lamers, F., Koster, J., Danen, E. H., van de Water, B., Versteeg, R., Fitzsimons, C. P. et al. (2010). Silencing of the microtubule-associated proteins doublecortin-like and doublecortin-like kinase-long induces apoptosis in neuroblastoma cells. *Endocr Relat Cancer* 17, 399-414.

Vigneri, P. G., Tirrò, E., Pennisi, M. S., Massimino, M., Stella, S., Romano, C. and Manzella, L. (2015). The Insulin/IGF System in Colorectal Cancer Development and Resistance to Therapy. *Front Oncol* 5, 230.

Vreugdenhil, E., Datson, N., Engels, B., de Jong, J., van Koningsbruggen, S., Schaaf, M. and de Kloet, E. R. (1999). Kainate-elicited seizures induce mRNA encoding a CaMK-related peptide: a putative modulator of kinase activity in rat hippocampus. *J Neurobiol* 39, 41-50.

Vreugdenhil, E., Kolk, S. M., Boekhoorn, K., Fitzsimons, C. P., Schaaf, M., Schouten, T., Sarabdjitsingh, A., Sibug, R. and Lucassen, P. J. (2007). Doublecortin-like, a microtubule-associated protein expressed in radial glia, is crucial for neuronal precursor division and radial process stability. *Eur J Neurosci* 25, 635-48.

Vázquez-Cedeira, M. and Lazo, P. A. (2012). Human VRK2 (vaccinia-related kinase 2) modulates tumor cell invasion by hyperactivation of NFAT1 and expression of cyclooxygenase-2. *J Biol Chem* 287, 42739-50.

Wang, C., Huang, Y. and Dai, W. (2015a). Tumor suppression function of FoxD3 in lung cancer. *Ir J Med Sci*.

Wang, T., Shigdar, S., Gantier, M. P., Hou, Y., Wang, L., Li, Y., Al Shamaileh, H., Yin, W., Zhou, S. F., Zhao, X. et al. (2015b). Cancer stem cell targeted therapy: progress amid controversies. *Oncotarget*.

Weigel, D. and Jäckle, H. (1990). The fork head domain: a novel DNA binding motif of eukaryotic transcription factors? *Cell* 63, 455-6.

Weiss, M. B., Abel, E. V., Dadpey, N. and Aplin, A. E. (2014). FOXD3 modulates migration through direct transcriptional repression of TWIST1 in melanoma. *Mol Cancer Res* 12, 1314-23.

Weng, W., Feng, J., Qin, H., Ma, Y. and Goel, A. (2015). An update on miRNAs as biological and clinical determinants in colorectal cancer: a bench-to-bedside approach. *Future Oncol* 11, 1791-808.

Werneck, M. B., Vieira-de-Abreu, A., Chammas, R. and Viola, J. P. (2011). NFAT1 transcription factor is central in the regulation of tissue microenvironment for tumor metastasis. *Cancer Immunol Immunother* 60, 537-46.

Westphalen, C. B., Asfaha, S., Hayakawa, Y., Takemoto, Y., Lukin, D. J., Nuber, A. H., Brandtner, A., Setlik, W., Remotti, H., Muley, A. et al. (2014). Long-lived intestinal tuft cells serve as colon cancer-initiating cells. *J Clin Invest* 124, 1283-95.

Wewer, U. M., Albrechtsen, R., Fisher, L. W., Young, M. F. and Termine, J. D. (1988). Osteonectin/SPARC/BM-40 in human decidua and carcinoma, tissues characterized by de novo formation of basement membrane. *Am J Pathol* 132, 345-55.

Weygant, N., Qu, D., Berry, W. L., May, R., Chandrakesan, P., Owen, D. B., Sureban, S. M., Ali, N., Janknecht, R. and Houchen, C. W. (2014). Small molecule kinase inhibitor

LRRK2-IN-1 demonstrates potent activity against colorectal and pancreatic cancer through inhibition of doublecortin-like kinase 1. *Mol Cancer* 13, 103.

Weygant, N., Qu, D., May, R., Tierney, R. M., Berry, W. L., Zhao, L., Agarwal, S., Chandrakesan, P., Chinthalapally, H. R., Murphy, N. T. et al. (2015). DCLK1 is a broadly dysregulated target against epithelial-mesenchymal transition, focal adhesion, and stemness in clear cell renal carcinoma. *Oncotarget* 6, 2193-205.

White, B. D., Chien, A. J. and Dawson, D. W. (2012). Dysregulation of Wnt/β-catenin signaling in gastrointestinal cancers. *Gastroenterology* 142, 219-32.

Whorton, J., Sureban, S. M., May, R., Qu, D., Lightfoot, S. A., Madhoun, M., Johnson, M., Tierney, W. M., Maple, J. T., Vega, K. J. et al. (2015). DCLK1 is detectable in plasma of patients with Barrett's esophagus and esophageal adenocarcinoma. *Dig Dis Sci* 60, 509-13.

Wiese, A. H., Auer, J., Lassmann, S., Nährig, J., Rosenberg, R., Höfler, H., Rüger, R. and Werner, M. (2007). Identification of gene signatures for invasive colorectal tumor cells. *Cancer Detect Prev* 31, 282-95.

Wijchers, P. J., Burbach, J. P. and Smidt, M. P. (2006). In control of biology: of mice, men and Foxes. *Biochem J* 397, 233-46.

Wiklund, T. A., Elomaa, I., Blomqvist, C. P., Risteli, L. and Risteli, J. (1992). Type III collagen metabolism in soft tissue sarcomas. *Br J Cancer* 65, 193-6.

Wu, T. H., Chu, L. J., Wang, J. C., Chen, T. W., Tien, Y. J., Lin, W. C. and Ng, W. V. (2012a). Meta-analytical biomarker search of EST expression data reveals three differentially expressed candidates. *BMC Genomics* 13 Suppl 7, S12.

Wu, Y., Borde, M., Heissmeyer, V., Feuerer, M., Lapan, A. D., Stroud, J. C., Bates, D. L., Guo, L., Han, A., Ziegler, S. F. et al. (2006). FOXP3 controls regulatory T cell function through cooperation with NFAT. *Cell* 126, 375-87.

Wu, Y., Wang, X., Wu, F., Huang, R., Xue, F., Liang, G., Tao, M., Cai, P. and Huang, Y. (2012b). Transcriptome profiling of the cancer, adjacent non-tumor and distant normal tissues from a colorectal cancer patient by deep sequencing. *PLoS One* 7, e41001.

Xiong, G., Deng, L., Zhu, J., Rychahou, P. G. and Xu, R. (2014). Prolyl-4-hydroxylase α subunit 2 promotes breast cancer progression and metastasis by regulating collagen deposition. *BMC Cancer* 14, 1.

Yan, J. H., Zhao, C. L., Ding, L. B. and Zhou, X. (2015). FOXD3 suppresses tumor growth and angiogenesis in non-small cell lung cancer. *Biochem Biophys Res Commun* 466, 111-6.

Yang, E., Kang, H. J., Koh, K. H., Rhee, H., Kim, N. K. and Kim, H. (2007). Frequent inactivation of SPARC by promoter hypermethylation in colon cancers. *Int J Cancer* 121, 567-75.

Yiu, G. K. and Toker, A. (2006). NFAT induces breast cancer cell invasion by promoting the induction of cyclooxygenase-2. *J Biol Chem* 281, 12210-7.

Yoeli-Lerner, M., Chin, Y. R., Hansen, C. K. and Toker, A. (2009). Akt/protein kinase b and glycogen synthase kinase-3beta signaling pathway regulates cell migration through the NFAT1 transcription factor. *Mol Cancer Res* 7, 425-32.

Yoeli-Lerner, M., Yiu, G. K., Rabinovitz, I., Erhardt, P., Jauliac, S. and Toker, A. (2005). Akt blocks breast cancer cell motility and invasion through the transcription factor NFAT. *Mol Cell* 20, 539-50.

Yudoh, K., Matsui, H., Kanamori, M., Ohmori, K., Tsuji, H. and Tatezaki, S. (1994). Serum levels of laminin, type IV collagen and type III procollagen peptide as markers for detection of metastasis. *Jpn J Cancer Res* 85, 1263-9.

Zeuner, A., Todaro, M., Stassi, G. and De Maria, R. (2014). Colorectal cancer stem cells: from the crypt to the clinic. *Cell Stem Cell* 15, 692-705.

Zhang, X., Zhang, Z., Cheng, J., Li, M., Wang, W., Xu, W., Wang, H. and Zhang, R. (2012). Transcription factor NFAT1 activates the mdm2 oncogene independent of p53. *J Biol Chem* 287, 30468-76.

Zhao, H., Chen, D., Wang, J., Yin, Y., Gao, Q. and Zhang, Y. (2014). Downregulation of the transcription factor, FoxD3, is associated with lymph node metastases in invasive ductal carcinomas of the breast. *Int J Clin Exp Pathol* 7, 670-6.

Zoratto, F., Rossi, L., Verrico, M., Papa, A., Basso, E., Zullo, A., Tomao, L., Romiti, A., Lo Russo, G. and Tomao, S. (2014). Focus on genetic and epigenetic events of colorectal cancer pathogenesis: implications for molecular diagnosis. *Tumour Biol* 35, 6195-206.

# Vita

Malaney Ravae O'Connell was born in Rankin TX, on March 10th 1989 to Jo Nell and Luis Valdez Lopez. Malaney was raised in Crane TX and attended Elementary/Middle/High school there. In 2007, Malaney graduated from high school as her class valedictorian. In December of 2010, Malaney graduated Cum laude from McMurry University with a Bachelor's of Science in Biochemistry. She graduated from McMurry with both University Honor's and Biochemistry Honor's. Following graduation, Malaney worked as a Research Associate at Receptor Logic, Inc. In 2011, Malaney joined the Cell Biology program within the Graduate School of Biomedical Sciences at the University of Texas Medical Branch, Galveston. During her time at UTMB, Malaney has served a student representative on the Cell Biology Admissions Committee and the BBSC Core Curriculum Committee. Malaney was also Treasurer for the Society of Cell Biology. Malaney has had the opportunity to teach Chemical Carcinogenesis I & II in the Environmental Toxicology course at the Texas A&M University at Galveston. She has also had the opportunity to mentor a PREP student and 2 undergraduate volunteers. During the course of her studies, Malaney has won a total of 14 national and local awards for her Academic Excellence Achievements and her work in Cancer Biology. Malaney will be graduating from UTMB with 19 published abstracts, 17 poster/oral presentations, 10 publications, and contributed to 2 patent/invention disclosure applications. Following graduation, Malaney will join the faculty at McMurry University in Abilene TX. She will be initiating and maintaining a new Biotechnology degree program.

## PUBLICATIONS

**O'Connell M***, Sarkar S*, Luthra G, Okugawa Y, Toiyama Y, Goel A, Gajjar A, Qiu S, Sowers L, and Singh P. Use of alternate promoter in IntronV by human colon cancers for expressing DCLK1-Short: clinical implications. Nature Scientific Reports 2015;5:14983. *=Shared first authors.

Huynh P, Beswick E, Coronado Y, **O'Connell M**, Watts T, Singh P, Qiu S, Morris K, Powell D, Pinchuk I. CD90+ stromal cells are the major source of IL-6 which supports cancer stem cells and inflammation in CRC. Int J Cancer. 2015 Nov 23. doi: 10.1002/ijc.29939. [Epub ahead of print].

Kantara C, **O'Connell MR**, Luthra G, Gajjar A, Sarkar S, Ulrich RL, Singh P. Methods for detecting circulating cancer stem cells (CCSCs) as a novel approach for diagnosis of colon cancer relapse/metastasis. Lab Invest. 2015; 95(1):100-12.

Kantara C, **O'Connell M**, Sarkar S, Moya S, Ullrich R, Singh, P. Curcumin promotes autophagic survival of a sub-set of colon cancer stem cells, which are ablated by DCLK1-siRNA. Can Research. 2014 May 1; 74(9):2487-98.

Andey T, Marepally S, Patel A, Jackson T, Sarkar S, **O'Connell M**, Singh, P, Singh M. Cationic lipid guided short-hairpin RNA interference of AnnexinA2 attenuates tumor growth and metastasis in a mouse lung cancer stem cell model. J Control Release. 2014 Apr12; 184C:67-78.

**O'Connell M,** Sarkar S, Luthra G, Okugawa, Y, Toiyama Y, Ward D, Goel A, Singh P. FOXD3 is a novel repressor of the expression of short isoform of DCLK1

(DCLK1-S) from IntronV(β)-promoter of hDCLK1-gene, and is epigenetically silenced in hCRCs: Prognostic/Diagnostic implications of FOXD3/DCLK1-S expression in hCRCs. To be submitted to Oncotarget Febuary 2016.

**O'Connell M**, Sarkar S, Luthra G, Spratt H, Widen S, Wood T, Singh P. DCLK1-S enhances the invasive potential of colon cancer cells via a novel NFATC2 mediated pathway, resulting in enhanced expression of extracellular matrix protein, COL3A1. To be submitted to Cancer Research March 2016.

Sarkar S, **O'Connell M**, Popov P. Luthra G. Singh P. A mono-specific antibody against short Isoform of DCLK1 (DCLK1-S) is a novel biomarker of colon carcinogenesis in patients. To be submitted to Journal of Immunological Methods Febuary 2016.

Sarkar S, **O'Connell M**, Kantara C, Singh P. Dietary Chemopreventive agent (curcumin), Hypomethylates 5`Promoter of DCLK1 Gene in Human Colon Cancer Cells and Restores Expression of Long Isoform of DCLK1. To be submitted to Cancer Prevention Research March 2016.

**O'Connell M**, Sarkar S, Singh P. Short (S) isoform of cancer-stem-cell marker, DCLK1, is critically required to maintain proliferative/tumorigenic potential of colon cancer cells independent of DCLK1-L isoform. To be submitted to Laboratory Investigations May 2016.

## PATENTS

Singh P, Sarkar S, **O'Connell M**, Inventors.

Invention disclosure titled "Increased expression of the Short isoform of DCLK1 (a stem cell marker), is an early biomarker of transformation (cancer) of epithelial cells: Normal (non-transformed) epithelial cells mainly express the Long isoform of DCLK1" submitted to UTMB tech office in April, 2013. (Singh-P-13A)

Singh P, Sarkar S, **O'Connell M**, Inventors

A utility application 14/246,090 titled "Methods and composition for assessing and treating Cancer" filed as final patent on 4/5/14, which was published as US 2014/0315754 A1 on 10/23/14.

Singh P, Sarkar S, and **O'Connell M**. Co-inventors

Invention disclosure Singh-P-15A submitted in March of 2015. Technology office filed a provisional patent titled: "DCLK1 Short form specific Binding Agents", Provisional patent number UTMB0513USP1/SING-P-15A in 2015.

## ABSTRACTS

**O'Connell M**, Sarkar S, Luthra G, Okugawa, Y, Toiyama Y, Ward D, Goel A, Singh P. FOXD3 is a Novel Negative Regulator of IntronV(β)-Promoter Within hDCLK1-Gene in Normal Colonic Cells, But Gets Epigenetically Silenced in hCRCs, Resulting in the Expression of a Short Isoform of DCLK1 (DCLK1-S): Prognostic/Diagnostic Implications of FOXD3/DCLK1-S Expression in hCRCs. Proceedings of the Digestive Disease Week, May 21-22 2016. Abstract #241125.

***POSTER OF DISTINCTION.**

**O'Connell M**, Sarkar S, Ward D, Singh P. Short (S) Isoform of Cancer-Stem-Cell Marker, DCLK1, Is Critically Required for Maintaining Proliferative/Tumorigenic/Potenial of Human Colon Cancer Cells (hCCCs) Independent of DCLK1-L Isoform. Proceedings of the Digestive Disease Week, May 21-22 2016. Abstract #2439559.

***POSTER OF DISTINCTION.**

Sarkar S, **O'Connell M**, Popov L, Luthra G, Singh P. A Mono-Specific Antibody Against Short Isoform of DCLK1 (DCLK1-S) Is A Novel Biomarker of Colon Cancer Carcinogenesis in Patients. Proceedings of the Digestive Disease Week, May 21-22 2016. Abstract #2441150.

Sarkar S, **O'Connell M**, Singh P. Curcumin and its Bioavailable Analog (EF24), Differentially Regulate Expression of Long (L) Versus Short (S) Isoforms of DCLK1 in Human Cancer (Colon/Pancreatic) Cells, Dose-Dependently, in vitro and in vivo. Proceedings of the Digestive Disease Week, May 21-22 2016. Abstract #2444776.

**O'Connell M**, Sarkar S, Luthra G, Okugawa, Y, Toiyama Y, Ward D, Goel A, Singh P. FOXD3 is a novel repressor of the expression of short isoform (DCLK1-S) from IntronV(β)-promoter of hDCLK1-gene, and is epigenetically silenced in hCRCs: prognostic/diagnostic implications of FOXD3/DCLK1-S expression in hCRCs. American Association of Cancer Research annual meeting, April 16-20, 2016, New Orleans, LA. Abstract #1528.

Sarkar S, **O'Connell M**, Popov L, Luthra G, Singh P. Generation of a novel, mono-specific, antibody against short isoform of DCLK1 (DCLK1-S): a novel biomarker of colon carcinogenesis in patients. American Association of Cancer Research annual meeting, April 16-20, 2016, New Orleans, LA. Abstract #2957.

Sarkar S, **O'Connell M**, Singh P. Differential, dose-dependent effects of Curcumin/analogs, on Long (L) versus Short (S) Isoforms of a cancer stem cell marker, DCLK1 in colon and pancreatic cancer cells: Biological impact. American Association of Cancer Research annual meeting, April 16-20, 2016, New Orleans, LA. Abstract #5242.

**O'Connell M**, Sarkar S, Luthra G, Okugawa Y, Toiyama Y, Goel A, Gajjar A, Qiu S, Singh P.A short isoform of DCLK1 is a novel prognostic marker for human colon cancers, and can be used as a specific target for preventing and/or treating colon cancers, while sparing normal cells. Proceeding of the Digestive Disease Week, May 15-19, 2015. Gastroenterology Vol 148, Issue 4, Page S-18.

***SELECTED FOR ORAL PRESENTATION.**

**O'Connell M**, Sarkar S, Luthra G Okugawa Y, Toiyama Y, Goel A, Gajjar A, Qiu S, Singh P. A short isoform of DCLK1, transcribed from an alternate promoter in human colon cancers, represents a novel biomarker and target for diagnostic and

treatment purposes. American Association of Cancer Research annual meeting, April 18-22, 2015, Philadelphia, PA. Abstract #543.

Sarkar S, **O'Connell M**, Singh P. Dietary Chemopreventive agent (curcumin), hypomethylates 5' promoter of DCLK1 gene in human colon cancer cells and restores expression of long isoform of DCLK1. American Association of Cancer Research annual meeting, April 18-22, 2015, Philadelphia. Abstract #2817.

**O'Connell M**, Sarkar S, Kantara C, Singh P. Curcumin Induces Autophagic Survival of DCLK1+VE Colon Cancer Stem Cells (CSCs), While Co-Treatment With Curcumin and DCLK1-siRNA Eliminates CSCS: Role of Long and Short Isoforms of DCLK1. Proceedings of the Digestive Disease Week, May 3-6 2014. Gastroenterology Vol. 146, Issue 5, Page S-340.

Sarkar S, **O'Connell M**, Luthra G, Singh P. Progastrin Up-Regulates the Expression of Both Long and Short Isoforms of Cancer Stem Cell Marker, DCLK1, by Transcriptionally Activating Their Respective Promoters: Role of β-Catenin and NfκB Response Elements. Proceedings of the Digestive Disease Week, May 3-6 2014. Gastroenterology Vol. 146, Issue 5, Page S-516.

**O'Connell M**, Sarkar S, Singh P. Short (S) isoform of cancer-stem-cell marker, DCLK1, is critically required to maintain proliferatinve/tumorigenic potential of colon cancer cells: Identification of associated molecular pathways. American Association of Cancer Research annual meeting, April 5-9, 2014. Abstract #1940.

Sarkar S, **O'Connell M**, Kantara C, Singh P. A sub-set of DCLK1+ve colon cancer stem cells (CSCs) survive curcumin induced autophagy, while co-treatment with

curcumin+DCLK1-siRNA eliminates CSCs: Role of long and short isoforms of DCLK1. American Association of Cancer Research annual meeting, April 5-9, 2014. Abstract #3903.

**O'Connell M**, Sarkar S, Kantara C, Singh P. Prevention and treatment strategies for colon cancer stem cells. International Conference on Recent Advances in Colon Cancer Prevention and Therapeutics. November 19-21, 2013; Ahmedabad, India (Singh P: Invited Speaker).

**O'Connell M**, Sarkar S, Luthra G, Qui S, Gajjar A, Maxwell C, Singh P. The short (s) isoform of stem-cell-marker DCLK1 is increasingly up-regulated during colon carcinogenesis: Role of autocrine/endocrine progastrin. Proceedings of the Digestive Disease Week, May 18-21 2013. Gastroenterology Vol. 144, Issue 5, Supplement 1, Page S-596.

Sarkar S, **O'Connell M**, Moya S, Singh P. Opposite effects of curcumin on the expression of short (S) form of stem-cell-marker, DCLK1, in non-transformed vs. transformed cells, resulting in either stabilization or inhibition of cell proliferation, respectively. Proceedings of the Digestive Disease Week, May 18-21 2013. Gastroenterology Vol. 144, Issue 5, Supplement 1, Page 596.

***POSTER OF DISTINCTION.**

**O'Connell M**, Sarkar S, Luthra G, Qui S, Gajjar A, Maxwell C, Singh P. The short isoform of stem-cell-marker DCLK1 (DCLK1-S) is strongly up-regulated during adenoma-carcinoma sequence of colon cancer disease: Role of autocrine/endocrine progastrin. American Association of Cancer Research annual meeting, April 6-10, 2013. Abstract #4891.

Sarkar S, **O'Connell M**, Moya S, Singh P. Curcumin either stimulates or inhibits expression of short isoform of stem-cell-marker DCLK1 (DCLK1-S) in non-transformed vs. transformed cells, resulting in stabilization/inhibition of growth, respectively. American Association of Cancer Research annual meeting, April 6-10, 2013. Abstract #2574.

Permanent address: 2027 FM 646 N Santa Fe TX 77510

This dissertation was typed by Malaney Ravae O'Connell.